Deciphering the genome of *Desulfovibrio gigas*: the role of the hydrogenases

The participation of the Ech and HynAB hydrogenases in the energy metabolism

Fabio de Oliveira Morais e Silva

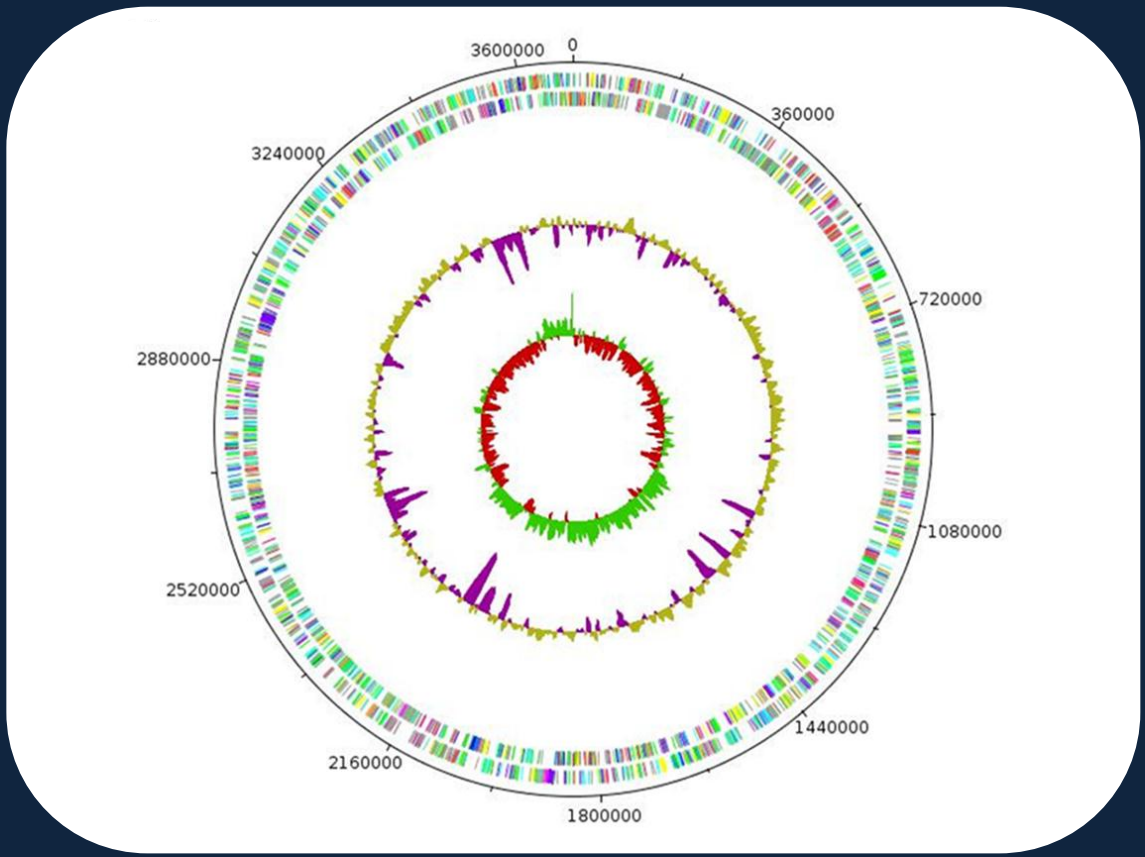

Dissertation presented to obtain the Ph.D degree in Biochemistry

Instituto de Tecnologia Química e Biológica António Xavier | Universidade Nova de Lisboa

Oeiras,
December, 2013

INSTITUTO
DE TECNOLOGIA
QUÍMICA E BIOLÓGICA
ANTÓNIO XAVIER /UNL

Knowledge Creation

ITQB-UNL | Av. da República, 2780-157 Oeiras, Portugal
Tel (+351) 214 469 100 | Fax (+351) 214 411 277

www.itqb.unl.pt

Deciphering the genome of *Desulfovibrio gigas*: the role of the hydrogenases

The participation of the Ech and Hyn hydrogenases in the energy metabolism

Fabio de Oliveira Morais e Silva

Dissertation presented to obtain the Ph.D degree in Biochemistry

Instituto de Tecnologia Química e Biológica António Xavier | Universidade Nova de Lisboa

Oeiras, December, 2013

INSTITUTO
DE TECNOLOGIA
QUÍMICA E BIOLÓGICA
ANTÓNIO XAVIER /UNL

Knowledge Creation

Financial support from Fundação para a Ciência e a Tecnologia (No.SFRH/BD/45211/2008) and Instituto de Tecnologia Química e Biológica – Antonio Xavier

Cover image

Circular representation of the genome of *Desulfovibrio gigas*

Work performed at:

Genomics and Stress Laboratory

and

Energy Metabolism Laboratory

Instituto de Tecnologia Química e Biológica – António Xavier

Av. da República, Estação Agronómica Nacional

2781-901 Oeiras, Portugal,

Tel:. (+351) 214469624

Supervisor:

Professora Doutora Claudina Rodrigues-Pousada

Professora Catedrática Convidada, Head of the Genomics and Stress Laboratory

Instituto de Tecnologia Química e Biológica – António Xavier, UNL

Co-Supervisor:

Doutora Inês Cardoso Pereira

Investigadora Principal, Head of the Bacterial Energy Metabolism Laboratory

Instituto de Tecnologia Química e Biológica – António Xavier, UNL

Jury Members:

Professor Paula Tamagnini – Head of the Bioengineering and Synthetic Microbiology Group, Instituto de Biologia Molecular e Celular, Universidade do Porto (*Principal Examiner*)

Professor Solange Gomes – Head of the Soil Microbiology Group, Instituto de Ciência Agrárias e Ambientais Mediterrânicas, Universidade de Évora (*Principal Examiner*)

Professor Isabel Sá Nogueira – Head of the Microbial Genetics Group, Faculdade de Ciências e Tecnologia, Universidade Nova de Lisboa

Dr. Pedro Matias – Head of the Industry and Medicine Applied Crystalography Group, Instituto de Tecnologia Química e Biológica, Universidade Nova de Lisboa

Esta tese é dedicada a memória

do meu avô João Coelho

This thesis is dedicated to the memory

of my grandfather João Coelho

Foreword

This thesis is the result of five years of research done at the Genomics and Stress and Bacterial Energy Metabolism laboratories at the Instituto de Tecnologia Química e Biológica – António Xavier (ITQB), Universidade Nova de Lisboa (UNL), Portugal, under the supervision of Professor Claudina Rodrigues-Pousada and Dr. Inês Cardoso Pereira. I have to mention the work performed in collaboration with the Bioinformatics and Genome Annotation group of Centro de Pesquisas René Rachou – Instituto Fiocruz, Brazil, during June 2012 under the supervision of Dr. Jeronimo C. Ruiz regarding the manual annotation of the genome *of Desulfovibrio gigas*.

The studies here reported were performed during the term of a four year PhD fellowship from Fundação para a Ciência e Tecnologia (FCT), from January 2009 to December 2013.

The thesis comprises five chapters. The first chapter provides a general understanding of the energetic metabolism of the *Desulfovibrio* genus of the Sulfate-Reducing Bacterial group (SRB) and the function of the hydrogenases in these organisms. The second chapter addresses the deciphering of the genome of *Desulfovibrio gigas*, our model organism and its comparison with other members of the *Desulfovibrio* genus. These results were already submitted to publication. The third chapter describes the physiological function of the two hydrogenases of *D. gigas* during respiratory and fermentative sulfidogenic conditions. The results obtained in those analyses were published in the Journal of Bacteriology. The fourth chapter describes the investigation of the function of these same hydrogenases during non-sulfidogenic conditions. The last chapter of the thesis presents a final discussion of the integrated results obtained and proposes two main pathways that could be followed to continue the investigation of the hydrogenases and energy metabolism in *D. gigas*.

Acknowledgements

The work presented in this thesis is the result of a long experience, both at the professional and personal levels. This would not be possible without the participation of several people throughout this journey and to whom I owe my acknowledgements.

First and foremost I must thank my supervisor, **Professor Claudina Rodrigues Pousada** in the first place for giving me the opportunity to perform my doctoral studies in her laboratory and to live in a different country, which is also a very unique experience. Also I have to appreciate that she was always there for me to listen, help, guide, but also call my attention to what was important when needed be.

I also owe a great debt of gratitude to my co-supervisor, **Dr. Inês Cardoso Pereira** for all the important discussions, suggestions and comments regarding the specific aspects of SRB and *Desulfovibrio´*s metabolism that helped to develop and reach the conclusions of this work.

To three other people in particular, for having key contributions directly involved in the work presented here. Firstly to **Catia Santos** from the *D. gigas* TEAM to whom I am indebted for the help to perform several experiments and analysis that were essential for this work. Secondly, to **Monica Martins**, from the Bacterial Energy Metabolism Lab, with whom I had numerous and long discussions about the data helping me to understand and to make sense out of the results of some experiments. Thirdly, to **Cristina Leitão** from the Analytical Services from ITQB that made possible the analysis of several hundred different samples for the substrate analysis due to her expertise in HPLC systems. I am positively sure that without her help I would not be able test so many different growth conditions.

To **Jeronimo C. Ruiz**, **Antonio Resende** and the other members of the Informatics and Biosystems group from René Rachou Research Center, FIOCRUZ, Brazil for not only receiving me and teaching me how to annotate a genome sequence, but also for being so kind to me during my stay in their laboratory.

To all my colleagues that worked in both Bacterial Energy Metabolism Lab, namely **Sofia Venceslau, Raquel, Marta, André, Gonçalo, Claudia, Will**; and especially in the Genomics and Stress laboratory: **Regina, Catarina Pimentel, Catarina Amaral, Sofia Silva, Marcos, Jorge, Liliana, Soraia, Rita, Daiane, Aninha, Ana Raposo, Cristina, Carol, Mariana, Joana, Pimpas, and Xana** for their patience, support, help and most of all for providing such a great environment to do science.

To other people from different labs from the ITQB, namely present and former members of the **InteraQB** group, as well as **Joana Lamego** and **Barbara Cunha** for their friendship and for the good time spent both in the ITQB events and outside.

To Instituto de Tecnologia Química e Biológica (ITQB) and its personnel for the facilities, access and training for using the equipment available, help and support in various technical and logistic areas, and for the stimulating conditions provided for learning and developing science.

To the “Fundação para a Ciência e Tecnologia”, for the financial support (SFRH/BD/45211/2008).

In the more personal side I have to acknowledge a very especial group of people that were part of my life during these years in Portugal and that I consider as my European family, the Saldanha Apartment crew: **Marta, Kim, Alessandro, Luka, Igor, Manuela, Gabriel, Ricardo, Joana, Sara, Marija, Filipe, Patricia, Rodrigo, Arianna, Anna, Thomas, Guido, Nadia, Lucas, Verica, Robert, José,**

Raphael, Alice, Benny, Stan, Christian, Claudia and many other people that made part of this group. Their friendship and companionship during the moments outside of the Lab made possible to live abroad for so many years and helped me deal with the struggle of a PhD life. I could not have done it without them as well.

I would also like to thank all my friends and family in Brazil, specially to my parents **Celso Morais e Silva** and **Marli Lefort** for all their love, support and care for me since I first started studying Biology in the university till when I decided to commit myself to the PhD in a different country and that kept me apart from them for many years. Despite that they always believed in me and were always there during difficult times and when I missed home.

Finally, I have to thank **Filipa Nunes** that entered in my life during the course of this PhD and that changed everything. Without her I would neither have had the strength to conclude this thesis nor I would be so happy.

TABLE OF CONTENTS

LIST OF PUBLICATIONS

Thesis publications

Morais-Silva F, Santos C, Rodrigues R, Pereira I, Rodrigues-Pousada C. (2013). "Role of HynAB and Ech, the only two hydrogenases found in the model sulfate reducer *Desulfovibrio gigas*." Journal of Bacteriology 195(20):4753-60

Morais-Silva F.*, Rezende A.*, Pimentel C., Santos C., Clemente C., Varela-Raposo A., Resende D., da Silva S., de Oliveira L., Costa D., Matos M., Flores O., Ruiz J. and Rodrigues-Pousada C. (2013) Genome sequence of the model sulfate reducer *Desulfovibrio gigas*: a comparative analysis within the *Desulfovibrio* genus. Submitted for publication.

Additional publications not included in the thesis

Varela-Raposo A, Pimentel C, **Morais-Silva F,** Rezende A, Ruiz J, Rodrigues-Pousada C. 2013. "Role of NorR-like transcriptional regulators under nitrosative stress of the δ-proteobacterium, *Desulfovibrio gigas*." Biochemical and Biophysical Research Communications 431(3):590–6

ABBREVIATIONS

16S = 16S ribosomal RNA

[Fe-S] = iron sulfur clusters

Δp = proton gradient

ATCC = American Type Culture Colection

ATP = adenosine triphosphate

Cas = CRISPR-associated sequences

CDS = coding sequence for a gene

CoA = coenzyme A

Coo = cytoplasmic [NiFe] carbon monoxide induced hydrogenase

CRISPR = clustered regularly interspaced short palindromic repeats

D. = *Desulfovibrio*

DNA = deoxyribonucleic acid

e^- = electron

E_0 = standard reduction potential

Ech = cytoplasmic membrane-bound energy-conserving [NiFe] hydrogenase

F = fumarate growth condition

FAD = flavin adenine dinucleotide cofactor

Fd = Ferredoxin

Fd_{red} = Reduced ferredoxin

FMN = flavin mononucleotide

g = gravity acceleration

HS = hydrogen plus sulfate growth condition

HPLC = High-Performance Liquid Chromatography

Hdr = heterodisulfide reductase

HydAB = periplasmic [FeFe] hydrogenase

HynAB = periplasmic [NiFe] hydrogenase

HysAB = periplasmic [NiFeSe] hydrogenase

kan^R = kanamycin

kb = kilobase

Ldh = lactate dehydrogenase

LF = lactate plus fumarate growth condition

LS = lactate plus sulfate growth condition

LS* = lactate fermentation

MK = menaquinone

mRNA = messenger RNA

mV = millivolts

NAD^+ = nicotinamide adenine dinucleotide coenzyme

NADH = reduced nicotinamide adenine dinucleotide coenzyme

$NADP^+$ = nicotinamide adenine dinucleotide phosphate coenzyme

NAD(P)H = reduced nicotinamide adenine dinucleotide phosphate coenzyme

Nuo = NADH:quinone oxidoreductase complex

ORF = Open Reading Frame

PCR = Polymerase Chain Reaction

pfl = pyruvate formate lyase gene

PS = pyruvate plus sulfate growth condition

PS* = pyruvate with limiting sulfate growth condtion

P = pyruvate fermentation

RNA = ribonucleic acid

RNase = ribonuclease

rpm = rotations per minute

rRNA = ribosomal RNA

spp. = species

SRB = Sulfate-Reducing Bacteria

TpI-c_3 = tetraheme cytochrome c_3

tRNA = transfer RNA

TCA cycle = tricarboxylic acid cycle

UV = ultraviolet

WT = wild type

SUMMARY

The work presented in this thesis describes the functional characterization of hydrogenases in the overall energy metabolism of the sulfate reducing bacterium *Desulfovibrio gigas*. With the complete annotation of the *D. gigas* genome, we were able to verify that only the two previously described hydrogenases are present in this organism, the periplasmic [NiFe] HynAB and the cytoplasmic membrane-bound [NiFe] Ech. Given its low number of hydrogenases, *D. gigas* is an excellent model organism to explore the specific function of each of these enzymes during different growth conditions and the possible mechanisms of energy conservation involved.

In Chapter 2 we present the sequencing and analysis of the *D. gigas* ATCC19364 genome. The genome is formed by a circular chromosome with approximately 3.7mb that contains 3,370 genes and also a megaplasmid of 102kb with 72 protein coding genes. The full analysis of the *D. gigas* encoding genes allowed us to have a complete overview of the proteins and regulatory mechanisms contained within this organism. Several gene duplications were identified for proteins that participate in metabolic pathways, such as fumarate reductases and formate dehydrogenases, and proteins involved in the response to O_2 and NO stress. We have detected unique genes and complexes for the *Desulfovibrio* genus in this species. Transmembrane complexes that might participate in electron transfer reactions were identified while key genes participating in CO and formate cycling mechanism (*codh* and *pfl*) were absent in *D. gigas*. This suggests that alternative cycling mechanism for energy conservation does not play an important role in this organism. Furthermore, comparison with other *Desulfovibrio* spp reveals the presence of high number of CRISPR systems in *D. gigas* as well as two distinct Cas gene operons in this organism. A phylogenetic analysis based on the conserved Cas1 gene, showed that in *Desulfovibrio* three different groups are present: I-C, I-E and I-F. However the Cas1 distribution among different species does not correlate well with the

separation of *Desulfovibrio* spp into separate clades, obtained by phylogenetic analyzes performed using genetic sequences of structural proteins, such as *rpoB* and *gyrB*. This strongly suggests the divergence after speciation of an ancestor gene common for the Cas genes from subtype I-F in this genus. Moreover, the acquisition of the other Cas subtypes by different Desulfovibrio appears to be the result of multiple horizontal gene transfer events.

In Chapter 3 we report the analysis of the physiological role of the two hydrogenases of *D. gigas* during respiratory and fermentative conditions. We have used two single mutant strains, Δ*echBC* and Δ*hynAB*, each containing a single active hydrogenase. Growth performance of these strains, as well as H_2 production was compared to the wild type during growth using the lactate, pyruvate and H_2 as electron donors. The expression of the genes coding for these enzymes was assessed by qRT-PCR in the three strains analyzed. The results indicate that none of the hydrogenases are essential during sulfate respiration with either lactate or pyruvate and that other mechanisms of energy conservation besides hydrogen cycling may be operating in these growth conditions. However, during sulfate respiration with H_2, the periplasmic HynAB is essential for H_2 oxidation supplying electrons for sulfate reduction, as the Δ*hynAB* is unable to grow. Furthermore the HynAB is also essential for H_2 production during pyruvate fermentative growth. As such this enzyme presents a bifunctional activity, being able to produce H_2 as well as oxidizing it according to the conditions present. It seems therefore to play a dominant role in *D. gigas* hydrogen metabolism.

In Chapter 4, we have further investigated hydrogenase function and its participation in energy conservation mechanisms in *D. gigas* during non sulfidogenic conditions. We compared growth and H_2 production of *D. gigas* wild type and hydrogenase mutants during lactate fermentative conditions or using fumarate as an alternative electron acceptor for lactate oxidation. During fumarate fermentation, the absence of either hydrogenase appears to have no effect in growth. However when lactate was tested as electron donor and fumarate as

electron acceptor, both these enzymes appear to contribute to energy conservation since the wild type grew more than any of the mutants. In addition, during lactate fermentation, both Ech and HynAB appear to produce H_2 from reducing equivalents generated during oxidation of the substrate. A similar mechanism of hydrogen production from lactate fermentation by different hydrogenases was observed using *D. vulgaris* Hildenborough deletion mutants for the [NiFe], [NiFeSe] and [FeFe] periplasmic hydrogenases. This indicates that in *Desulfovibrio* spp. H_2 production during lactate fermentation is produced not only by cytoplasmic hydrogenases, as expected, but also by periplasmic enzymes.

In conclusion, the work described in this thesis represents an important contribution to the elucidation of the physiological role of the two hydrogenases in *Desulfovibrio gigas*. The periplasmic HynAB is a bifunctional enzyme that produces H_2 during fermentative growth, is essential in hydrogen oxidation during sulfate respiratory growth and contributes to energy conservation in lactate plus fumarate growth. The cytoplasmic Ech produces H_2 using reducing equivalents from lactate oxidation during fermentative and respiratory growth and contributes to energy conservation. However, other mechanisms of energy conservation involving transmembrane complexes identified in *D. gigas* genome may play a role during sulfate respiration, providing alternatives for electron transfer, in which the participation of the hydrogenases is not essential.

RESUMO

O trabalho apresentado nesta tese constitui uma contribuição para o estudo funcional das hidrogenases no metabolismo energético da bactéria redutora de sulfato *Desulfovibrio gigas*. Com a descodificação de todo o genoma de *D. gigas* foi possível verificar que apenas duas hidrogenases previamente descritas nesta bactéria, a [NiFe] HynAB periplásmica e a [NiFe] Ech, citoplásmica associada à membrana, são únicas neste organismo. Por esta razão, a bactéria *D. gigas* se torna um excelente organismo modelo para estudar o papel específico de cada uma destas enzimas em diferentes condições de crescimento, bem como os possíveis mecanismos de conservação de energia que estão envolvidos com a sua atividade.

No Capítulo 2, apresenta-se o genoma da bactéria *D. gigas* ATCC 19364, que é constituido por um cromossoma circular de 3,7 megabases contendo aproximadamente 3.370 genes e também um mega plasmídeo com um tamanho de 102 kilobases composto por 72 genes. Com a análise de todos os genes codificantes presentes no genoma de *D. gigas* foi possível obter uma visão global de todas as proteínas e mecanismo regulatórios que este organismo contém. Foram identificadas inúmeras duplicações génicas em proteínas que participam não somente em importantes vias metabólicas, tal como as redutases do fumarato ou deshidrogenases do formato, mas também proteínas que estão envolvidas na resposta ao stress gerado por O_2 e NO. Os genes que codificam para proteínas e complexos pela primeira vez observados no gênero *Desulfovibrio* foram também detetados no genoma de *D. gigas*. Ainda, foram identificados diversos complexos transmembranares que podem estar envolvidos em reações de transferência eletrónica. Contudo, genes chave, que participam em mecanismos de ciclagem de CO e formato (*codh* e *pfl*) não foram identificados no genoma deste organismo.

Isto sugere que estes mecanismos alternativos de conservação de energia envolvendo a ciclagem de compostos intermediários não são participativos no metabolismo energético deste organismo. Além disso, as comparações feitas entre *D. gigas* e outras espécies do gênero *Desulfovibrio* revelaram a presença de um elevado número de elementos CRISPR no genoma e dois operões de genes Cas distintos. A análise filogenética feita com base nos genes conservados Cas1 revelou a presença de três grupos distintos (I-C, I-E e I-F) presentes em *Desulfovibrio*. Porém a distribuição destes grupos de genes Cas não correlaciona com a divisão do género *Desulfovibrio* em diferentes clados, obtida com base em análises filogenéticas feitas com sequências gênicas de proteínas estruturais conservadas (*rpoB e gyrB*). Isto indica uma divergência após especiação de um ancestral comum para o gene Cas do subtipo I-F em *Desulfovibrio* e ainda a aquisição dos demais tipos destes genes via múltiplos eventos de transferência horizontal.

No Capítulo 3, foi avaliada a função específica de cada uma das duas hidrogenases presentes na bactéria *D. gigas* em diversas condições de crescimento fermentativas e respiratórias. Para tal, foram construídas duas estirpes mutantes, Δ*echBC* and Δ*hynAB*, cada uma contendo uma única hidrogenase ativa. A performance de crescimento e a respetiva produção de H_2 foi comparada entre estas estirpes mutantes e a estirpe selvagem cujo crescimento foi feito utilizando lactato, piruvato e gás hidrogénio como fontes doadoras de eletrões. Também foi avaliado o nível de expressão dos mRNAs codificando para estas enzimas, através de qRT-PCR, nas três estirpes estudadas. Os resultados obtidos indicam que nenhuma destas enzimas é essencial para o crescimento celular em condições respiratórias na presença de sulfato e ácidos orgânicos como fonte de energia. Nestas condições é de supor que estarão ativos outros mecanismos de conservação de energia que não dependem da participação do H_2 como intermediário, como sugerido na hipótese da Ciclagem de Hidrogenio. Entretanto, quando utilizamos H_2 como fonte de

energia durante condições de crescimento respiratórias, a hidrogenase periplásmica HynAB é essencial, oxidando este H_2 e fornecendo eletrões para a redução do sulfato no citoplasma, visto que a ausência deste gene impede o crescimento celular. Além disso, esta enzima é também essencial para o crescimento fermentativo de *D. gigas* quando o piruvato é utilizado como fonte de energia, demonstrando que a hidrogenase HynAB é uma enzima bifuncional oprando na produção e consumo de H_2 e apresenta um papel dominante no metabolismo do hidrogénio.

No Capítulo 4, nós aprofundamos os estudos sobre a função das hidrogenase e sua concomitante participação em processos de conservação de energia em *D. gigas* durante condições de crescimento na ausência de sulfato. Ambas as estirpes mutadas para as hidrogenases e a estirpe selvagem foram avaliadas, em termos de performance de crescimento e produção de H_2, durante condições fermentativas e ainda em condições de crescimento onde o sulfato foi substituído pelo composto orgânico fumarato como aceitador final de eletrões durante oxidação de lactato. Durante o crescimento fermentativo utilizando fumarato, observou-se que a ausência de qualquer das hidrogenases presentes não alterou o perfil de crescimento das estirpes avaliadas. Porém, quando o fumarato foi testado como aceitador de eletrões durante a oxidação de lactato, a presença das duas hidrogenases parece contribuir para um maior crescimento celular, uma vez que a estirpe selvagem cresce mais que qualquer das estirpes mutantes. Nestas condições ambas as hidrogenases parecem participar num mecanismo de conservação de energia. Adicionalmente, quando o lactato é utilizado como fonte de energia durante o metabolismo fermentativo a função da Ech e da HynAB é a produção de H_2 a partir de eletrões e protões gerados da oxidação do substrato. Este mecanismo parece não estar somente restrito a *D. gigas*, mas ser comum para outras espécies do gênero *Desulfovibrio*, uma vez que em expericiências realizadas com mutantes de hidrogenases periplasmáticas de *D. vulgaris* Hildenborough contendo diferentes centros ativos ([NiFe], [NiFeSe]

e [FeFe]) revelam resultados similares. Estes resultados sugerem que em *Desulfovibrio* spp. a produção de H_2 durante a fermentação de lactato é realizada não somente por hidrogenases citoplasmáticas, como seria esperado, mas também por aquelas encontradas no periplasma independentemente da composição dos seus centros ativos.

Em conclusão, os resultados apresentados neste trabalho demonstram o papel específico de cada uma das duas hidrogenases presentes em *D. gigas*. A hidrogenase periplasmática HynAB possui uma função efetivamente reversível, produzindo H_2 durante o crescimento fermentativo, é essencial durante o crescimento respiratório na presença de sulfato oxidando H_2 e ainda contribui para conservação de energia durante a oxidação de lactato com redução do fumarato. A hidrogenase citoplasmática Ech participa na produção de H_2 utilizando o potencial redutor (eletrões e protões) produzidos durante a oxidação de lactato em ambas condições respiratórias e fermentativas, e também contribuindo para a conservação de energia. Porém, como observado em algumas condições de crescimento, outros mecanismos relacionados com o metabolismo energético envolvendo complexos transmembranares identificados no genoma de *D. gigas* podem fornecer alternativas para a transferência de eletrões na ausência das hidrogenases.

Chapter 1

General Introduction: an overview of the Sulfate Reducing Bacteria (SRB)

1.1. General features of sulfate reducing bacteria

Organic and inorganic compounds such as fumarate, carbon dioxide, nitrate, iron oxides, sulfur and sulfate are used as terminal electron acceptors for respiratory electron transfer chain reactions in anaerobes that are equivalent to the aerobic respiration (Rabus *et al.*, 2006). The sulfate reducing bacteria (SRB) are a widespread group of microorganisms existing in many anoxic habitats, which employ a respiratory mechanism using sulfate as the main terminal electron acceptor to gain energy for cell synthesis and growth. During dissimilatory sulfate reduction, these organisms use inorganic sulfate as an external electron acceptor for the oxidation of energy substrates, generating hydrogen sulfide, a toxic end product (Rabus *et al.*, 2006; Muyzer and Stams, 2008; Barton and Fauque, 2009).These organisms have a great impact in the global cycling of elements, mainly the sulfur and carbon natural cycles, reason why they are extensively studied (Fig 1.1).

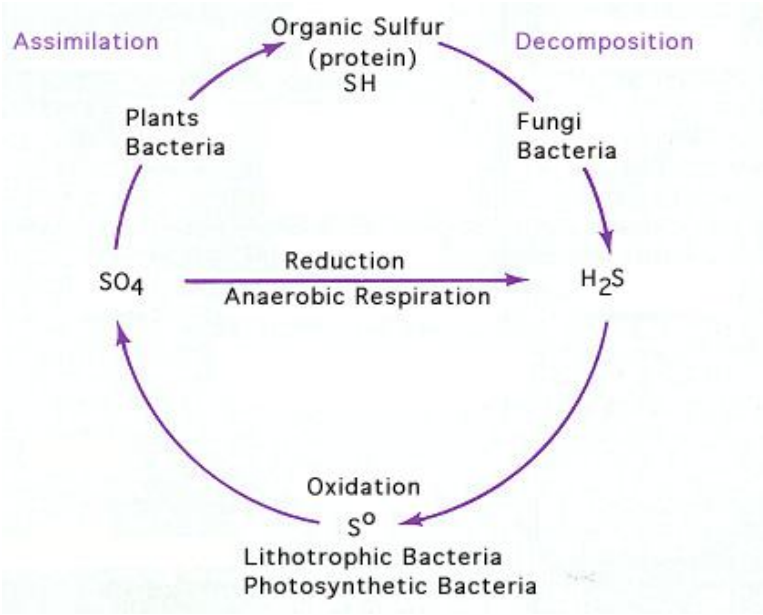

Fig 1.1. Participation of the Sulfate-Reducing Bacteria (SRB) in the anaerobic respiration during the Sulfur cycle.

Source: http://textbookofbacteriology.net/themicrobialworld/environmental.html

Hydrogen sulfide serves as an electron donor for aerobic chemotrophic and anaerobic phototrophic microorganisms in sulfidic habitats. In the carbon cycle, SRB play a key role in anaerobic degradation of organic matter whenever sulfate is present and also in its absence, in certain systems (Hansen, 1994) (Fig1.2).

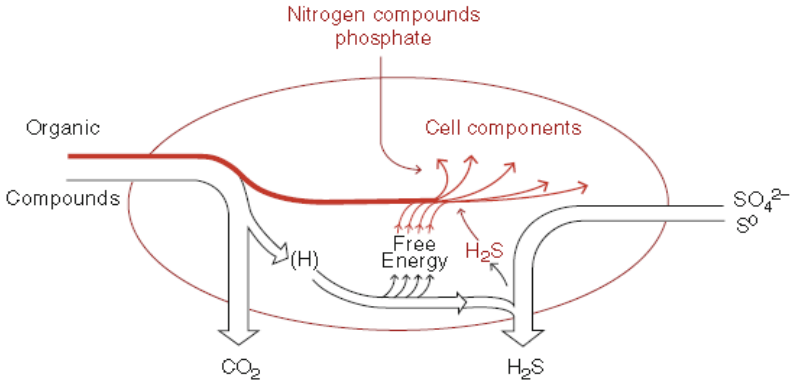

Fig 1.2. Metabolic principle of Sulfate-Reducing Bacteria (Rabus *et al*. 2006). Catabolic fluxes (energy metabolism) are shown in black arrows; anabolic fluxes (cell synthesis) are shown in red arrows.

They contribute in particular to carbon re-mineralization in marine environments where approximately 50% of organic carbon in the sediments is mineralized by the sulfate reducing processes (Jorgensen, 1982). Moreover, they also participate in the biogeochemistry of these environments, through sulfide production, in metal reduction, such as ferric iron, and in the formation ferrous carbonates (Lovley, 1993). In addition to their importance in these cycles, mainly in the marine habitat, they are also important agents in a variety of processes in wetland soils and sediments, such as organic matter turnover or biodegradation of contaminants (Fauque, 1995). These organisms are ubiquitous and may be found in most diverse natural and engineered anaerobic environments, such as marine sediments, hydrothermal vents, hydrocarbon seeps, mud volcanoes, hypersaline microbial mats, oil fields, water-clogged soils, rhizosfere of plants, aquifers, human

gastrointestinal tract, anaerobic waste-water treatment plants or even in environments where microaerophilic or oxygen saturating conditions are present (Muyzer and Stams, 2008)

In some conditions, the SRB can cause serious problems. These organisms are involved in several biocorrosion processes involving: a) biofilm formation and fixation on metallic surfaces, where ferrous surface is formed; b) cathodic depolarization, causing iron corrosion by the dissociation of H_2 through the action of hydrogenases; c) formation of iron sulfide deposits on iron surface; or d) formation of occluded areas on metal surface. Sulfate reduction can also be prejudicial resulting in lower methane yields in anaerobic treatment of agro-industrial waste waters. In the petrochemical and oil industry, besides metal corrosion of pipe lines and also platform structures under anaerobic environments, such as deep-sea bed, souring of oilfields is a great problem. In this process, the hydrogen sulfide is produced inside the oil field due to pumping of sea-water that might contain up to 300mM of sulfate, thus becoming a contaminant of crude oil. This is possible because species of SRB are able to degrade hydrocarbons present in the oil (Rabus *et al*., 2006; Barton and Fauque, 2009). The presence of SRB has also health consequences as they are implicated in inflammatory bowel diseases caused by the toxic effects of sulfide on epithelial cells located in the colon (Loubinoux *et al*., 2002).

On the other hand, these organisms present a great biotechnological potential. Heavy metals can be removed from groundwater and waste-water through the formation of precipitated metal sulfides, during sulfate reduction. Organisms that are able to perform such process are referred to as dissimilatory metal-reducing bacteria (DMRB) (Barton and Fauque, 2009). The recovery of precious metals for industrial applications can also, to some extent, be performed by SRB (Lloyd *et al*., 1999; Lloyd *et al*., 2001). They are also capable of removal and reutilization of sulfur compounds from contaminated water and gases. In contrast to their effect in oil degradation inside oil fields, they can be used in bioremediation cleaning processes of hydrocarbon contaminated areas, such as oil spills or oil contaminated soil (Widdel and Rabus, 2001; Widdel *et al*., 2007). Chemical reduction of azo dyes through

biological hydrogen sulfide is also proposed to be carried out by these organisms via the hydrogenases activity (Mutambanengwe *et al*., 2007).

The group of SRB presents a great metabolic flexibility as they can use a great variety of organic and inorganic substrates being able to grow heterotrophically, autotrophically or lithoautotrophically. SRB does not usually use polymeric organic compounds as direct substrates. The most common electron donors utilized by these bacteria are typically products of fermenting bacteria such as low-molecular-mass organic compounds including mono and dicarboxylic aliphatic acids and alcohols, as well as intermediate breakdown products such as sugars, amino acids, glycerol, fatty acids and aromatic compounds (Hansen, 1994; Rabus *et al*., 2006; Barton and Fauque, 2009). The organic compounds are either completely oxidized, forming only carbon dioxide, or incompletely to acetate and CO_2. This ability to fully oxidize such substrates is often used as criteria to separate the SRB in two major groups: complete and incomplete oxidizers. The SRB that are able to fully oxidize organic compounds usually use acetate as growth substrate and one of two possible pathways for acetate oxidation: a modified citric acid cycle or the acetyl-CoA pathway (Muyzer and Stams, 2008). More recently characterized SRB species can grow in less degradable substrates, such as hydrocarbons, alkanes, toluene, xylenes and naphtalenes (Rabus *et al*., 1996; Galushko *et al*., 1999; Harms *et al*., 1999; So and Young, 1999). Inorganic electron donors such as H_2, which is a very important substrate, or sulfur species can also be used under anoxic conditions, resulting in purely inorganic redox reactions for energy conservation (lithotrophic growth).

Due to the fact that these organisms can be found in environments with low concentrations or even in the absence of sulfate, e. g. anaerobic freshwater sediments, some species can carry out other energy processes such as fermentative growth, using pyruvate or fumarate, or syntrophic growth coupled with other organisms. Furthermore, the capability of aerobic respiration was also demonstrated. Some species of SRB, which were considered to be strict anaerobes, such as members of the *Desulfovibrio* genus, are able to perform a microaerobic respiration

coupled to energy conservation (Cypionka, 2000). Also growth of *D. desulfuricans* ATCC 27774 at low oxygen levels has been demonstrated (Lobo *et al*., 2007).

The SRB importance in different ecosystems and their ability to grow using electron donors and acceptors, as well as the fact that these organisms can be used in biotechnological application justifies their intensive scientific interest. Among the various species of these organisms, rRNA sequenced based analysis allowed their organization into four distinct groups: mesophilic gram-negative; spore forming gram-positive; thermophilic bacterial; and thermophilic archeal SRB (Castro *et al*., 2000). Further comparative analysis using 16S rRNA sequences showed that SRB can be divided into seven phylogenetic lineages. However, the majority of the SRB belongs to approximately 23 genera of *Deltaproteobacteria* (Muyzer and Stams, 2008).

1.2. *Desulfovibrio* species

Among the representatives of the *Deltaproteobacteria*, the most intensive studied are those from the genus *Desulfovibrio* (Barton and Fauque, 2009) (Fig 1.3).

Fig 1.3. Electron microscopy of *Desulfovibrio desulfuricans*. Source: Microbewiki

Important biochemical information regarding organic degradation pathways leading to ATP synthesis during sulfate reduction, as well as bioenergetics studies to identify electron transfer components during respiration was obtained using these

organisms (Hansen, 1994; Matias *et al*., 2005; Rabus *et al*., 2006; Zhang *et al*., 2006). Structural information of diverse enzymes and electron carriers that participate in the sulfate respiratory energy transfer reactions, such as hydrogenases, cytochromes, ferredoxins were obtained using *Desulfovibrio* spp (Volbeda *et al*., 1995; Matias *et al*., 1996; Frazao *et al*., 2000).

Desulfovibrio species were the first SRB to be genetically manipulated and modified by marker exchange mutagenesis (Rousset *et al*., 1991). Further molecular biology and genetics studies, due to the ease of cultivation and the applicability of antibiotics as selecting agents for mutants, included analysis of hydrogenases, cytochromes, nitrogenases, biosynthetic enzymes and plasmids (Rabus *et al*., 2006). After sequencing the genome of *Desulfovibrio vulgaris*, another set of molecular tools including microarray data and random transposon mutant libraries were also available to explore and provide insights into the electron flow pathways during different growth conditions (Heidelberg *et al*., 2004; Keller and Wall, 2011).

1.2.1.Sulfate respiration

Sulfate reduction to sulfide occurs in the cytoplasm after its transport to the cell, through an eight electron reduction process, requiring at least four enzymes (Fig 1.4). Sulfate transport from the environment into the cell appears to be largely an electro neutral process, unless sulfate concentrations are limited (Cypionka and Barton, 1995). In the first step, sulfate must be activated by ATP sulfurylase at expenses of up to ATP molecules, since the $E^{0'}$redox couple sulfate-sulfite, (-516mV), is too negative to allow reduction by ferredoxin or NADH ($E^{0'}$ -398mV and -314mV, respectively) (Muyzer and Stams, 2008) (Table I.I).

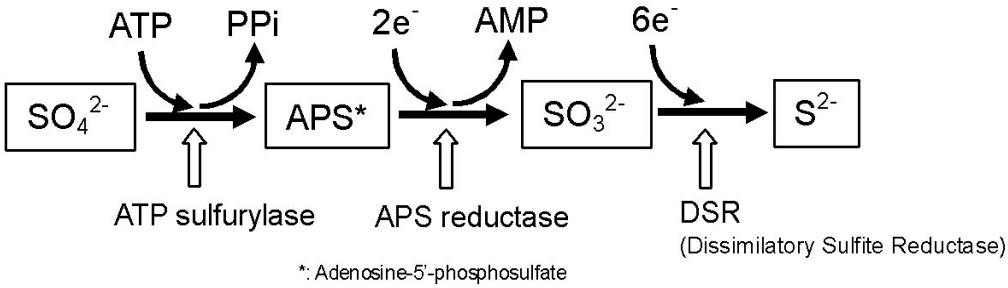

Fig 1.4. Scheme of the three step and eight electron sulfate reduction process in the SRB. Source: www.biochemeng.bio.titech.ac.jp/research/biofilm/mic/mic.html

This results in the formation of APS, which is the actual electron acceptor, and pyrophosphate, which is hydrolyzed to orthophosphate to drive the endergonic formation of APS. APS is then reduced to sulfite (HSO_3^{2-}) by APS reductase (AprAB), in a two electron step. Sulfite, or bisulfite, is then reduced to sulfide, in a six electron transfer, by the bisulfite reductase (DsrAB). Two different pathways were originally proposed. The first one consisted of a sequential reduction in three steps of two-electron transfer that would lead to the formation of trithionate and thiosulfate as intermediates in the trithionate pathway. The enzymes participating in this pathway are the trithionate reductase and thiosulfate reductase (Akagi *et al*., 1994). However, formation of trithionate and thiosulfate is regarded as secondary reactions as by-products of the bisulfite-reductase reaction (Rabus *et al*., 2006). The second pathway is a direct six-electron reduction performed by bisulfite reductase. In *Desulfovibrio*, desulfoviridin is the high-spin bisulfite reductase enzyme responsible for sulfite reduction to sulfide. Interestingly, besides desulfoviridin, a second type low-spin sulfite reductase, which is assimilatory-type sulfite reductases is present in *Desulfovibrio* spp. These sequential reactions suggest the consumption of eight moles of electrons with eight and a half moles of protons in the reduction of sulfate (Keller and Wall, 2011). The energy gain of the overall reaction is much lower in the case of sulfate respiration in comparison for example to oxygen respiration.

Table 1.1. Redox potentials ($E^{o'}$) of intermediates involved in dissimilatory sulfate reduction. $E^{o'}$ at pH7.0 are given for H_2, CO_2 and CO at 10^5Pa. Adapted from Barton and Fauque., 2009.

Redox couple	**$E^{o'}$ (mV)**
CO_2 + acetate/pyruvate	-660
CO_2/CO	-520
SO_4^{2-}/HSO_3^-	-516
Acetyl-CoA + CO_2/pyruvate	-498
CO_2/formate	-432
CO_2 + acetate/lactate	-430
H^+/H_2	-414
H^+/H_2	(-270 to -300)[a]
Acetyl-CoA/acetaldehyde	-396
Acetate/etanol	-390
SO_4^{2-}/HS^-	-217
Acetaldehyde/etanol	-197
Pyruvate/lactate	-190
SO_3H^-/HS^-	-116
APS/AMP+HSO^{3-}	-60
Fumarate/succinate	+33

[a] H2 partial pressures between 1 and 10Pa observed in sediments

Despite the overall mechanism of sulfate reduction being well understood, the molecular understanding of those involved in energy conservation as well as the enzymes involved in the sulfate respiration are not completely elucidated (Matias *et al.*, 2005). For instance, the terminal reductases, which are located in the cytoplasm, do not participate in charge translocation across the membrane and generation of transmembrane electrochemical potential. The exact electron-transfer pathways linking the dehydrogenases to the terminal reductase by which this chemiosmotic electron potential is generated from different substrates, leading to oxidative phosphorylation, is thus not completely understood. Also the identity of the electron donors responsible for the transfer for the terminal reductases AprAB and DsrAB were only recently proposed to be the QmoABC complex (Pires *et al.*, 2003; Venceslau *et al*., 2010) and the DsrMKJOP (Pires *et al*., 2006).

1.2.2 Other electron acceptors

Besides sulfate, other sulfur compounds can be used as final electron acceptors. In contrast to sulfate, thiosulfate does not need to be activated. Elemental sulfur can also be used by some *Desulfovibrio* in dissimilatory sulfur reduction (Barton and Fauque, 2009). Other compounds used for respiratory growth include nitrate and nitrite. Dissimilatory reduction of nitrate and (or) nitrite to ammonia (also referred to as ammonification), as sole energy conserving process, was demonstrated with cells of *Desulfovibrio* and membranes of *D. gigas* (Barton *et al*., 1983).

Organic compounds such as fumarate, found in their environment resulting from degradation of proteins and amino acids, can also be used by some *Desulfovibrio* spp. during respiratory processes (Zaunmuller *et al*., 2006). In this respiratory growth, reduction of fumarate to succinate is performed by the fumarate reductase (Frd) (Lemos *et al*., 2002), composed of three subunits. FdrC is a membrane bound subunit that has a cytochrome b. The electrons coming from either a hydrogenase or formate dehydrogenase are transferred to the final reductase via

menaquinone. Thus, the electron transport chain for fumarate reduction, in contrast to what is observed in sulfate reduction, occurs entirely in membrane.

1.2.3 Electron donors

The bioenergetics of sulfate respiration is very influenced by the electron donors, as each of these substrates may use different electron pathways and mechanisms of energy conservation. The finding of different electron donors helped to understand the structure and function of the enzymes participating in the process and contributed to the discovery of new anaerobic pathways (Rabus *et al*., 2006).

Several electron donors can be used in sulfate respiration. Depending on the electron donors, different enzymes catalyzing the redox reactions, and electron-carrier proteins, participating in electron transport chains, were described. A single mechanism of electron transport cannot be considered. *Desulfovibrio* spp. usually uses H_2 or organic compounds that are preferable energy substrates for sulfate respiration (Table 1.2). The catabolism of an organic electron donor connected to the reduction of an external electron acceptor provides advantages to purely fermentative reactions. With the presence of external electron acceptors more energy is obtained than from oxidation at the level of substrate. The reduction of the external electron acceptor associated to an electron transport chain, enables the generation of transmembrane proton gradient and a correspondent chemiosmotic ATP synthesis (Rabus *et al*., 2006). The most important and relevant electron donors to the work performed in this thesis will be described in more detail.

Table 1.2. Estimated standard Gibs free energy for the various reactions in *Desulfovibrio* spp. Adapted from (Magee *et al*., 1978); Voordouw 2002; and Barton and Fauque 2009

Energy yielding reaction	$\Delta G^{0'}$ **(kJ/mol)**
Sulfate respiration	
$4H_2 + SO_4^{2-} + H^+ \rightarrow HS^- + 4H_2O$	-151.8
Lactate + 0.5 SO_4^- –> acetate + HCO_3^- + 0.5 H_2S	-84.5
Pyruvate + 0.25 SO_4^- –> acetate+ HCO_3^- + 0.25 H_2S	-89.1
Formate + 0.25 SO_4^- –> HCO_3^- + 0.25 H_2S	-45.6
SO_4^{2-} + ATP + $2H^+$ –> APS + PPi	-46
Fumarate respiration	
H_2 + $Fumarate^{2-}$ –> $succinate^{2-}$	-85.8
Lactate + 2 fumarate –> acetate + HCO_3^- + 2 succinate	-179.1
Pyruvate + fumarate –> acetate + HCO_3^- + succinate	-136.4
Fermentation processes	
$Lactate^-$ + H_2O –> $acetate^-$ + CO_2 + $2H_2$	-8.8
Lactate –> pyruvate + H_2	+43.2
Pyruvate + $2H_2O$ –> acetate + HCO_3^- + H_2 + H^+	-47.1
Pyruvate –> acetate + CO	-32.0
$Pyruvate^-$ + CoA –> acetyl-CoA + $formate^-$	-16.3
H_2O + formate –> HCO_3^- + H_2	+1.4

1.2.3.1 Hydrogen

Molecular hydrogen (H_2) is a central molecule in the energetic metabolism of *Desulfovibrio* spp. In the presence of sulfate, these organisms are able to use this compound as sole energy source and as an intermediate being transiently produced and consumed during degradation of organic compounds (Brandis and Thauer, 1981). It can also be a product of the energetic metabolism in syntrophy or fermentation. This flexibility depends on the growth conditions. Regardless of its specific function, the main enzymes metabolizing H_2 are the hydrogenases, one of the most extensively studied enzymatic groups of SRB (see Section 1.5). In the absence of sulfate or other external electron acceptors, H_2 can be produced as a metabolic product during organic fermentative metabolism or participate as an interspecies electron transfer carrier during syntrophic growth (Walker *et al*., 2009; Plugge *et al*., 2010; Meyer *et al*., 2013). During sulfate respiration, H_2 produced by other fermenting or syntrophic organisms can serve as a main external electron donor. At standard pressure, H_2 is a favorable electron donor ($2\ H^+/H_2$, $E_0' = -0.414$ V) for chemolithoheterotrophic growth, where cell materials are synthesized from acetate and CO_2 (Table 1.1). H_2 is oxidized in the periplasm by the periplasmic hydrogenases, generating protons and electrons in the periplasmic side of the membrane. The electrons are transferred by electron carriers to the cytoplasm, for the exergonic process of sulfate reduction, while the protons remain in the periplasm, creating a proton gradient. This proton gradient is then used by the ATP synthase F_0F_1 to generate energy through oxidative phosphorylation. The primary physiological electron carrier for the periplasmic hydrogenases is the tetrahaem type-I cytochrome *c_3* (TpI-c_3), although the Hmc complex has already been shown to accept electrons directly from hydrogenase (Chen *et al*., 1994). TpI-*c_3* accepts the electrons directly from the hydrogenase and transfers them to other multihaem cytochrome associated membrane-bound complexes that will, in turn, transfer the electrons to sulfate reduction directly or indirectly. The identity and participation of such complexes is not yet clearly established. The high-molecular cytochrome c was shown to accept the

electrons from TpI-c3 (Voordouw, 1995; Pereira *et al.,* 1998). The electrons are transferred from the periplasm to the cytoplasm directly or via the quinone pool. The quinone reductase complex (QrcABCD) was recently demonstrated to be able to accept electrons from the TpI-c3 and transfer them to menaquinone (Venceslau *et al*., 2010).

From the oxidation of H_2 approximately 1 3/4 to 2 1/3 mol of ATP may be generated by chemiosmotic energy conservation, if the 3-4 H^+/ATP ratio in assumed (Stock *et al*., 1999). However, as described above, the reduction of sulfate to APS demands 2 ATP equivalents due to the hydrolysis of PPi. The net result of up to 1/3 mol of ATP is not sufficient for the corresponding cell growth that is observed for *Desulfovibrio* spp.(Rabus *et al*., 2006). This indicates that besides proton gradient, other mechanisms of energy conservation, such as proton pumping (vectorial proton transport) across the membrane should be in place to provide extra energy for cell growth. The Qrc complex together with the Qmo one may constitute such protein-pumping redox mechanism involving the menaquinone in a Q-loop process.

1.2.3.2 Lactate and pyruvate

Lactate found in anoxic environments as a result of fermentative bacterial metabolism, is one of the most common substrates used by many SRB. It is oxidized by the L- and D-lactate dehydrogenase to pyruvate. In *Desulfovibrio* spp. these enzymes are $NAD(P)^+$-independent dehydrogenases associated to the membrane. After lactate oxidation, pyruvate is oxidized to acetyl-CoA by the pyruvate:ferredoxin oxidoreductase enzyme (Pfor) with ferredoxin or flavodoxin as the electron acceptors. The acetyl-CoA produced by pyruvate oxidation is then converted to acetate by the phosphotransacetylase (Pta) and the acetate kinase (Ak) generating ATP by substrate-level phosphorylation. Reductant in the form of seven protons and eight electrons are generated through the conversion from lactate to pyruvate ($4e^- + 4H^+$), pyruvate to acetyl-CoA ($4e^- + 2H^+$) and acetyl-CoA to acetylphosphate (H^+).

The ATP gain by substrate-level oxidation alone during this process, with sulfate as electron acceptor, is zero, since the two moles of ATP generated by the oxidation of two molecules of lactate oxidized are needed for the activation of one molecule of sulfate, specifically one for the ATP sulfurylase reaction and one for regeneration of ADP from AMP (adenylate kinase reaction) formed during APS reduction (Barton and Fauque, 2009). Hence, additional mechanisms for ATP formation must be involved.

Odom and Peck suggested the hydrogen cycling mechanism for the generation of a proton gradient under lactate/sulfate metabolism (Odom and Peck, 1981). In this model H_2 is a key intermediate for energy conservation (Fig 1.5).

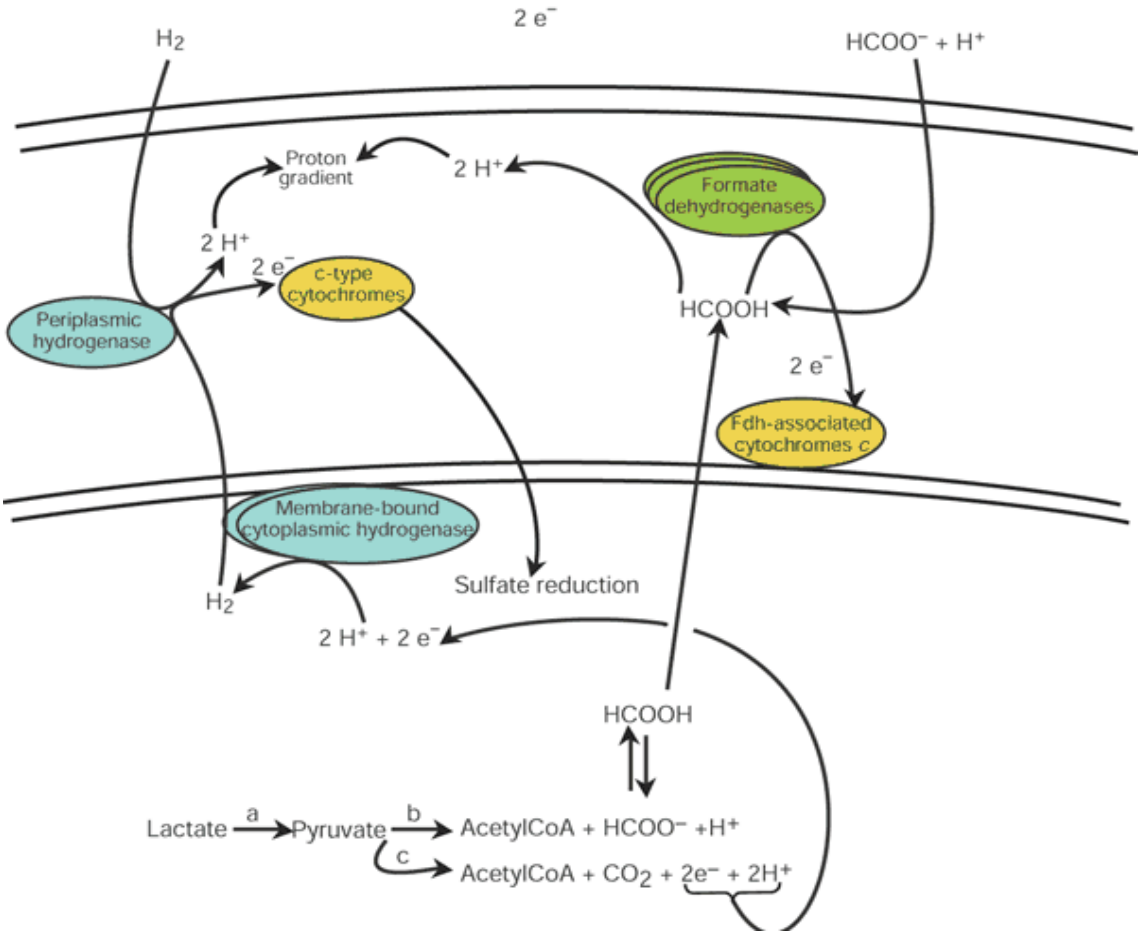

Fig 1.5. Participation of the hydrogenases in the energy conservation of *Desulfovibrio* spp. proposed by hydrogen cycling model (Heidelberg 2004).

The protons and electrons coming from lactate and pyruvate oxidation (first two oxidation steps) would be converted to H_2 by a cytoplasmic hydrogenase. This H_2 would then diffuse to the periplasm of the cell where another hydrogenase would re-oxidize it similarly to what was described when H_2 is the electron donor. The electrons would be shuttled back across the membrane for sulfate reduction whereas the protons would generate a proton potential and ultimately ATP. This model was proposed based on experiments with spheroplasts of *D. gigas* where they demonstrated that without the periplasmic proteins responsible for H_2 oxidation (hydrogenase and TpI-c_3) lactate oxidation couple with sulfate reduction was not possible. Further evidence by Peck and collaborators was provided using *D. vulgaris*, during growth in pyruvate by membrane-inlet mass spectrometry (Peck *et al.,* 1987). This theory also helps to explain the fact that during growth with lactate and pyruvate, a transient accumulation of H_2 is observed (termed hydrogen burst), which is later consumed. As discussed by Rabus and colleagues hydrogen formation during growth in lactate might reflect the high investment of ATP to transport and activate sulfate to APS. Thus, sulfate independent lactate degradation might be a way to produce the ATP that is needed to initiate sulfate metabolism (Rabus *et al.*, 2006). However, since its proposal the hydrogen cycling hypothesis was subjected to a controversial debate and till date it was neither proven nor disregarded. As a major criticism for this hypothesis is the fact that hydrogen formation from lactate oxidation to pyruvate is energetically unfavorable and it would demand an energy input. The $E^{0'}$ of the pyruvate/lactate couple is -190 mV for lactate oxidation whereas, the acetyl-CoA + CO_2/pyruvate couple is -498 mV. Even at much higher lactate concentration, the redox potential remains too high for lactate oxidation to occur (Pankhania *et al.*, 1988). Thus, the formation of H_2 from the reducing equivalents generated by the lactate dehydrogenases is thermodynamically unfavorable. The standard reduction potential of the pyruvate/lactate couple is above that of the H^+/H_2 couple ($E^{0'}$ of -414

mV), even if H_2 at more environmental concentrations is considered ($E^{0'}$ of -270 mV at 1Pa:H_2). It would thus required energy-driven reverse electron flow to accomplish H_2 generation from the conversion of lactate to pyruvate (Keller and Wall, 2011). The second criticism is the lack of inhibition of lactate oxidation by the addition of H_2 during lactate/sulfate respiratory growth (Pankhania *et al.*, 1986). Thirdly, in the context of the *Desulfovibrionales*, some closely related species such as *Desulfomicrobium baculatum* do not present any cytoplasmic hydrogenases or in the cases of *Desulfococcus oloevorans* and *D. sapovorans* no hydrogenases at all (Keller and Wall, 2011; Pereira *et al.,* 2011).

Alternatively, it was proposed that the production and consumption of H_2 was used as mechanism to control redox state of electron carriers (Lupton *et al.,* 1984). These authors showed that during growth with thiosulfate as terminal electron acceptor, which does not require prior activation; H_2 was still produced and consumed. Transient H_2 accumulation could be due to a result of an imbalance between reductant produced or consumed by the cells during organic acid oxidation. However, the production of some H_2 during growth on lactate and sulfate was neither a proof for H_2 cycling nor a proof for a specific mechanism that controls the redox state of electron carriers involved in lactate oxidation. As *Desulfovibrio* participates in interspecies H_2 transfer in the absence of sulfate, the release of H_2 could derive from the inability to redirect electrons completely when sulfate is available, thus driving the release of electrons as H_2 (Rabus *et al.*, 2006).

It was more recently suggested that hydrogen cycling could be one of many possible pathways that might be used by *Desulfovibrio* spp. during lactate/sulfate respiration. Other pathways may include intracellular cycling of other reduced intermediates, such as CO or formate, which might also be involved in the energy conservation mechanisms (Voordouw, 2002). Noguera *et al.* (1998) proposed a model where dual pathways would be in operation simultaneously. In this model a combination of kinetic and thermodynamic conditions determines the flow of electrons between each pathway (Noguera *et al*., 1998). In one of the pathways hydrogen, which is an obligatory intermediate, is been produced and consumed, as in hydrogen

cycling model. In the other pathway, direct transport of electrons from the donor to the acceptor occurs without the participation of H_2. The presence of two different pathways may provide a mechanism by which *Desulfovibrio* spp respond more efficiently to changes in environmental conditions. Corroborating these ideas Keller and Wall suggested different pathways for the electrons obtained from lactate and pyruvate oxidation (Keller and Wall, 2011) (Fig 1.6).

Based on experimental results performed with Tpl-c_3 and Coo hydrogenases mutants, there are indications that: i) some proportion of the electrons generated from substrate oxidation should not cycle as molecular H_2; and ii) there is an exclusive pathway for production of H_2 originated from pyruvate oxidation that is not available for lactate. Indeed, thermodynamically, pyruvate oxidation with ferredoxin reduction has sufficient redox potential to generate H_2. As such, in each pathway the electrons coming from either lactate or pyruvate can be transported to the Qmo and/or DsrMKJOP via the menaquinone pool or to membrane-bound hydrogenases, such as the Coo, and generate H_2 that will cycle.

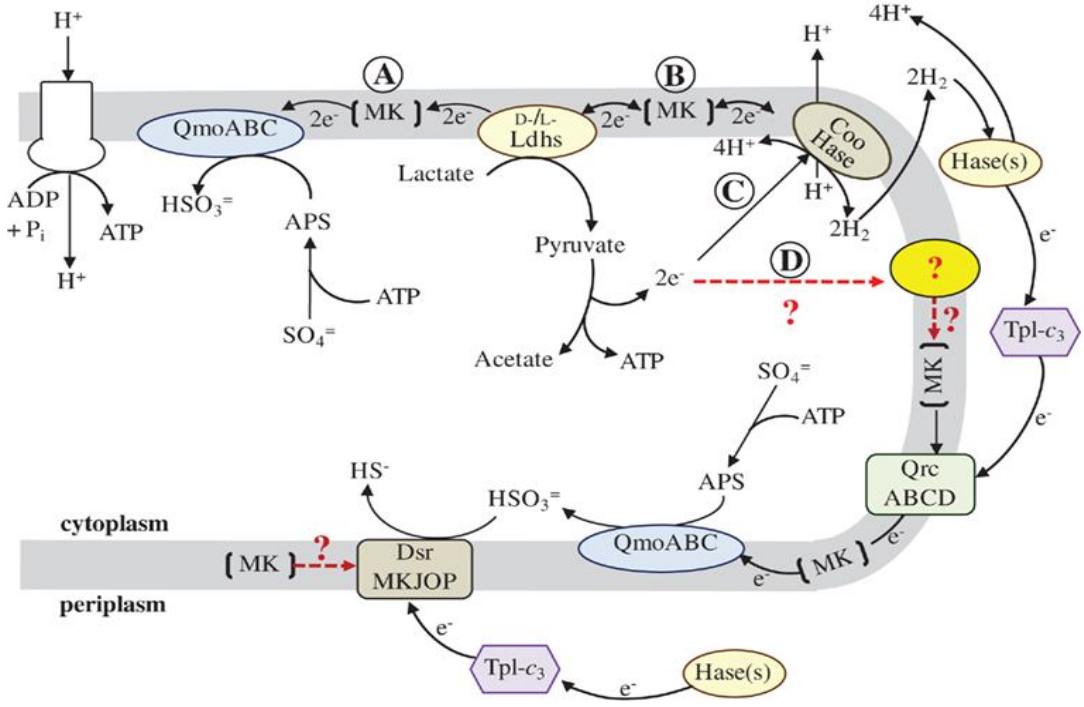

Fig 1.6. The proposed dual pathways for electron flow derived from the oxidation of organic substrates during respiratory growth of *Desulfovibrio* spp. (Keller and Wall, 2011). In pathways A) and D), electron flow occurs via the menaquinone in the membrane, while in pathways B) and C), electrons flow across the membrane through the action of the hydrogenases, in the form of H_2.

However, it is important to notice that the electron acceptor for electrons generated in lactate oxidation to pyruvate is not known. As mentioned, lactate dehydrogenase is a membrane-bound flavoprotein that is capable of transferring electrons directly to the menaquinone in the membrane (Thauer *et al*., 2007). Another possible mechanism of energy conservation from lactate oxidation, which supports hydrogen production, was proposed by Keller and Wall (Keller and Wall, 2011). This mechanism relies in flavin-based electron bifurcation (Herrmann *et al.*, 2008) performed by the Coo membrane-bound hydrogenase complex. When concentrations of H_2 are at low levels, the exergonic reduction of protons to form H_2 from the reduced ferredoxin generated by the pyruvate:ferredoxin oxidoreductase, could be coupled to endergonic formation of H_2 with electrons transferred by the menaquinone. However, the Coo hydrogenase is not a flavoprotein and there is no evidence to indicate that these enzymes might be involved in bifurcation.

1.2.3.3 Formate

Formate is also a fermentation product from anaerobic degradation performed by enterobacteria, for instance that is a common substrate for *Desulfovibrio* spp. Furthermore, in natural bacterial communities it can participate in interspecies transfer reactions as an alternative to H_2. Similarly to H_2, formate is a favorable electron donor, presenting a redox potential around -410 mV. Differently from lactate, which does not need to be internalized for its oxidation, in *Desulfovibrio* spp. formate can be oxidized to CO_2, both in the cytoplasm as well as in the periplasm, due to the presence periplasmic dehydrogenases. The electron acceptor for the periplasmic

formate dehydrogenases was proposed to be the tetrahaem cytochrome c_3 (Riederer-Henderson and Peck Jr, 1986). It then transfers these electrons to the cytoplasm for sulfate reduction through the participation of multi-heme-containing membrane-bound complexes such as Qrc. This creates a proton gradient across the membrane, generating energy through oxidative phosphorylation via ATP synthase, as in the case of H_2. Besides the external sources, formate can be generated in the cytoplasm from lactate oxidation by the pyruvate:formate lyase enzyme. This formate can then diffuse to the periplasm where it is re-oxidized by periplasmic formate dehydrogenases, in a cycling mechanism that resembles the proposed H_2 cycling (Voordouw, 2002). Furthermore, transcriptional analysis carried out using *D. vulgaris* Hildenborough suggested that formate cycling can also occur during hydrogen/sulfate growth from CO_2 and acetate contributing to energy gain by the creation of a proton motive force (Pereira *et al*., 2008; da Silva *et al*., 2013). In summary, the presence of multiple formate dehydrogenases implies that the oxidation of this compound from external sources or from the cytoplasm may be catalyzed by different specialized enzymes (Heidelberg *et al*., 2004).

1.2.3.4 Ethanol and acetaldehyde

Ethanol, a common electron donor and carbon source, is oxidized in *Desulfovibrio* spp. via acetaldehyde to acetate in the presence of sulfate. In the first step, ethanol is oxidized to acetaldehyde by an alcohol dehydrogenase (Adh). In *D. gigas* this enzyme is NAD^+-dependent and the electron acceptor is reduced to NADH. Aldehyde is further oxidized by either a molybdenum or tungsten containing aldehyde oxidoreductase (Kremer *et al*., 1988a). Further conversion of aldehyde to acetate, proceeds via acetyl-CoA and acetyl phosphate, similarly to what is observed in pyruvate oxidation. As shown before, in this pathway energy is obtained by substrate-level oxidation. This indicates that, similar to what was described for lactate, the ATP generated by substrate-level oxidation would be consumed for the activation of sulfate, and other mechanisms of energy conservation must be present to allow cell

growth. However in this case, instead of the cytochrome pool, NADH/NAD(P)H is involved in the reducing power transfer reactions. A mechanism for the transfer of reducing equivalents generated in ethanol oxidation during sulfate reduction was proposed in *D. vulgaris* Hildenborough, by Haveman and collaborators involving the heterodissulfide reductase (HdrABC) complex (Haveman *et al.*, 2003). These authors suggested that the protons and electron generated by ethanol oxidation are converted into hydrogen or hydrogen equivalents by the H_2-heterodisulfide oxidoreductase complex (Hdr). However, this complex does not include a hydrogenase but a NADH dehydrogenase. The presence of the flavin oxidoreductase genes (*floxABCD*) in the same cluster as the *hdrABC* in *Desulfovibrio spp*. provide the component for NAD(P)H oxidation and electron transfer to the HdrABC protein. As such, the HdrA proteins could be involved in electron bifurcation mechanisms (Thauer *et al*., 2008).

Interestingly, as observed by Haveman and collaborators, Adh is functional during lactate, pyruvate, formate and hydrogen sulfate reduction. This suggests that this enzyme reoxidizes ethanol that may be formed during the metabolism of these compounds implying that energy conservation through the HdrABC complex could contribute to the energy budget in different electron donor metabolisms. In agreement, transcriptional analysis showed an upregulation of both Adh and Hdr enzymes during hydrogen growth compared to lactate in sulfate respiration (Pereira *et al.,* 2008). As such a HdrA-associated pathway could provide a soluble route for sulfite reduction through electron bifurcation instead of through the creation of chemiosmotic energy (Pereira *et al.*, 2011).

1.2.3.5 Dicarboxylic acids

C^4-dicarboxylic acids, such as malate, fumarate and succinate, known to participate in the standard TCA cycle, are relatively common substrates for SRB. In *Desulfovibrio* strains, these compounds are internalized mainly by membrane-bound

TRAP transporters (tripartite ATP-independent periplasmic carriers) as anaerobic fumarate/succinate antiporters are not found (Zaunmuller *et al.*, 2006).

Oxidation of these dicarboxylic acids occurs via a reaction sequence with the presence of a $NADP^+$-dependent malate dehydrogenase (malic enzyme). The malic enzyme is responsible for the oxidation of malate to pyruvate, with the formation of NADPH. It is also proposed to participate in the transfer of reducing equivalents to sulfate reduction in an energy conservation mechanism, since the ATP generated by substrate-level phosphorylation of pyruvate to acetate would be consumed in sulfate activation. Experimental analysis demonstrated that in the presence of sulfite, which does not need prior activation like sulfate, higher cell mass was obtained using malate when compared to pyruvate. Since both compounds are oxidized via the same pathway, this clearly shows the presence of another pathway of energy conservation (Kremer *et al.*, 1988b). Such pathway was proposed by Chen and colleagues stating that by action of a $NAD(P)^+$ transhydrogenase, reducing power would be transferred from NAD(P)H to NADH (Chen *et. al*; 1995). Reduction of APS-reductase could then be achieved by NADH via an unknown pathway, constituting a soluble alternative to electron flow to sulfate reduction.

Fumarate is oxidized to malate by a fumarase localized in the cytoplasm. In the case of succinate, oxidation occurs by a membrane-bound succinate dehydrogenase (Sdh) enzyme that has a site for menaquinone reduction. However, succinate oxidation by menaquinone is an endergonic process that requires a transmembrane potential for functioning. As such, in some *Desulfovibrio* spp., succinate reduction does not allow cell growth and appears to be relevant for specific metabolic reactions. (Zaunmuller *et al.*, 2006).

1.2.4 Fermentative and synthropic growth

When sulfate and other inorganic electron acceptors are unavailable, SRB can grow by fermentation of several organic substrates or in syntrophic association with other organisms, mainly methanogens. This ability of fermentative growth

explains the widespread presence of high numbers of SRB in environments with low or no sulfate. In fact, experiments performed with biofilm reactors containing *Desulfovibrio* spp. in the absence of sulfate for an extended period of time showed that addition of sulfate resulted in its rapid reduction (Raskin *et al*., 1996).

From the diverse organic compounds that can be used by *Desulfovibrio*, pyruvate that can be generated from the metabolism of other substrates is easily fermented. Energy is obtained at the level of substrate oxidation, being acetate, carbon dioxide and H_2 the main products generated (Postgate, 1984). Even species that do not present hydrogenases, e. g. *D. sapovorans* are able to grow by pyruvate fermentation (Rabus *et al*., 2006).

Desulfovibrio spp. are also able to ferment C^4-dicarboxylic acids such as fumarate or malate with succinate, acetate and CO_2 are the main products (Fig 1.7).

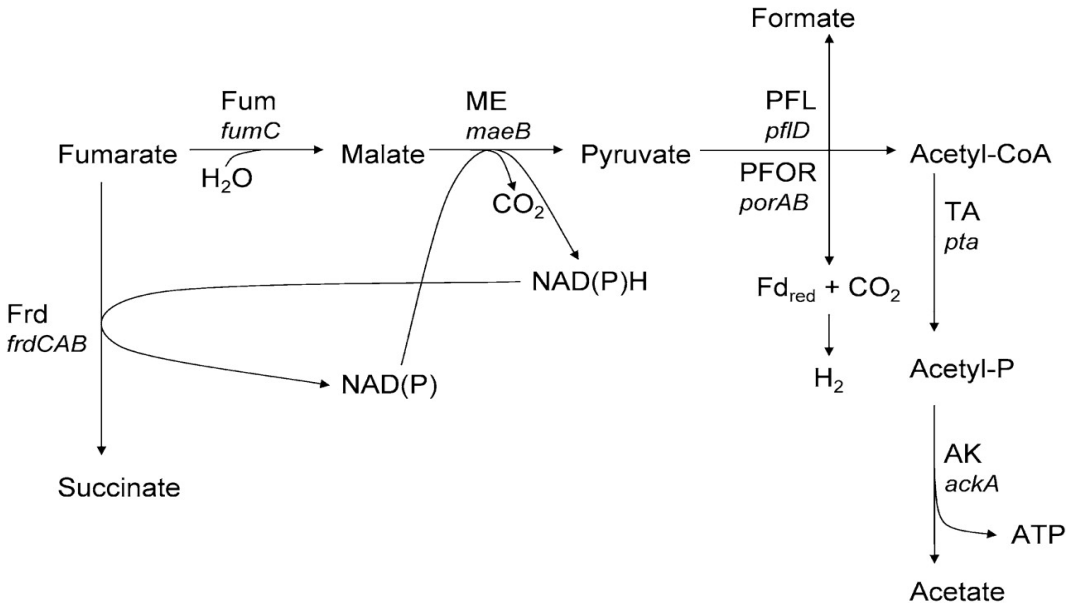

Fig 1.7. Scheme of the metabolic pathway involved in fumarate fermentative growth in *Desulfovibrio* spp (Zaunmuller et. al 2006). The enzymes participating in the pathway are: Frd, fumarate reductase; Fum, fumarase; ME, malic enzyme; PFOR, pyruvate-ferredoxin oxidoreductase; PFL, pyruvatel formate lyase; TA, phosphotransacetylase; and AK, acetate kinase.

In the case of fumarate, a special type of fermentative growth referred as disproportionation (previously called dismutation) occurs (Zaunmuller *et al.,* 2006). In disproportionation growth, fumarate is used both as electron donor/carbon source and as electron acceptor with different stoichiometries. One pool of the substrate is oxidized via malate dehydrogenase to acetate and the second pool is used as the electron acceptor, being reduced to succinate. In *D. vulgaris* Hildenborough and *D. desulfuricans* (Essex 6) the succinate:acetate ratio is approximately 2:1.

Two other very important substrates lactate and ethanol can also be fermented generating acetate, CO_2 and H_2 as products. Lactate fermentation with H_2 formation has been reported, although cell growth was not observed, unless a syntrophic organism is present. In fact lactate oxidation to pyruvate ($E^{0'}$ = -190 mV) is energy-dependent and requires reverse electron transport (Pankania *et al.*, 1988). Experimental data have indicated that in this case, reducing equivalents from lactate dehydrogenation were converted to H_2 in an energy-driven process, with the energy derived from the subsequent exergonic conversion of pyruvate via acetyl-CoA. However, in both cases, fermentative metabolism originating growth can only be developed if the H_2 generated by these SRB processes is efficiently removed and maintained at low levels by the presence of hydrogen-consuming methanogens in syntrophic associations (Barton and Fauque, 2009). These syntrophic communities play an important role in the degradation of organic acids under sulfate limiting conditions.

In several SRB other unusual compounds can be fermented as for instance in *D. fructosovorans*, which ferments fructose producing succinate and acetate as main products and small amounts of ethanol. Other SRB such as *Desulfobulbus propionicus* are also able to perform propionic fermentation (Rabus *et al.,* 2006). Furthermore, the energetic metabolism of *Desulfovibrio sulfodismutans* involves inorganic fermentation of sulfur compounds. It is able to conserve energy for anaerobic growth by disproportionation of sulfite or thiosulfate to sulfate and sulfide which is thermodynamically unfavorable, using acetate as carbon source (Barton and Fauque, 2009).

1.2.5 Electron carriers

A great variety of electron carriers appears to be involved in the flow of reducing equivalents ([H], electrons) from the electron donors to the electron acceptors during respiratory energetic metabolism. Among the SRB group, *Desulfovibrio* organisms are characterized by the presence of a particularly high number of multiheme *c*-type cytochromes and low redox potential iron-sulfur proteins (Matias *et al*., 2005; Pereira *et al*., 2011). This may reflect the fact that, the final reductases for sulfate reduction are not associated to the cytoplasmic membrane.

1.2.5.1 Soluble electron transfer proteins

Despite several types of cytochromes being identified in the SRB, the cytochrome *c* is the main cytochrome type observed, which is either soluble or associated to membrane redox complexes. Remarkably, many components of the energy metabolism, like periplasmic hydrogenases and formate dehydrogenases, do not have a membrane-bound cytochrome containing subunit, indicating the importance of cytochrome *c* pool in the periplasmic electron transfer pathways (Pereira *et al.*, 2011).

Among the cytochrome *c* type, the tetraheme cytochrome c_3 is predominant and can be found in all members of *Desulfovibrio* spp, associated with periplasmic hydrogenases and formate dehydrogenases or in its monocystronic form. These cytochromes play a central role in the bioenergetics of sulfate reduction as they transfer the electrons from the periplasmic hydrogenases to the respiratory transmembrane electron transport complexes (Matias *et al*., 2005). There are two types (I and II) of the tetraheme cytochrome c_3. The type I (TpI-c_3) has a molecular mass of 13 kDa, containing four low redox potential hemes (-120 to -400 mV) and is able to capture protons and electrons simultaneously (Barton and Fauque, 2009). It has been suggested to be the electron acceptor for all the periplasmic hydrogenases and to serve as a capacitor for electrons in the periplasm. TpI-c_3 of different organisms have a low sequence homology but their three-dimensional structure and

haem arrangement is well conserved (Matias *et al*., 2005). A dimeric cytochrome c_3 (Dic_3), containing two tetrahaem subunits similar to TpI-c_3 was also identified in some *Desulfovibrio* organisms (Frazao *et al*., 1999). Its physiological function is believed to be similar to TpI-c_3 as it was shown to be reduced by the [NiFe] hydrogenase of *D. gigas* and the [NiFeSe] hydrogenase of *D. africanus*. The type II tetraheme cytochrome c_3 (TpII-c_3) is a genetic and structurally different group from the one of TpI-c_3 presenting different reactivity (Valente *et al.*, 2001). Its genetic organization in the genome of *D. vulgaris* and *D. alaskensis* G20 indicates that it is part of a transmembrane protein complex with redox centers in the periplasm, membrane and cytoplasm named the Tmc complex. These TpII-c_3 cytochromes appear to be reduced by TpI-c_3 and transfer electrons to other proteins of their respective transmembrane complexes that will deliver the electrons to APS reductase or dissimilatory sulfite reductase, thus participating in respiratory electron transfer reactions (Matias *et al*., 2005).

Besides the tetraheme cytochrome *c* present in some *Desulfovibrio* spp, the periplasmic monoheme cytochrome c_{553}, with a molecular mass of 9 KDa, can be found (Barton and Fauque, 2009). This electron carrier was originally isolated as a natural electron acceptor of formate dehydrogenase in *D. vulgaris* (Sebban *et al.*, 1995). It is also able to accept electrons from [FeFe] hydrogenase, although less efficiently than TpI-c_3 (Matias *et al*., 2005). Furthermore, its genomic location in the same locus as cytochrome c oxidase, suggests that it could possibly act as its electron donor (Pereira *et al*., 2011).

Another important and widespread group of electron carriers are the ferredoxins (Fd). These soluble iron-sulfur proteins with a molecular mass of ~6 KDa present a low redox potential, and more than one can be found in the cells, with different biological reactivities. In *D. gigas*, ferredoxin I is a trimer which contains one [4Fe-4S] cluster with a redox potential of -440mV participating during the phosphoroclastic reaction of hydrogen formation from the oxidation of pyruvate (Bruschi *et al*., 1976; Peck and LeGall, 1994) Ferredoxin II is a tetramer containing one [3Fe-4S] cluster with a redox potential of -130mV and it acts during hydrogen

oxidation as electron donor in bisulfate reduction to sulfide (Rodrigues *et al*., 2001; Hsieh *et al*., 2005; Barton and Fauque, 2009). Whereas all SRB so far analyzed contain ferredoxin I in single or multiple copies, ferredoxin II was only detected in some of these organisms (Pereira *et al*., 2011). The participation of ferredoxins in anaerobic metabolism became in recent years, more important with the discovery of flavin-based electron bifurcation mechanism of energy conservation that only involves soluble proteins (Herrmann *et al*., 2008; Li *et al*., 2008). As suggested by Pereira and collaborators energy conservation could result from reduced ferredoxin produced during electron bifurcating reactions with the participation of membrane-associated ion-translocating complexes, such as the Ech hydrogenase or the Rnf complex (Pereira *et al.,* 2011).

Another important component that has brought about attention is its participation in electron bifurcating reactions by the heterodisulfide reductases (Hdr) like proteins. Hdr-related proteins are found associated to a variety of enzymes that participate in the energetic metabolism or in membrane complexes, such as the Qmo, Dsr, Tmc and Hmc. According to the classification proposed these proteins are divided into two main families: those containing an HdrA-like domain and the ones containing an HdrD-like domain (Strittmatter *et al.*, 2009)

In *Desulfovibrio* spp. one of the HdrA-like proteins are found in all members with available genomic information and is present in a genomic arrangement, with *hdr*ABC genes, and four genes encoding the subunits of the flavin oxidoreductase, floxABCD. The *hdr* genes code for a HdrA, which is an iron–sulfur flavoprotein; a HdrB, that contains two CCG domains and harbors a special [4Fe4S] catalytic site and HdrC which is a small iron-sulfur protein. Originally the *floxABCD* were thought to code for a hydrogenase-HDR complex. However it was later observed that these genes do not code for a catalytic hydrogenase subunit. The *floxABCD* operon codes for a FloxA, which contains FAD and NAD(P)-binding domains; FloxB and FloxC which are iron-sulfur proteins; and FloxD which is involved in electron transfer. The HdrABC proteins are thought to catalyzed the exergonic reduction of heterodisulfide coupled to the endergonic reduction of ferredoxin, while the FloxABCD proteins

provide the electrons obtained through the oxidation of NAD(P)H. This mechanism, in *D. vulgaris* was proposed to be involved in the alcohol degradation pathway, with Adh reducing NAD^+ to NADH which will be oxidized by Flox (Haveman *et al*., 2003). However, in other gene loci encoding a formate dehydrogenase and pyruvate:ferredoxin oxidoreductase (Por), genes encoding proteins similar to the HdrA proteins are found, suggesting that these substrates could also provide electrons for HdrA reduction (Pereira *et al*., 2011).

HdrD-like proteins are found as subunits associated to other electron donors like lactate dehydrogenase (Ldh) and molybdopterin oxidoreductase (Mop). HdrD is a protein that has both HdrB and HdrC-like domains, with a similar catalytic cofactor as the HdrB. As such, the presence of HdrD-like subunits in these enzymes suggests that other pathways involving those electron donors are possibly involved in the reduction of heterodisulfide or even in the menaquinone pool (Pereira *et al*., 2011).

Menaquinones are found in all members of SRB and in *Desulfovibrio* are apparently obligate components of various electron transport chains participating in fumarate reduction. The most frequent menaquinones are Mk-6 and Mk-7 and their involvement in electron transport during lactate and acetate oxidation has been proposed (Rabus *et al*., 2006; Barton and Fauque, 2009). Menaquinone was shown to be an important component in the mechanisms of energy conservation together with membrane complexes such as Qmo, Qrc and DsrMKJOP (Pires *et al*., 2006; Venceslau *et al*., 2010; Ramos *et al*., 2012).

Flavoproteins are also another group of electron carriers that can be used by SRB. In *Desulfovibrio* genus there are two types: flavodoxins and flavoredoxins. The flavodoxin are small molecular mass (15-22 KDa) monomeric electron carriers that contain a single riboflavin (FMN). Its function is related to the fact that it is able to substitute both ferredoxin I and II types, participating in hydrogen consuming and hydrogen producing reactions, since it presents two redox potential states (-440 mV and -150mV) (Barton and Fauque, 2009). Flavoredoxins are homodimers, where one FMN molecule is observed per monomer, presenting a molecular mass of 40kDa. Rather than participating in sulfite reduction electron transfer reactions, as the most

of electron carriers, flavoredoxins were shown to have a key function as the electron carrier in thiosulfate reduction (Broco *et al*., 2005).

1.2.5.2 Membrane associated electron carriers

Although the importance of soluble electron carriers have been amply investigated, the importance of the transmembrane electron carriers in various electron transfer pathways have only been more recently studied in detail. From these membrane-bound complexes existing in SRB, two of them are conserved and are proposed to play key functions in sulfate reduction: the Qmo and Dsr complexes (Pires *et al*., 2003; Pires *et al*., 2006; Ramos *et al*., 2012; Krumholz *et al*., 2013). Microarray transcriptional analysis performed with the mRNAs isolated from *D. vulgaris* Hildenborough revealed that Qmo and Dsr gene expression during sulfate respiratory growth, were among the top 20% of all genes (Keller and Wall, 2011). Their up-regulation was also observed using sulfate/lactate or sulfate/pyruvate as substrates compared to the sulfate with hydrogen. These experiments suggest that electron transport through the Qmo and Dsr complexes have a more important role during growth with these organic electron donors (Pereira *et al*., 2008).

The DsrMKJOP complex, previously referred as Hme in *Archeoglobus fulgidus*, is proposed to be involved in the electron transfer to the dissimilarity bisulfite reductase (DsrAB) (Mander *et al*., 2002; Pires *et al*., 2006). Given that it presents redox subunits both in the periplasm and in the cytoplasm, electrons could flow on either direction. It is suggested to have two modules, one being involved in electron transfer from a periplasmic component to the menaquinone, composed of triheme cytochrome DsrJ, the iron-sulfur protein DsrO and the NrfD family DsrP proteins and the second one composed of cytochrome b DsrM and the iron-sulfur protein DsrK. This protein has a special [4Fe-4S] cluster similar to HdrD catalytic subunit responsible for heterodisulfide reduction, and is suggested to reduce a cytoplasmic substrate through menaquinol oxidation (Pereira *et al*., 2011). The possible cytoplasmic substrate for oxidation by DsrMK module is DsrC, with the Dsr persulfide

($DsrC_{ox}$) being reduced by the catalytic Hdr-like iron-sulfur center of the DsrK subunit, possibly with proton translocation associated to this process.

The quinone-interacting membrane-bound oxidoreductase complex (QmoABC) was originally isolated from D. *desulfuricans* ATCC 27774 (Pires *et al.*, 2003). Its genes encode two soluble proteins, QmoA and QmoB, that present similarity with the HdrA and a protein, QmoC, containing a transmembrane cytochrome b and a soluble iron-sulfur domain. These three subunits bind two hemes b, two FAD groups and a number of iron-sulfur clusters (Pereira *et al*., 2011). A *qmoABC* mutant strain of *D. vulgaris* Hildenborough was unable to grow using sulfate as its sole electron acceptor with a range of electron donors, whereas growth with sulfite was unaffected (Zane *et al*., 2010). As such the function of this complex was proposed to be implicated in the transfer of electrons from the quinone pool to the APS reductase (AprAB) (Ramos *et al*., 2012). Such an energy conservation mechanism might involve the Qrc complex (Venceslau *et al*., 2010).

The quinone reductase complex (QrcABCD), also isolated from *D. vulgaris* Hildenborough, is composed of the hexaheme cytochrome (QrcA), a non-binding molybdopterin-family protein (QmoB), the periplasmic iron-sulfur protein (QrcC) and the NrfD family membrane protein. QmoABC does not contain a cytoplasmic component being put forward the idea that the Qrc complex would accept the electrons coming from periplasmic H_2 or formate oxidation via TpI-c_3 with the subsequent transfer to the Qmo complex, for sulfate reduction, via menaquinone (Venceslau *et al*., 2010). As such, these two complexes would contribute to energy conservation from H_2 or formate by the generation of a proton motive force via a redox loop process. In accordance, *D. alaskensis* G20 *qrcB* mutant strain was not able to grow with H_2 or formate as electron donor (Li *et al.*, 2009). Remarkably the *D. vulgaris* Δ*qrcBCD* mutant strain was shown to be able to grow on lactate plus sulfate indicating that when lactate is the electron donor this complex is not necessary or eventually other mechanism could compensate for the absence of Qrc (Keller and Wall, 2011).

Other cytochrome *c* containing transmembrane complexes include the 16 haem high-molecular-weight cytochrome *c* (HmcABCDEF) that presents similar subunit composition when compared to the Dsr complex. However, differently from the DsrJ subunit, the HmcA can accept electrons from periplasmic hydrogenases via TpI-c_3 (Pereira *et al*., 1998). As such, its primary function was attributed to be the acceptance of electrons from H_2 oxidation, via TpI-c_3 and their transfer to the cytoplasmic reduction of sulfate (Rossi *et al*., 1993; Matias *et al*., 2005). However, transcriptional profiling showed that growth in the presence of hydrogen plus sulfate, the genes encoding this complex were down-regulated compared to the growth with lactate (Caffrey *et al*., 2007; Pereira *et al*., 2008). During *D. vulgaris* syntrophic experiments it was suggested that in the presence of lactate, the Hmc complex functions in the opposite direction, transferring electrons from the cytoplasm to the periplasm for H_2 reduction (Walker *et al*., 2009). Notwithstanding, it appears that Hmc is not essential during lactate plus sulfate growth because low levels of Hmc transcripts and multiple transposon insertion in a mutant library analysis were observed under these conditions (Keller and Wall, 2011). This would indicate that Hmc role is only observed when H_2 levels are low. As such, the exact function of Hmc is still a matter of debate. It may be possible that, according to the redox conditions, it could transfer electrons from the periplasm to the cytoplasm or, if the conditions change, in the opposite direction.

The Tmc complex (TmcABCD) is composed of typeII-c_3 (TmcA), a cytochrome *b* integral membrane subunit (TmcC) and a two cytoplasmic proteins (TmcB and TmcD), and it appears to function as a transmembrane electron channel from the periplasm. In fact, it was demonstrated that the Tmc complex accepts electrons from the periplasmic hydrogenase via TpI-c_3 (Valente *et al*., 2001; Pereira *et al*., 2006). The genes encoding this complex are upregulated upon hydrogen plus sulfate growth when compared to lactate as the electron donor. This indicates that it is more important in this role than Hmc. (Pereira *et al*., 2008).

The nine-heme cytochrome (NhcABC) complex is present in some *Desulfovibrio* spp and was proposed to function as another alternative to periplasmic

electron acceptor due to similarities with Hmc (Saraiva *et al.*, 2001). The octa-heme cytochrome (OhcABC) shows some differences regarding its cytochrome OhcA subunit compared to the other transmembrane multi-heme complexes (Pereira *et al*., 2007). Low Ohc mRNA expression when thiosulfate is the electron acceptor compared to sulfate was observed in *D. vulgaris* cells grown in lactate and formate. Moreover, Ohc down-regulation in the transition from exponential to stationary phase suggests a role in sulfate reduction (Pereira *et al*., 2008).

Other membrane complexes mediating electron transfer with the participation of NADH and ferredoxin are present in some *Desulfovibrio* spp. The most commonly observed is the Na^+-translocating ferredoxin:NAD^+-oxidoreductase complex (RnfABCDEF) that transfers electron between NADH and Fd (Muller *et al*., 2008). This complex transport electrons from reduced Fd to NAD^+, coupled to electrogenic translocation of Na^+ thus contributing to the generation of a proton motive force (Schlegel *et al*., 2012). However experimental confirmation was not yet obtained. Furthermore, as observed by the group of Pereira the presence of a cytochrome gene encoded in the *rnfABCDEF* operon could provide an electron periplasmic input/output connecting the cytochrome *c* pool to NADH and Fd (Pereira *et al*., 2011).

Finally, the proton-translocating NADH:ubiquinone oxidoreductase complex (nuo), an analogue of complex I, is present in several genomes of *Desulfovibrio* spp but little is known about its participation in the energy metabolism. The activity of this complex in proton translocation through the cytoplasmic membrane would contribute to the formation of a proton potential translated into energy conservation. However, in most cases the NADH dehydrogenase module (NuoEFG) does not exist in *Desulfovibrio* spp., so the electron donor to this complex is not known.

1.3 Hydrogenases

Hydrogenases are enzymes found in all domains of life, especially in a wide variety of microorganisms in anaerobic but also in aerobic environments. The study of these enzymes, found mainly in anaerobic ecosystems, might give insights to the Earth´s earliest life conditions. In fact, the SRB are regarded as one of the oldest forms of microorganism that can be traced back to 3.5 billion years ago (Shen and Buick, 2004). These enzymes have been extensively studied in the SRB group (Matias *et al*., 2005).

They catalyze the reversible oxidation of molecular hydrogen into protons and electrons:

$$H_2 \quad <\!\!-\!\!> \quad 2H^+ + 2e^-$$

Although these enzymes are able to catalyze *in vitro* this reaction in either direction, each enzyme is prone to catalyze *in vivo* either H_2 oxidation or H_2 evolution, according to its physiological function. The direction of this reaction is greatly dependent on the substrates, pH and redox potential of the elements that interact with this enzyme. It will act as H_2 uptake enzyme if H_2 and an electron acceptor is present, or in the presence of an electron donor, this enzyme will produce H_2 (Vignais *et al*., 2001).

These enzymes can be located in the cytoplasm or periplasm of the cell, associated or not to the membrane. The characteristic that directs the localization of the hydrogenase is the presence of a signal peptide at the N-terminus of a subunit of the periplasmic hydrogenases. These signal peptides are 30-70 aminoacids long and present conserved motifs recognized by two major translocation pathways: the membrane targeting and translocation (MTT)/twin-arginine translocator (TAT) pathway and the ubiquitous Sec pathway (Voordouw, 2000; Wu *et al*., 2000; Dubini and Sargent, 2003). This subcellular localization is often associated to their function, with the periplasmic hydrogenases regarded as H_2 oxidizing enzymes, while cytoplasmic hydrogenases are often responsible for H_2 production. However, a group of the cytoplasmic hydrogenases are proposed to work bidirectionally.

The majority of the hydrogenases are metalloenzymes that possess metal sites of two categories. One of them is the active site itself that contains either [NiFe] or [Fe] (Albracht, 1994; Nicolet *et al*., 2002). The second is composed of iron sulfur clusters ([2Fe-2S], [3Fe-3S] and [4Fe-4S]) which are responsible for the shuttling of electrons between the active site and redox partners of the enzyme. However, another group of hydrogenases (Hmd) were found in some methanogenic archaea that do not contain Fe-S clusters or nickel (Zirngibl *et al*., 1992). Initially termed metal-free hydrogenases, it was later discovered that the activity of this enzyme was dependent on an iron-containing cofactor (Lyon *et al*., 2004). As such they should not be designated as iron-free hydrogenases but rather as iron-sulfur cluster free hydrogenases (Vignais and Colbeau, 2004; Matias *et al*., 2005).

Due to their diversity (size, quaternary structure, electron donors and acceptors) the hydrogenase enzymatic group is divided in three distinct families characterized by a unique functional core which is conserved within each class: [NiFe], [FeFe] and the iron-sulfur cluster free (Vignais *et al*., 2001; Vignais and Colbeau, 2004; Vignais and Billoud, 2007). Marked differences are found between these groups regarding their H_2-uptake and H_2-evolving activities, their sensitivity towards molecules, such as CO and NO, and their molecular structures (Fontecilla-Camps *et al*., 2007). Each of these hydrogenase families will be described in more detail.

1.3.1 [NiFe] Hydrogenases

This family of hydrogenases is the most numerous and best studied in bacteria. The [NiFe] hydrogenases contain a minimum of two subunits that are the large and the small subunits, encoded by a multicistronic operon. The first [NiFe] hydrogenases identified were composed of αβ heterodimers. Phylogenetic analyses have shown that the two subunits of [NiFe] hydrogenases hydrogenases have evolved conjointly (Vignais *et al*., 2001).

The large subunit has an average molecular mass of 60kDa, containing the heteronuclear diatomic [NiFe] active site that is buried deep inside the protein (Fig 1.8).

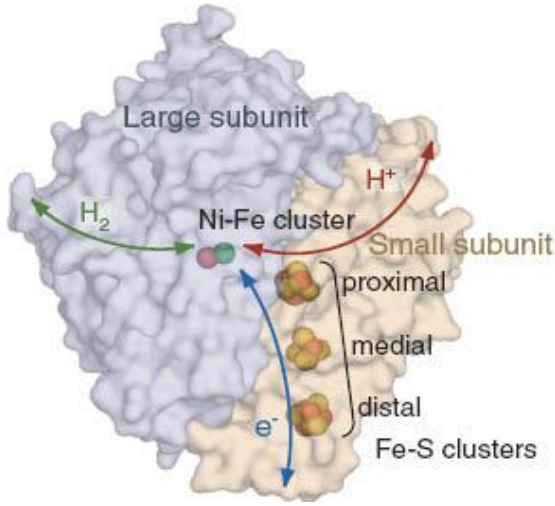

Fig 1.8. Structural aspects of the periplasmic [NiFe]-hydrogenase. Hydrogen oxidation (red arrow) and/or reduction (green arrow) occurs in the active site (Ni-Fe cluster) of the large subunit (light blue mesh), while electron flow to and from the active site is mediated by the three Fe-S clusters localized in the small subunit (light orange mesh). Source: Reviews in Inorganic Chemistry (2013) DOI: 10.1515/revic-2013-0005.

The binuclear core is coordinated by four cysteine residues. Two of these cysteine residues coordinate specifically the Ni atom while the other two residues are responsible for the bridging between the two metal atoms (Matias *et al*., 2005). The Fe atom is further coordinated by two types of diatomic species, that were identified spectroscopically: two CN^- and one CO ligand (Volbeda *et al*., 1995). This arrangement leaves two open positions (Fig 1.8, pink and green circles) that are important to the activation cycle of this enzyme. The small subunit has an average of

30KDa and binds up to three [4Fe-4S] or [3Fe-4S] centers responsible for conducting the electrons from the H_2-active site to the redox partner at the surface of the hydrogenases. The proximal [4Fe-4S] cluster, closest to the active site, is essential for the H_2 activation. The two subunits interact extensively by a large contact surface aerea. H_2 diffusion from the surface of the heterodimer to the catalytic site is achieved through hydrophobic channels (Montet *et al*., 1997; Baltazar *et al*., 2012).

In some [NiFe] hydrogenases however, one of the cysteine residues that are bound to the Ni atoms is substituted by selenocystein. This subgroup, designated [NiFeSe], is structurally very similar to the [NiFe] hydrogenases. Besides the presence of a selenocysteine, another major difference is the presence of a medial $[4Fe\text{-}4S]^{2+/+}$ cluster instead of the $[3Fe\text{-}4S]^{+/0}$ cluster found in the standard [NiFe] enzymes. However, the [NiFeSe] hydrogenase presents higher activities values than the [NiFe] hydrogenases and are more resistant to inactivation by oxygen (Valente *et al*., 2006).

The characterized [NiFe] hydrogenases reveal differences at the structural level as well as at their function in the hydrogen metabolism and redox partners. As such, a classification of these enzymes in four main groups was proposed (Vignais and Billoud, 2007). The respiratory uptake hydrogenases (Group 1) are the enzymes that are located at the periplasm of the cells and that are capable of supporting growth with H_2 as energy source. This group, which is characterized by a long signal peptide at the N-terminus of their small subunit, is further subdivided in two main types. The membrane-bound uptake hydrogenases are enzymes attached to the membrane by a cytochrome *b* containing subunit that link H_2 oxidation to the reduction of different electron acceptors, such as oxygen, sulfate, fumarate or CO_2, via the quinone pool. The electron transfer in this respiratory chain conserves energy by coupling vectorial proton translocation with the establishment of electrochemical proton gradient (Gross *et al*., 1998). The periplasmic soluble uptake hydrogenases, on the other hand, do not have the cytochrome b subunit. The electrons deriving from H_2 oxidation are transferred by low-potential *c*-type cytochromes to the cytoplasm via transmembrane electron carriers. These complexes generate in the process a proton

gradient across the membrane. In the case of sulfate reducers of the *Desulfovibrio* genus, that present a great number of these enzymes, this electron transfer during sulfate respiration is performed by the TpI-c_3 and the Qrc complex (Rabus *et al*., 2006; Venceslau *et al*., 2010).

The cytoplasmic heterodimeric hydrogenases (Group 2) are composed of cyanobacterial hydrogenases and the soluble H_2 sensing hydrogenases. Because they are found in the cytoplasm they do not present a signal peptide in the small subunit. These hydrogenases have the function of detecting environmental H_2 triggering a cascade of reactions that control the synthesis of other respiratory hydrogenases. Thus, they are not directly involved in energy transduction and conservation reactions. The cyanobacterial uptake hydrogenases have been proposed to recycle reducing equivalents (electrons) lost to hydrogen evolution and provide reductant to the reductive TCA cycle for CO_2 fixation (Vignais and Billoud, 2007).

The cytoplasmic heteromultimeric reversible hydrogenases (Group 3) present distinct subunits that are capable of binding a soluble cofactor (F420, NAD or NAPD). These enzymes are referred to as bidirectional because they can either function as H_2-production enzymes or as H_2 consuming, reoxidizing the cofactors, under anaerobic conditions, using the protons of water as the electron acceptors. In cyanobacteria they function primarily as a redox regulator for maintaining a proper oxidation/reduction state in the cell (Carrieri *et al*., 2011). In methangens they are implied in electron bifurcation mechanisms where they catalyze the reduction of the low potential ferredoxin with concomitant oxidation higher potential acceptors such as crotonyl-CoA, NAD(+) or heterodisulfide (Buckel and Thauer, 2013)

The last group (Group 4) is composed of membrane-associated respiratory hydrogenases, such as the hydrogenase 3 of *E. coli*, the CO-induced hydrogenase of *Rhodospirillum rubrum* or the Ech hydrogenase present in methanogens and in *Desulfovibrio* spp. These enzyme complexes present a high similarity with the subunits of complex I, not only regarding the electron (Fontecilla-Camps *et al*., 2007) transfer subunits but also the transmembrane subunits, which are responsible for

proton pumping and energy conservation (Hedderich and Forzi, 2005). The membrane-bound hydrogenases are able to use the reducing equivalents from anaerobic oxidation of C^1 organic compounds such as formate, acetate or carbon monoxide, through H_2 reduction. This mechanism creates a proton motive force across the membrane that conserves energy.

1.3.2 [FeFe] hydrogenases

Unlike the [NiFe] hydrogenases which are composed of at least two subunits, several [FeFe] hydrogenases are constituted by a single catalytic subunit, including both active site and the electron transfer domains (Fig 1.9).

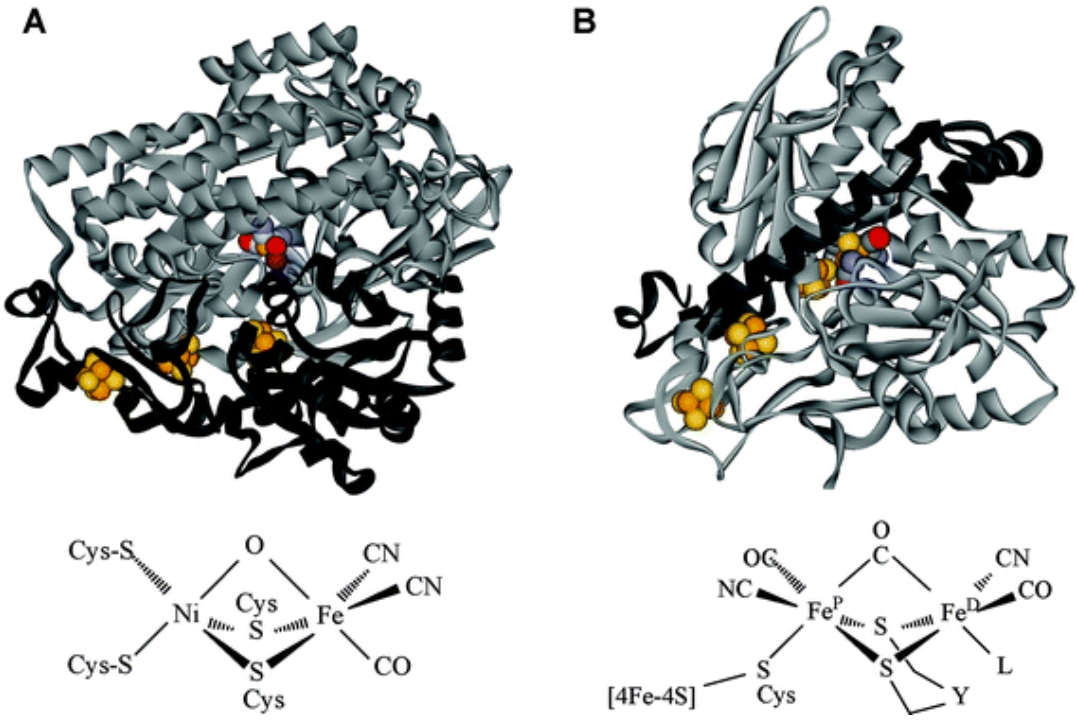

Fig 1.9. Differences in the 3D-structure and active site coordination from the [NiFe] and [FeFe] hydrogenases (Vincent *et al.*, 2005). (A) Ribbon representation of the [NiFe] hydrogenase structure of *D. gigas* (PDB: 1FRV) and schematic representation of the Ni-Fe coordination center (below); (B) Ribbon representation of the [FeFe]

hydrogenase from *D. desulfuricans* (PDB: 1HFE) and schematic representation of the Fe-Fe coordination center (below).

However, dimeric, trimeric and tetrameric enzymes were also characterized. The catalytic subunit of the monomeric enzymes is composed of a conserved domain called the H-cluster, of around 350 aminoacids, that contains the active site and additional domains with the iron-sulfur clusters. The C-terminal H-cluster domain is highly conserved consisting of the binuclear iron site bound by a bridging cysteine residue, to a [4Fe-4S] cluster, four other cysteine residues coordinating the iron site and other conserved aminoacids that are proposed to be involved in the formation of a H_2 channel linking the surface of the protein to the deeply buried active site. Besides the highly conserved C-terminal domain, some [FeFe] hydrogenases contain also an N-terminal domain that presents high homology with [4Fe-4S] bacterial ferredoxins. In the [FeFe] hydrogenases that are not monomeric the small subunit is similar to the C-terminal domain of the monomeric enzymes and embraces the large subunit containing the H-cluster in a circular manner. It is also responsible to carry the signal peptide sequence that allows the export of the complete enzyme to the periplasm of the cell. In terms of function, the [FeFe] hydrogenases are versatile enzymes as they are able to use different electron donors and acceptors, such as ferredoxins, flavodoxins, c-type cytochromes and even NADP as for example in the case of the tetrameric hydrogenase of *D. fructosovorans* (Malki *et al.*, 1995). Furthermore, in terms of activity [FeFe] hydrogenases are generally involved in the production of molecular hydrogen, regardless of their localization in the cytoplasm or in the periplasm

1.3.3. Iron-sulfur cluster free hydrogenases

The hydrogenases found in some methanogenic archea, termed Hmd, constitute a very restrict group of hydrogenase that are much different from the other two families by the main fact that they do not contain iron- sulfur clusters. They are composed of two identical subunits of 40KDa, that catalize the reversible reduction of

the cofactor N5,N10-methenyltetrahydromethanopterin with H_2 to methylenetetrahydromethanopterin (methylene-H4MPT) and a proton (Schworer *et al*., 1993). Lyon and collaborators verified that each monomer contain a single Fe atom with the function of protecting from light inactivation, which is the reason why they are no longer referred as “metal-free” hydrogenases (Lyon *et al*., 2004). This hydrogenase group is not only different from the [NiFe] and the [FeFe] families by not having iron-sulfur clusters, but also by the fact that the Fe atom required for the enzyme activity, is not in the redox center.

1.4. General aspects of hydrogenase gene organization and expression

The separation of the hydrogenases into three families according to the metal content of their active site was further reinforced by phylogenetic data. Alignments using a great number of genetic and genomic sequences from different hydrogenases confirmed that, in fact, they belong to phylogenetic distinct families (Vignais *et al*., 2001). In the [NiFe] family of hydrogenases, both [NiFe] and [NiFeSe] hydrogenases share significantly structural homology confirming that this is a monophyletic group (Matias *et al*., 2005). The [Fe] hydrogenases also constitute a monophyletic group that is completely separated from the [NiFe] branch. However, despite having different structures and evolutionary basis, these two families share common features, namely endogenous CO and CN^- ligands bound to the Fe center in the active site, the presence of an iron-sulfur cluster proximal to the dinuclear metallo-center and a hydrophobic channel for H_2 connecting the surface of enzyme to the deep buried active site. This suggests these two families of hydrogenases may be a case of convergent evolution (Vignais *et al*., 2001; Vignais and Billoud, 2007). Furthermore, this same sequence data analysis revealed that the hydrogenases present similarity with other redox proteins and enzymes e. g. ferredoxins and Complex I.

The genes encoding hydrogenases are usually organized in clusters. These clusters comprise not only the structural genes but also accessory genes for

maturation and insertion of the transition metals (Ni and Fe) and the ligands (CO and CN^-) in the active site. Maturation of the hydrogenases involves the protein products of the *hyp* genes, namely HypA, HypB, HypC, HypD, HypE and HypF in a complex pathway. These proteins are responsible for: a) the synthesis and incorporation of the metal center into the apo protein; b) fidelity of insertion of the correct metal in the target protein; c) maintaining the folding state of the protein for metal addition; and d) allowing the correct conformational changes for the internatilization of the metal center (Casalot and Rousset, 2001; Vignais and Colbeau, 2004).

In some organisms, the hydrogenase gene cluster also includes regulatory genes that control the expression of the structural genes. Hydrogenase regulation is exerted at the transcriptional level as a mean to respond efficiently and rapidly to environmental changes (Colbeau and Vignais, 1992). Control of the transcription of these genes involves one or several two-component regulatory systems, acting positively or negatively at the hydrogenase operon. The transcription of mRNAs for hydrogenase responds to several types of signals (Vignais and Colbeau, 2004):

i. Molecular hydrogen, which normally activates hydrogenase gene expression;
ii. Molecular oxygen, which inhibits most of the hydrogenases;
iii. Metabolites, either as electron acceptor or as electron donors, such as formate, carbon monoxide, nitrate, sulfate, etc;
iv. Metal ions such as Ni, Fe and Se

The organisms exposed to several environmental cues reveal that different hydrogenases can be expressed. Accordingly, each of these enzymes, present in the cytoplasm, periplasm or in both subcelullar compartments, may play a different physiological role in the energy metabolism of the cell.

1.5 Hydrogenase function in the *Desulfovibrio* genus

In the *Desulfovibrio* spp. a high number and diversity of hydrogenase enzymes can be found. From the genome sequences already available, all members of this genus contain at least one hydrogenase in both periplasm and cytoplasm.

The periplasmic uptake [NiFe] hydrogenase (Group 1) is the most commonly found. At least one copy of the two-subunit HynAB [NiFe] hydrogenase is present (Pereira *et al*., 2011) in all *Desulfovibrio* spp. These enzymes are characterized by the presence of two [4Fe-4S] and one [3Fe-4S] clusters and use the Type I cytochrome c_3 (TpI-c_3) as their electron acceptor (Matias *et al*., 2005; Pereira *et al*., 2011). Similar to the HynAB, the HysAB hydrogenase, which contain a seleno-cystein residue coordinating the active site, is also found in several species. On the other hand, the membrane anchored subgroup of uptake [NiFe] hydrogenases, containing an adicional subunit for quinone reduction (HynABC) was identified so far in only three species: *D.vulgaris* Hildenborough, *D. alaskensis* G20 and *D.desulfuricans* ATCC 27774 (Pereira *et al*., 2011)

Periplasmic [FeFe] hydrogenases are also found in the great majority of the *Desulfovibrionacae*. With the exception of the *D. piger* all other species contain one copy of the dimeric [FeFe] hydrogenase. Similarly to the [NiFe] uptake hydrogenases, these enzymes also use TpI-c_3 as their electron acceptor. No membrane-bound periplasmic [FeFe] hydrogenases were identified in this genus. This demonstrates that the cytochrome c_3 is the preferred redox partner for the electrons coming from periplasmic H_2 uptake for both families of hydrogenases in *Desulfovibrio*.

In the cytoplasm, either an Ech or Coo-type of the membrane-bound energy conserving [NiFe] hydrogenases (Group 4) is found in all *Desulfovibrio* spp, with the exception of *D. alaskensis* G20. In some cases, such as in *D. vulgaris* Hildenborough and *D. desulfuricans* ATCC27774, both these enzymes are present, suggesting that multiple mechanisms of energy conservation may be in place. Interestingly, the organisms that contain these energy-conserving hydrogenases do not contain other cytoplasmic [NiFe]-type enzymes, suggesting that energy coupling through [NiFe] hydrogenases involves either a chemiosmotic or an electron bifurcating mechanism (Pereira *et al*., 2011). In accordance, cytoplasmic heterodimeric (Group 2) or heteromultimeric reversible hydrogenases (Group 3) were not characterized in this group of SRB.

Regarding the [FeFe] family, a high number of soluble cytoplasmic hydrogenases are present in the diverse *Desulfovibrio* spp. With the exception of *D. aespoeensis* and *D. desulfuricans* ATCC27774, the other species of this genus contains at least one cytoplasmic [FeFe] hydrogenase. Besides the monomeric [FeFe] hydrogenases that are related to H_2 production, soluble multimeric [FeFe] are also present in these organisms. In some cases, these enzymes are associated with electron bifurcating mechanisms, such as the tetrameric [FeFe] NADP-dependent of *D. fructosovorans* (Malki *et al*., 1995). Furthermore, a group of [FeFe] hydrogenases that may form the soluble formate–hydrogen lyase complexes (FHLs) can be found in at least three species. Such complexes composed by genes that code for the [FeFe] hydrogenase, the formate dehydrogenase catalytic subunit of FDH and two [4Fe-4S] electron-transfer proteins. At last, in a few *Desulfovibrio* spp. a specific [FeFe] hydrogenase, that includes a PAS sensor domain and which is thought to be involved in H_2 sensing and regulation was identified (Pereira *et al*., 2011).

Although many hydrogenases have already been characterized, the exact physiological role of each of these enzymes is still unclear. In the case of *Desulfovibrio* spp., the multiplicity and redundancy of the hydrogenases may also contribute to the complexity of determining their function, since organisms such as *D. vulgaris* Hildenborough present seven hydrogenases, with four of them located just in the periplasm and composed by different active sites ([NiFe], [NiFeSe] and [FeFe]).

Analysis using mutant strains and expression profiles performed in *D. vulgaris* Hildenborough, the most extensively *Desulfovibrio* studied with respect to the hydrogenase function, have shown that during respiratory growth using H_2 as energy source the periplasmic [NiFe] HynAB and the [NiFeSe] HysAB perform a similar role in H_2 oxidation (Valente *et al*., 2006; Caffrey *et al*., 2007; Pereira *et al*., 2008). Interestingly, while [FeFe] hydrogenases usually act as H_2 evolving enzymes, the *D. vulgaris* Hildenborough [FeFe] Hyd hydrogenase is also involved in H_2 uptake (Pohorelic *et al*., 2002). The participation of each enzyme during H_2 oxidation may reside in different expression levels related to metal availability or hydrogen

concentration to which the cells are exposed (Valente *et al*., 2006; Caffrey *et al*., 2007).

With regard to the metal content, it was elegantly demonstrated in the same organism that not only Ni, but also Se are involved in the regulation of periplasmic hydrogenases (Valente *et. al* 2006). When Se is present the mRNA expression of the gene encoding the periplasmic [NiFeSe] hydrogenase is enhanced, while the expression of [FeFe] and [NiFe] hydrogenase genes is negatively regulated. Also, the gene expression of all three hydrogenases is increased in the presence of hydrogen, corroborating their function in H_2 uptake. Caffrey and collaborators have demonstrated that the mRNAs levels of the [FeFe] Hyd hydrogenase are higher in elevated H_2 partial pressures (50%) when compared to low H_2 pressures (5%). In this last condition however, the increased mRNA expression levels of [NiFeSe] compared to the other hydrogenases indicate that this is the main active enzyme (Caffrey *et al.*, 2007).

Another observation is that no single hydrogenase appears to be essential for H_2 oxidation. Besides the analysis performed in *D. vulgaris* Hildenborough (Caffrey *et al*., 2007), in *D.fructosovorans*, single and double mutations in the periplasmic [NiFe] Hyn, the cytoplasmic NADP-reducing HnD and the [FeFe] Hyd hydrogenases, showed that the mutant strains were still able to grow with H_2 as the only electron source (Malki *et al*., 1997).

The participation of each of these enzymes in the energy metabolism can vary according to the substrate available and growth conditions. In *D. fructosovorans*, double (Δ*hnd*Δ*hyn*) and triple (Δ*hnd*Δ*hyn*Δ*hyd*) mutants revealed a decrease in the growth efficiency when lactate or pyruvate was used as electron donor for sulfate reduction when compared to cells growing in H_2 (Malki *et al*., 1997; Casalot *et al*., 2002). Also, due to its reversible function, a single enzyme may switch function, participating in H_2 evolution during certain growth conditions and in H_2 oxidation if substrate or redox conditions change. In *D. vulgaris* Hildenborough, it has been demonstrated that periplasmic [FeFe] Hyd hydrogenase functions as an uptake hydrogenase during lactate respiration, similarly to what is observed when H_2 is the

sole energy source (Pohorelic *et al*., 2002; Caffrey *et al*., 2007). In contrast, during lactate and pyruvate fermentative metabolism, the same Hyd [FeFe] hydrogenase functions as an H_2 producing enzyme (Voordouw, 2002).

After uncovering the genome of *D. vulgaris* Hildenborough (Heidelberg *et al*., 2004) the elaboration of microarray chips for analysis of transcriptional profiles enabled a better understanding of the phenotypical differences observed during distinct growth conditions (Zhang *et al*., 2006; Caffrey *et al*., 2007; Pereira *et al*., 2008; Keller and Wall, 2011). Transcriptional analysis performed in *D. vulgaris* Hildenborough wild type and corresponding mutants for periplasmic hydrogenases have revealed that the levels of each hydrogenase gene expression in H_2/sulfate differs from lactate/sulfate respiratory conditions (Caffrey *et al*., 2007; Pereira *et al*., 2008). The *hyd* hydrogenase gene expression is induced when compared to the *hys* gene expression during lactate respiratory growth, while the *hyn1* hydrogenase did not show any changes in expression using either lactate/sulfate or H_2/sulfate conditions. However, the latter gene expression was decreased is response to the exponential to stationary shift in lactate/sulfate conditions (Zhang *et al*., 2006). This suggests that this hydrogenase plays a primary role in the early phase of growth, since it is the only hydrogenase differentially regulated during growth. Further studies confirmed that changes in the growth conditions affect differently the expression of several, seemingly redundant enzymes, indicating that they have specialized roles not being completely interchangeable (Pereira *et al*., 2008). Under respiratory conditions, when pyruvate is the energy source, the periplasmic *hyn1* hydrogenase is up-regulated compared to its expression in cells grown using lactate, while at the same time the [NiFe] *hyn2* shows a slight down-regulation (Keller and Wall, 2011). However, this same *hyn2* hydrogenase is up-regulated during pyruvate fermentative conditions (Pereira *et al*., 2008) compared to lactate fermentation. Metal availability also influences hydrogenase protein formation differently, since the synthesis of the [FeFe] Hyd hydrogenase in Fe-only medium was higher in pyruvate/sulfate compared to lactate/sulfate, while in the presence of Ni a significant reduction of this

hydrogenase occurs only in lactate/sulfate compared to pyruvate and H_2 respiratory conditions (Valente *et al*., 2006).

In the case of the [NiFe] cytoplasmic hydrogenases (Group 4), Ech and Coo enzymes were proposed to function in hydrogen generation in the cytoplasm. Ech hydrogenases coupled the oxidation of reduced ferredoxin with the production of H_2, while creating an electrochemical proton potential. In the methanogenic archaea the Ech hydrogenase can also act in reduction of ferredoxin by H_2, driven by reverse electron transport (Meuer *et al*., 2002; Welte *et al*., 2010b; Welte *et al*., 2010a). The Coo hydrogenase of chemolithoautotrophic bacteria couples the oxidation of CO to CO_2, performed by the carbon monoxide dehydrogenases (CODH) enzyme, with reduction of H^+ to H_2 (Fox *et al*., 1996).

The physiological role of the cytoplasmic-facing hydrogenases in the respiratory metabolism of *Desulfovibrio* spp. with different substrates is much less clear than with the periplasmic hydrogenases. In *D. vulgaris* Hildenborough, transcriptional data suggested a different role for each of these enzymes. Comparative analysis using different electron donors showed that the *ech* genes were more expressed using H_2 or pyruvate as electron donor compared to lactate during sulfate respiratory conditions, whereas the *coo* genes were less expressed in H_2 (Pereira *et al*., 2008). In accordance, the *ech* genes (*echACDE*) were up-regulated while the *coo* genes (*cooHLUX*) were down-regulated in formate/sulfate when compared to lactate/sulfate. These results indicate a possible bifunctional role for Ech hydrogenase in *Desulfovibrio* spp. In H_2/sulfate this enzyme would reduce ferredoxin with the electrons obtained from H_2 oxidation for carbon fixation. On the other hand, in pyruvate/sulfate, where carbon fixation is not required it would oxidize ferredoxin, which is reduced by the pyruvate:ferredoxin oxidoreductase, forming H_2. As such, it may participate in the hydrogen cycling energy conserving mechanism, in a similar fashion as observed in methanogens. However, differently from what was observed for the periplasmic hydrogenases, no physiological analysis was performed in mutant strains lacking a functional Ech hydrogenase.

The Coo hydrogenase appears to participate in the energy metabolism when lactate is the electron donor. Transcriptional arrays showed that gene expression of this enzyme is among the top 15% of expressed genes during lactate/sulfate growth and it is up-regulated when compared to pyruvate/sulfate conditions (Keller and Wall, 2011) Furthermore, random transposon mutant libraries indicated that the Coo complex is essential in lactate metabolism, as no insertion in the *coo* operon was observed in cells growing in lactate/sulfate conditions. Based on these results, Keller and Wall proposed that this hydrogenase may allow the bifurcation of electrons from reduced ferredoxin and menaquinone. However, there is no clear evidence to support this idea. In contrast, in other analysis performed in *D. vulgaris* Hildenborough the Coo hydrogenase was proposed to participate, together with carbon moxonide dehydrogenase (CODH), in CO cycling during growth using pyruvate as the electron donor (Voordouw, 2002). This mechanism would constitute another metabolic cycling mechanism to conserve energy besides hydrogen and formate cycling. In agreement, in a *D. vulgaris* Hildenborough *coo* deletion mutant strain it was shown that despite the up-regulation obtained in transcriptional arrays, the Coo hydrogenase was not required for lactate/sulfate respiratory growth (Walker *et al*., 2009) . In this analysis, the Coo hydrogenase was proposed to produce H_2 and perform an important role during lactate synthrophic growth.

Indeed, other transcriptional and physiological analysis using wild type and hydrogenase mutant strains of *D. vulgaris* Hildenborough and D*. alaskensis* G20 grown under syntrophy with methanogenic bacteria, showed that the function of the hydrogenases during syntrophic growth may change when compared to sulfate respiratory growth (Walker *et al*., 2009; Plugge *et al*., 2010; Meyer *et al*., 2013).

In *D. vulgaris* Hildenborough, transcriptional data showed that the periplasmic [NiFe] *hyn1* and [FeFe] *hyd* gene had increased expression in lactate media during syntrophic growth when compared to monocultures. In this analysis, the mutant strains lacking the periplasmic hydrogenases (Δ*hyn* and Δ*hyd*) also showed slow growth using both lactate and pyruvate during syntrophy. As such, the activity of the periplasmic hydrogenases is proposed to be as H_2 evolving enzymes during

syntrophic growth, instead of H_2 oxidation during respiratory growth (Walker *et al*., 2009) (Fig 1.10).

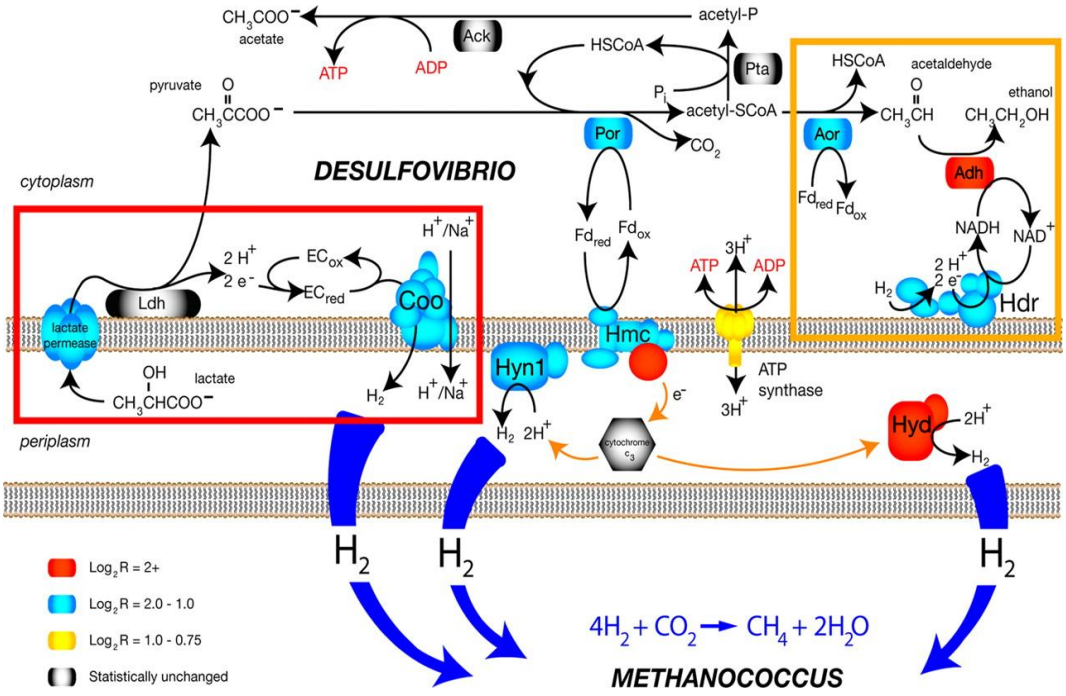

Fig 1.10. Participation of the hydrogenases (Coo, Hyn1 and Hyd) in the H_2 production, contributing to the energy conservation of *D. vulgaris* Hildenborough growing with lactate as energy source, during syntrophy with *Methanococcus* sp. (Walker *et al* 2009).

The *coo* genes for the cytoplasmic energy conserving [NiFe] hydrogenase also appeared as some of the most up-regulated during syntrophy and its deletion inhibit cell growth during syntrophy, using both lactate and pyruvate. The authors proposed a model where electrons from lactate oxidation are shuttled to the Coo hydrogenase that produces H_2 with the concomitant translocation of protons, while pyruvate is oxidized generating reduced ferredoxin. The membrane-associated Hmc complex then couples the oxidation of this reduced ferredoxin to the reduction of a periplasmic hydrogenase (Hyn-1 and Hyd), yielding more hydrogen. In other similar

syntrophic studies with *D. vulgaris* Hildenborough using a different methanogen, an up-regulation of the Ech hydrogenase was observed when growth shifted from syntrophy back to lactate/sulfate metabolism, indicating that Ech could also be acting as proton pump due to its similarity with Complex I (Plugge *et al*., 2010).

Syntrophic studies were recently performed using *D. alaskensis* G20 (Meyer *et al*., 2013). The results of the expression profiles and hydrogenases mutant physiological analysis were different from *D. vulgaris*. The periplasmic [NiFe] *hyn1* showed an upregulation during syntrophic growth in lactate, indicating that it is the main hydrogenase in H_2 production, while the periplasmic [NiFeSe] *hys* hydrogenases was down-regulated. However, despite its down-regulation the mutant strain for this same enzyme (Δ*hysA*) was impaired in coculture growth, while the Δ*hyn1* mutant only showed an extended lag-phase. This indicates the Hys hydrogenase is important during the early stages of the syntrophic growth while the Hyn1 enzyme is more important under steady-state conditions during lactate fermentation. Furthermore, it is interesting to notice that *D. alaskensis* strain G20 does not possess a cytoplasmic membrane-bound [NiFe] hydrogenase, such as the Coo or Ech, which are essential for syntrophic growth in *D. vulgaris* strain Hildenborough, an indication that in other *Desulfovibrio* spp. there are different molecular mechanisms acting during syntrophic processes. In addition, during this type of growth, independent energy generation pathways from those used during sulfate respiratory processes may be at place.

Finally, the hydrogenases present in the *Desulfovibrio* spp. may also perform different physiological functions when sulfate is not the final electron acceptor, during respiratory growth conditions. Fumarate can serve as electron acceptor in the presence of H_2 and formate (Zaunmuller *et al*., 2006). In *W. succinogenes*, a bacterium in which this process is well described, fumarate respiration is catalyzed by an electron transport chain consisting of a hydrogenase, menaquinone, and a fumarate reductase (Kroger *et al*., 2002). Fumarate reduction is coupled to the generation of an electrochemical proton potential across the membrane that is generated by MK reduction with H_2. However, little is known about the exact role of

the hydrogenases in fumarate respiration of *Desulfovibrio*, as no physiological or expression analysis using hydrogenase mutants were performed under these conditions.

1.6 *Desulfovibrio gigas* as SRB model

The matrix of redox carriers and enzymes participating in the energy metabolism of the SRB and, in particular, of the *Desulfovibrio* spp. can vary quite significantly, both in number of the enzymes and in the presence/absence of specific energy transduction pathways. As already observed by Hansen, despite similarities in physiological properties observed among the *Desulfovibrio* strains, one has to be careful in generalizing models proposed for one strain to other strains since many species-specific differences have been found in the elements involved in energy transduction (Hansen, 1994). Although *D. gigas* (Legall, 1963) was used by many different groups to elucidate the structure of key enzymes that participate in sulfate reduction (cytochromes, ferredoxins, dehydrogenases, etc), as well as its functional processes, a complete genome sequence was not yet available (Fig 1.11).

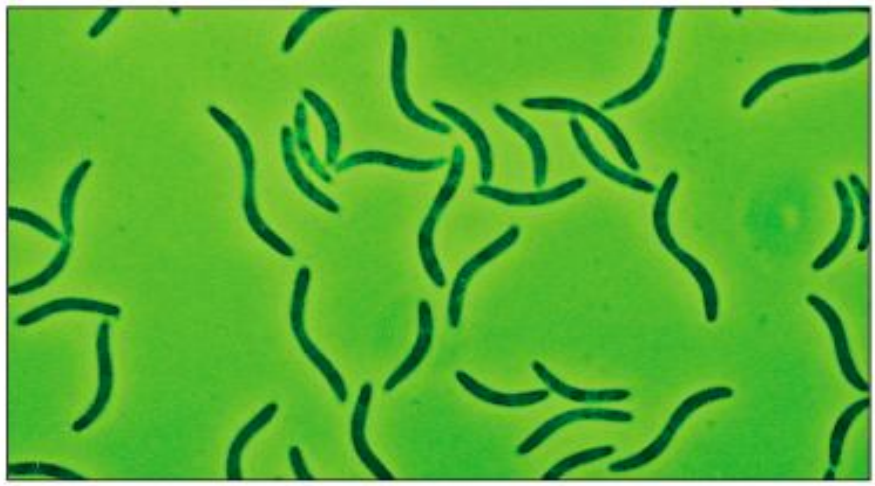

Fig 1.11. Image of the anaerobic bacterium *Desulfovibrio gigas.* Source: http://blog.daum.net/daumcos/1307

As such, the identification of energy metabolism related proteins, especially transmembrane complexes and structures for energy conservation during sulfate respiration remains to be elucidated in *D. gigas*.

In the particular case of hydrogenases, the presence of different types of these enzymes, their number and cellular location in the *Desulfovibrio* genus, can vary quite significantly (Pereira *et al*., 2011). Due to the presence of multiple hydrogenases genes in the genome of the *Desulfovibrio* species sequenced so far, the identification of the function of each of these enzymes in different growth conditions represents a complex task.

However, in the case of *D. gigas* only two [NiFe] hydrogenases were described, the HynAB and the Ech (Li *et al*., 1987; Rodrigues *et al*., 2003) enzymes (Fig 1.12).

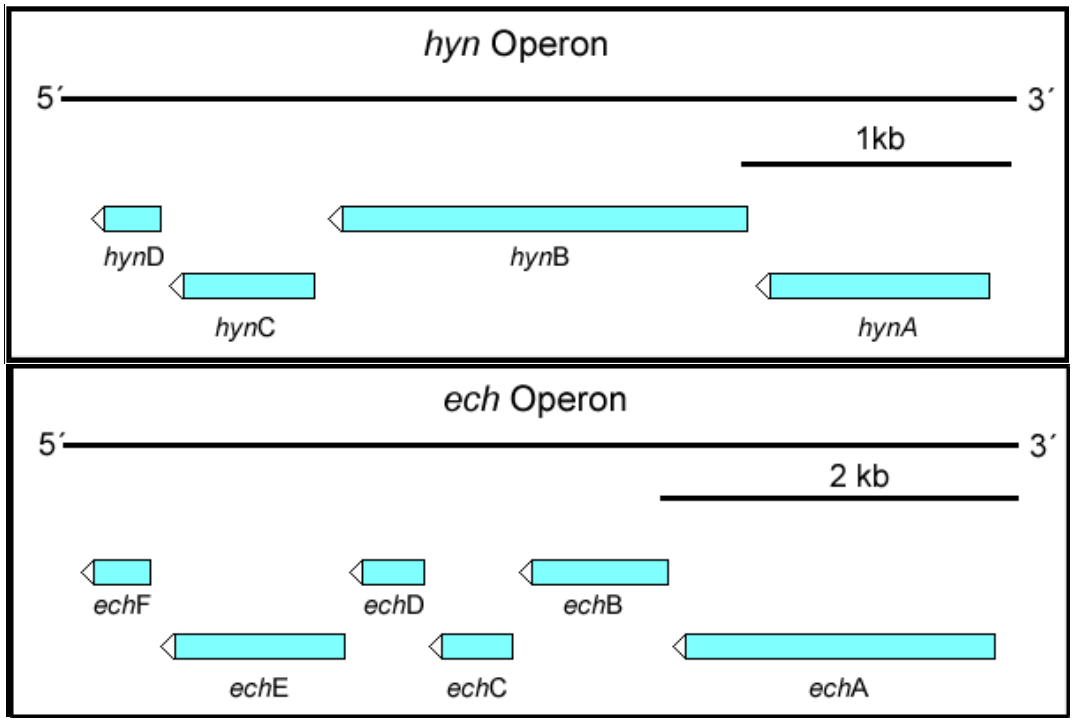

Fig 1.12. Genomic arrangment of the operons coding for the HynAB and Ech hydrogenases described for *D. gigas*

Among the SRB hydrogenases, the HynAB of *D. gigas* was the first [NiFe] hydrogenase from which a crystal structure was obtained (Volbeda *et al*., 1995). This enzyme has the basic configuration of periplasmic uptake hydrogenases (Group 1) composed of two subunits (αβ) (Fig 1.12). Besides the genes conding for the small and large subunits of this enzyme (*hyn*A and *hyn*B), two other genes coding for maturation proteins (*hyn*C and *hyn*D) are present in the same operon.

The HynA large subunit comprises the [NiFe] active site coordinated by four conserved cysteine residues (Fig 1.13). The HynB small subunit contains three FeS clusters responsible for electron transfer, the proximal and distal [4Fe-4S] clusters and the medial [3Fe-4S] cluster, and has a signal peptide for export to the periplasm (Rousset *et al*., 1998; Hedderich and Forzi, 2005).

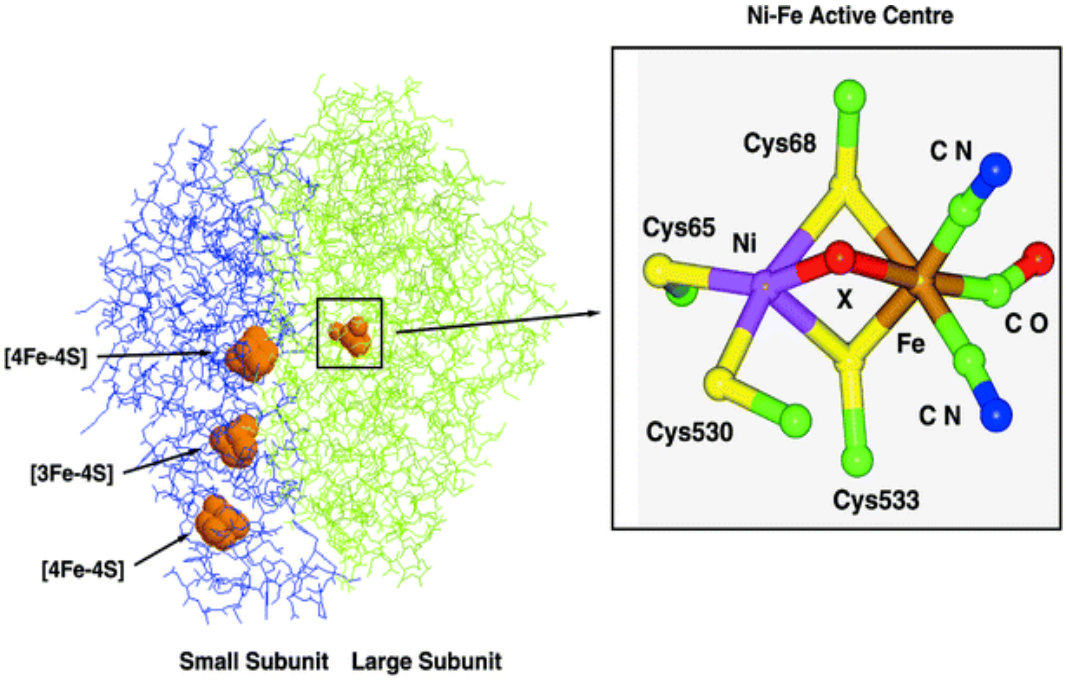

Fig 1.13. The 3D-structure and active site representation (enlargement) of the HynAB hydrogenase from *D. gigas* (PDB: 2FRV) showing the four cystein residues, as well as the two CN and one CO ligands, that coordinates the Ni-Fe active site.

Its function is proposed to be in H_2 oxidation. Molecular hydrogen is oxidized at the active site and the electrons generated in the process flow through the Fe-S clusters to be accepted by TpI-c_3 (Aubert *et al*., 2000; Rabus *et al*., 2006)

The Ech enzyme of *D. gigas* was also the first [NiFe] hydrogenase belonging to group of membrane-associated H_2-evolving respiratory hydrogenases (Group 4) to be characterized in the *Desulfovibrio* genus (Rodrigues *et al*., 2003). It presents great similarity with the *Escherichia coli* hydrogenase 3 found also in *Methanosarcina* (Kunkel *et al*., 1998), and to subunits of the proton-pumping NADH:ubiquinone oxidoreductase (complex I) (Vignais and Colbeau, 2004). It is composed of six genes encoded by the same operon (*ech*ABCDEF) (Fig 1.12). The EchC subunit presents a single conserved iron–sulfur-binding motif typic of the small subunit of [NiFe] hydrogenases and does not show the twin-arginine motif belonging to the signal peptide, confirming that the Ech faces the cytoplasm. The EchE subunit is similar to the [NiFe] hydrogenases large subunit and presents the two conserved motifs in the amino-terminal region and near the carboxy terminus containing the Cys residues coordinating the active site. The EchA and the EchB are hydrophobic subunits containing 13 and 6 transmembrane helices, while the EchD and EchF are hydrophilic. The latter also contains two conserved binding motifs of [4Fe-4S] type clusters. Overall, the Ech hydrogenase of *D. gigas* shows high similarity to the one from *M. barkeri*. In the methanogens this enzyme plays a central role in energy conservation mechanisms as it is able to evolve hydrogen from reduced ferredoxin, creating a proton motive force in the process that can be used to generate ATP (Meuer *et al*., 2002). It can also perform ferredoxin reduction from H_2 driven by reverse electron transport.

Despite that the genes coding for these enzymes were sequenced and the structure of HynAB was determined, their global role in the energy metabolism and

their direct physiological function was not yet evaluated in *D. gigas*. Furthermore, the presence of only two [NiFe] hydrogenases makes *D. gigas* an excellent model organism to investigate the function of these hydrogenases in terms of hydrogen production and physiological role through the generation of single gene deletions. Moreover, the fact that each of these enzymes is located in different subcelullar compartments (HynAB in the periplasm whereas Ech is in the cytoplasm) enable us to investigate if the hydrogen cycling mechanism of energy conservation is operating in *D. gigas* as originally proposed, and its importance in the global energetic metabolism of the cell (Odom and Peck, 1981).

1.7 Scope of the dissertation

The global focus of this thesis is the investigation of the hydrogenase function in *Desulfovibrio gigas* ATCC 19364 during respiratory and fermentative growth. In order to achieve this, we have followed the following steps:

i) Search the *D. gigas* genome for genes encoding hydrogenases;

ii) Elucidate the physiological role of each of the hydrogenase enzymes, the periplasmic HynAB and the cytoplasmic Ech, during respiratory and fermentative conditions. The strategy developed was based on the analysis and comparison of mutant strains in each of the hydrogenases with the wild type, evaluating: a) substrate consumption and metabolites formation in each condition, using high-performance liquid chromatography (HPLC); and b) the concentration of molecular hydrogen (H_2) accumulated during growth, by gas chromatography (GC);

iii) Study of the expression of both hydrogenase genes encoding these by quantitative Real Time PCR as well as Ech protein levels by Western-Blot.

iv) Analysis and annotation of the genome to get further insights into the physiology of the organism;

1.8 References

Akagi, J., Drake, H., Kim, J., and Gevertz, D. (1994) Thiosulfate and trithionate reductases. *Methods in enzymology*.

Albracht, S.P. (1994) Nickel hydrogenases: in search of the active site. *Biochimica Et Biophysica Acta* **1188**: 167-204.

Aubert, C., Brugna, M., Dolla, A., Bruschi, M., and Giudici-Orticoni, M.T. (2000) A sequential electron transfer from hydrogenases to cytochromes in sulfate-reducing bacteria. *Biochimica Et Biophysica Acta* **1476**: 85-92.

Baltazar, C.S., Teixeira, V.H., and Soares, C.M. (2012) Structural features of [NiFeSe] and [NiFe] hydrogenases determining their different properties: a computational approach. *J Biol Inorg Chem* **17**: 543-555.

Barton, L.L., and Fauque, G.D. (2009) Biochemistry, physiology and biotechnology of sulfate-reducing bacteria. *Adv Appl Microbiol* **68**: 41-98.

Barton, L.L., LeGall, J., Odom, J.M., and Peck, H.D., Jr. (1983) Energy coupling to nitrite respiration in the sulfate-reducing bacterium Desulfovibrio gigas. *J Bacteriol* **153**: 867-871.

Brandis, A., and Thauer, R.K. (1981) Growth of Desulfovibrio Species on Hydrogen and Sulfate as Sole Energy-Source. *Journal of General Microbiology* **126**: 249-252.

Broco, M., Rousset, M., Oliveira, S., and Rodrigues-Pousada, C. (2005) Deletion of flavoredoxin gene in Desulfovibrio gigas reveals its participation in thiosulfate reduction. *Febs Letters* **579**: 4803-4807.

Bruschi, M., Hatchikian, C., Le Gall, J., Moura, J.J., and Xavier, A.V. (1976) Purification, characterization and biological activity of three forms of ferredoxin

from the sulfate-reducing bacterium Desulfovibrio gigas. *Biochimica Et Biophysica Acta* **449**: 275-284.

Buckel, W., and Thauer, R. (2013) Energy conservation via electron bifurcating ferredoxin reduction and proton/Na(+) translocating ferredoxin oxidation. *Biochimica Et Biophysica Acta* **1827**: 94-113.

Caffrey, S.M., Park, H.S., Voordouw, J.K., He, Z., Zhou, J., and Voordouw, G. (2007) Function of periplasmic hydrogenases in the sulfate-reducing bacterium Desulfovibrio vulgaris Hildenborough. *J Bacteriol* **189**: 6159-6167.

Carrieri, D., Wawrousek, K., Eckert, C., Yu, J., and Maness, P.C. (2011) The role of the bidirectional hydrogenase in cyanobacteria. *Bioresour Technol* **102**: 8368-8377.

Casalot, L., and Rousset, M. (2001) Maturation of the [NiFe] hydrogenases. *Trends Microbiol* **9**: 228-237.

Casalot, L., Valette, O., De Luca, G., Dermoun, Z., Rousset, M., and de Philip, P. (2002) Construction and physiological studies of hydrogenase depleted mutants of Desulfovibrio fructosovorans. *Fems Microbiology Letters* **214**: 107-112.

Castro, H.F., Williams, N.H., and Ogram, A. (2000) Phylogeny of sulfate-reducing bacteria(1). *Fems Microbiology Ecology* **31**: 1-9.

Chen, L., Pereira, M.M., Teixeira, M., Xavier, A.V., and Le Gall, J. (1994) Isolation and characterization of a high molecular weight cytochrome from the sulfate reducing bacterium Desulfovibrio gigas. *FEBS Lett* **347**: 295-299.

Colbeau, A., and Vignais, P.M. (1992) Use of hupS::lacZ gene fusion to study regulation of hydrogenase expression in Rhodobacter capsulatus: stimulation by H2. *J Bacteriol* **174**: 4258-4264.

Cypionka, H. (2000) Oxygen respiration by desulfovibrio species. *Annu Rev Microbiol* **54**: 827-848.

Cypionka, H., and Barton, L. (1995) Sulfate-Reducing Bacteria. *Springer*.

da Silva, S.M., Voordouw, J., Leitao, C., Martins, M., Voordouw, G., and Pereira, I.A. (2013) Function of formate dehydrogenases in Desulfovibrio vulgaris Hildenborough energy metabolism. *Microbiology* **159**: 1760-1769.

Dubini, A., and Sargent, F. (2003) Assembly of Tat-dependent [NiFe] hydrogenases: identification of precursor-binding accessory proteins. *FEBS letters* **549**: 141-146.

Fauque, G. (1995) Ecology of sulfate-reducing bacteria. *Biotechnology Handbooks* **8**: 217-217.

Fontecilla-Camps, J., Volbeda, A., Cavazza, C., and Nicolet, Y. (2007) Structure/function relationships of [NiFe]- and [FeFe]-hydrogenases. *Chemical Reviews* **107**: 4273-4303.

Fox, J.D., Kerby, R.L., Roberts, G.P., and Ludden, P.W. (1996) Characterization of the CO-induced, CO-tolerant hydrogenase from Rhodospirillum rubrum and the gene encoding the large subunit of the enzyme. *Journal of Bacteriology* **178**: 1515-1524.

Frazao, C., Sieker, L., Sheldrick, G., Lamzin, V., LeGall, J., and Carrondo, M.A. (1999) Ab initio structure solution of a dimeric cytochrome c3 from Desulfovibrio gigas containing disulfide bridges. *J Biol Inorg Chem* **4**: 162-165.

Frazao, C., Silva, G., Gomes, C.M., Matias, P., Coelho, R., Sieker, L. *et al*. (2000) Structure of a dioxygen reduction enzyme from Desulfovibrio gigas. *Nature Structural Biology* **7**: 1041-1045.

Galushko, A., Minz, D., Schink, B., and Widdel, F. (1999) Anaerobic degradation of naphthalene by a pure culture of a novel type of marine sulphate-reducing bacterium. *Environmental Microbiology* **1**: 415-420.

Gross, R., Simon, J., Theis, F., and Kroger, A. (1998) Two membrane anchors of Wolinella succinogenes hydrogenase and their function in fumarate and polysulfide respiration. *Archives of Microbiology* **170**: 50-58.

Hansen, T.A. (1994) Metabolism of sulfate-reducing prokaryotes. *Antonie Van Leeuwenhoek* **66**: 165-185.

Harms, G., Zengler, K., Rabus, R., Aeckersberg, F., Minz, D., Rossello-Mora, R., and Widdel, F. (1999) Anaerobic oxidation of o-xylene, m-xylene, and homologous alkylbenzenes by new types of sulfate-reducing bacteria. *Appl Environ Microbiol* **65**: 999-1004.

Haveman, S.A., Brunelle, V., Voordouw, J.K., Voordouw, G., Heidelberg, J.F., and Rabus, R. (2003) Gene expression analysis of energy metabolism mutants of Desulfovibrio vulgaris Hildenborough indicates an important role for alcohol dehydrogenase. *Journal of Bacteriology* **185**: 4345-4353.

Hedderich, R., and Forzi, L. (2005) Energy-converting [NiFe] hydrogenases: more than just H2 activation. *J Mol Microbiol Biotechnol* **10**: 92-104.

Heidelberg, J.F., Seshadri, R., Haveman, S.A., Hemme, C.L., Paulsen, I.T., Kolonay, J.F. *et al*. (2004) The genome sequence of the anaerobic, sulfate-reducing bacterium Desulfovibrio vulgaris Hildenborough. *Nature Biotechnology* **22**: 554-559.

Herrmann, G., Jayamani, E., Mai, G., and Buckel, W. (2008) Energy conservation via electron-transferring flavoprotein in anaerobic bacteria. *J Bacteriol* **190**: 784-791.

Hsieh, Y.C., Liu, M.Y., Le Gall, J., and Chen, C.J. (2005) Anaerobic purification and crystallization to improve the crystal quality: ferredoxin II from Desulfovibrio gigas. *Acta Crystallogr D Biol Crystallogr* **61**: 780-783.

Jorgensen, B.B. (1982) Ecology of the bacteria of the sulphur cycle with special reference to anoxic-oxic interface environments. *Philos Trans R Soc Lond B Biol Sci* **298**: 543-561.

Keller, K.L., and Wall, J.D. (2011) Genetics and molecular biology of the electron flow for sulfate respiration in desulfovibrio. *Front Microbiol* **2**: 135.

Kremer, D.R., Nienhuis-Kuiper, H.E., and Hansen, T.A. (1988a) Ethanol dissimilation in Desulfovibrio. *Archives of Microbiology* **150**.

Kremer, D.R., Nienhuis-Kuiper, H.E., Timmer, C.J., and Hansen, T.A. (1988b) Catabolism of malate and related dicarboxylic acids in various Desulfovibrio strains and the involvement of an oxygen-labile NADPH dehydrogenase. *Archives of Microbiology* **151**.

Kroger, A., Biel, S., Simon, J., Gross, R., Unden, G., and Lancaster, C.R. (2002) Fumarate respiration of Wolinella succinogenes: enzymology, energetics and coupling mechanism. *Biochimica Et Biophysica Acta* **1553**: 23-38.

Krumholz, L., Wang, L., Beck, D., Wang, T., Hackett, M., Mooney, B. *et al*. (2013) Membrane protein complex of APS reductase and Qmo is present in Desulfovibrio vulgaris and Desulfovibrio alaskensis. *Microbiology (Reading, England)* **159**: 2162-2168.

Kunkel, A., Vorholt, J.A., Thauer, R.K., and Hedderich, R. (1998) An Escherichia coli hydrogenase-3-type hydrogenase in methanogenic archaea. *European Journal of Biochemistry* **252**: 467-476.

Legall, J. (1963) A New Species of Desulfovibrio. *J Bacteriol* **86**: 1120.

Lemos, R.S., Fernandes, A.S., Pereira, M.M., Gomes, C.M., and Teixeira, M. (2002) Quinol:fumarate oxidoreductases and succinate:quinone oxidoreductases: phylogenetic relationships, metal centres and membrane attachment. *Biochimica Et Biophysica Acta* **1553**: 158-170.

Li, C., Peck, H.D., Jr., LeGall, J., and Przybyla, A.E. (1987) Cloning, characterization, and sequencing of the genes encoding the large and small subunits of the periplasmic [NiFe]hydrogenase of Desulfovibrio gigas. *DNA* **6**: 539-551.

Li, F., Hinderberger, J., Seedorf, H., Zhang, J., Buckel, W., and Thauer, R.K. (2008) Coupled ferredoxin and crotonyl coenzyme A (CoA) reduction with NADH catalyzed by the butyryl-CoA dehydrogenase/Etf complex from Clostridium kluyveri. *J Bacteriol* **190**: 843-850.

Li, X., Luo, Q., Wofford, N.Q., Keller, K.L., McInerney, M.J., Wall, J.D., and Krumholz, L.R. (2009) A molybdopterin oxidoreductase is involved in H2 oxidation in Desulfovibrio desulfuricans G20. *J Bacteriol* **191**: 2675-2682.

Lloyd, J.R., Mabbett, A.N., Williams, D.R., and Macaskie, L.E. (2001) Metal reduction by sulphate-reducing bacteria: physiological diversity and metal specificity. *Hydrometallurgy* **59**.

Lloyd, J.R., Ridley, J., Khizniak, T., Lyalikova, N.N., and Macaskie, L.E. (1999) Reduction of technetium by Desulfovibrio desulfuricans: biocatalyst characterization and use in a flowthrough bioreactor. *Appl Environ Microbiol* **65**: 2691-2696.

Lobo, S.A., Melo, A.M., Carita, J.N., Teixeira, M., and Saraiva, L.M. (2007) The anaerobe Desulfovibrio desulfuricans ATCC 27774 grows at nearly atmospheric oxygen levels. *FEBS Lett* **581**: 433-436.

Loubinoux, J., Bronowicki, J.-P., Pereira, I., Mougenel, J.-L., and Faou, A. (2002) Sulfate-reducing bacteria in human feces and their association with inflammatory bowel diseases. *Fems Microbiology Ecology* **40**: 107-112.

Lovley, D.R. (1993) Dissimilatory metal reduction. *Annu Rev Microbiol* **47**: 263-290.

Lupton, F.S., Conrad, R., and Zeikus, J.G. (1984) Physiological function of hydrogen metabolism during growth of sulfidogenic bacteria on organic substrates. *J Bacteriol* **159**: 843-849.

Lyon, E.J., Shima, S., Buurman, G., Chowdhuri, S., Batschauer, A., Steinbach, K., and Thauer, R.K. (2004) UV-A/blue-light inactivation of the 'metal-free' hydrogenase (Hmd) from methanogenic archaea. *Eur J Biochem* **271**: 195-204.

Magee, E., Ensley, B., and Barton, L. (1978) An assessment of growth yields and energy coupling in Desulfovibrio. *Archives of Microbiology*.

Malki, S., Saimmaime, I., De Luca, G., Rousset, M., Dermoun, Z., and Belaich, J.P. (1995) Characterization of an operon encoding an NADP-reducing hydrogenase in Desulfovibrio fructosovorans. *J Bacteriol* **177**: 2628-2636.

Malki, S., De Luca, G., Fardeau, M.L., Rousset, M., Belaich, J.P., and Dermoun, Z. (1997) Physiological characteristics and growth behavior of single and double hydrogenase mutants of Desulfovibrio fructosovorans. *Archives of Microbiology* **167**: 38-45.

Mander, G., Duin, E., Linder, D., Stetter, K., and Hedderich, R. (2002) Purification and characterization of a membrane-bound enzyme complex from the sulfate-reducing archaeon Archaeoglobus fulgidus related to heterodisulfide reductase from methanogenic archaea. *European journal of biochemistry / FEBS* **269**: 1895-1904.

Matias, P.M., Pereira, I.A., Soares, C.M., and Carrondo, M.A. (2005) Sulphate respiration from hydrogen in Desulfovibrio bacteria: a structural biology overview. *Prog Biophys Mol Biol* **89**: 292-329.

Matias, P.M., Morais, J., Coelho, R., Carrondo, M.A., Wilson, K., Dauter, Z., and Sieker, L. (1996) Cytochrome c3 from Desulfovibrio gigas: crystal structure at 1.8 A resolution and evidence for a specific calcium-binding site. *Protein Sci* **5**: 1342-1354.

Meuer, J., Kuettner, H.C., Zhang, J.K., Hedderich, R., and Metcalf, W.W. (2002) Genetic analysis of the archaeon Methanosarcina barkeri Fusaro reveals a central role for Ech hydrogenase and ferredoxin in methanogenesis and carbon fixation. *Proceedings of the National Academy of Sciences of the United States of America* **99**: 5632-5637.

Meyer, B., Kuehl, J., Deutschbauer, A.M., Price, M.N., Arkin, A.P., and Stahl, D.A. (2013) Variation among Desulfovibrio species in electron transfer systems used for syntrophic growth. *J Bacteriol* **195**: 990-1004.

Montet, Y., Amara, P., Volbeda, A., Vernede, X., Hatchikian, E.C., Field, M.J. *et al*. (1997) Gas access to the active site of Ni-Fe hydrogenases probed by X-ray crystallography and molecular dynamics. *Nature Structural Biology* **4**: 523-526.

Muller, V., Imkamp, F., Biegel, E., Schmidt, S., and Dilling, S. (2008) Discovery of a ferredoxin:NAD+-oxidoreductase (Rnf) in Acetobacterium woodii: a novel potential coupling site in acetogens. *Ann N Y Acad Sci* **1125**: 137-146.

Mutambanengwe, C.C., Togo, C.A., and Whiteley, C.G. (2007) Decolorization and degradation of textile dyes with biosulfidogenic hydrogenases. *Biotechnol Prog* **23**: 1095-1100.

Muyzer, G., and Stams, A. (2008) The ecology and biotechnology of sulphate-reducing bacteria. *Nature reviews Microbiology* **6**: 441-454.

Nicolet, Y., Cavazza, C., and Fontecilla-Camps, J.C. (2002) Fe-only hydrogenases: structure, function and evolution. *J Inorg Biochem* **91**: 1-8.

Noguera, Brusseau, Rittmann, and Stahl (1998) A unified model describing the role of hydrogen in the growth of desulfovibrio vulgaris under different environmental conditions. *Biotechnology and bioengineering* **59**: 732-746.

Odom, J.M., and Peck, H.D.J. (1981) Hydrogen cycling as a general mechanism for energy coupling in the sulfate-reducing bacteria Desulfovibrio sp. *Fems Microbiology Letters* **12**: 47-50.

Pankania, I.P., Alfred M Spormann, W. Allan Hamilton, and Thauer, a.R.K. (1988) Lactate conversion to acetate, CO2 and H2 in cell suspensions of Desulfovibrio vulgaris (Marburg): indications for the involvement of an energy driven reaction. *Archives Microbiology* **150**: 26-31.

Pankhania, I.P., Gow, L.A., and Hamilton, W.A. (1986) The Effect of Hydrogen on the Growth of Desulfovibrio vulgaris (Hildenborough) on Lactate. *Microbiology* **132**.

Pankhania, I.P., Alfred, M.S., Hamilton, W.A., and Rudolf, K.T. (1988) Lactate conversion to acetate, CO2 and H2 in cell suspensions of Desulfovibrio vulgaris (Marburg): indications for the involvement of an energy driven reaction. *Archives of Microbiology* **150**.

Peck, H.D., and LeGall, J. (1994) Inorganic microbial sulfur metabolism. *Academic Press*.

Peck, H.D., LeGall, J., Lespinat, P.A., Berlier, Y., and Fauque, G. (1987) A direct demonstration of hydrogen cycling by< i> Desulfovibrio vulgaris</i> employing membrane-inlet mass spectrometry. *Fems Microbiology Letters* **40**: 295-299.

Pereira, I.A., Ramos, A.R., Grein, F., Marques, M.C., da Silva, S.M., and Venceslau, S.S. (2011) A comparative genomic analysis of energy metabolism in sulfate reducing bacteria and archaea. *Front Microbiol* **2**: 69.

Pereira, I.A.C., Haveman, S.A., and Voordouw, G. (2007) Biochemical, genetic and genomic characterization of anaerobic electron transport pathways in sulphate-reducing delta-proteobacteria. *Sulphate-reducing bacteria: environmental and engineered systems*: 215-240.

Pereira, I.A.C., Célia, V.R., António, V.X., LeGall, J., and Miguel, T. (1998) Electron transfer between hydrogenases and mono- and multiheme cytochromes in Desulfovibrio ssp. *Journal of Biological Inorganic Chemistry* **3**.

Pereira, P.M., Teixeira, M., Xavier, A.V., Louro, R.O., and Pereira, I.A. (2006) The Tmc complex from Desulfovibrio vulgaris hildenborough is involved in transmembrane electron transfer from periplasmic hydrogen oxidation. *Biochemistry* **45**: 10359-10367.

Pereira, P.M., He, Q., Valente, F.M., Xavier, A.V., Zhou, J., Pereira, I.A., and Louro, R.O. (2008) Energy metabolism in Desulfovibrio vulgaris Hildenborough: insights from transcriptome analysis. *Antonie Van Leeuwenhoek* **93**: 347-362.

Pires, R., Lourenço, A., Morais, F., Teixeira, M., Xavier, A., Saraiva, L., and Pereira, I. (2003) A novel membrane-bound respiratory complex from Desulfovibrio desulfuricans ATCC 27774. *Biochimica et biophysica acta* **1605**: 67-82.

Pires, R.H., Venceslau, S.S., Morais, F., Teixeira, M., Xavier, A.V., and Pereira, I.A. (2006) Characterization of the Desulfovibrio desulfuricans ATCC 27774 DsrMKJOP complex--a membrane-bound redox complex involved in the sulfate respiratory pathway. *Biochemistry* **45**: 249-262.

Plugge, C.M., Scholten, J.C., Culley, D.E., Nie, L., Brockman, F.J., and Zhang, W. (2010) Global transcriptomics analysis of the Desulfovibrio vulgaris change from syntrophic growth with Methanosarcina barkeri to sulfidogenic metabolism. *Microbiology* **156**: 2746-2756.

Pohorelic, B.K.J., Voordouw, J.K., Lojou, E., Dolla, A., Harder, J., and Voordouw, G. (2002) Effects of deletion of genes encoding Fe-only hydrogenase of Desulfovibrio vulgaris Hildenborough on hydrogen and lactate metabolism. *Journal of Bacteriology* **184**: 679-686.

Postgate, J.R. (1984) *The sulphate-reducing bacteria*. Cambridge Cambridgeshire ; New York: Cambridge University Press.

Rabus, R., Hansen, T.A., and Widdel, F. (2006) Dissimilatory sulfate- and sulfur-reducing prokaryotes. In. Dworkin, M., Falkow, S., Rosenberg, E., Schleifer, K.H., and Stackebrandt, E. (ed).

Rabus, R., Fukui, M., Wilkes, H., and Widdle, F. (1996) Degradative capacities and 16S rRNA-targeted whole-cell hybridization of sulfate-reducing bacteria in an anaerobic enrichment culture utilizing alkylbenzenes from crude oil. *Appl Environ Microbiol* **62**: 3605-3613.

Ramos, A.R., Keller, K.L., Wall, J.D., and Pereira, I.A. (2012) The Membrane QmoABC Complex Interacts Directly with the Dissimilatory Adenosine 5'-Phosphosulfate Reductase in Sulfate Reducing Bacteria. *Front Microbiol* **3**: 137.

Raskin, L., Rittmann, B.E., and Stahl, D.A. (1996) Competition and coexistence of sulfate-reducing and methanogenic populations in anaerobic biofilms. *Appl Environ Microbiol* **62**: 3847-3857.

Riederer-Henderson, M.A., and Peck Jr, H.D. (1986) Properties of formate dehydrogenase from Desulfovibrio gigas. *Canadian Journal of Microbiology* **32**: 430-435.

Rodrigues, P., Graca, F., Macedo, A.L., Moura, I., and Moura, J.J. (2001) Characterization of recombinant Desulfovibrio gigas ferredoxin. *Biochem Biophys Res Commun* **289**: 630-633.

Rodrigues, R., Valente, F.M., Pereira, I.A., Oliveira, S., and Rodrigues-Pousada, C. (2003) A novel membrane-bound Ech [NiFe] hydrogenase in Desulfovibrio gigas. *Biochem Biophys Res Commun* **306**: 366-375.

Rossi, M., Pollock, W.B., Reij, M.W., Keon, R.G., Fu, R., and Voordouw, G. (1993) The hmc operon of Desulfovibrio vulgaris subsp. vulgaris Hildenborough encodes a potential transmembrane redox protein complex. *J Bacteriol* **175**: 4699-4711.

Rousset, M., Dermoun, Z., Chippaux, M., and Belaich, J.P. (1991) Marker exchange mutagenesis of the hydN genes in Desulfovibrio fructosovorans. *Mol Microbiol* **5**: 1735-1740.

Rousset, M., Magro, V., Forget, N., Guigliarelli, B., Belaich, J.P., and Hatchikian, E.C. (1998) Heterologous expression of the Desulfovibrio gigas [NiFe] hydrogenase in Desulfovibrio fructosovorans MR400. *J Bacteriol* **180**: 4982-4986.

Saraiva, L.M., da Costa, P.N., Conte, C., Xavier, A.V., and LeGall, J. (2001) In the facultative sulphate/nitrate reducer Desulfovibrio desulfuricans ATCC 27774, the nine-haem cytochrome c is part of a membrane-bound redox complex mainly expressed in sulphate-grown cells. *Biochimica Et Biophysica Acta* **1520**: 63-70.

Schlegel, K., Welte, C., Deppenmeier, U., and Müller, V. (2012) Electron transport during aceticlastic methanogenesis by Methanosarcina acetivorans involves a sodium-translocating Rnf complex. *The FEBS journal* **279**: 4444-4452.

Schworer, B., Fernandez, V.M., Zirngibl, C., and Thauer, R.K. (1993) H2-forming N5,N10-methylenetetrahydromethanopterin dehydrogenase from Methanobacterium thermoautotrophicum. Studies of the catalytic mechanism of H2 formation using hydrogen isotopes. *Eur J Biochem* **212**: 255-261.

Sebban, C., Blanchard, L., Bruschi, M., and Guerlesquin, F. (1995) Purification and characterization of the formate dehydrogenase from Desulfovibrio vulgaris Hildenborough. *FEMS Microbiol Lett* **133**: 143-149.

Shen, Y., and Buick, R. (2004) The antiquity of microbial sulfate reduction. *Earth-Science Reviews* **64**.

So, C.M., and Young, L.Y. (1999) Isolation and characterization of a sulfate-reducing bacterium that anaerobically degrades alkanes. *Appl Environ Microbiol* **65**: 2969-2976.

Stock, D., Leslie, A.G., and Walker, J.E. (1999) Molecular architecture of the rotary motor in ATP synthase. *Science* **286**: 1700-1705.

Thauer, R., Kaster, A.-K., Seedorf, H., Buckel, W., and Hedderich, R. (2008) Methanogenic archaea: ecologically relevant differences in energy conservation. *Nature reviews Microbiology* **6**: 579-591.

Thauer, R.K., Stackebrandt, E., and Hamilton, W.A. (2007) Energy metabolism phylogenetic diversity of sulphate-reducing bacteria. *Sulphate-reducing bacteria: environmental and engineered systems*: 1-37.

Valente, F.M., Saraiva, L.M., LeGall, J., Xavier, A.V., Teixeira, M., and Pereira, I.A. (2001) A membrane-bound cytochrome c3: a type II cytochrome c3 from Desulfovibrio vulgaris Hildenborough. *Chembiochem* **2**: 895-905.

Valente, F.M., Almeida, C.C., Pacheco, I., Carita, J., Saraiva, L.M., and Pereira, I.A. (2006) Selenium is involved in regulation of periplasmic hydrogenase gene expression in Desulfovibrio vulgaris Hildenborough. *J Bacteriol* **188**: 3228-3235.

Venceslau, S.S., Lino, R.R., and Pereira, I.A. (2010) The Qrc membrane complex, related to the alternative complex III, is a menaquinone reductase involved in sulfate respiration. *Journal of Biological Chemistry* **285**: 22774-22783.

Vignais, P.M., and Colbeau, A. (2004) Molecular biology of microbial hydrogenases. *Curr Issues Mol Biol* **6**: 159-188.

Vignais, P.M., and Billoud, B. (2007) Occurrence, classification, and biological function of hydrogenases: an overview. *Chemical Reviews* **107**: 4206-4272.

Vignais, P.M., Billoud, B., and Meyer, J. (2001) Classification and phylogeny of hydrogenases. *Fems Microbiology Reviews* **25**: 455-501.

Vincent, K., Cracknell, J., Parkin, A., and Armstrong, F. (2005) Hydrogen cycling by enzymes: electrocatalysis and implications for future energy technology. *Dalton transactions (Cambridge, England : 2003)*: 3397-3403.

Volbeda, A., Charon, M.H., Piras, C., Hatchikian, E.C., Frey, M., and Fontecilla-Camps, J.C. (1995) Crystal structure of the nickel-iron hydrogenase from Desulfovibrio gigas. *Nature* **373**: 580-587.

Voordouw, G. (1995) The genus desulfovibrio: the centennial. *Appl Environ Microbiol* **61**: 2813-2819.

Voordouw, G. (2000) A universal system for the transport of redox proteins: early roots and latest developments. *Biophysical Chemistry* **86**: 131-140.

Voordouw, G. (2002) Carbon monoxide cycling by Desulfovibrio vulgaris Hildenborough. *J Bacteriol* **184**: 5903-5911.

Walker, C.B., He, Z., Yang, Z.K., Ringbauer, J.A., Jr., He, Q., Zhou, J. *et al*. (2009) The electron transfer system of syntrophically grown Desulfovibrio vulgaris. *J Bacteriol* **191**: 5793-5801.

Welte, C., Kratzer, C., and Deppenmeier, U. (2010a) Involvement of Ech hydrogenase in energy conservation of Methanosarcina mazei. *FEBS J* **277**: 3396-3403.

Welte, C., Kallnik, V., Grapp, M., Bender, G., Ragsdale, S., and Deppenmeier, U. (2010b) Function of Ech hydrogenase in ferredoxin-dependent, membrane-bound electron transport in Methanosarcina mazei. *J Bacteriol* **192**: 674-678.

Widdel, F., and Rabus, R. (2001) Anaerobic biodegradation of saturated and aromatic hydrocarbons. *Current Opinion in Biotechnology* **12**: 259-276.

Widdel, F., Musat, F., Knittel, K., and Galushko, A. (2007) Anaerobic degradation of hydrocarbons with sulphate as electron acceptor. *Sulphate-reducing bacteria: environmental and engineered systems*: 265-303.

Wu, L.F., Chanal, A., and Rodrigue, A. (2000) Membrane targeting and translocation of bacterial hydrogenases. *Archives of Microbiology* **173**: 319-324.

Zane, G.M., Yen, H.C., and Wall, J.D. (2010) Effect of the deletion of qmoABC and the promoter-distal gene encoding a hypothetical protein on sulfate reduction in Desulfovibrio vulgaris Hildenborough. *Appl Environ Microbiol* **76**: 5500-5509.

Zaunmuller, T., Kelly, D.J., Glockner, F.O., and Unden, G. (2006) Succinate dehydrogenase functioning by a reverse redox loop mechanism and fumarate reductase in sulphate-reducing bacteria. *Microbiology* **152**: 2443-2453.

Zhang, W., Culley, D.E., Scholten, J.C., Hogan, M., Vitiritti, L., and Brockman, F.J. (2006) Global transcriptomic analysis of Desulfovibrio vulgaris on different electron donors. *Antonie Van Leeuwenhoek* **89**: 221-237.

Zirngibl, C., Van Dongen, W., Schworer, B., Von Bunau, R., Richter, M., Klein, A., and Thauer, R.K. (1992) H2-forming methylenetetrahydromethanopterin dehydrogenase, a novel type of hydrogenase without iron-sulfur clusters in methanogenic archaea. *Eur J Biochem* **208**: 511-520.

Chapter 2

The genome of SRB model organism *Desulfovibrio gigas*

The work presented in this chapter includes data of a manuscript in submission: Morais-Silva F.*, Rezende A.*, Pimentel C., Santos C., Clemente C., Varela-Raposo A., Resende D., da Silva S., de Oliveira L., Costa D., Matos M., Flores O., Ruiz J. and Rodrigues-Pousada C. (2013) Genome sequence of the model sulfate reducer *Desulfovibrio gigas*: a comparative analysis within the *Desulfovibrio* genus.

The author of this dissertation had a major participation in all aspects of this work, except in the assembly of the genome sequences, which was performed by Dr. Antonio Rezende and Dr. Jeronimo Ruiz and his group.

2.1 Summary

Desulfovibrio gigas is a model organism of the sulfate reducing bacteria group of which aspects of the energy metabolism and stress response have been extensively studied. The complete genomic context of this organism was however not yet available. The sequencing of the *D. gigas* genome provides insights into the integrated network of energy conserving complexes and structures present in this bacterium. Comparison with other *Desulfovibrio spp.* reveals the presence of two different CRISPR/Cas systems in *D. gigas.* Phylogenetic analysis using conserved proteins (*rpoB* and *gyrB*) indicates two main groups of *Desulfovibrio* spp, being *D. gigas* more closely related to *D. vulgaris* and *D. desulfuricans* strains. Gene duplications were identified: fumarate reductase, formate dehydrogenase and super oxide dismutase. Complexes not yet described for the *Desulfovibrio* genus were detected: Mnh complex; a v-type ATP-synthase; and an aerobic-type CO dehydrogenase. A low number of hydrogenase and absence of the *codh/acs* and *pfl* genes indicate that intermediate cycling mechanisms may contribute much less to the energy gain in *D. gigas* when compared to other *Desulfovibrio spp.* This might be compensated by the presence of other unique genomic arrangements of complexes such as the Rnf and the Hdr/Flox, or by the presence of NAD(P)H related complexes, like the *nuo*, *nfnAB* or *mnh*.

2.2 Introduction

Sulfate reducing bacteria (SRB) are probably one of the most ancient forms of life on Earth. This group of anaerobic microorganisms, widespread in anoxic habitats, uses sulfate as main terminal electron acceptor to degrade organic compounds, with the consequent production of sulfide (Muyzer and Stams, 2008). This process is extremely important in the sulfur and carbon cycles, since approximately 50% of the organic carbon mineralization in marine sediments is due to sulfate reduction (Jorgensen, 1982). The sulfide produced by these organisms is incorporated into sulfur containing amino acids and proteins with enzymatic activity. SRB are metabolically very versatile microorganisms, being able to use organic and inorganic carbon substrates, as well as other short-chain fatty acids or ethanol for sulfate reduction. In recent years, new species were found to be able to grow on more diverse and less degradable substrates such as hydrocarbons or aromatic compounds (Rabus *et al*., 2006). Furthermore, due to the fact that many SRB use H_2 as an important substrate for sulfate reduction, they are able to participate in interspecies hydrogen transfer processes in synthropic communities with archea (Walker *et al*., 2009; Plugge *et al*., 2010; Li *et al*., 2011). As a result of its metabolic flexibility, SRB can be found in almost all ecological environments on the planet. Moreover, these bacteria possess a wide biotechnology potential especially in bioremediation by helping removal of sulfate and heavy metals from natural environments and of industrial waste liquids and sewage (Janssen *et al*., 2001; Lenz *et al*., 2008). On the other hand, due to the production of high amounts of hydrogen sulfide, SRB have a large negative economic impact mainly as causative agents of microbial corrosion processes in anaerobic environments like offshore oil production or waterlogged clay soils, resulting in economic losses, especially, for oil industry (Hamilton, 1985). Furthermore, they can create problems regarding the change of oil composition and souring of petroleum reservoirs (Huang and Larter, 2005; Vance and Thrasher, 2005).

Recent advances in genomics, biochemistry and genetics of the SRB have greatly helped to identify the essential enzymes and complexes that participate in sulfate respiration. The reduction of sulfate to sulfide during the respiratory process occurs in the cytoplasm. As such, electron transport chains and carriers must provide a link for the flow of the reducing equivalents ($[H^+]$ and electrons) between dehydrogenases and the terminal reductases (Rabus *et al*., 2006). Despite many efforts to understand the sites and mechanisms of energy conservation in sulfate respiration, the electron-transfer pathways that generate ATP from oxidative phosphorylation and create a proton gradient are not yet fully understood (Pereira *et al*., 2011). Most of the studies are focused in the understanding of the principles of sulfate reduction using *Desulfovibrio* genus. Among the various members of this genera, *Desulfovibrio gigas,* a curved rod bacterium, whose name was inspired by its unusual size (up to 11µm) was for the first time isolated in 1963 by Jean LeGall from a water pond (Legall, 1963). After its isolation, this bacterium was used by many different groups to elucidate the structure of enzymes participating in energy transfer reactions such as hydrogenases, formate dehydrogenases, ferredoxins, cytochromes, and the xantine oxidase-related aldehyde oxido-reductase (MOP) (Ambler *et al*., 1969; Romao *et al*., 1995; Volbeda *et al*., 1995; Matias *et al*., 1996; Frazao *et al*., 2000; Raaijmakers *et al*., 2002; Hsieh *et al*., 2005). Mechanistic and functional processes related to the energy metabolism and stress response have been as well studied in *D. gigas* (Silva *et al*., 2001; Broco *et al*., 2005; Rodrigues *et al*., 2006a; Morais-Silva *et al*., 2013). However, despite all these important information acquired after many years of research using this bacterium as model organism, a clear whole-genomic context of the genes and structures was not yet available for *D. gigas*. Previous analyses and comparison between the different species of SRB revealed that the composition of energy metabolism proteins, as well as stress related proteins can vary quite significantly (Rabus *et al*., 2006; Pereira *et al*., 2008; Pereira *et al*., 2011). *D. giga*s may therefore react to environmental cues and adapt to different environments by using different metabolic and structural

components. Genome sequencing and analysis is an important tool in order to fully understand which components may be involved in these adaptation and survival mechanisms. Because we were already involved in the study of many metabolic aspects of *D. gigas* ATCC19364, we decided to examine the whole-genome sequence of this organism and to perform a comparative genomic analysis with other *Desulfovibrionaceae*.

2.3 Materials and Methods

DNA extraction and sequencing

D. gigas ATCC19364 was grown anaerobically in 50mL flasks, at 37°C in a basal medium as described in (Varela-Raposo *et al*., 2013). RNase treated genomic DNA was extracted using Wizard Genomic DNA Purification Kit (Promega). Sequencing of *Desulfovibrio gigas* ATCC19364 was performed with a combination of several approaches. Two small-insert (2-6 kb) plasmid libraries were constructed in pZero1 vector (Invitrogen) or Zero Blunt TOPO PCR Cloning Kit (Invitrogen), after partial digestion of genomic DNA with Sau3AI or DNA sonication (Branson Sonifier 450D), respectively. Sequencing was performed with an ABI PRISM 3700 DNA analyser, using dye-terminator chemistry (Sanger sequencing) with a pair of universal primers (M13 Fwd and M13 Rev). In addition, high throughput random sequencing was performed using Roche Diagnostics 454 GS20 sequencing platform (Keygene) and Illumina´s Solexa sequencing technology. Moreover, Illumina´s sequencing was performed using two pair-ended libraries of 290 and 4100bp. Final gap closure was obtained either by primer walking or by gDNA re-sequencing in the Personal Genome Machine (PGM) platform set up, using Ion Torrent sequencing technology, from STAB-VIDA.

Assembly, sequence analysis and annotation

Reads were trimmed for platform dependent systematic errors, then quality

evaluated using Phred parameter with cutoff ranging from Q=20 to Q=26 (Ewing and Green, 1998; Ewing *et al*., 1998). *Ab initio* assembly with high quality reads was performed using Velvet version 0.7.55 software (Zerbino and Birney, 2008), and the consensus genomic sequence were obtained with Phrap (http://www.phrap.org/phredphrapconsed.html). In addition, reference genome assembly strategies were applied using publicly available *Desulfovibrio* genomes (*Desulfovibrio vulgaris* str. Hildenborough GenBank ID: NC_002937; *Desulfovibrio alaskensis* G20; GenBank ID: NC_007519; and *Desulfovibrio magneticus* RS-1; GenBank ID: NC_012796). Contigs and scaffolds were ordered and oriented with ABACAS software (Assefa *et al*., 2009). All assemblies were merged using in house developed Perl scripts. Each sequencing strategy contributed to the total genome coverage, as follows: Sanger sequencing 25,975 reads (coverage =~7.39x); 454 Sequencing™ on the Genome Sequencer FLX ™ System 275549 (coverage =~7.5); Ion Torrent™ technology: 3693899 reads (coverage=~98.48); and Solexa Sequencing Technology 3693899 reads (coverage =~46.31). The completed genome achieved an average of 159.7 fold sequence coverage per base.

The annotation procedures involved the use of several algorithms in a multi-step process. Structural annotation was performed using the following softwares: FgenesB: gene predictor (www.softberry.com); RNAmmer: rRNA predictor (Lagesen *et al*., 2007) tRNA-scan-SE: tRNA predictor (Lowe and Eddy, 1997); and Tandem Repeat Finder: repetitive DNA predictor (tandem.bu.edu/trf/trf.html). Functional annotation was performed by similarity analyses, using public databases and InterProScan analysis (Zdobnov and Apweiler, 2001). Manual annotation was performed using Artemis (Rutherford *et al*., 2000). Codon usage bias was evaluated using the EMBOSS package.

Comparative genome analysis

Comparative analyses for *Desufovibrio* were performed using the BLAST –

NCBI (Altschul *et al*., 1990) and InterProScan databases. The Mauve algorithm (gel.ahabs.wisc.edu/mauve) and the ACT (Carver *et al*., 2005) tool were used to explore genome synteny.

Phylogenomics analysis

Evolutionary relationship was constructed using multiple concatenated genes. This approach has retrieved a more robust phylogeny (Delsuc *et al*., 2003; Teeling *et al*., 2003; Hedges *et al*., 2004; Wolf *et al*., 2004)**.** The protein sequences coded by rpoB and gyrB genes of ten *Desulfovibrio* species were downloaded from GenBank ftp site (ftp://ftp.ncbi.nlm.nih.gov/). A total of 21 isolates were analysed. The protein sequences of *Escherichia coli* K12 were used as an outgroup. The rpoB and gyrB sequences were concatenated in a super-protein sequence and aligned using MAFFT software (Katoh *et al*., 2002). Subsequently, in order to choose the evolutionary model which best fits the alignment, 120 models were tested using the ProtTest version 2. (Abascal *et al.*, 2005). The chosen model was LG (Le and Gascuel, 2008) including invariant sites and number of rate categories of change by the gamma distribution. The alignment was used as input for the PhyML version 3.0 that is a simple, fast and accurate algorithm to estimate large phylogenies by Maximum Likelihood which is a probabilistic method for evolutionary inference (Guindon *et al.*, 2010).

The evolutionary history of Cas1 proteins was inferred by using the Maximum Likelihood method based on the JTT matrix-based model (Jones *et al*., 1992). Initial tree(s) for the heuristic search were obtained automatically by applying Neighbor-Join and BioNJ algorithms to a matrix of pairwise distances estimated using a JTT model, and then selecting the topology with superior log likelihood value. The analysis involved 11 amino acid sequences. All positions containing gaps and missing data were eliminated. There were a total of 247 positions in the final dataset. Evolutionary analyses were conducted in MEGA5 (Tamura *et al*., 2011).

2.4 Results and Discussion

2.4.1 General genome features

The genome of *D. gigas* (CP006585) consists of one circular chromosome of 3,693,899 base-pairs (bp) having 3,370 genes of which 3,273 are protein coding (see Table 2.1 and Fig 2.1A). Its genome has a G+C content of 63.4% that reflects a biased codon usage. Indeed *D. gigas* prefers high G+C codons, with a clear preference for cytosine (C) in the 3rd position using. (see Table 2.2). The genome is very compact as observed by its gene density of 1,128 bp per gene and the average length of each gene is 993 bp. It contains 19 transposases that represents a low number when compared with other SRB genomes in which the average number is 34, indicating a low rate of re-organization of its genome (Bennett, 2004). The genome presents 47 pseudogenes, 48 tRNAs and 9 selenocysteine containing proteins. Surprisingly, it was found one single operon of rRNA in contrast to what was detected in other *Desulfovibrio* spp that do contain between 3 and 6 operons. The recently sequenced genome of the new strain *Salinarchaeum* sp. HArcht-Bsk1T, that is able to grow in high salt concentrations, also contains one single rRNA operon (Dominova *et al*., 2013) as well as the bacterium *Mycobacteria,* a fact that was associated to its slow growth (Arnvig *et al*., 2005). The high generation time of *D. gigas* of around 8 hours may be related to this fact (Morais-Silva *et al*., 2013). It is also relevant to note the presence of 6 repeats of clustered regularly interspaced short palindromic repeats (CRISPR), with two of them being flanked by Cas operons (Table S26 and Fig 2.2A).

Table 2.1. General genome features of *Desulfovibrio gigas.*

Features	Value	% of total
Genome size (bp)	3,693,899	100
DNA coding region (bp)	3,249,714	87.98
G+C content (bp)	2,341,530	63.39
Extracromossomal elements	1	
Number of replicons	1	
Total Number of genes	3,370	100

Stable rRNAS		
rRNAs	3	0.09
tRNAs	48	1.42
Protein-coding genes	3,273	97.09
Genes density (bp/gene)	1,128	
Average length of a gene (bp)	993	
Pseudogenes	47	1.39
Genes with assigned COG	2,273	67.45
Selenocysteine-containing proteins[a]	9	
Genes without assigned function	999	29.64
Poorly chracterized genes	395	11.72
Other elements		
CRISPR repeats	6	
Cas operons	2	
Transposases	19	
Mobile elements	1	

Table 2.2. Codon usage of the genome of *D. gigas*

Codon	Aminoacid	Fraction	Frequency	Nº# AA
GCA	A	0.071	8.530	9240
GCC	**A**	**0.667**	**79.523**	**86142**
GCG	A	0.211	25.164	27259
GCT	A	0.051	6.097	6604
TGC	**C**	**0.866**	**12.429**	**13464**
TGT	C	0.134	1.919	2079
GAC	**D**	**0.651**	**34.018**	**36850**
GAT	D	0.349	18.221	19738
GAA	**E**	**0.500**	**30.000**	**32497**
GAG	**E**	**0.500**	**29.988**	**32484**
TTC	**F**	**0.673**	**24.381**	**26410**
TTT	F	0.327	11.865	12853
GGA	G	0.069	5.376	5823
GGC	**G**	**0.674**	**52.803**	**57198**
GGG	G	0.194	15.179	16443
GGT	G	0.064	5.034	5453
CAC	**H**	**0.609**	**14.522**	**15731**
CAT	H	0.391	9.337	10114
ATA	I	0.028	1.219	1320
ATC	**I**	**0.752**	**32.578**	**35290**

ATT	I	0.220	9.547	10342
AAA	K	0.255	8.861	9599
AAG	**K**	**0.745**	**25.923**	**28081**
CTA	L	0.005	0,591	640
CTC	L	0.178	20.402	22100
CTG	**L**	**0.666**	**76.346**	**82701**
CTT	L	0.058	6.699	7257
TTA	L	0.004	0,505	547
TTG	L	0.088	10.086	10925
ATG	**M**	**1.000**	**26.235**	**28419**
AAC	**N**	**0.709**	**17.105**	**18529**
AAT	N	0.291	7.009	7592
CCA	P	0.053	2.885	3125
CCC	**P**	**0.482**	**26.167**	**28345**
CCG	P	0.385	20.890	22629
CCT	P	0.080	4.327	4687
CAA	Q	0.144	5.685	6158
CAG	**Q**	**0.856**	**33.926**	**36750**
AGA	R	0.019	1.282	1389
AGG	R	0.044	2.992	3241
CGA	R	0.038	2.608	2825
CGC	**R**	**0.525**	**35.646**	**38613**
CGG	R	0.291	19.763	21408
CGT	R	0.082	5.556	6018
AGC	S	0.282	13.864	15018
AGT	S	0.043	2.103	2278
TCA	S	0.029	1.426	1545
TCC	**S**	**0.446**	**21.918**	**23742**
TCG	S	0.150	7.360	7973
TCT	S	0.050	2.456	2660
ACA	T	0.061	3.089	3346
ACC	**T**	**0.605**	**30.508**	**33047**
ACG	T	0.290	14.607	15823
ACT	T	0.044	2.220	2405
GTA	V	0.026	1.893	2051
GTC	V	0.242	17.782	19262
GTG	**V**	**0.687**	**50.416**	**54613**
GTT	V	0.045	3.306	3581
TGG	**W**	**1.000**	**12.594**	**13642**
TAC	**Y**	**0.641**	**14.248**	**15434**
TAT	Y	0.359	7.966	8629
TAA	*	0.243	0,735	796
TAG	*	0.310	0,937	1015
TGA	*****	**0.447**	**1.353**	**1466**

A)

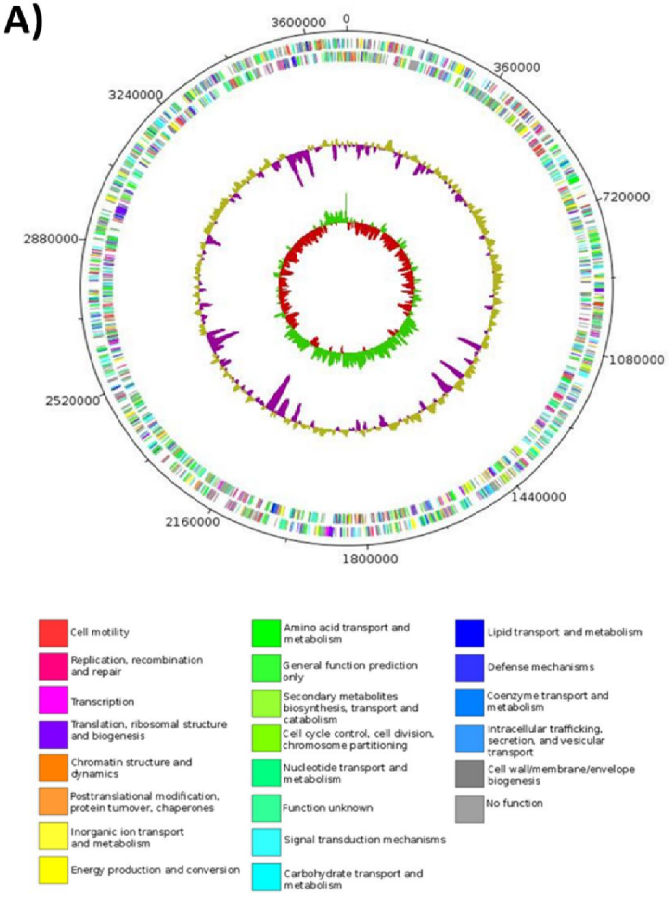
0
360000
720000
1080000
1440000
1800000
2160000
2520000
2880000
3240000
3600000
Cell motility
Replication, recombination and repair
Transcription
Translation, ribosomal structure and biogenesis
Chromatin structure and dynamics
Posttranslational modification, protein turnover, chaperones
Inorganic ion transport and metabolism
Energy production and conversion
Amino acid transport and metabolism
General function prediction only
Secondary metabolites biosynthesis, transport and catabolism
Cell cycle control, cell division, chromosome partitioning
Nucleotide transport and metabolism
Function unknown
Signal transduction mechanisms
Carbohydrate transport and metabolism
Lipid transport and metabolism
Defense mechanisms
Coenzyme transport and metabolism
Intracellular trafficking, secretion, and vesicular transport
Cell wall/membrane/envelope biogenesis
No function

B)

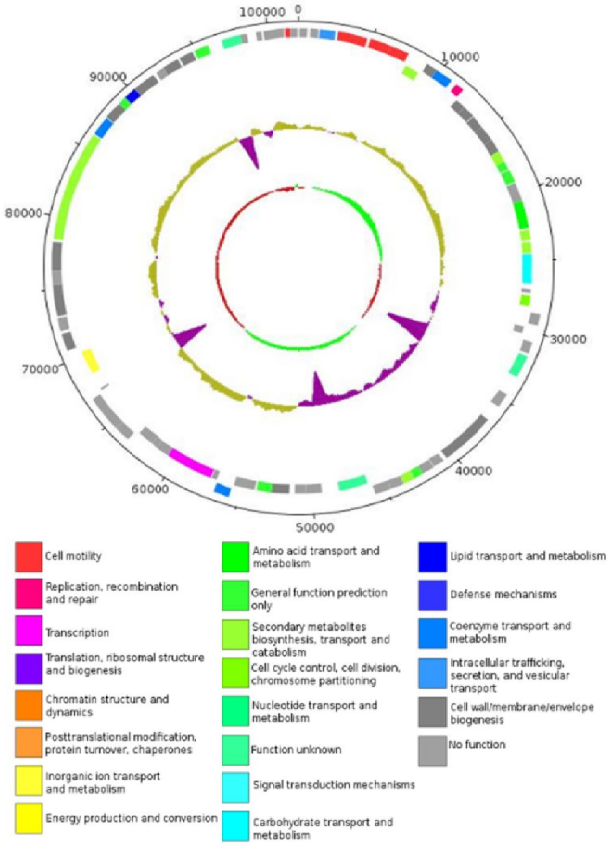
0
10000
20000
30000
40000
50000
60000
70000
80000
90000
100000
Cell motility
Replication, recombination and repair
Transcription
Translation, ribosomal structure and biogenesis
Chromatin structure and dynamics
Posttranslational modification, protein turnover, chaperones
Inorganic ion transport and metabolism
Energy production and conversion
Amino acid transport and metabolism
General function prediction only
Secondary metabolites biosynthesis, transport and catabolism
Cell cycle control, cell division, chromosome partitioning
Nucleotide transport and metabolism
Function unknown
Signal transduction mechanisms
Carbohydrate transport and metabolism
Lipid transport and metabolism
Defense mechanisms
Coenzyme transport and metabolism
Intracellular trafficking, secretion, and vesicular transport
Cell wall/membrane/envelope biogenesis
No function

Fig 2.1: Structural representation of the circular chromosome (A) and plasmid (B) of *Desulfovibrio gigas*. Circular representations, from inside to the outside represent: (i) GC skew, richness of guanine over cytosine in the positive strand represented in green and cytosine over guanine represented in red; (ii) GC content, below average in purple, above average in gold; (iii) positive strand coding regions (below) and negative strand coding regions (above) colored according to COG functional terms of the best hit obtained from *Blastp* program; (iv) nucleotide position indicated in circular scale.

The plasmid of this bacterium (CP006586) has a size of 101,949 bp, containing 76 ORFs, of which 73 are coding regions (Table 2.3 and Fig 2.1B). Approximately one third (36%) of the encoded polypeptides are annotated as of hypothetical function. In the other 49 annotated ORFs the most representative functional group was composed of 12 proteins encoding acetyl, methyl and glycosyl transferases.

Table 2.3. General plasmid features of *Desulfovibrio gigas*

Features	Value
Size (bp)	101,949
G+C contente (bp)	64,081
DNA coding region (bp)	79,425
Pseudogenes	3
Protein coding genes	72
Gene density (bp/gene)	1,415
Average length of a gene (bp)	1,103

Interestingly, we could also identify an operon of 12 ORFs (DGIp_00010-00120) encoding a type II secretory system (T2SSs) which is involved in the secretion of folded and/or oligomeric exoproteins (Douzi *et al*., 2012). We have also identified a 30kb operon encoding a set of capsule polysaccharide biosynthesis (*kps*) and transporter (*tag*) proteins. These features may indicate a

mechanism used by *D. gigas* to secret and transport folded exoproteins. Another remarkable feature of *D. gigas* plasmid is related to the presence of the *apsK* gene encoding a predicted bi-functional protein, shown to have a sulfate adenylyltransferase and an adenylylsulfate kinase activities (Marchler-Bauer *et al*., 2013).

2.4.2 CRISPR /Cas system a bacterial innate immune system

CRISPRs are loci encompassing several short repeats, that are found in nearly all archaea and in about 40% of bacteria, for which genome sequences are available (Mojica *et al*., 2000; Jansen *et al*., 2002; Grissa *et al*., 2007; Kunin *et al*., 2007; Sorek *et al*., 2008). CRISPR functions as an adaptive microbial immune system, providing immunity against viruses (Gasiunas *et al*., 2013). Moreover, CRISPR is supposed to also limit horizontal gene transfer by preventing conjugation and plasmid transformation (Marraffini and Sontheimer, 2008).

Several types of CRISPR-associated proteins (Cas) are encoded by *cas* genes located in the vicinity of CRISPRs. Cas proteins are required for the multistep defense against intruder genetic elements mediated by crRNAs. The number and identity of *cas* genes as well as their operonic organization appear to be extremely variable. Makarova *et al*, have proposed a classification of CRISPR/Cas systems in which the *cas1* and *cas2* genes constitute the core of three distinct types of system (Makarova *et al*., 2011). Each system was further divided into different subtypes, on the basis of the gene composition and architecture of the respective operons.

In the particular case of *Desulfovibrio* spp. little is known about the presence of CRISPR sequences and Cas associated genes. *D.vulgaris* appears to have a plasmidic CRISPR/Cas locus that falls into the subtype I-C system, according to the abovementioned classification criteria (see Fig 2.2A and (Haft *et al*., 2005; Makarova *et al*., 2011). A survey of the genome of *D. gigas* for CRISPR repeats, revealed the presence of two distinct CRISPR/Cas systems: one of the I-

F type, for the first time reported in *Yersinia pestis*, and another one that does not fit in any of the known types of CRISPR/Cas systems (Fig 2.2A). Using a dedicated database (http://crispi.genouest.org/) (Rousseau *et al*., 2009), we have next searched for CRISPR sequences that have adjacent *cas* genes using the different species of *Desulfovibrio* genus. We have focused on CRISPR/Cas arrays that possess the ubiquitous core protein Cas1, which is involved in new spacer acquisition. We then used the conserved Cas1 protein as a scaffold to investigate the evolution of the CRISPR/Cas system in the *Desulfovibrio* genus (Fig 2.2B). Remarkably, CRISP/Cas sytems are absent from the genome of *D.aespoeensis* Aspo-2, *D.africanus* Walvis Bay, *D.piezophilus* C1TLV30 and *D.salexigens* DSM2638.

Three distinct groups within several *Desulfovibrio* spp. were found, on the basis of the conserved Cas1 phylogenetic tree (Fig 2.2B). Group I comprises the Cas1 proteins from *D. gigas* ATCC19364, *D. hydrotermalis* AM13 and *D. magneticus* RS-1; group II includes Cas1 sequences from *D. desulfuricans* ATCC2774 and *D. alaskensis* G20 and group III encompasses another Cas1 protein found in *D. magneticus* RS-1, the already described Cas1 from *D. vulgaris* Hildenborough and its orthologues from *D. desulfuricans* ND132 and *D. vulgaris* Miyazaki. Notably, in terms of *cas* gene composition and organization each group embraces different CRISPR/Cas subtypes (Fig 2.2A). Accordingly, Cas1 proteins of each group cluster with the archetypal orthologue of the assigned CRISPR/Cas subtype (Fig 2.2B), namely *Yersinia pestis* CO92 (group I, subtype I-F), *Escherichia coli* DH1 (group II, subtype I-E) and *D. vulgaris* Hildenborough (group III, subtype I-C).

A)

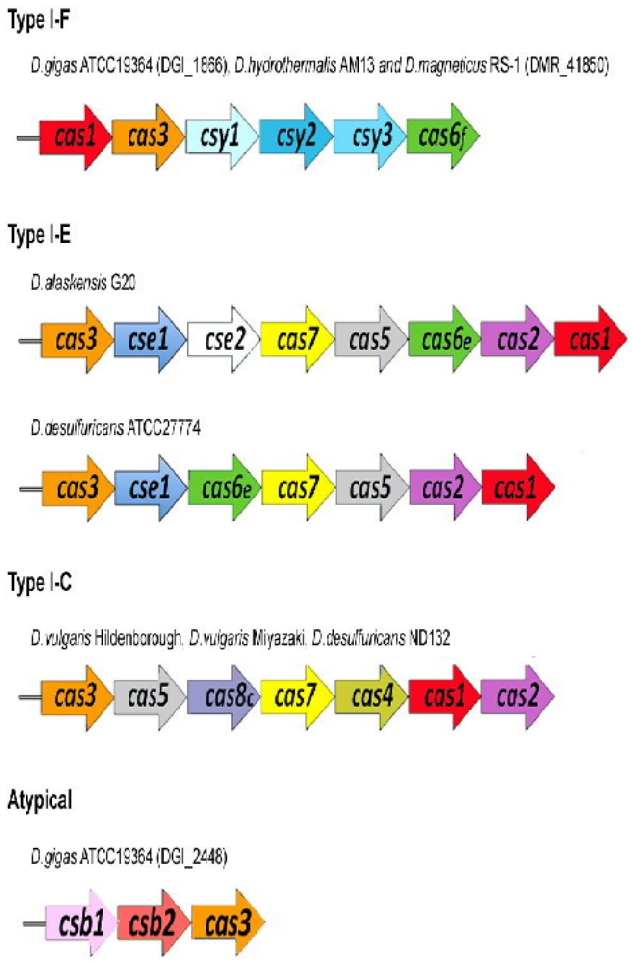
Type I-F
D.gigas ATCC19364 (DGI_1866), D.hydrothermalis AM13 and D.magneticus RS-1 (DMR_41850)
cas1
cas3
csy1
csy2
csy3
cas6f
Type I-E
D.alaskensis G20
cas3
cse1
cse2
cas7
cas5
cas6e
cas2
cas1
D.desulfuricans ATCC27774
cas3
cse1
cas6e
cas7
cas5
cas2
cas1
Type I-C
D.vulgaris Hildenborough, D.vulgaris Miyazaki, D.desulfuricans ND132
cas3
cas5
cas8c
cas7
cas4
cas1
cas2
Atypical
D.gigas ATCC19364 (DGI_2448)
csb1
csb2
cas3

B)

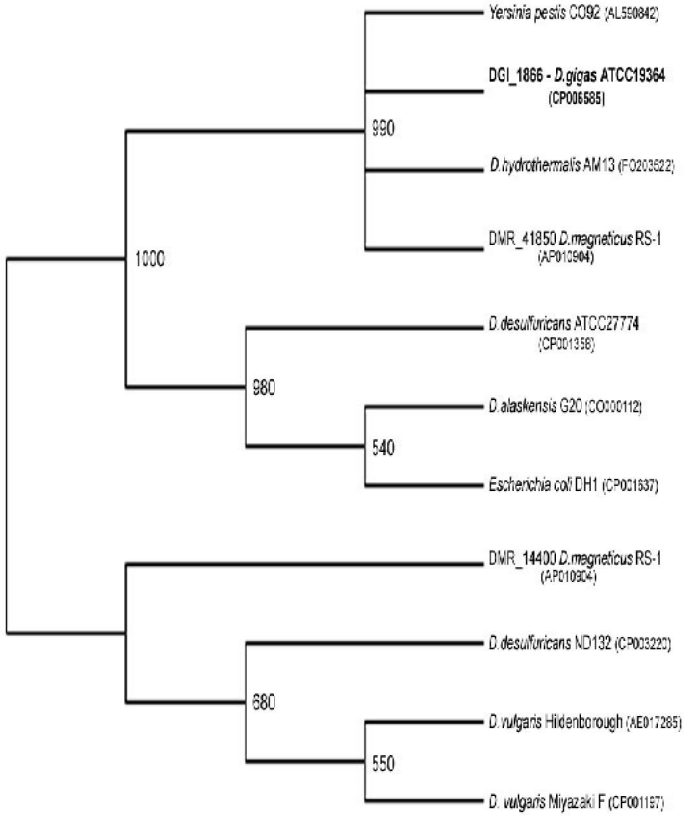
Yersinia pestis CO92 (AL590842)
DGI_1866 - D.gigas ATCC19364 (CP006585)
990
D.hydrothermalis AM13 (FQ203522)
DMR_41850 D.magneticus RS-I (AP012904)
1000
D.desulfuricans ATCC27774 (CP001338)
980
D.alaskensis G20 (CO000112)
540
Escherichia coli DH1 (CP001637)
DMR_14400 D.magneticus RS-I (AP010804)
D.desulfuricans ND132 (CP003220)
680
D.vulgaris Hildenborough (AE017285)
550
D. vulgaris Miyazaki F (CP001197)

Fig 2.2: Distribution of different types of CRISPR/Cas systems among *Desulfovibrio* spp. (A) Operon structure of Cas proteins from the indicated *Desulfovibrio* spp. The operonic organization was assessed through the DOE Joint Genome Institute (JGI) website (http://www.jgi.doe.gov/). Classification into the distinct Type I subtypes is according to Makarova *et al.* 2011. (B) The evolutionary history of Cas1 proteins was inferred by using the Maximum Likelihood method. The bootstrap consensus tree inferred from 1000 replicates was taken t o represent the evolutionary history of the taxa analyzed. Branches corresponding to partitions reproduced in less than 50% bootstrap replicates were collapsed. The percentage of replicate trees in which the associated taxa clustered together in the bootstrap test (1000 replicates) is shown next to the branches. Accession numbers are indicated after species name.

The phylogenetic tree of *Desulfovibrio* genus was used in order to explore the evolutionary bases of the CRISPR/cas loci (Fig 2.3). In the particular case of group I, the topology of Cas1 phylogenetic tree (Fig 2.2B) together with the *rpoB* and *gyrB* based phylogeny of the genus *Desulfovibrio* (Fig 2.3), strongly suggests the divergence after speciation of an ancestor gene common to *D. gigas* ATCC19364, *D. hydrotermalis* AM13 and *D. magneticus* RS-1. Furthermore, the Cas1 phylogeny shows *D. desulfuricans* ATCC2774, *D. alaskensis* G20 grouping separately from the other *Desulfovibrio* spp. and of *E. coli* DH1 (Fig 2.2B). These phylogenetic relationships together with the *rpo_gyrB* phylogenetic tree indicate that CRISPR/Cas system I-E (group II) might have been acquired from horizontal gene transfer (HGT) during prokaryotic evolution. Indeed, a comprehensive phylogenetic analysis of CRISPR/Cas loci points towards their propagation via HGT events (Godde and Bickerton, 2006). Regarding group III, it seems that the CRISPR/Cas subtype I-C is scattered across several *Desulfovibrio* spp. (Fig 2.2B and Fig 2.3). The absence of additional *Desulfovibrio* orthologues suggests that the acquisition of this CRISPR/Cas subtype may rely as well in HGT occurrences throughout evolution. Notably, *D. vulgaris* Hildenborough contains the

CRISPR/Cas locus in its megaplasmid, whereas the closely related *D. vulgaris* Miyazaki (Fig 2.3) possesses a similar CRISPR/cas array in the genome. Godde and Bickerton have proposed that most megaplasmids should not be stably maintained in their host cells (Godde and Bickerton, 2006). Consistently, the lack of a megaplasmid in *D.vulgaris* Miyazaki indicates that a recent HGT event might have been responsible for the appearance of CRISPR locus in *D.vulgaris* Hildenborough.We show now that *D. gigas* possesses a different CRISPR/cas system when compared to *D.vulgaris*. Moreover, we have identified in *D. gigas* an atypical CRISPR/cas array (Fig 2.2A – DGI_2448). These arrays are spread across several species of bacteria and archaea (Bhaya *et al*., 2011) but it remains to be elucidated whether they represent an active loci.

2.4.3 Phylogenetic analysis of Desulfovibrio genus

A phylogenetic tree was built based on protein sequences coded by the conserved *rpoB* and *gyrB* genes from 21 isolates of *Desulfovibrio* genus whose genomic sequences are available and annotated.

The analysis originated two well-supported deep-branching main clades (Fig 2.3). Within the upper clade, two groups emerge: one group contains *D. gigas* clustering with *D. alaskensis* G20, *D. piger* ATCC29098, *D. desulfuricans* ATCC27774 and *D. vulgaris* spp; the other group embraces *D. magneticus RS-1*, two *D. africanus* strains and two not yet assigned *Desulvofibrio* species (Fig 2.3). The lower clade contains a single group of *Desulfovibrio* species with many of them found in higher depths (piezophilic environment). The tree topology points towards a more divergent evolutionary history of the species included in the lower clade.

D. vulgaris Hildenborough (AE017285)
D. vulgaris DP4 (CP000527)
D. vulgaris RCH1 (CP002297)
D. vulgaris Miyazaki F (CP001197)
Desulfovibrio sp. A2 (GCA_000226255)
Desulfovibrio sp. 3_1_syn3 (GCA_000145315)
Desulfovibrio sp. 6_1_46AFAA (GCA_000244635)
D. piger ATCC 29098 (GCA_000153375)
D. desulfuricans ATCC 27774 (GPD01358)
D. alaskensis G20 (CP000112)
D. gigas ATCC 19364 (CP016585)
Desulfovibrio sp. U5L (GCA_000240065)
Desulfovibrio sp. 1012B (CMC01388)
D. magneticus RS-1 (AP010904)
D. africanus Walvis Bay (CP003221)
D. africanus PCS (GCA_000344315)
D. aespoeensis Aspo-2 (CP002431)
D. piezophilus C1TLV30 (FQ203427)
D. desulfuricans ND132 (CP003220)
D. hydrothermalis AM13 (FC203522)
D. salexigens DSM 2638 (CP001648)
Escherichia coli K12 (CP000948)
298
1000
769
1000
998
1000
616
1000
997
881
706
1000
1000
626
1000
617
1000
808
1000
1.0

Fig 2.3:.Evolutionary relationship of *Desulfovibrio* species. This tree was built based on RpoB and GyrB protein sequences using a Maximum Likelihood approach with 1000 iterations for the Bootstrap test, both implemented in the PhyML tool. The number at each node corresponds to the frequency of that branching occurred during the 1000 iterations. The sequences of the *E. coli* proteins were applied as an outgroup. Accession numbers are indicated after the species names

In fact, gene structures associated with oxygen resistance and detoxification present in *D. gigas* genome are also detected in the subgroup containing *D. magneticus* RS-1. This is the case of the superoxide dismutase (SOD) genes (DGI_1536 and DGI_3082), as well as the gene encoding the peroxiredoxin (DGI_3518), which does not have homologous sequences with the species observed in the lower clade. These results are in agreement with the fact that species such as *D.piezophilus* and *D. hydrothermalis*, are found in environments where O_2 is absent or present at very low levels (Ji *et al*., 2013).

Remarkably, according to this phylogenetic analysis, the isolates within *Desulfovibrio* genus not yet classified, namely *Desulfovibrio* sp. 3_1_syn3 together with *Desulfovibrio* sp. 6_1_46AFAA, *Desulfovibrio* sp. U5L along with *Desulfovibrio* sp. 1012B and *Desulfovibrio* sp. A2, are clustered with *D.desulfuricans, D.magneticus and D.vulgaris*, respectively. Corroborating our data with respect to the *Desulfovibrio* sp. A2, it was shown using 16S rRNA gene sequence a 99.1% overall sequence similarity with *D.vulgaris* Miyazaki (Mancini *et al*., 2011). These findings indicate that they are close related species and merit further investigation, in order to clarify their classification within the *Desulfovibrio* genus.

Another interesting aspect of this analysis relies in the positioning of *D.desulfuricans* ND132 within the lower clade of the phylogenetic tree, rather than in the upper clade, where *D. desulfuricans* appears (Fig 2.3). This finding has

already been observed by others and strongly indicates that its classification should be reconsidered (Brown *et al*., 2011; Gilmour *et al*., 2011)

2.4.4 Strategies to survive to Oxygen and NO

SRB, in the diverse environmental niches they occupy, can come across with reactive oxygen or nitrogen species that cause great damage to the cells. Formerly classified as strict anaerobes there is, however, growing evidence that they are able to cope with oxygen and to use it to produce ATP even if they are unable to grow in its presence. As such, the organisms have developed several strategies to avoid such damage.

The response to different oxygen concentrations in microorganisms, aerotaxis, is often initiated by the transmembrane chemoreceptors methyl-accepting chemotaxis proteins, and involves many other proteins organized in a cascade of reactions activating the flagellar motor, allowing the cells to move to an optimal oxygen gradient (Armitage, 1997). SRB within the microbial mats and oxic environments are motile, and active movements are observed in response to change in oxygen gradients which were interpreted as a strategy to survive in these environments (Krekeler *et al*., 1989; Canfield and Des Marais, 1991; Teske *et al*., 1998; Eschemann *et al*., 1999). SRB respond to oxygen by sensing extra and/or intracellular signals followed by their transduction to the transcriptional and post-transcriptional machineries. *D. gigas* contains an operon of 7 cistrons of which 5 encoding the chemotaxis proteins CheB, CheR, CheW, CheY and CheA. All these units are co-transcribed as an 11Kb mRNA whose expression is not altered either by O_2 or NO (Felix *et al*., 2006). However, this bacterium also contains many other chemotaxis coding regions scattered throughout the genome (Table S27). The encoded polypeptides present a high homology with the ones of *D. desulfuricans*, *D. vulgaris* and *D. magneticus.* Besides aerotaxis, aggregation and attachment to surfaces, these microorganisms have developed a network of defense mechanisms against ROS, being the toxic O_2 eliminated by dismutation to

H_2O_2 and O_2, a reaction catalyzed by the superoxide reductase (SOR) (Dos Santos *et al*., 2000). *D. gigas* contains in its genome two superoxide dismutase genes, one a small blue protein named neelaredoxin (Silva *et al*., 1999) and a second one (DGI_1536) here described for the first time (see Table S19). Neelaredoxin contains one mononuclear iron sites showing high homology with the second domain of desulfoferrodoxin (Moura *et al*., 1977; Archer *et al*., 1995). The complementation of an *E.coli* Δ*sodA*Δ*sodB* double mutant with *nlr* gene of *D. gigas* recovers the wild type phenotype in the presence of H_2O_2 indicating that neelaredoxin can function as a SOD (Silva *et al*., 1999). The accumulation of potentially toxic H_2O_2 is also prevented by the action of catalases (Dos Santos *et al*., 2000) that is found in *D. gigas* genome as a single gene. It is believed that in some anaerobic bacteria, as in aerobic organisms, SOD and catalase play a role in the detoxification of oxygen by-products. SOD activity was shown to be present in sulfate-reducing bacteria, such as *Desulfomicrobium norvegicum* (formerly known as *Desulfovibrio desulfuricans* strain Norway 4), *D. vulgaris* and *D. gigas* (Dos Santos *et al*., 2000). *D. gigas* genome also contains genes encoding for three rubrerythrins, one peroxiredoxin, one rubredoxin-like protein and three F390 synthetase proteins (Table S19), which have been shown to be related to defense mechanisms against oxidative stress.

A flavodiiron protein, rubredoxin:oxygen reductase (ROO), involved in the detoxification of O_2, (Chen *et al*., 1993) was as well shown to protect *D. gigas* against nitrosative stress by acting as a nitric oxide (NO) reductase (Rodrigues *et al*., 2006b). Under nitrosative stress, *roo* transcription is regulated by NorR (NorR1L) and a second putative *norR* gene designated as *norR2L* which was found in *D. gigas* genome (Table S17) being its function still unknown (Varela-Raposo *et al*., 2013). *D. gigas* genome also includes one copy of 'hybrid cluster protein' (HCP), a protein with an unusual structure (Cooper *et al*., 2000) proposed to have a function in nitrogen cycle due to its hydroxylamine reductase activity (Wolfe *et al*., 2002; Cabello *et al*., 2004; Overeijnder *et al*., 2009). A role in defense against oxidative stress has also been suggested on basis of HCP

peroxidase activity (Almeida *et al*., 2006). The specific function of HCP in the cell remain however elusive. Other studies in *D. vulgaris* Hildenborough have shown that *hcp* is upregulated by nitrite (Haveman *et al*., 2004; Haveman *et al*., 2005; He *et al*., 2006) and it may protect the cell from nitrite and NO stresses although NO reductase activity was not detected (Johnston *et al*., 2009; Yurkiw *et al*., 2012; Figueiredo *et al*., 2013). It seems clear though, that HCP must have an important role in protection against nitrosative and oxidative stresses. In *E. coli*, and other facultative anaerobic microorganisms, *hcp* is found in an operon together with an NADH oxidoreductase (van den Berg *et al*., 2000) while in *Desulfovbrio* spp. it is co-expressed with a hypothetical ferredoxin (*frdx*) gene (Rodionov *et al*., 2004). Interestingly, in *D. gigas* genome HCP is encoded by a monocistronic gene (Fig 2.4A). A gene encoding a transcriptional regulator (*hcpR)* of *hcp* gene expression present in other *Desulfovibrio* spp. was also identified upstream of *hcp* although localized in an opposite direction. *D. gigas* genome codes also for the membrane complex cytochrome *c* nitrite reductase (NrfHA), which is suggested to play a role in nitrite detoxification. Indeed, *D. gigas* as well as *D. vulgaris* do not grow under nitrite or nitrate (Greene *et al*., 2003; He *et al*., 2006). Nitrate reductases as well as nitroreductases encoded in *D. gigas* genome (Table S17) might be involved in NO detoxification mechanisms.

2.4.5 Central Carbon Metabolism

D. gigas accumulates large amounts of polyglucose as an endogenous carbon and energy reserve, utilizing these sugars compounds for growth (Fareleira *et al*., 1997). We have conducted a broad analysis in its genome to identify the elements of the central carbon metabolism involved in many different pathways. Biochemical studies have shown (Fareleira *et al*., 1997), that *D. gigas* contains all the genes encoding proteins of the Embden-Meyerhof pathway (Table S4), whereas the genes coding for the hexokinase and the KDGP aldolase of the Entner-Doudoroff pathway are lacking (Table S5). *D. gigas* belongs to SRB group

of incomplete-oxidizers, producing acetate and CO_2 as its main end-products from substrate oxidation.

Inspection of the genome reveals that the genes corresponding to 2-oxoglutarate dehydrogenase, 2-oxoglutarate synthases and both subunits of the succinyl Co-A ligase, *sucC* and *sucD* (Table S7) from the tricarboxylic acid (TCA) cycle are absent.

Both copies of the succinate:quinone oxidoreductase (SQR), one here identified for the first time (DGI_0826 to DGI_0828 - Table S14), appear to function mainly as fumarate reductases rather than a succinate dehydrogenases, due to a conserved glutamine residue (Glu180) in the Sdh/FdrC subunit (Zaunmuller *et al*., 2006). These results indicate that both oxidative and reductive TCA cycle pathways are not fully functional and are likely to have a biosynthetic function, as suggested for *D. vulgaris* Hildenborough (Heidelberg *et al*., 2004). In the Wood-Ljungdahl pathway (Table S8), the genes coding for a key element from this pathway (Ragsdale and Pierce, 2008), the bifunctional carbon monoxide dehydrogenase/acetyl-CoA synthase (CODH/ACS) enzyme, were not identified. Instead, unlike the other *Desulfovibrio* spp., *D. gigas* genome codes for an aerobic-type carbon monoxide dehydrogenase of the *coxSLM* type (Fig 2.4B), similar to the CO dehydrogenase of *Oligotropha carboxidovorans* (Dobbek *et al*., 1999). This enzyme shows a high sequence similarity with the aldehyde oxidoreductase (MOP) from *D. gigas* (Romao *et al*., 1995). This may suggest that this CO dehydrogenase could play a function in oxygen metabolism and resistance in *D. gigas* rather than being part of the Wood-Ljungdahl pathway. Furthermore, the absence of this enzyme in *D. gigas* indicates that in contrast to *D.vulgaris* Hildenborough, CO cycling (Voordouw, 2002) is not an effective mechanism of energy conservation.

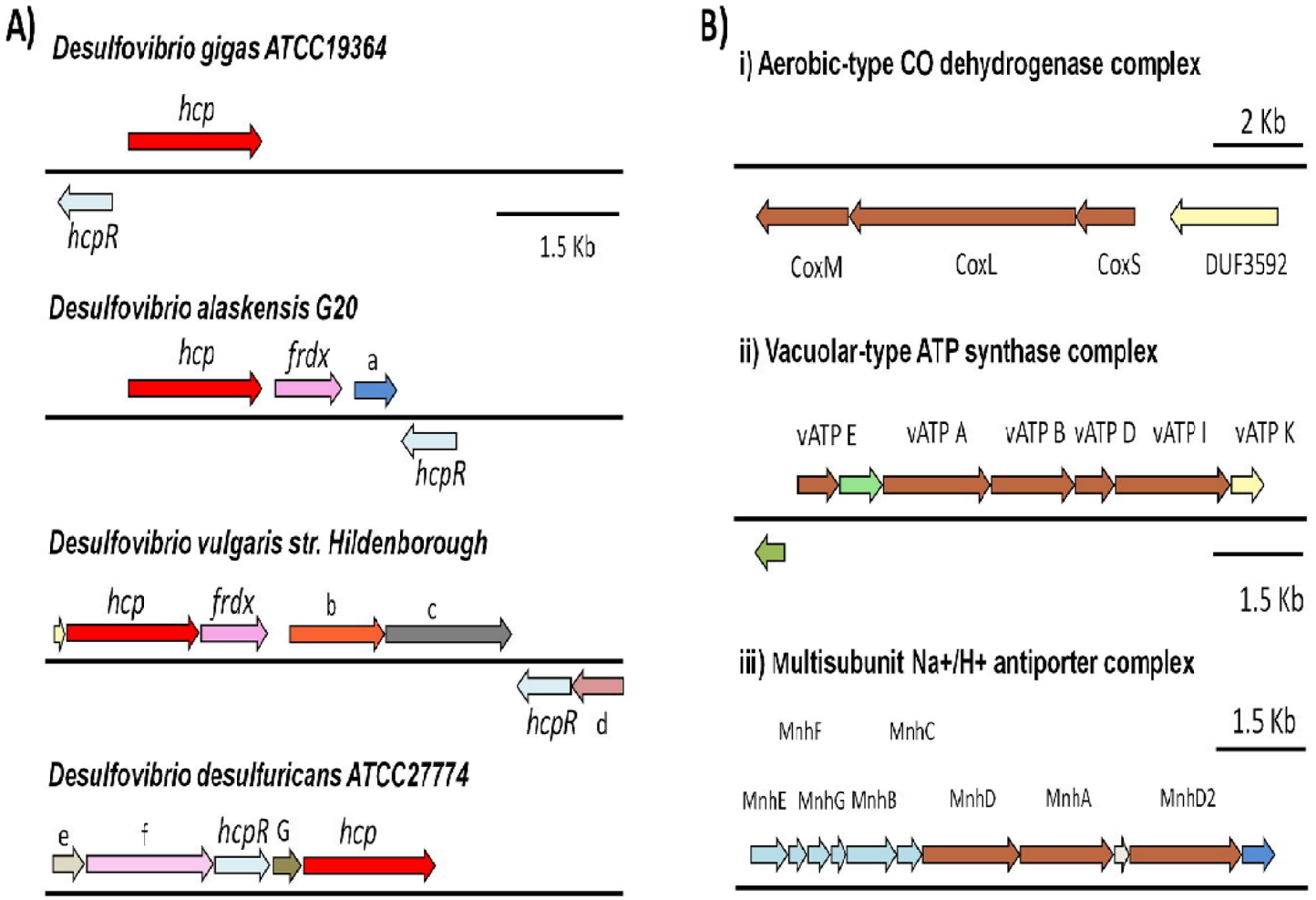
A)
Desulfovibrio gigas ATCC19364
hcp
hcpR
1.5 Kb
Desulfovibrio alaskensis G20
hcp
frdx
a
hcpR
Desulfovibrio vulgaris str. Hildenborough
hcp
frdx
b
c
hcpR
d
Desulfovibrio desulfuricans ATCC27774
e
f
hcpR
G
hcp
B)
i) Aerobic-type CO dehydrogenase complex
2 Kb
CoxM
CoxL
CoxS
DUF3592
ii) Vacuolar-type ATP synthase complex
vATP E
vATP A
vATP B
vATP D
vATP I
vATP K
1.5 Kb
iii) Multisubunit Na+/H+ antiporter complex
MnhF
MnhC
1.5 Kb
MnhE
MnhG
MnhB
MnhD
MnhA
MnhD2

Fig 2.4: Genomic organization of operons in *D. gigas*. (A) Organization of the *hcp* and *hcpR* monocistronic operons in *D. gigas* in comparison with other *Desulfovibrio* species, where: *frdx*, ferredoxin; *a*, Upsa-like protein; *b*, alcohol dehydrogenase; *c*, sensory box histidine kinase; *d*, acpD:acyl carrier protein phosphodiesterase; *e*, putative lipoprotein; *f*, polysaccharide export protein; *g*, cupin 2 conserved barrel domain protein. Gene cluster organization from *D. vulgaris* Hildenborough, *D. alaskensis* G20 and *D. desulfuricans* ATCC27774 were obtained at the DOE Joint Genome Institute (http://www.jgi.doe.gov/). (B) Organization of operons characterized exclusively in *D. gigas* when compared to other *Desulfovibrio* spp.: i) aerobic-type carbon monoxide dehydrogenase complex; ii) vacuolar-type ATP synthase complex; and iii) multisubunit Na+/H+ antiporter complex. Genes were assigned according to the predicted protein function. Nameless coding regions are either hypothetical proteins or proteins of unknown function. Color code for CDSs is based on COG functional categories, are as follows: brown, energy production and conversion; blue, signal transduction; light blue, inorganic ion transport and metabolism; green, RNA processing and modification; light green, unknown function; light yellow, cytoskeleton; and white, hypothetical protein.

2.4.6 Energy metabolism

A survey of *D. gigas* genome revealed several genes encoding dehydrogenases that oxidize organic acids and alcohols, as well as putative transporters and permeases for these substrates (Tables S1, S11 and S13). Pyruvate, the main metabolic intermediate of organic carbon oxidation can be oxidized by the two pyruvate oxidoreductases (DGI_0996 and DGI_1712/DGI_1713) as well as by other oxo-organic acid ferredoxin: oxidoreductases enzymes present (Table S10). Although *D. gigas* genome reveals many genes encoding such complexes, the pyruvate:formate lyase (*pfl*), a gene involved in fermentative metabolism, was not identified. This enzyme produces

acetyl-CoA and formate when pyruvate is the main carbon and energy source. As suggested for *D. vulgaris* Hildenborough, formate cycling could contribute to energy conservation in a mechanism similar to CO or hydrogen cycling (Voordouw, 2002; Heidelberg *et al*., 2004). The absence of this gene suggests that this mechanism is not operating in this bacterium albeit *D. gigas* is able to grow using formate as the main electron donor (our unpublished results) since it presents two genes encoding formate dehydrogenases (Table S13). One of these enzymes, a tungsten selenoprotein, was already described (Almendra *et al*., 1999), whereas the second is firstly identified in this work (DGI_3334 and DGI_3335).

As other *Desulfovibrio* spp*., D. gigas* grows chemolitotrophically deriving energy from oxidative phosphorylation using hydrogen oxidized in the periplasm by hydrogenases, coupled to sulfate reduction in the cytoplasm, creating a proton gradient ultimately used to generate ATP through F_1F_0-ATP synthase (Table S2). The electrons generated in the periplasm, by periplasmic hydrogenase activity, are transferred through the membrane for the sulfate reduction, in the cytoplasm, by multiheme c_3-type cytochromes (at the periplasmic side) and membrane-bound electron transport complexes.

The presence of at least three c_3-type cytochromes was found in *D. gigas* genome (Table S22). The full set of genes necessary for the dissimilatory sulfate reduction to sulfide were also detected, as well as specific sulfate permeases (Table S16). Interestingly enough, in the case of the ATP-synthase, not only the genes encoding the F_1F_0-ATP synthase were identified (Table S2) but another ATP-synthase which apparently is not present in other *Desulfovibrio* spp, was identified (Fig 2.4B). This enzyme is similar to the Vacuolar-type ATPases (V_oV_1) and in some anaerobic bacteria, such as *Enterococcus hirae*, it functions as a sodium pump (Kakinuma *et al*., 1999). In *D. gigas* this second ATPase could enhance ATP production derived from transmembrane electrochemical proton gradient.

In contrast to other *Desulfovibrio* spp. genomes so far sequenced (Pereira *et al*., 2011), only two [NiFe] type hydrogenase are present in *D. gigas*: the periplasmic HynBA (Volbeda *et al*., 1995) and the energy conserving Ech hydrogenase (Rodrigues *et al*., 2003) (Table S21). Recent work performed using mutant strains for these genes indicates that, although it is possible that the hydrogen cycling model of energy conservation (Odom and Peck, 1981) is effective, it appears to contribute substantially less to the final energy yield *of D. gigas* as proposed for other *Desulfovibrio* spp. (Morais-Silva *et al*., 2013). This could be a reflex of the unusual low number of these enzymes in *D. gigas*.

2.4.7 Energy conservation

Sulfate reducers contain several transmembrane redox complexes involved in energy metabolism and conservation (Pereira *et al*., 2011). The genome of *D. gigas* encodes the Ohc, Tmc and Hmc (Fig 2.5 and Table S20) multiheme cytochrome *c* complexes described as participating in electron transfer from periplasmic hydrogen oxidation to sulfate reduction as transmembrane electron circuits (Rossi *et al*., 1993; Pereira *et al*., 2006). We have also identified the membrane complexes QmoABC and DsrMKJOP directly related to sulfate reduction and suggested to transfer electrons to the final reductases Apr (*aprAB*) and Dsr (*dsrABC*) (Pires *et al*., 2003; Dahl *et al*., 2005). Furthermore, the presence of the Qrc (*qrcABCD*) complex, which was shown to transfer electrons from the Tpl-c_3 cytochrome to the menaquinone during sulfate respiration in a quinone:menaquinone loop together with the Qmo complex (Venceslau *et al*., 2010), suggests the existence in *D. gigas* of a mechanism of energy conservation linking periplasmic hydrogen or formate oxidation to cytoplasmic sulfate reduction. In addition, the complexes involved in NAD(P)H and ferredoxin oxidation were identified (Table S20). An operon coding for the NADH:quinone oxidoreductase (*nuo*), firstly reported in *D. magneticus* RS-1 (Nakazawa *et al*., 2009) was also detected in *D. gigas* genome. This enzyme complex is proposed to couple NADH

oxidation to proton translocation (Spring *et al*., 2012). However, the genes encoding the NADH dehydrogenase module (*nuoEFG*) are absent, suggesting a different electron donor, such as ferredoxin (Fd), instead of NADH (Pereira *et al*., 2011). Notably, the Mnh Na+/H+ antiporter complex with high similarity to the *nuo* complex that was not detected in other *Desulfovibrio* spp. genomes is present in *D. gigas* (Fig 2.4B). This complex is suggested to function as a transmembrane electron potential-generating NADH dehydrogenase rather than as a secondary transmembrane electron potential-consuming antiporter, directly accounting for the great transmembrane electron potential in *Staphylococcus aureus* (Bayer *et al*., 2006).

The presence of a similar mechanism in *D. gigas* might compensate for the apparent lack of energy conservation through metabolite cycling mechanisms, such as CO, formate or hydrogen cycling, deduced from its genome.

A search of the *D. gigas* genome also revealed the presence of the Rnf complex (*rnfCDGEABF*), proposed to function as a Na^+-translocating, ferredoxin:NAD^+ oxidoreductase (Biegel and Muller, 2010) and a multiheme cytochrome *c* in the same operon (Fig 2.6A – *w*), hypothesized to mediate the electron transfer between the periplasmic cytochrome *c* pool and the cytoplasmic NAD(P)H/Fd (Li *et al*., 2006; Pereira *et al*., 2011). Another gene with similarity to cytochrome *c* is found adjacent to the Rnf complex in *D. gigas*, corresponding to cytochrome c subunit of D-lactate dehydrogenase (Fig 2.6A – *a*). Interestingly, the *rnf* operon is not present in the genomic context of this dehydrogenase in other *Desulfovibrio spp.*, being replaced by the pyruvate:oxidoreductase (*poR*). This fact may indicate that the Rnf complex in *D. gigas* could be directly involved in the electron transport from lactate to Fd/NADH or between these two elements.

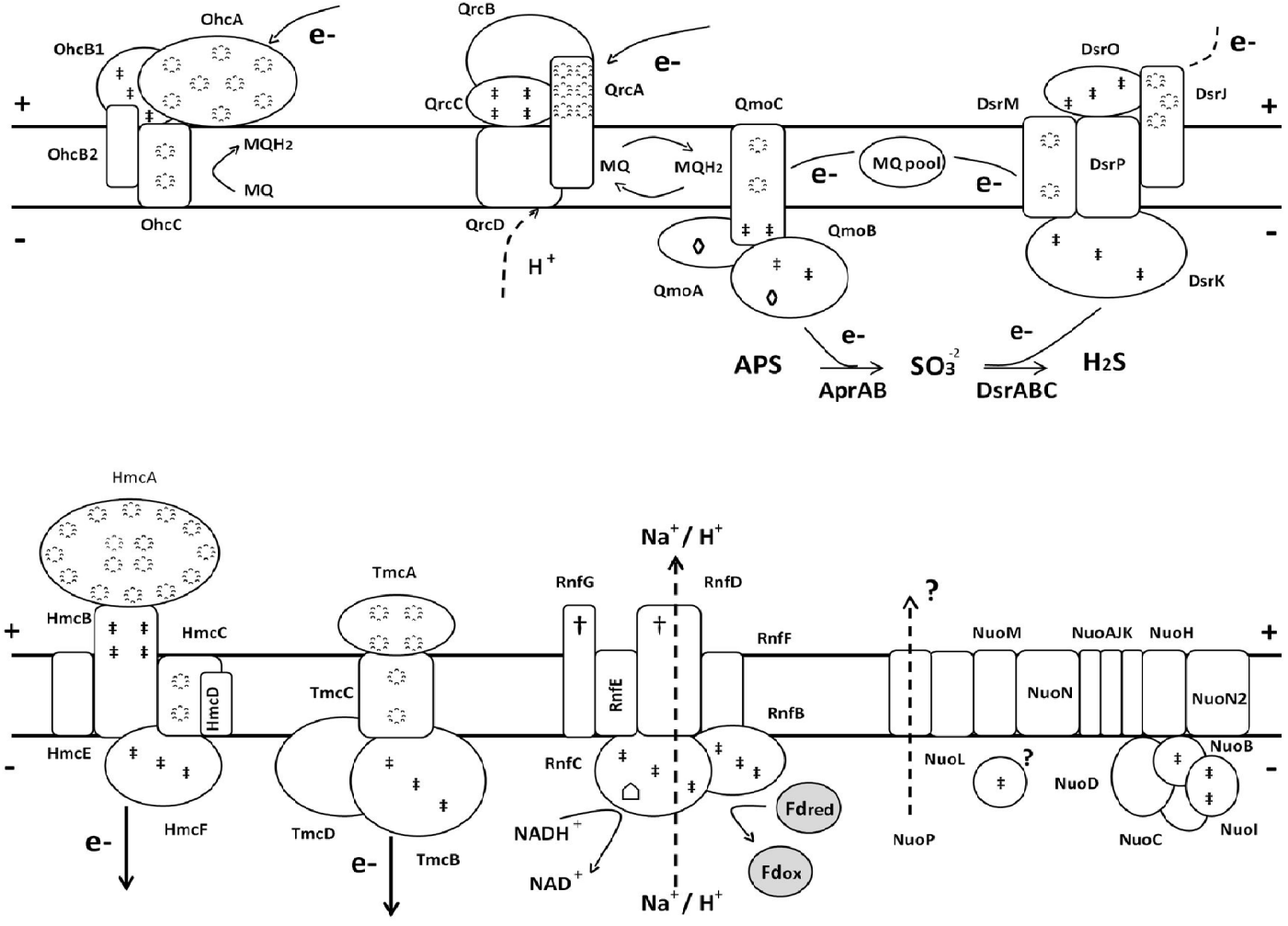
OhcA
OhcB1
OhcB2
OhcC
e-
MQH2
MQ
QrcB
QrcC
QrcA
QrcD
H+
MQ
MQH2
QmoC
QmoB
QmoA
MQ pool
DsrM
DsrO
DsrJ
DsrP
DsrK
APS
AprAB
SO3-2
DsrABC
H2S
HmcA
HmcB
HmcC
HmcD
HmcE
HmcF
TmcA
TmcC
TmcD
TmcB
RnfG
RnfD
RnfE
RnfF
RnfB
RnfC
Na+ / H+
NADH+
NAD+
Fdred
Fdox
NuoM
NuoAJK
NuoH
NuoN
NuoN2
NuoB
NuoL
NuoD
NuoC
NuoI
NuoP

Fig 2.5: Schematic representation of *D. gigas* membrane-bound electron-transfer complexes. The complexes were identified in the genome according to their predicted function*:* quinone reduction, Ohc and Qrc; quinol oxidation, Qmo; transmembrane electron transfer/sulfite reduction DsrMKJOP, Hmc and Tmc; and NADH/Fd oxidation, Rnf and Nuo. Symbols represent: heme; ‡, iron sulfur center; †, FMN cofactor; ⌂, flavin cofactor and ◊, FAD cofactor. Dashed lines represent hypothetical pathways for electron/proton flow.

Another group of energy conserving enzymes and complexes are those related to electron bifurcation processes. *D. gigas* genome encodes two paralogous (Table S24) of the heterodimeric transhydrogenase (NfnAB), responsible for the reversible NADH-dependent reduction of $NADP^+$ by Fd (Wang *et al*., 2010).

D. gigas has only one cytoplasmic hydrogenase but its genome encodes a sequence of an electron bifurcating complex: the HdrABC/FloxABCD (Fig 2.6B). Flox gene products are likely to oxidize NAD(P)H and transfer electrons to the HdrABC proteins (Pereira *et al*., 2011) (Table S23). These genes are found in other *Desulfovibrio* spp. between two alcohol dehydrogenases (Fig 2.6B – *a*), suggesting that they might be involved in the electron transfer from alcohol substrates. The presence of an aldehyde dehydrogenase (Fig 2.6B – *b*), found downstream of this operon in *D. gigas*, might indicate that this complex could also use aldehydes as another electron source to this complex. This genomic arrangement suggests that not only alcohol but also aldehyde oxidation could participate in mechanisms of energy conservation in *D. gigas*.

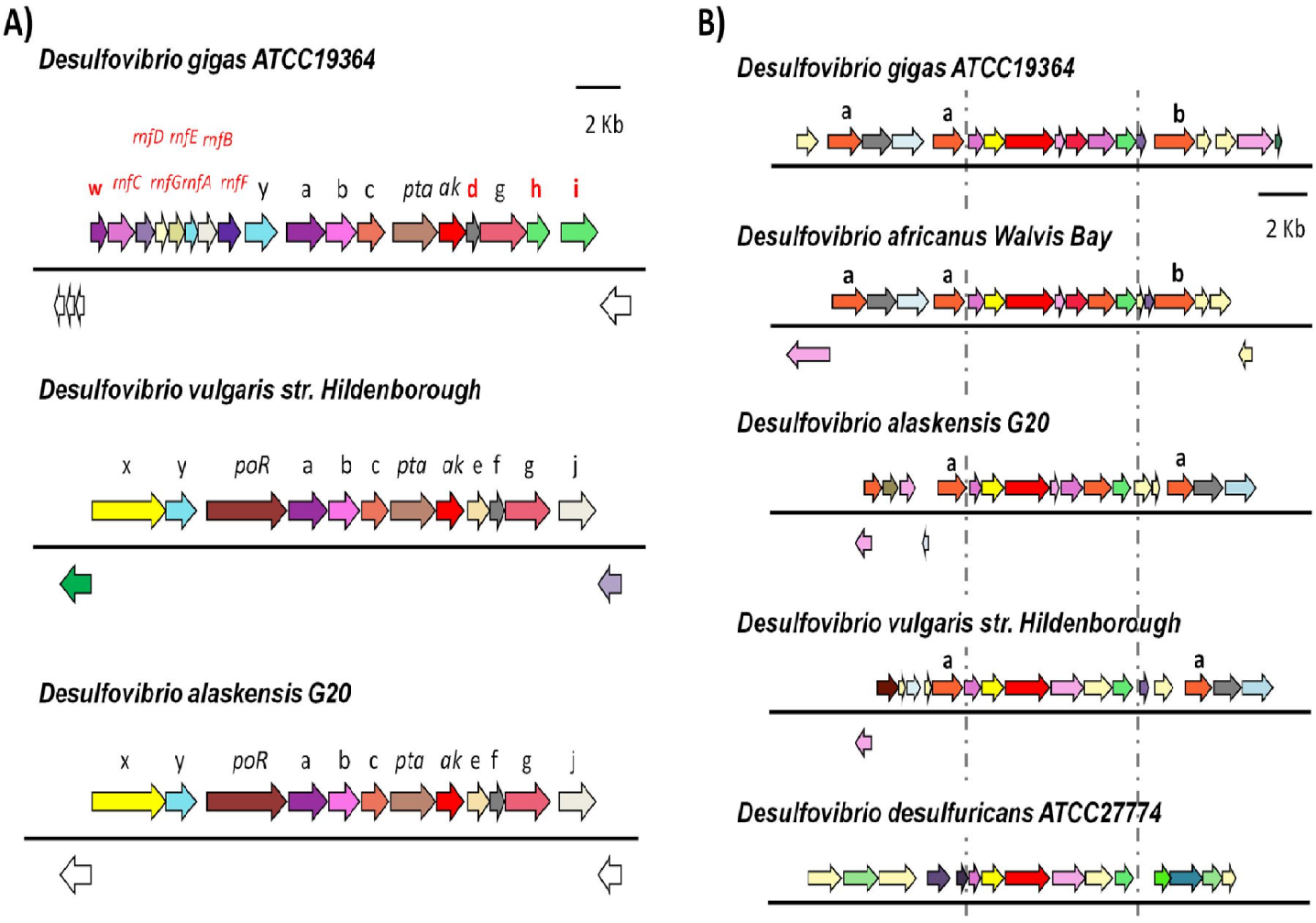
A)
Desulfovibrio gigas ATCC19364
2 Kb
rnfD rnfE rnfB
w rnfC rnfGrnfA rnfF y a b c pta ak d g h i
Desulfovibrio vulgaris str. Hildenborough
x y poR a b c pta ak e f g j
Desulfovibrio alaskensis G20
x y poR a b c pta ak e f g j
B)
Desulfovibrio gigas ATCC19364
a a b
2 Kb
Desulfovibrio africanus Walvis Bay
a a b
Desulfovibrio alaskensis G20
a a
Desulfovibrio vulgaris str. Hildenborough
a a
Desulfovibrio desulfuricans ATCC27774

Fig 2.6: Genomic organization of the operons involved in the energy metabolism of *D. gigas*. **(A)** Comparison of the *Desulfovibrio spp.* genomic regions containing the D-Lactate dehydrogenase operon. Differences in genomic organization are with red letters and genes are indicated as follows: *poR* - Pyruvate-ferredoxin oxidoreductas; *pta* - phosphate acetyltransferase; *ak* - acetate kinase; *rnfC, rnfD, rnfE, rnfG, rnfA, rnfB, rnfF* - Rnf complex; *w* - cytochrome c type protein; *x* - response regulator; *y* - sigma-54 response regulator; *a*, *b* and *c* - cytochrome c, lactate permease, and iron sulfur cluster protein (Ldh1a) subunits of the D-lactate dehydrogenase; *d* - lactate utilization protein B/C; e and f - hypothetical proteins; *g* - iron sulfur cluster binding protein (Ldh1b); *h* - FMN-dependent α-hydroxyacid dehydrogenase; *i* - Sodium-dependent transporter; *j* - methyl-accepting chemotaxis protein. Identification of the single letter genes was made according to BLAST best hit value. Gene cluster organization of *D. vulgaris* Hildenborough and *D. alaskensis* G20 were obtained at the DOE Joint Genome Institute: http://www.jgi.doe.gov/. **(B)** Organization of genomic regions containing the HdrABC/FloxABCD operon and neighboring genes. Hdr/Flox operon appears between dashed lines and is composed of three subunits of Hdr-like proteins and four subunits of the flavin oxidoreductase genes (Flox) in *D. gigas*, *D. africanus* and *D. alaskensis* or three subunits in *D. vulgaris* Hindelborough and *D. desulfuricans* ATCC27774. *a* – alcohol dehydrogenase; b – aldehyde dehydrogenase.

2.5 Conclusions

The observations herewith reported for the genome of *D. gigas* ATCC19364 highlight the differences found within several species of the *Desulfovibrio* genus. *D. gigas* presents a great number of CRISPR elements and a different CRISPR/Cas system when compared to the archetypal array from *D. vulgaris.* Besides it also contains an atypical CRISPR/Cas system not found in other *Desulfovibrio* spp.

Duplication of genes involved in stress responses, such as a new superoxide dismutase (SOD) besides the neelaredoxin also designated as *sor,*, a second *norR* transcriptional factor, NorRL2 (in addition to the NorRL1), several putative nitrate reductases and a unique aerobic-type carbon monoxide dehydrogenase indicates a highly developed and flexible enzymatic machinery to overcome the deleterious effects of an aerobic environment. Likewise, the identification of a second fumarate reductase (FrdABC) and a second formate dehydrogenase (Fdh) suggest that this flexibility is also present in the energetic metabolism. Furthermore, the presence of a low number of hydrogenases and the absence of *codh* and *pfl genes* indicates that intermediate compounds (H_2, CO and formate) do not contribute to cycling mechanisms of energy conservation in *D. gigas* as much as they do in other *Desulfovibrio* spp. The presence of other complexes, in particular: a secondary vacuolar type ATPase, two complexes linking NAD(P)H and ferredoxins with electron transfer (*nuo* and *mnh*), a heterodimeric transhydrogenase, a cytochromes c in the Rnf complex and an aldehyde dehydrogenase in the vicinity of the Hdr/Flox operon may provide alternative routes for energy conservation processes. This might indicate that different substrates (alcohols and aldehydes) and coenzymes (NAD^+/$NADP^+$) could play a more important role in redox reactions of *D. gigas* than previously thought.

2.6 Acknowledgements

We thank Teresa Barata and Mario Vicente for their support in the first part of this work. We also would like to thank Edson Luiz Folado, Leilane Oliveira Gonçalves and Elvira C. A. Horácio for their help in processing the genomic data. This work was supported by Fundação para Ciência e Tecnologia (FCT) through grants PTDC/BIA-IC/104030/2008 given to C.R.P., Pest-OE/EQB/LA0004/2011 given to ITQB. Agência de Inovação (ADI) also supported our research through the grant ADI/2006/M2.3/003 given to C.R.P. and O.F. We are also greatly indebted to

STAB Vida and BIOCANT for their financial support. F.M.S (SFRH/BD/45211/2008), C.P. (SFRH/BPD/90823/2012) S.S. (grant SFRH / BPD / 80244 / 2011), were supported by FCT fellowships. The work conducted in CPqRR – FIOCRUZ, was supported by Coordenação de Aperfeiçoamento de Pessoal de Ensino Superior (CAPES); Fundação de Amparo à Pesquisa do Estado de Minas Gerais, National Counsel of Technological and Scientific Development (CNPq) and Rede Integrada de Estudos Genômicos e Proteômicos (GENOPROT) through grants APQ-02382-10, PRI-00197-12, APQ-01085-12, and grants 476539/2010-2, 301652/2012-0 and 560943/2010-5.

Supplemental Material

Additional supporting information, found in the Supplemental Material – Chapter 1, contain the following lists of identified genes:

Table S0: COG functional groups
Table S1: Alcohol metabolism
Table S2: ATP synthesis
Table S3: Beta oxidation
Table S4: Embden-Meyerhof-Parnas Pathway
Table S5: Entner-Doudoroff Pathway
Table S6: Pentose phosphate Pathway
Table S7: TCA Cycle
Table S8: WoodLjungahl Pathway
Table S9: Oxidation of pyruvate to acetyl-CoA and acetate formation
Table S10: Lactate metabolism
Table S11: Beta Lactamase proteins
Table S12: Formate Metabolism
Table S13: Fumarate Metabolism
Table S14: Glyoxylate Cycle
Table S15: Methylglyoxylate Cycle

2.7 References

Abascal, F., Zardoya, R., and Posada, D. (2005) ProtTest: selection of best-fit models of protein evolution. *Bioinformatics* **21**: 2104-2105.

Almeida, C.C., Romao, C.V., Lindley, P.F., Teixeira, M., and Saraiva, L.M. (2006) The role of the hybrid cluster protein in oxidative stress defense. *J Biol Chem* **281**: 32445-32450.

Almendra, M.J., Brondino, C.D., Gavel, O., Pereira, A.S., Tavares, P., Bursakov, S. *et al*. (1999) Purification and characterization of a tungsten-containing formate dehydrogenase from Desulfovibrio gigas. *Biochemistry* **38**: 16366-16372.

Altschul, S.F., Gish, W., Miller, W., Myers, E.W., and Lipman, D.J. (1990) Basic local alignment search tool. *Journal of Molecular Biology* **215**: 403-410.

Ambler, R.P., Bruschi, M., and Le Gall, J. (1969) The structure of cytochrome c'(3) from desulfovibrio gigas (NCIB 9332). *FEBS Lett* **5**: 115-117.

Archer, M., Huber, R., Tavares, P., Moura, I., Moura, J.J., Carrondo, M.A. *et al*. (1995) Crystal structure of desulforedoxin from Desulfovibrio gigas determined at 1.8 A resolution: a novel non-heme iron protein structure. *Journal of Molecular Biology* **251**: 690-702.

Armitage, J.P. (1997) Behavioural responses of bacteria to light and oxygen. *Archives of Microbiology* **168**: 249-261.

Arnvig, K.B., Gopal, B., Papavinasasundaram, K.G., Cox, R.A., and Colston, M.J. (2005) The mechanism of upstream activation in the rrnB operon of Mycobacterium smegmatis is different from the Escherichia coli paradigm. *Microbiology* **151**: 467-473.

Assefa, S., Keane, T.M., Otto, T.D., Newbold, C., and Berriman, M. (2009) ABACAS: algorithm-based automatic contiguation of assembled sequences. *Bioinformatics* **25**: 1968-1969.

Bayer, A.S., McNamara, P., Yeaman, M.R., Lucindo, N., Jones, T., Cheung, A.L. *et al*. (2006) Transposon disruption of the complex I NADH oxidoreductase gene (snoD) in Staphylococcus aureus is associated with reduced susceptibility to the microbicidal activity of thrombin-induced platelet microbicidal protein 1. *J Bacteriol* **188**: 211-222.

Bennett, P.M. (2004) Genome plasticity: insertion sequence elements, transposons and integrons, and DNA rearrangement. *Methods Mol Biol* **266**: 71-113.

Bhaya, D., Davison, M., and Barrangou, R. (2011) CRISPR-Cas systems in bacteria and archaea: versatile small RNAs for adaptive defense and regulation. *Annu Rev Genet* **45**: 273-297.

Biegel, E., and Muller, V. (2010) Bacterial Na+-translocating ferredoxin:NAD+ oxidoreductase. *Proc Natl Acad Sci U S A* **107**: 18138-18142.

Broco, M., Rousset, M., Oliveira, S., and Rodrigues-Pousada, C. (2005) Deletion of flavoredoxin gene in Desulfovibrio gigas reveals its participation in thiosulfate reduction. *FEBS Lett* **579**: 4803-4807.

Brown, S.D., Gilmour, C.C., Kucken, A.M., Wall, J.D., Elias, D.A., Brandt, C.C. *et al*. (2011) Genome sequence of the mercury-methylating strain Desulfovibrio desulfuricans ND132. *J Bacteriol* **193**: 2078-2079.

Cabello, P., Pino, C., Olmo-Mira, M.F., Castillo, F., Roldan, M.D., and Moreno-Vivian, C. (2004) Hydroxylamine assimilation by Rhodobacter capsulatus E1F1. requirement of the hcp gene (hybrid cluster protein) located in the nitrate assimilation nas gene region for hydroxylamine reduction. *J Biol Chem* **279**: 45485-45494.

Canfield, D.E., and Des Marais, D.J. (1991) Aerobic sulfate reduction in microbial mats. *Science* **251**: 1471-1473.

Carver, T.J., Rutherford, K.M., Berriman, M., Rajandream, M.A., Barrell, B.G., and Parkhill, J. (2005) ACT: the Artemis Comparison Tool. *Bioinformatics* **21**: 3422-3423.

Chen, L., Liu, M.Y., Legall, J., Fareleira, P., Santos, H., and Xavier, A.V. (1993) Purification and characterization of an NADH-rubredoxin oxidoreductase involved in the utilization of oxygen by Desulfovibrio gigas. *Eur J Biochem* **216**: 443-448.

Cooper, S.J., Garner, C.D., Hagen, W.R., Lindley, P.F., and Bailey, S. (2000) Hybrid-Cluster Protein (HCP) from Desulfovibrio vulgaris (Hildenborough) at 1.6 Å Resolution†,‡. *Biochemistry* **39**: 15044-15054.

Dahl, C., Engels, S., Pott-Sperling, A.S., Schulte, A., Sander, J., Lubbe, Y. *et al*. (2005) Novel genes of the dsr gene cluster and evidence for close interaction of Dsr proteins during sulfur oxidation in the phototrophic sulfur bacterium Allochromatium vinosum. *J Bacteriol* **187**: 1392-1404.

Delsuc, F., Stanhope, M.J., and Douzery, E.J. (2003) Molecular systematics of armadillos (Xenarthra, Dasypodidae): contribution of maximum likelihood and Bayesian analyses of mitochondrial and nuclear genes. *Molecular Phylogenetics and Evolution* **28**: 261-275.

Dobbek, H., Gremer, L., Meyer, O., and Huber, R. (1999) Crystal structure and mechanism of CO dehydrogenase, a molybdo iron-sulfur flavoprotein containing S-selanylcysteine. *Proc Natl Acad Sci U S A* **96**: 8884-8889.

Dominova, I.N., Sorokin, D.Y., Kublanov, I.V., Patrushev, M.V., and Toshchakov, S.V. (2013) Complete Genome Sequence of Salinarchaeum sp. Strain HArcht-Bsk1T, Isolated from Hypersaline Lake Baskunchak, Russia. *Genome Announc* **1**.

Dos Santos, W.G., Pacheco, I., Liu, M.Y., Teixeira, M., Xavier, A.V., and LeGall, J. (2000) Purification and characterization of an iron superoxide dismutase and a catalase from the sulfate-reducing bacterium Desulfovibrio gigas. *J Bacteriol* **182**: 796-804.

Douzi, B., Filloux, A., and Voulhoux, R. (2012) On the path to uncover the bacterial type II secretion system. *Philos Trans R Soc Lond B Biol Sci* **367**: 1059-1072.

Eschemann, A., Kuhl, M., and Cypionka, H. (1999) Aerotaxis in Desulfovibrio. *Environmental Microbiology* **1**: 489-494.

Ewing, B., and Green, P. (1998) Base-calling of automated sequencer traces using phred. II. Error probabilities. *Genome Res* **8**: 186-194.

Ewing, B., Hillier, L., Wendl, M.C., and Green, P. (1998) Base-calling of automated sequencer traces using phred. I. Accuracy assessment. *Genome Res* **8**: 175-185.

Fareleira, P., Legall, J., Xavier, A.V., and Santos, H. (1997) Pathways for utilization of carbon reserves in Desulfovibrio gigas under fermentative and respiratory conditions. *J Bacteriol* **179**: 3972-3980.

Felix, R., Rodrigues, R., Machado, P., Oliveira, S., and Rodrigues-Pousada, C. (2006) A chemotaxis operon in the bacterium Desulfovibrio gigas is induced under several growth conditions. *DNA Seq* **17**: 56-64.

Figueiredo, M.C.O., Lobo, S.A.L., Sousa, S.H., Pereira, F.P., Wall, J.D., Nobre, L.S., and Saraiva, L.M. (2013) Hybrid Cluster Proteins and Flavodiiron Proteins Afford Protection to Desulfovibrio vulgaris upon Macrophage Infection. *J Bacteriol* **195**: 2684-2690.

Frazao, C., Silva, G., Gomes, C.M., Matias, P., Coelho, R., Sieker, L. *et al*. (2000) Structure of a dioxygen reduction enzyme from Desulfovibrio gigas. *Nature Structural Biology* **7**: 1041-1045.

Gasiunas, G., Sinkunas, T., and Siksnys, V. (2013) Molecular mechanisms of CRISPR-mediated microbial immunity. *Cellular and molecular life sciences : CMLS*.

Gilmour, C.C., Elias, D.A., Kucken, A.M., Brown, S.D., Palumbo, A.V., Schadt, C.W., and Wall, J.D. (2011) Sulfate-reducing bacterium Desulfovibrio desulfuricans ND132 as a model for understanding bacterial mercury methylation. *Appl Environ Microbiol* **77**: 3938-3951.

Godde, J.S., and Bickerton, A. (2006) The repetitive DNA elements called CRISPRs and their associated genes: evidence of horizontal transfer among prokaryotes. *J Mol Evol* **62**: 718-729.

Greene, E.A., Hubert, C., Nemati, M., Jenneman, G.E., and Voordouw, G. (2003) Nitrite reductase activity of sulphate-reducing bacteria prevents their inhibition by nitrate-reducing, sulphide-oxidizing bacteria. *Environmental Microbiology* **5**: 607-617.

Grissa, I., Vergnaud, G., and Pourcel, C. (2007) The CRISPRdb database and tools to display CRISPRs and to generate dictionaries of spacers and repeats. *BMC Bioinformatics* **8**: 172.

Guindon, S., Dufayard, J.F., Lefort, V., Anisimova, M., Hordijk, W., and Gascuel, O. (2010) New algorithms and methods to estimate maximum-likelihood phylogenies: assessing the performance of PhyML 3.0. *Syst Biol* **59**: 307-321.

Haft, D.H., Selengut, J., Mongodin, E.F., and Nelson, K.E. (2005) A guild of 45 CRISPR-associated (Cas) protein families and multiple CRISPR/Cas subtypes exist in prokaryotic genomes. *PLoS Comput Biol* **1**: e60.

Hamilton, W.A. (1985) Sulphate-reducing bacteria and anaerobic corrosion. *Annu Rev Microbiol* **39**: 195-217.

Haveman, S.A., Greene, E.A., and Voordouw, G. (2005) Gene expression analysis of the mechanism of inhibition of Desulfovibrio vulgaris Hildenborough by nitrate-reducing, sulfide-oxidizing bacteria. *Environmental Microbiology* **7**: 1461-1465.

Haveman, S.A., Greene, E.A., Stilwell, C.P., Voordouw, J.K., and Voordouw, G. (2004) Physiological and gene expression analysis of inhibition of Desulfovibrio vulgaris hildenborough by nitrite. *J Bacteriol* **186**: 7944-7950.

He, Q., Huang, K.H., He, Z., Alm, E.J., Fields, M.W., Hazen, T.C. *et al*. (2006) Energetic consequences of nitrite stress in Desulfovibrio vulgaris Hildenborough, inferred from global transcriptional analysis. *Appl Environ Microbiol* **72**: 4370-4381.

Hedges, S.B., Blair, J.E., Venturi, M.L., and Shoe, J.L. (2004) A molecular timescale of eukaryote evolution and the rise of complex multicellular life. *Bmc Evolutionary Biology* **4**: 2.

Heidelberg, J.F., Seshadri, R., Haveman, S.A., Hemme, C.L., Paulsen, I.T., Kolonay, J.F. *et al*. (2004) The genome sequence of the anaerobic, sulfate-reducing bacterium Desulfovibrio vulgaris Hildenborough. *Nature Biotechnology* **22**: 554-559.

Hsieh, Y.C., Liu, M.Y., Le Gall, J., and Chen, C.J. (2005) Anaerobic purification and crystallization to improve the crystal quality: ferredoxin II from Desulfovibrio gigas. *Acta Crystallogr D Biol Crystallogr* **61**: 780-783.

Huang, H., and Larter, S. (2005) Biodegradation of petroleum in subsurface geological reservoirs. In *Petroleum Microbiology*. Olliver, B., and Magot, M. (eds). Washington, DC, USA: ASM Press, pp. 91–122.

Jansen, R., van Embden, J.D., Gaastra, W., and Schouls, L.M. (2002) Identification of a novel family of sequence repeats among prokaryotes. *OMICS* **6**: 23-33.

Janssen, A.J., Ruitenberg, R., and Buisman, C.J. (2001) Industrial applications of new sulphur biotechnology. *Water Sci Technol* **44**: 85-90.

Ji, B., Gimenez, G., Barbe, V., Vacherie, B., Rouy, Z., Amrani, A. *et al*. (2013) Complete Genome Sequence of the Piezophilic, Mesophilic, Sulfate-Reducing Bacterium Desulfovibrio hydrothermalis AM13(T.). *Genome Announc* **1**.

Johnston, S., Lin, S., Lee, P., Caffrey, S.M., Wildschut, J., Voordouw, J.K. *et al*. (2009) A genomic island of the sulfate-reducing bacterium Desulfovibrio vulgaris Hildenborough promotes survival under stress conditions while decreasing the efficiency of anaerobic growth. *Environmental Microbiology* **11**: 981-991.

Jones, D.T., Taylor, W.R., and Thornton, J.M. (1992) The rapid generation of mutation data matrices from protein sequences. *Comput Appl Biosci* **8**: 275-282.

Jorgensen, B.B. (1982) Ecology of the bacteria of the sulphur cycle with special reference to anoxic-oxic interface environments. *Philos Trans R Soc Lond B Biol Sci* **298**: 543-561.

Kakinuma, Y., Yamato, I., and Murata, T. (1999) Structure and function of vacuolar Na+-translocating ATPase in Enterococcus hirae. *Journal of Bioenergetics and Biomembranes* **31**: 7-14.

Katoh, K., Misawa, K., Kuma, K., and Miyata, T. (2002) MAFFT: a novel method for rapid multiple sequence alignment based on fast Fourier transform. *Nucleic Acids Research* **30**: 3059-3066.

Krekeler, C., Ziehr, H., and Klein, J. (1989) Physical methods for characterization of microbial surfaces. *Experientia* **45**: 1047-1055.

Kunin, V., Sorek, R., and Hugenholtz, P. (2007) Evolutionary conservation of sequence and secondary structures in CRISPR repeats. *Genome Biol* **8**: R61.

Lagesen, K., Hallin, P., Rodland, E.A., Staerfeldt, H.H., Rognes, T., and Ussery, D.W. (2007) RNAmmer: consistent and rapid annotation of ribosomal RNA genes. *Nucleic Acids Research* **35**: 3100-3108.

Le, S.Q., and Gascuel, O. (2008) An improved general amino acid replacement matrix. *Mol Biol Evol* **25**: 1307-1320.

Legall, J. (1963) A New Species of Desulfovibrio. *J Bacteriol* **86**: 1120.

Lenz, M., Hullebusch, E.D., Hommes, G., Corvini, P.F., and Lens, P.N. (2008) Selenate removal in methanogenic and sulfate-reducing upflow anaerobic sludge bed reactors. *Water Res* **42**: 2184-2194.

Li, Q., Li, L., Rejtar, T., Lessner, D.J., Karger, B.L., and Ferry, J.G. (2006) Electron transport in the pathway of acetate conversion to methane in the marine archaeon Methanosarcina acetivorans. *J Bacteriol* **188**: 702-710.

Li, X., McInerney, M.J., Stahl, D.A., and Krumholz, L.R. (2011) Metabolism of H2 by Desulfovibrio alaskensis G20 during syntrophic growth on lactate. *Microbiology* **157**: 2912-2921.

Lowe, T.M., and Eddy, S.R. (1997) tRNAscan-SE: a program for improved detection of transfer RNA genes in genomic sequence. *Nucleic Acids Research* **25**: 955-964.

Makarova, K.S., Haft, D.H., Barrangou, R., Brouns, S.J., Charpentier, E., Horvath, P. *et al*. (2011) Evolution and classification of the CRISPR-Cas systems. *Nat Rev Microbiol* **9**: 467-477.

Mancini, S., Abicht, H.K., Karnachuk, O.V., and Solioz, M. (2011) Genome sequence of Desulfovibrio sp. A2, a highly copper resistant, sulfate-reducing bacterium isolated from effluents of a zinc smelter at the Urals. *J Bacteriol* **193**: 6793-6794.

Marchler-Bauer, A., Zheng, C., Chitsaz, F., Derbyshire, M.K., Geer, L.Y., Geer, R.C. *et al*. (2013) CDD: conserved domains and protein three-dimensional structure. *Nucleic Acids Research* **41**: D348-352.

Marraffini, L.A., and Sontheimer, E.J. (2008) CRISPR interference limits horizontal gene transfer in staphylococci by targeting DNA. *Science* **322**: 1843-1845.

Matias, P.M., Morais, J., Coelho, R., Carrondo, M.A., Wilson, K., Dauter, Z., and Sieker, L. (1996) Cytochrome c3 from Desulfovibrio gigas: crystal structure at 1.8 A resolution and evidence for a specific calcium-binding site. *Protein Sci* **5**: 1342-1354.

Mojica, F.J., Diez-Villasenor, C., Soria, E., and Juez, G. (2000) Biological significance of a family of regularly spaced repeats in the genomes of Archaea, Bacteria and mitochondria. *Mol Microbiol* **36**: 244-246.

Morais-Silva, F.O., Santos, C.I., Rodrigues, R., Pereira, I.A., and Rodrigues-Pousada, C. (2013) Role of HynAB and Ech, the only two hydrogenases found in the model sulfate reducer Desulfovibrio gigas. *J Bacteriol*.

Moura, I., Bruschi, M., Le Gall, J., Moura, J.J., and Xavier, A.V. (1977) Isolation and characterization of desulforedoxin, a new type of non-heme iron protein from Desulfovibrio gigas. *Biochem Biophys Res Commun* **75**: 1037-1044.

Muyzer, G., and Stams, A. (2008) The ecology and biotechnology of sulphate-reducing bacteria. *Nature reviews Microbiology* **6**: 441-454.

Nakazawa, H., Arakaki, A., Narita-Yamada, S., Yashiro, I., Jinno, K., Aoki, N. *et al*. (2009) Whole genome sequence of Desulfovibrio magneticus strain RS-1 revealed common gene clusters in magnetotactic bacteria. *Genome Res* **19**: 1801-1808.

Odom, J.M., and Peck, H.D., Jr. (1981) Localization of dehydrogenases, reductases, and electron transfer components in the sulfate-reducing bacterium Desulfovibrio gigas. *J Bacteriol* **147**: 161-169.

Overeijnder, M.L., Hagen, W.R., and Hagedoorn, P.L. (2009) A thermostable hybrid cluster protein from Pyrococcus furiosus: effects of the loss of a three helix bundle subdomain. *J Biol Inorg Chem* **14**: 703-710.

Pereira, I.A., Ramos, A.R., Grein, F., Marques, M.C., da Silva, S.M., and Venceslau, S.S. (2011) A comparative genomic analysis of energy metabolism in sulfate reducing bacteria and archaea. *Front Microbiol* **2**: 69.

Pereira, P.M., Teixeira, M., Xavier, A.V., Louro, R.O., and Pereira, I.A. (2006) The Tmc complex from Desulfovibrio vulgaris hildenborough is involved in transmembrane electron transfer from periplasmic hydrogen oxidation. *Biochemistry* **45**: 10359-10367.

Pereira, P.M., He, Q., Valente, F.M., Xavier, A.V., Zhou, J., Pereira, I.A., and Louro, R.O. (2008) Energy metabolism in Desulfovibrio vulgaris Hildenborough: insights from transcriptome analysis. *Antonie Van Leeuwenhoek* **93**: 347-362.

Pires, R., Lourenço, A., Morais, F., Teixeira, M., Xavier, A., Saraiva, L., and Pereira, I. (2003) A novel membrane-bound respiratory complex from Desulfovibrio desulfuricans ATCC 27774. *Biochimica et biophysica acta* **1605**: 67-82.

Plugge, C.M., Scholten, J.C., Culley, D.E., Nie, L., Brockman, F.J., and Zhang, W. (2010) Global transcriptomics analysis of the Desulfovibrio vulgaris change from syntrophic growth with Methanosarcina barkeri to sulfidogenic metabolism. *Microbiology* **156**: 2746-2756.

Raaijmakers, H., Macieira, S., Dias, J.M., Teixeira, S., Bursakov, S., Huber, R. *et al*. (2002) Gene sequence and the 1.8 A crystal structure of the tungsten-containing formate dehydrogenase from Desulfovibrio gigas. *Structure* **10**: 1261-1272.

Rabus, R., Hansen, T.A., and Widdel, F. (2006) Dissimilatory sulfate- and sulfur-reducing prokaryotes. In. Dworkin, M., Falkow, S., Rosenberg, E., Schleifer, K.H., and Stackebrandt, E. (ed).

Ragsdale, S.W., and Pierce, E. (2008) Acetogenesis and the Wood-Ljungdahl pathway of CO(2) fixation. *Biochimica Et Biophysica Acta* **1784**: 1873-1898.

Rodionov, D.A., Dubchak, I., Arkin, A., Alm, E., and Gelfand, M.S. (2004) Reconstruction of regulatory and metabolic pathways in metal-reducing delta-proteobacteria. *Genome Biol* **5**: R90.

Rodrigues, P.M., Macedo, A.L., Goodfellow, B.J., Moura, I., and Moura, J.J. (2006a) Desulfovibrio gigas ferredoxin II: redox structural modulation of the [3Fe-4S] cluster. *J Biol Inorg Chem* **11**: 307-315.

Rodrigues, R., Valente, F.M., Pereira, I.A., Oliveira, S., and Rodrigues-Pousada, C. (2003) A novel membrane-bound Ech [NiFe] hydrogenase in Desulfovibrio gigas. *Biochem Biophys Res Commun* **306**: 366-375.

Rodrigues, R., Vicente, J.B., Felix, R., Oliveira, S., Teixeira, M., and Rodrigues-Pousada, C. (2006b) Desulfovibrio gigas flavodiiron protein affords protection against nitrosative stress in vivo. *J Bacteriol* **188**: 2745-2751.

Romao, M.J., Archer, M., Moura, I., Moura, J.J., LeGall, J., Engh, R. *et al*. (1995) Crystal structure of the xanthine oxidase-related aldehyde oxido-reductase from D. gigas. *Science* **270**: 1170-1176.

Rossi, M., Pollock, W.B., Reij, M.W., Keon, R.G., Fu, R., and Voordouw, G. (1993) The hmc operon of Desulfovibrio vulgaris subsp. vulgaris Hildenborough encodes a potential transmembrane redox protein complex. *J Bacteriol* **175**: 4699-4711.

Rousseau, C., Gonnet, M., Le Romancer, M., and Nicolas, J. (2009) CRISPI: a CRISPR interactive database. *Bioinformatics* **25**: 3317-3318.

Rutherford, K., Parkhill, J., Crook, J., Horsnell, T., Rice, P., Rajandream, M.A., and Barrell, B. (2000) Artemis: sequence visualization and annotation. *Bioinformatics* **16**: 944-945.

Silva, G., LeGall, J., Xavier, A.V., Teixeira, M., and Rodrigues-Pousada, C. (2001) Molecular characterization of Desulfovibrio gigas neelaredoxin, a protein involved in oxygen detoxification in anaerobes. *J Bacteriol* **183**: 4413-4420.

Silva, G., Oliveira, S., Gomes, C.M., Pacheco, I., Liu, M.Y., Xavier, A.V. *et al*. (1999) Desulfovibrio gigas neelaredoxin. A novel superoxide dismutase integrated in a putative oxygen sensory operon of an anaerobe. *Eur J Biochem* **259**: 235-243.

Sorek, R., Kunin, V., and Hugenholtz, P. (2008) CRISPR--a widespread system that provides acquired resistance against phages in bacteria and archaea. *Nat Rev Microbiol* **6**: 181-186.

Spring, S., Visser, M., Lu, M., Copeland, A., Lapidus, A., Lucas, S. *et al*. (2012) Complete genome sequence of the sulfate-reducing firmicute Desulfotomaculum ruminis type strain (DL(T)). *Stand Genomic Sci* **7**: 304-319.

Tamura, K., Peterson, D., Peterson, N., Stecher, G., Nei, M., and Kumar, S. (2011) MEGA5: molecular evolutionary genetics analysis using maximum likelihood, evolutionary distance, and maximum parsimony methods. *Mol Biol Evol* **28**: 2731-2739.

Teeling, E.C., Madsen, O., Murphy, W.J., Springer, M.S., and O'Brien, S.J. (2003) Nuclear gene sequences confirm an ancient link between New

Zealand's short-tailed bat and South American noctilionoid bats. *Molecular Phylogenetics and Evolution* **28**: 308-319.

Teske, A., Ramsing, N.B., Habicht, K., Fukui, M., Kuver, J., Jorgensen, B.B., and Cohen, Y. (1998) Sulfate-reducing bacteria and their activities in cyanobacterial mats of solar lake (Sinai, Egypt). *Appl Environ Microbiol* **64**: 2943-2951.

van den Berg, W.A., Hagen, W.R., and van Dongen, W.M. (2000) The hybrid-cluster protein ('prismane protein') from Escherichia coli. Characterization of the hybrid-cluster protein, redox properties of the [2Fe-2S] and [4Fe-2S-2O] clusters and identification of an associated NADH oxidoreductase containing FAD and [2Fe-2S]. *Eur J Biochem* **267**: 666-676.

Vance, I., and Thrasher, D.R. (2005) Reservoir souring: mechanisms and prevention. In *Petroleum Microbiology*. Olliver, B., and Magot, M. (eds). Washington, DC, USA: ASM Press, pp. 123-142.

Varela-Raposo, A., Pimentel, C., Morais-Silva, F., Rezende, A., Ruiz, J.C., and Rodrigues-Pousada, C. (2013) Role of NorR-like transcriptional regulators under nitrosative stress of the delta-proteobacterium, Desulfovibrio gigas. *Biochem Biophys Res Commun* **431**: 590-596.

Venceslau, S.S., Lino, R.R., and Pereira, I.A. (2010) The Qrc membrane complex, related to the alternative complex III, is a menaquinone reductase involved in sulfate respiration. *Journal of Biological Chemistry* **285**: 22774-22783.

Volbeda, A., Charon, M.H., Piras, C., Hatchikian, E.C., Frey, M., and Fontecilla-Camps, J.C. (1995) Crystal structure of the nickel-iron hydrogenase from Desulfovibrio gigas. *Nature* **373**: 580-587.

Voordouw, G. (2002) Carbon monoxide cycling by Desulfovibrio vulgaris Hildenborough. *Journal of Bacteriology* **184**: 5903-5911.

Walker, C.B., He, Z.L., Yang, Z.K., Ringbauer, J.A., He, Q., Zhou, J.H. *et al*. (2009) The Electron Transfer System of Syntrophically Grown Desulfovibrio vulgaris. *Journal of Bacteriology* **191**: 5793-5801.

Wang, S., Huang, H., Moll, J., and Thauer, R.K. (2010) NADP+ reduction with reduced ferredoxin and NADP+ reduction with NADH are coupled via an electron-bifurcating enzyme complex in Clostridium kluyveri. *J Bacteriol* **192**: 5115-5123.

Wolf, Y.I., Rogozin, I.B., and Koonin, E.V. (2004) Coelomata and not Ecdysozoa: evidence from genome-wide phylogenetic analysis. *Genome Res* **14**: 29-36.

Wolfe, M.T., Heo, J., Garavelli, J.S., and Ludden, P.W. (2002) Hydroxylamine reductase activity of the hybrid cluster protein from Escherichia coli. *J Bacteriol* **184**: 5898-5902.

Yurkiw, M.A., Voordouw, J., and Voordouw, G. (2012) Contribution of rubredoxin:oxygen oxidoreductases and hybrid cluster proteins of Desulfovibrio vulgarisHildenborough to survival under oxygen and nitrite stress. *Environmental Microbiology* **14**: 2711-2725.

Zaunmuller, T., Kelly, D.J., Glockner, F.O., and Unden, G. (2006) Succinate dehydrogenase functioning by a reverse redox loop mechanism and

fumarate reductase in sulphate-reducing bacteria. *Microbiology* **152**: 2443-2453.

Zdobnov, E.M., and Apweiler, R. (2001) InterProScan--an integration platform for the signature-recognition methods in InterPro. *Bioinformatics* **17**: 847-848.

Zerbino, D.R., and Birney, E. (2008) Velvet: algorithms for de novo short read assembly using de Bruijn graphs. *Genome Res* **18**: 821-829.

Chapter 3

Hydrogenase physiological role during respiratory and fermentative conditions

The work presented in this chapter was published in:

Morais-Silva F., C. Santos, R. Rodrigues, I. Pereira, and C. Rodrigues-Pousada. (2013). “Roles of HynAB and Ech, the only two hydrogenases found in the model sulfate reducer *Desulfovibrio gigas*.” *Journal of bacteriology* 195: 4753–60

The author of this thesis had a major contribution in the work presented in this chapter, namely in the planning of the experimental work, performing the experiments and analyzing the data. It is important to acknowledge that the construction of the *D. gigas* Ech hydrogenase mutant strain (Δ*ech*) was done previously by Dr. Rute Rodrigues.

3.1 Summary

Sulfate-reducing bacteria are characterized by a high number of hydrogenases, which have been proposed to contribute to the overall energy metabolism of the cell, but exactly in what role is not clear. *Desulfovibrio* spp. can produce or consume H_2 when growing on organic or inorganic substrates in the presence or absence of sulfate. Due to the presence of only two hydrogenases encoded in its genome, the periplasmic HynAB and the cytoplasmic Ech hydrogenases, *Desulfovibrio gigas* is an excellent model organism to investigate the specific function of each of these enzymes during growth. In this report we analyzed the physiological response of the deletion of the genes encoding each of the two hydrogenases in *D. gigas*, through the generation of single mutant strains, Δ*echBC* and Δ*hynAB*. These strains were analyzed for their ability to grow using different substrates, such as lactate, pyruvate and hydrogen in respiratory and fermentative conditions. Furthermore, expression of both hydrogenase genes was assessed through qRT-PCR, in the three strains studied. The results demonstrate that neither hydrogenase is essential for growth on lactate/sulfate, indicating that hydrogen cycling is not indispensable. In addition, the periplasmic HynAB enzyme has a bifunctional activity and is required for growth on H_2 or by fermentation of pyruvate. Therefore, this enzyme seems to play a dominant role in *D. gigas* hydrogen metabolism.

3.2 Introduction

Hydrogenases are key enzymes in hydrogen metabolism of *Desulfovibrio* spp. that catalyze the reversible oxidation of molecular hydrogen into protons and electrons (Matias *et al*., 2005). However, their role during sulfate respiration has not been clearly established. Odom and Peck proposed a hydrogen cycling model to explain energy conservation during growth on lactate and sulfate by *Desulfovibrio* spp., which belong to the deltaproteobacteria sub-group of the sulfate-reducing bacteria (SRB) (Odom and Peck, 1981). The model predicts that protons and electrons produced in the oxidation of lactate are used for the production of molecular hydrogen by a cytoplasmic hydrogenase. This hydrogen then diffuses across the membrane to the periplasm, where it is re-oxidized by a periplasmic hydrogenase. Electrons are transferred back to the cytoplasm for sulfate reduction, thus creating a proton gradient across the membrane that leads to ATP formation. In this model the presence of at least two hydrogenases on opposite sides of the membrane is a requirement for growth. In contrast, other studies suggested that the physiological role of these enzymes was to regulate the redox potential of the cell, controlling the flow of protons and electrons and generating a proton motive force (Lupton *et al*., 1984) . More recent models, proposed for *Desulfovibrio vulgaris*, suggested dual pathways for electron transfer from lactate to sulfate: one involving the cycling of H_2, and the other a route involving a membrane-associated electron transfer chain (Noguera *et al*., 1998; Keller and Wall, 2011). Several membrane complexes have been identified in SRB which could be involved in this process (reviewed in (Pereira *et al*., 2011)). It was estimated that about 48% of electrons transported from lactate to sulfate involved H_2 production (Noguera *et al*., 1998).

Several studies have tried to elucidate the function of hydrogenases in *Desulfovibrio* spp., but because most of these organisms present a multiplicity of hydrogenases, in the periplasm and/or in the cytoplasm, identifying the role of each enzyme is complex. In addition, the expression pattern of different

hydrogenases was shown to be different and to depend on the substrate, fermentative or respiratory growth or metal availability (Valente *et al*., 2006; Caffrey *et al*., 2007; Pereira *et al*., 2008; Walker *et al*., 2009; Plugge *et al*., 2010; Keller and Wall, 2011; Li *et al*., 2011; Meyer *et al*., 2013). Furthermore, the function of each hydrogenase in terms of hydrogen production or oxidation may vary depending on the conditions presented to the cell. Numerous studies reported hydrogenase mutant strains in *Desulfovibrio fructosovorans* and in *Desulfovibrio vulgaris* Hildenborough (Malki *et al*., 1997; Casalot *et al*., 2002a; Casalot *et al*., 2002b; Goenka *et al*., 2005; Caffrey *et al*., 2007). However, in most cases, due to the multiplicity of enzymes present, these studies were not conclusive. This indicates that each hydrogenase may contribute to the overall energy metabolism of the cell and that the loss of one enzyme might be compensated by the presence of the remaining ones. In spite of the extensive work performed using hydrogenase deletion strains and also transcriptomic analyses, the results so far obtained have not permitted a complete elucidation of the function and importance of each hydrogenase in the different growth conditions.

Desulfovibrio gigas is an excellent biological model to investigate hydrogenase function and importance in the energy metabolism, since its genome, recently sequenced in our laboratory, encodes only two hydrogenases: the HynAB and the Ech enzymes. Furthermore, because each hydrogenase is located in different cell compartments, *D. gigas* is also an excellent model to study the importance of hydrogen cycling towards energy conservation. The *D. gigas* periplasmic HynAB enzyme is one of the most studied enzymes of the [NiFe] type and was the first [NiFe] hydrogenase to have its crystal structure solved (Volbeda *et al*., 1995). In *Desulfovibrio* spp., as in other bacteria, the periplasmic hydrogenases are believed to be involved in the consumption of hydrogen, coming either from the environment or from intracellular H_2 cycling, generating protons and electrons. The electrons are then shuttled to the cytoplasm through the Type I

cytochrome c_3, the Qrc and Qmo complexes (Pires *et al*., 2003; Li *et al*., 2009; Venceslau *et al*., 2010), to be used for sulfate reduction.

The *D. gigas* cytoplasmic Ech hydrogenase (Rodrigues *et al*., 2003) belongs to the sub-group of multi-subunit membrane-bound energy-conserving [NiFe] hydrogenases (Vignais *et al*., 2001; Hedderich and Forzi, 2005), similarly to the Ech hydrogenase from *Methanosarcina barkeri* (Kunkel *et al*., 1998; Meuer *et al*., 2002). These enzymes have subunits showing high similarity to the energy-conserving Complex I (NADH:quinone oxidoreductase). The Ech hydrogenase in methanogenic archaea can catalyze H_2 formation from reduced ferredoxin, generating a proton motive force, or the reduction of ferredoxin by H_2, driven by reverse electron transport (Meuer *et al*., 2002; Soboh *et al*., 2004; Welte *et al*., 2010b; Welte *et al*., 2010a). However, the function of the Ech hydrogenase in *Desulfovibrio* spp. is still not clear.

To try to elucidate the function of each of these two hydrogenases in *D. gigas* metabolism we have generated single deletion mutants (Δ*echBC* and Δ*hynAB*). These strains were tested under respiratory *vs.* fermentative conditions using different energy sources (lactate, pyruvate or H_2), and the hydrogenase expression profiles at the mRNA level were studied.

3.3 Materials and Methods

Generation of the mutants

To construct the mutant strains, recombinant cassettes containing the DNA fragments of the flanking regions from the genes of interest were amplified from *D. gigas* wild-type (wt) ATCC 19364. A mutant *D. gigas* strain lacking a functional Ech hydrogenase (Δ*ech*) was produced by gene replacement of *ech*B (integral membrane subunit) and *ech*C (electron transfer subunit) with a kanamycin resistance gene (kan^R) amplified from the plasmid pJRD215 [27], through homologous recombination (Broco *et al*., 2005). Oligonucleotides (Table 3.1 *ech*)

were used to amplify ~1kb of adjacent DNA regions upstream subunit *ech*B (FlankI) and downstream subunit *ech*C (FlankII), respectively, from a DNA fragment containing the *ech* operon. *Pfx* DNA polymerase (Invitrogen) was used for amplifications. The PCR products were ligated with T4 DNA Ligase (Fermentas) into the plasmid pZErO-1 (Invitrogen) and this construct was transformed in *E. coli* XL-I Blue. Plasmid DNA was extracted with the plasmid purification kit from Eppendorf.

Table 3.1. Oligonucleotides used for the creation and confirmation of *D. gigas* mutant strains.

Primers	**Sequence**
∆***ech***	
EchFlankI_fwd	5´- GTA CGG ATC CGG TGC TGC GCA TGG CTC C - 3´
EchFlankI rev	5´- CAG CTC TAG AGA CCT CCC ACC ACC AGC AGC - 3´
Ech Flank II_fwd	5´- CGA GTC TAG AGG ATT GAG CCA TGC CCA TCC C - 3´
Ech Flank II_rev	5´- CTC AGG GCC CCG GTG TAG TCG TCC AGA ATG G – 3´
EchKan^{R}XbaI-fwd	5'- GAG TTC TAG ACA GCT ACT GGG CTA TCT G-3'
EchKan^{R}XbaI-rev	5'- GAG TTC TAG ACT GCA GTT CGG GGG CAT G-3'
EchBC-1	5´- GGG GGC CTC ATC ACC GGC G - 3´
EchBC-2	5´-GGG GCA GCT TGA ACA GCA TGG - 3´
∆***hynAB***	
HynABFlankI_fwd	5´- TGA TTA CGC CAA GCT TTC AGG CGG AAG AAT TGG -3´
HynABFlankI_rev	5´- CAG TAG CTG GTC GAC TTA CGT ACC CTC CGT CCT - 3´
HynABFlankII_fwd	5´- GAA CTG CAG GGA TCC GTT CCG GAC GCC AGA C - 3´
HynABFlank II_rev	5´- CAG TGA ATT CGA GCT CGA TTC TTC GGC TTC CTT G-3´
HynABKan^{R}SalI_fwd	5´- GTC GAC CAG CTA CTG GGC TAT CTG - 3´
HynABKan^{R}BHI_rev	5´- GGA TCC CTG CAG TTC GGG GGC ATG - 3´

For the *hynAB* gene, a *D. gigas* mutant strain lacking the entire di-cistronic operon was produced by replacement with kan^R as in the Δ*ech*. Oligonucleotides (Table 3.1 *hynAB*) were used to amplify ~1kb of adjacent DNA regions upstream and downstream of the operon directly from *D. gigas* wild type gDNA. *Phusion* High-fidelity DNA polymerase (Thermo Scientific) was used for amplifications. The PCR products were ligated and transformed into the vector YipLac211 according to the In-Fusion® HD Cloning Kit protocol (Clontech). Kanamycin resistant colonies for both constructs were selected and their plasmids analyzed by restriction enzyme pattern. These plasmids were used for *D. gigas* transformation.

D. gigas cells to be transformed were prepared based on the method previously described (Broco *et al*., 2005) from 500mL of an early stationary phase culture. Immediately before transformation, 6µg of the plasmid construct were mixed with the cells. Transformation was done aerobically in 0.1cm cuvettes by electroporation in a BIORAD Gene Pulser Apparatus, setting the resistance to ∞ and using a 0.7kV voltage and a 3µF capacitance.

Immediately after electroporation, cells were inoculated in lactate/sulfate medium at 37ºC. After a 5h recovery period, kanamycin was added to the medium (50µg/ml), and the cultures were allowed to grow overnight. Cells were then subcultured in lactate/sulfate medium with kanamycin (50µg/ml) for 3 consecutive times.

Colonies were grown for approximately 15 days to one month in medium supplemented with agar (15g/L) and kanamycin (50µg/ml), in Hungate culture tubes using the roll tube technique and/or in plates, inside an AnaeroPack Rectangular Jar 7L (Mitsubishi Gas Chemical Company, Inc) with the AnaeroPack System Sachets (bioMérieux).

The deletions of the *echBC* and *hynAB* genes in the respective mutant strains were confirmed by PCR and Southern-blot analysis (Supplementary Materials).

Culture media and growth conditions

D. gigas cells were grown anaerobically at 37ºC in 100mL flasks with 50mL of media. All media were inoculated with 10% (v/v) of fresh pre-culture cells grown in lactate/sulfate medium.

For most phenotypic analyses, wild type and mutant strains were grown in basal medium modified from (Malki *et al*., 1997) containing per liter: 1g NH_4Cl, 0.15g $CaCl_2$ $2H_2O$, 1g NaCl, 0.5g KCl, 0.4g $MgCl_2$ $7H_2O$, 4.9g KH_2PO_4, 0.1g Yeast extract, and 1.5mL of trace elements (Varela-Raposo *et al*., 2013). This medium was then supplemented with either lactate or pyruvate as electron donors at a concentration of 40mM. Sulfate was added as electron acceptor either at 40mM, 5mM or was absent. For all solutions pH was brought to 7.0 with NaOH. The growth conditions tested were: lactate/sulfate (40mM/40mM); pyruvate/sulfate (40mM/40mM); pyruvate/limiting sulfate (40mM/5mM) and pyruvate (40mM).

In the case of growth with H_2 as sole energy source, cells were grown on modified Postgate Medium C, containing per liter: 0.82g sodium acetate, 0.5g KH_2PO_4, 1g NH_4Cl, 1.14g Na_2SO_4, 0.05g $CaCl_2.2H_2O$, 0.5g $MgSO_4.7H_2O$, 0.2g yeast extract, 0.0071g $FeSO_4$.7H2O, 0.3g sodium citrate, 0.1g ascorbic acid, 0.1g sodium thioglicolate, 1µM Ni, 1µM Se and 0.1µM Mo.. The cultures were inoculated in 100mL flasks containing 50mL of medium and then gassed with H_2:CO_2 (80:20, v/v) at a pressure of 1atm. The 100mL flasks were grown at 37ºC in a horizontal position to enhance the gas-liquid surface area.

Growth of the cultures was monitored by determining the optical density at 600nm (OD_{600nm}). Biomass was determined by measuring the dry cell weight (dcw) and correlating it with OD_{600nm} values. One unit value of OD_{600nm} corresponded to $0.365g_{dcw}$/L.

Analytical procedures

H_2 quantification in the headspace of culture-containing serum bottles was performed by gas chromatography, with a THERMO Unicam Electron Cooperation Trace GC Ultra gas chromatograph fitted with a Alltech Molecular Sieve 5A 80/100 column. The carrier gas was N_2 and measurements were done at 130ºC. Headspace volumes of 30µL were withdrawn with a gastight syringe and injected into the gas chromatograph. The detection limit was 5nmol of molecular hydrogen. Cultures of wild type and both *D. gigas* mutant strains were compared.

Identification and quantification of the organic substrates and products generated during growth were performed by HPLC analyses, with a Waters chromatograph (Waters Chromatography, Milford, MA), consisting of: a Waters 510 Pump, a Waters 715 Autosampler and a Waters Temperature Control Module, connected to a LKB 2142 Differential Refractometer (Bromma, Sweden) detector. Chromatographic separation was undertaken with an Aminex HPX-87H column (300 x 7.8mm), 9 µm particle size (Bio-Rad, Hercules, California) at 45°C. Elution was carried out isocratically, at a flow rate of 0.6mL·min^{-1}, with 0.005N of H_2SO_4 and the injection volume was 20µL. The retention times of the compounds were compared with standards for identification and the peak area was used for quantification.

Sulfate concentration was measured either by HPLC analyses (Rethmeier, 1997) and/or by the SulfaVer4 method (Hach-Lange). HPLC analyses were performed with a Hitachi LaChrom Elite HPLC with a PDA detector. Injections of 20 µL were made in a 10µL loop operated in full-loop mode and the separation was achieved on a PRP-X100 (4.1 × 150mm), 10 µm particle size column (Hamilton Company, Reno, USA), and thermostatted at 25 º C. Isocratic conditions of mobile phase consisted of 3% (v/v) Methanol and 97% (v/v) 4mM 4-Hydroxybenzoic acid (pH 10 adjusted). The flow rate of the eluent was 2 mL.min^{-1}. The indirect UV detection was done at 310nm. The retention time of the compound

was compared with a standard for identification and the peak area was used for quantification.

RNA preparation and Real time reverse transcription quantitative PCR (qRT-PCR) analyses

D. gigas wild type and both mutant strains were grown at 37ºC in the same media composition as described in the growth experiments. Cells were harvested after 16h (mid exponential phase) or 32h of growth (stationary phase). Total RNA was extracted as described in (Silva *et al*., 2001; Rodrigues *et al*., 2006). However, DNAse treatment with Turbo DNAse (Ambion) had to be performed three times to avoid gDNA contamination in the RNA extracts. For each sample 1 µg of total RNA was reverse transcribed with Transcriptor Reverse Transcriptase (Roche Diagnostics). Specific primers amplifying a ~100bp region of *echE* and *hynB* were designed (Table 3.2). The 16S rRNA gene was used as an internal reference gene for each sample analyzed. qRT-PCR reactions were performed in a Light Cycler 480 Real-Time PCR System (Roche), with Light Cycler Fast Start DNA Master SYBR Green I (Roche). Relative standard curves and gene expression was calculated as in (Varela-Raposo *et al*., 2013). For the final results three biological replicates and two technical replicates were used for each condition.

Table 3.2. Oligonucleotides used in the qRT-PCR expression analyzes for *D. gigas* wild type and mutant strains.

Primers	**Sequence**
ech	
Ech_RT_fwd	5´- TCT GGT CCA CCA GCT TCG - 3´
Ech_RT_rev	5´- AGG CGG AAG ACA CCA TCC - 3´
hynAB	
HynAB_RT_fwd	5´- CCG ACG AAT ACG ATC TGA AC - 3´

HynAB_RT_rev	5´- TAC TTG ACG TGC TCC TCG AT - 3´
16S rRNA	
16S_RT_fwd	5´- CTC GTG CCG TGA GGT GTT - 3´
16S_RT_rev	5´- TCC CCA CCT TCC TCC TTG - 3´

Acession Numbers

The NCBI accession numbers for the *D. gigas* genome sequence mentioned in this work is CP006585. In addition, the acession numbers for hydrogenases and specific membrane complexes are as follows: *aprAB/qmoABCD*, KF113859; *dsrMKJOP*, KF113860; *echABCDEF*, AY282786; *hdrABC/floxABCD*, KF113861; *hynAB*, 18083; and *qrcABCD*, KF113862.

3.4 Results

A search of the *D. gigas* genome sequenced in our laboratory revealed the presence of genes encoding only the two known hydrogenases: the periplasmic HynAB and the cytoplasmic Ech hydrogenase. Two mutant strains deleted in these enzymes, the Δ*echBC and* Δ*hynAB* strains, were generated and then tested under different growth conditions.

3.4.1 Confirmation of the Ech and HynAB deletion mutants

For confirmation of the deletion of the *echBC* and *hynAB* genes, Southern-blot analyses were performed using gDNA from *D. gigas* wild-type and the respective mutant strains extracted with Wizard Genomic DNA Purification Kit (Promega).

For the Δ*hynAB* deletion, *BciI* (Roche) was used for the digestion of ~3µg of *D. gigas* wild type and Δ*hynAB* strain gDNA. A probe for the ~1kb upstream region of the *hynA* gene was amplified using *Phusion* High-fidelity DNA polymerase (Thermo Scientific). Southern blotting, prehybridisation and hybridisation were carried out using the DIG High Prime DNA labeling and

Detection Starter kit II (Roche), according to the manufactures protocol. The replacement of the *hynAB* genes for the *kanR* gene creates a new restriction site for *BciI* enzyme generating bands of different sizes. The results showed the expected higher size for the positive band in the *D. gigas* WT (4635bp) and a smaller size for the positive band in the Δ*hynAB* mutated strain (1623bp) as shown in Fig 3.1A.

In the case of the Ech mutation, ~2µg of *D. gigas* wild-type and Δ*echBC* gDNA was digested with *Nco*I (Fermentas). Specific probes for *echBC* and the *kanR* genes were amplified using *Taq* DNA polymerase (Invitrogen) and labeled with [32P]dATP. Southern blotting, prehybridisation and hybridisation were carried out as described.

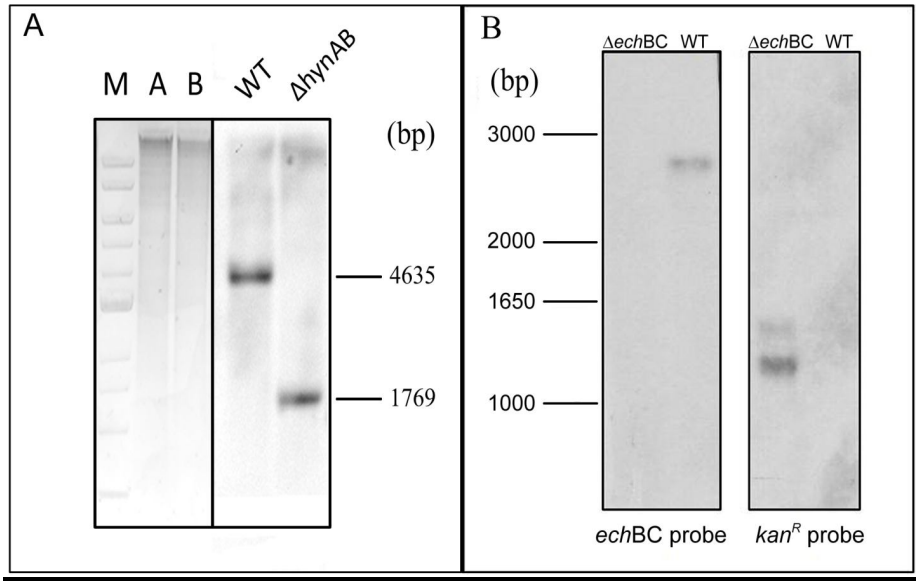

Fig 3.1. Confirmation of *echBC* and *hynAB* deletions. A- Southern-blot analysis of *BciI*-digested genomic DNA from *D. gigas* wild type and Δ*hynAB* strains. Expected band sizes are as follows: 4635bp for WT and 1769bp for the Δ*hynAB*. B- Southern-blot analysis of *Nco*I digested genomic DNA from *D. gigas* wild-type and Δ*echBC* strains. Expected radio-labeled bands are as follows: Δ*echBC* (*echBC* probe), none; WT (*echBC* probe), 2752bp; Δ*echBC* (*kanR* probe), 1230bp and 1623bp; WT (*kanR* probe), none.

Hybridisation with the *echBC* probe resulted in a single positive band of the expected size (2752bp) only in the lane corresponding to *D. gigas* wild-type, whereas hybridisation with the *kan*^{R} probe resulted in two positive bands of the predicted size (1230bp and 1623pb) only in the lane corresponding to *D. gigas* ∆*echBC,* as shown in Fig 3.1B.

Further confirmation was performed through PCR analyses using ~200ng of gDNA from *D. gigas* wild-type or the respective mutant strains as templates and specific oligonucleotides amplifying for the regions of interest (Table 3.1).

In the case of the ∆*echBC* mutant strain, PCR products of the expected size in *D. gigas* wild-type were obtained only with the primers for *echBC* (Fig 3.2A). In the *D. gigas* ∆*echBC* strainamplification was observed only with the primers for *kan*^{R}*.* Likewise, in the ∆*hynAB* mutant strain, amplification of the *hynAB* locus showed PCR products of the expected sizes in the *D. gigas* wild-type and in the *D. gigas* ∆*hynAB* strain (Fig 3.2B). The difference in size of the amplified bands is due to the fact that the *kan*^{R} gene has only ~1.5kb´s, whereas the *hynAB* genes have ~2.5kb´s. Furthermore, specific primers to amplify the *kan*^{R} genes presented PCR product of the expected size in the *D. gigas* ∆*hynAB* (1415bp), while for the wild type no amplification was observed (Fig 3.2B).

The results obtained by both PCR and Southern-blot confirmed the deletion of the *echBC* and *hynAB* genes and their replacement with the *kan*^{R} gene, creating two single mutant strains containing one hydrogenase each.

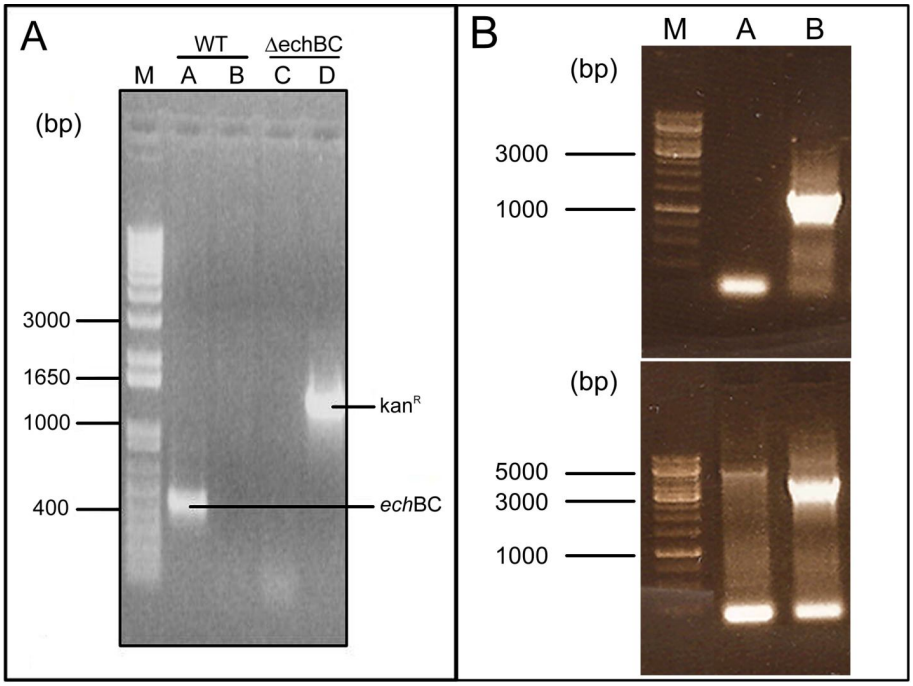

Fig 3.2. Confirmation of *echBC* and *hynAB* deletion by PCR analysis: A- PCR products amplified from *D. gigas* wild-type and Δ*echBC* genomic DNA are as follows: Lane A- WT (EchBC-1/EchBC-2), 422bp; Lane B- WT (EchKan^{R}XbaI-fwd / EchKan^{R}XbaI-rev), none; Lane C- Δ*echBC* (EchBC-1/EchBC-2), none; Lane D- Δ*echBC* (EchKan^{R}XbaI-fwd / EchKan^{R}XbaI-rev), 1425 bp. B – PCR products amplified from *D. gigas* wild-type and Δ*hynAB* genomic DNA. Top image, amplification of kanR gene (HynABKan^{R}SalI_fwd / HynABKan^{R}BHI_rev): Lane A- WT, none; Lane B - Δ*hynAB*, 1415bp. Lower image, amplification of the deletion site (HynABFlankI_fwd/ HynABFlank II_rev): Lane A – WT, 4637bp; Lane B - Δ*hynAB*, 3416bp.

3.4.2 Mutant phenotype in sulfate respiration

The growth of *D. gigas* wild type was compared to the growth of both Δ*ech* and Δ*hynAB* single mutant strains. In the presence of an excess of sulfate

(40mM), with either lactate (Fig 3.3A) or pyruvate (Fig 3.3B), both mutant strains reached a final cell density similar to the wild type.

However, the doubling time of the mutants was higher than that of the wild type for the Δ*echBC* strain growing on lactate, and for the Δ*hynAB* strain growing on pyruvate (Table 3.3). Also, the cell yield coefficient observed for the Δ*echBC* was higher than that of the wild type, especially in growth with pyruvate.

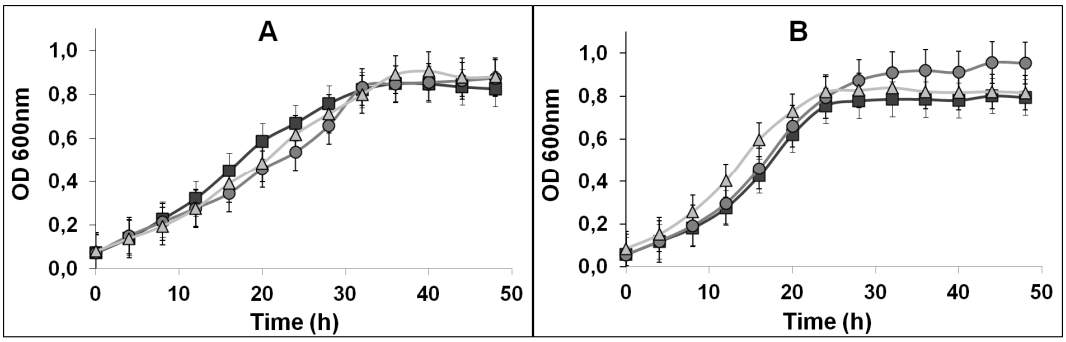

Fig 3.3. Growth curves of *D. gigas* wild-type, Δ*echBC* and Δ*hynAB* strains in medium containing: A- 40mM lactate/40mM sulfate; B- 40mM pyruvate/40mM sulfate. Wild-type, squares; Δ*echBC*, circles; and Δ*hynAB* triangles. Each data point is the average of three independent growth experiments.

Metabolite quantification (Table 3.4) revealed that both mutations did not affect substrate consumption or product formation, when compared to the wild type. The electron acceptor, sulfate, was reduced in agreement with the expected stoichiometry of 2:1 and 4:1, relative to lactate and pyruvate respectively, and at the same rate by the mutant strains and the wild type. No significant amounts of H_2 accumulated during growth, whenever sulfate was present. These results indicate that none of the two hydrogenases is essential for growth under sulfate respiratory conditions, with either lactate or pyruvate as carbon source.

Table 3.3. Doubling time and cell yield coefficient (YS) for the *D. gigas* wild type and hydrogenase mutant strains Δ*echBC* and Δ*hynAB*, during growth under different conditions.

Growth Condition	Doubling Time (h)			Y_S (g [dry wt] cells/mol)		
	WT	**Δ*echBC***	**Δ*hynAB***	**WT**	**Δ*echBC***	**Δ*hynAB***
Lactate/Sulfate	8.7	11.1	9.0	6.8	7.2	6.8
Pyruvate/Sulfate	6.7	6.7	7.9	6.0	7.3	6.1
Pyruvate/Sulfate*	6.9	7.1	8.0	5.2	6.3	4.7
Pyruvate	14.2	16.7	-	4.8	6.7	-
H_2/Sulfate	33.3	24.1	-	-	-	-

However, with H_2 as the energy source in the presence of sulfate a different phenotype was observed (Fig 3.4). The doubling time for this respiratory condition was much higher for the wild type when compared to conditions where organic acids (lactate or pyruvate) were the energy source (Table 3.4).

Also, the behavior of the mutant strains was quite different. The Δ*echBC* mutant strain reached a final cell density similar to the wild type and presented an even higher doubling time. In contrast, the Δ*hynAB* strain did not grow at all revealing that, as expected, the periplasmic hydrogenase is essential for growth under these conditions.

Growth Condition	Compound	Strains					
		WT		Δ*ech*		Δ*hynAB*	
		0h	48h	0h	48h	0h	48h
Lactate/ Sulfate	Lactate	40.0±0.3	0.0±1.4	40.4±0.8	0.0±0.2	40.5±0.6	0.0±0.2
	Sulfate	42.2±5.8	25.7±5.3	40.0±0.3	21.0±3.4	43.6±1.5	23.6±3.9
	Acetate	1.7±0.5	42.0±2.9	1.2±0.7	39.5±1.5	2.0±1.0	42.3±1.5
Pyruvate/ Sulfate	Pyruvate	45.0±1.7	0.0±0.2	43.3±5.2	0.0±0.4	41.1±3.9	0.0±0.2
	Sulfate	42.5±4.1	34.0±2.7	40.2±4.7	32.2±5.9	39.0±3.6	31.2±1.3
	Acetate	2.9±0.3	34.5±3.8	2.7±0.4	34.9±2.2	2.5±1.8	30.7±5.3
Pyruvate/ Sulfate*	Pyruvate	44.6±6.4	0.0±0.2	45.3±2.9	0.0±0.4	42.0±3.8	0.0±0.2
	Sulfate	5.3±0.9	0.0±0.2	5.2±0.7	0.0±0.2	5.3±0.8	0.0±0.2
	Acetate	2.8±0.5	32.6±1.0	2.7±0.3	31.8±1.7	3.0±1.3	29.4±3.9
Pyruvate	Pyruvate	41.5±5.5	0.0±0.2	39.5±8.6	0.0±0.2	45.6±6.3	29.3±2.5
	Acetate	2.6±0.2	29.6±3.5	2.4±0.2	28.7±4.5	2.4±0.6	5.3±5.6
H_2/Sulfate	Acetate	9.9±0.5	9.2±0.7	10.9±0.5	12.6±1	-	-
	Sulfate	19.3±0.5	16.4±0.5	19.2±0.5	16.5±0.5	-	-

Table 3.4. HPLC quantification of substrates and products from of *D. gigas* wild-type (WT), Δ*echBC* and Δ*hynAB* strains from growth experiments in basal medium modified from [2] containing: Lactate 40mM/Sulfate 40mM, Pyruvate 40mM/Sulfate 40mM, Pyruvate 40mM/Sulfate* 5mM, Pyruvate 40mM and H_2/Sulfate 20mM. Quantifications where performed after inoculation (~4h) and at the end of stationary phase (~48h). Each data point is the average of three independent growth experiments. Standard deviation for each value is shown.

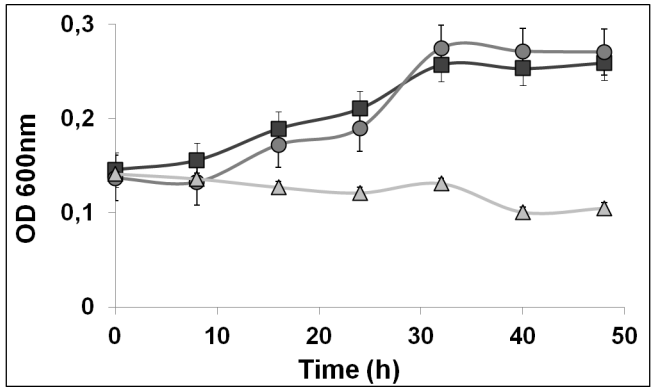

Fig 3.4. Growth curves of *D. gigas* wild-type, Δ*echBC* and Δ*hynAB* strains in H_2/Sulfate. Cells were grown on modified Medium C, containing 10mM acetate and 20mM sulfate, with a gas phase composed of H_2:CO_2 (80:20% v/v) at a pressure of 1atm. Wild-type, squares; Δ*echBC*, circles; and Δ*hynAB* triangles. Each data point is the average of three independent growth experiments.

3.4.3 Mutant phenotype in sulfate limitation and fermentation

Desulfovibrio spp. are unable to grow fermentatively in the presence of lactate, unless H_2 partial pressures are kept low by hydrogenotrophic organisms, such as methanogenic archaea. This is due to the fact that oxidation of lactate to pyruvate is an endergonic reaction. However, these bacteria can grow fermentatively with pyruvate. Thus, we evaluated the effect of deleting each

hydrogenase in fermentative conditions using pyruvate. As such, the wild type and both mutant strains were grown in pyruvate with sulfate limitation (5 mM), or in its absence, (Fig 3.5A and 3.5B, respectively).

In the first case, although sulfate was limiting, growth of *D. gigas* wild type and mutant strains reached similar cell densities to when sulfate was present in excess (see Fig 3.3), revealing that enough sulfate was present to allow respiratory growth. In agreement with this, the doubling time was similar to pyruvate respiratory conditions and once again the deletion of the *hynAB* genes slowed growth (Table 3.3). When comparing yield coefficients, a decrease in cell yield was observed for all strains in this condition, especially in the case of the Δ*hynAB* mutant, which possibly correlates with the lower sulfate concentration available.

Once again it is noticeable that the absence of the *echBC* genes appears to increase cell yield of the mutant strain when compared to the wild type. Interestingly, after sulfate was completely reduced at 20-24h (Fig 3.5A), the cells stopped growing and started to accumulate H_2 (Fig 3.5E), and the Δ*echBC* strain, containing only the periplasmic hydrogenase, accumulated much more H_2 than the wild type strain. On the other hand, the Δ*hynAB* strain, having the cytoplasmic hydrogenase, did not accumulate any H_2. No difference was observed in terms of pyruvate consumption or acetate formation, as shown in Fig 3.5C, indicating that the difference in H_2 accumulation was due to HynAB activity.

In fermentative conditions where no sulfate was added, a small amount of sulfate (~1-3mM) was nevertheless present in the beginning of growth, coming from the inoculum. After this sulfate was reduced (~16h), we could observe a different phenotype compared to pyruvate respiratory growth. The Δ*hynAB* strain did not show fermentative growth once the small amount of residual sulfate was consumed, whereas the Δ*echBC* and wild type strains were able to grow, albeit to lower cell densities (Fig 3.5B) and with reduced cell yields (Table 3.3) than in pyruvate/sulfate.

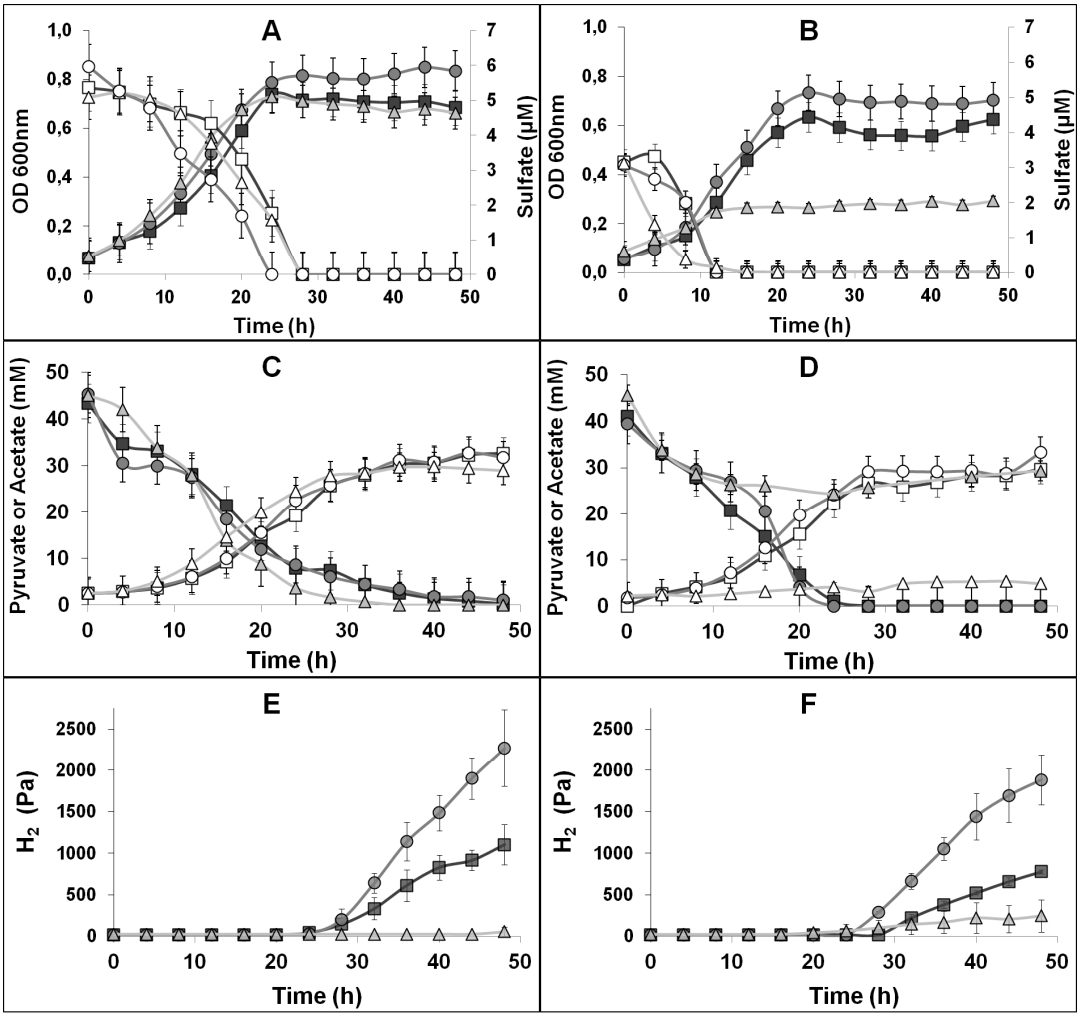

Fig 3.5. *D. gigas* wild-type, Δ*echBC* and Δ*hynAB* strains grown in pyruvate with sulfate limitation (A, C and E) or no sulfate added (B, D and F). A and B: Growth curves (filled symbols) and sulfate quantification (open symbols); C and D: quantification of pyruvate (filled symbols) and acetate (open symbols); E and F: hydrogen accumulation in the head space. *D. gigas* wild type, squares; Δ*echBC*, circles; and Δ*hynAB*, triangles.

Furthermore, the doubling time for these strains in pyruvate fermentation was at least double of that when sulfate was present. From the metabolite analysis it is

clear that, after the residual sulfate was reduced, the absence of the HynAB hydrogenase prevented the cells from fermenting pyruvate, resulting in the absence fermentative growth for this strain (Fig 3.5B and 3.5D). Furthermore, the expression of the *ech* genes is also lower in this condition in the Δ*hynAB* strain than in the wild type strain (see below), which may also have contributed to the lack of growth.

Similarly to what happened under sulfate limiting conditions, H_2 accumulation in the Δ*echBC* strain was much higher than in the wild type (Fig 3.5F). Interestingly, this accumulation only started after all pyruvate was consumed, as previously reported for *D. vulgaris* [32]. A slight accumulation of H_2 could be observed in the Δ*hynAB* strain as well, showing that the Ech hydrogenase can contribute to some H_2 production in these conditions.

These results indicate that under fermentative conditions, the HynAB is an essential enzyme to allow cell growth, and that in its absence cells are unable to ferment pyruvate. Furthermore, the periplasmic HynAB is the main hydrogenase responsible for the H_2 accumulation observed under the fermentative conditions.

3.4.4 Expression profiles of the ech and hyn genes

The higher H_2 accumulation by the Δ*echBC* strain, relative to the wild type, during pyruvate fermentation is very surprising, since it could be expected that the cytoplasmic Ech hydrogenase would be responsible for H_2 production from reduced ferredoxin produced by the pyruvate:ferredoxin oxidoreductase. To evaluate if this was due to an increase of HynAB transcripts in the deletion strain, we analysed the expression levels of genes coding for both HynAB and Ech hydrogenases, in *D. gigas* wild type and deletion strains. Quantitative real time PCR was performed to analyze the mRNA expression level of the HynAB hydrogenase, both in the *D. gigas* wild type (Fig 3.6A) and the Δ*echBC* strain (Fig 3.6B), at mid-exponential (16h) and stationary phases (32h), in pyruvate/limiting sulfate and pyruvate fermentation, as well as in lactate/sulfate and H_2/sulfate

conditions, where microarray expression data has been reported for other *Desulfovibrio* spp (Pereira *et al*., 2008; Keller and Wall, 2011).

Expression of the Ech hydrogenase was similarly evaluated in *D. gigas* wild type (Fig 3.7A) and in the Δ*hynAB* strain (Fig 3.7B). Quantification of all samples was performed relative to the 16S rRNA gene.

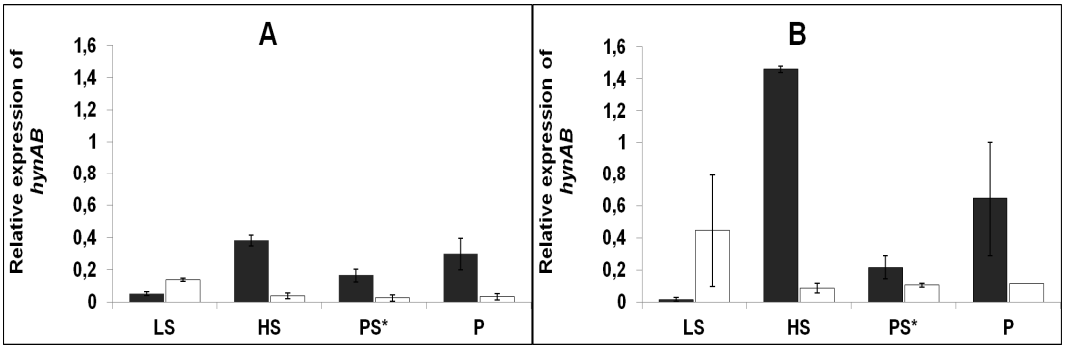

Fig 3.6. Quantification of the mRNA levels of the *hynB* hydrogenase gene, through qRT-PCR, at mid-exponential (16h) and stationary phases (32h) of both wild type (Panel A) and Δ*echBC* (Panel B) strains grown under different conditions, where: LS -Lactate 40mM/Sulfate 40mM; PS* - Pyruvate 40mM/Sulfate 5mM; P- Pyruvate 40mM; and H – H_2 1atm/Sulfate 20mM. Black bars, 16h; white bars, 32h. The expression of *hynAB gene* was normalized against the one of 16S rRNA. Standard errors are shown for each value.

The *hynB* gene showed highest expression in the wild-type strain during exponential growth in hydrogen respiration and in pyruvate fermentation (Fig 3.6A), whereas it was lower in pyruvate/sulfate and even less in lactate/sulfate. After cells entered stationary phase, the *hynB* gene expression dropped to very low levels in hydrogen/sulfate, pyruvate/sulfate and pyruvate fermentation, whereas it increased in lactate/sulfate conditions.

An increase of the *hynB* gene expression, compared to the wild type, was observed in the Δ*echBC* mutant strain in those conditions where the *hynAB* deletion prevented growth, i.e. hydrogen respiration and pyruvate fermentation (compare Fig 3.6B to Fig 3.6A). This increase is more prominent at the exponential phase, but can also be observed at the stationary phase, where in the wild type we observe a more accentuated drop in the expression of *hynB*. In the respiratory conditions with organic substrates (LS and PS*), the *hynB* expression at exponential phase is similar to the wild type, and once again an increase is observed in the stationary phase relative to the wild type. These increased levels of *hynB* at stationary phase observed for Δ*echBC* mutant may account for the greater accumulation of H_2 observed in pyruvate limitation/fermentation during physiological analyses. As such, in the Δ*echBC* strain the absence of the Ech hydrogenase appears to be compensated by an increased level of HynAB (except in lactate/sulfate exponential growth).

We also measured the expression level of *echE* in the wild type and the Δ*hynAB* strain. The *echE* mRNA levels are highest in the *D. gigas* wild type strain during exponential growth on organic substrates (lactate or pyruvate) in the presence of sulfate (Fig 3.7A, 16h). After cells enter the stationary phase (32h), the levels of *echE* gene expression decrease significantly, especially in lactate growth. In respiratory growth with H_2 as the energy source, the opposite behavior is observed, where the level of the *echE* mRNA is almost undetectable at the exponential phase (16h), but increases after cells enter the stationary phase. In pyruvate fermentative growth, the transcript levels of *echE* are low in the exponential phase and further decrease to undetectable levels after cells enter the stationary phase. This suggests that the Ech activity is mainly related to the initial phase of respiratory growth (i.e. where sulfate is still present) with organic substrates, whereas in fermentative growth, the Ech appears to play a much less important role.

When the *echE* gene expression is analyzed in the Δ*hynAB* mutant strain (Fig 3.7B), a major overall decrease in expression can be observed for all

conditions, when compared to the wild type (Fig 3.7A), suggesting that the HynAB hydrogenase is involved in the regulation of Ech expression. These results indicate that in hydrogen/sulfate respiration and in pyruvate fermentation, the Ech hydrogenase is poorly expressed and thus cannot compensate for the absence of the HynAB hydrogenase, preventing growth in these conditions.

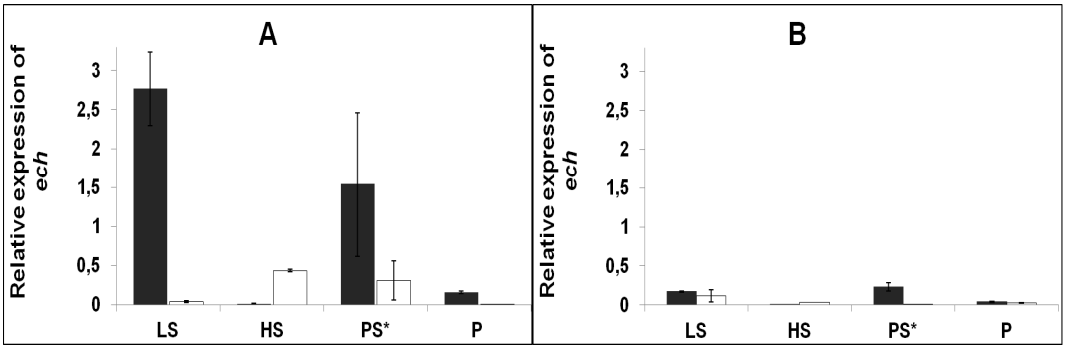

Fig 3.7. Quantification of the mRNA levels of the *echE* hydrogenase gene, through qRT-PCR, at mid-exponential (16h) and stationary phases (32h) of both wild type (Panel A) and Δ*hynAB* (Panel B) strains grown under different conditions, where: LS -Lactate 40mM/Sulfate 40mM; PS* - Pyruvate 40mM/Sulfate 5mM; P- Pyruvate 40mM; and H – H_2 1atm/Sulfate 20mM. Black bars, 16h; white bars, 32h. The expression of *hynAB gene* was normalized against the one of 16S rRNA. Standard errors are shown for each value.

3.5 Discussion

Previous studies have addressed the role of hydrogenases in *Desulfovibrio* spp. In a *D. vulgaris* strain deleted for the periplasmic Hyn1 [NiFe] hydrogenase, cells were able to grow to almost the same level as the wild type in lactate/sulfate media (Goenka *et al*., 2005). Similar results were obtained in a double mutant of the periplasmic *hynABC* and cytoplasmic *hnd* hydrogenases in *D. fructosovorans*

that was able to grow on all conditions tested (Malki *et al*., 1997). A further triple mutant lacking all described periplasmic hydrogenases was also shown to grow in fructose-sulfate medium (Casalot *et al*., 2002a) . However, in these studies there were additional hydrogenases present that could compensate for the absence of the missing genes.

D. gigas is uniquely positioned among *Desulfovibrio* spp. to test the function of hydrogenases and the importance of hydrogen cycling towards energy conservation, since it contains only two enzymes, one periplasmic and one cytoplasmic. Furthermore, the genomic analyses revealed no sequences related to the pyruvate:formate lyase gene in *D. gigas*, and as such, formate cycling should not be participating in the energy conservation processes as an alternative to hydrogen cycling.

The results obtained in this work demonstrate that none of the two hydrogenases is essential for growth of *D. gigas* under respiratory conditions with organic substrates (lactate or pyruvate) in the presence of sulfate. In addition, the absence of *hynAB* or the *echBC* genes also did not lead to any significant accumulation of molecular hydrogen. Since no other hydrogenase, either periplasmic or cytoplasmic, is present in the genome of *D. gigas*, and formate is not participating in the energy conservation process, this suggests that the hydrogen cycling pathway appears not to play a major part in the bioenergetics of *D. gigas*. Cell yield coefficients calculated for sulfate respiration with lactate and pyruvate are almost identical for the wild type and the hydrogenase mutant strains. Nevertheless, a slightly lower growth rate is observed for the Δ*echBC* strain growing on lactate/sulfate and for the Δ*hyn*AB strain in both lactate/sulfate and pyruvate/sulfate, suggesting that a small fraction of the electron flow to sulfate may involve production of H_2. In *D. vulgaris*, a mathematical model of metabolism, supported by experimental results, indicated that two simultaneous pathways for electron flow during growth in lactate/sulfate co-exist: one requiring the obligate cycling of H_2, and the other not (Noguera *et al*., 1998). The model estimated that 48% of electron flow from lactate to sulfate involved H_2 production. Our results

suggest that this value may be significantly lower for *D. gigas*. This would be in line with the reduced number of hydrogenases in this organism compared to *D. vulgaris*, which has seven hydrogenases. Nevertheless, we have been unable to date to generate a double hydrogenase mutant in *D. gigas*. However, given the difficulty to transform this organism, we cannot clearly conclude that this is due to the required presence of at least one hydrogenase.

Thus, as suggested before, the mechanism of hydrogen cycling does not seem to be strictly essential for the *Desulfovibrio* genus (Caffrey *et al*., 2007), and may have different contributions to the overall electron flow in different organisms. This is not entirely surprising since it was previously shown that some sulfate reducing bacteria do not have any hydrogenases at all (e.g. *Desulfococcus oleovorans*), or have no cytoplasmic hydrogenases (as *Desulfomicrobium baculatum*, which is closely related to *Desulfovibrionacae*) (Pereira *et al*., 2011).

Thus, H_2 is not an obligatory intermediate in the oxidation of organic compounds by *D. gigas* since the deletion of the hydrogenases does not affect the ability of the cells to grow. This agrees with the observation by Lupton that H_2 added to lactate/sulfate medium did not competitively inhibit the oxidation of lactate nor did it increased growth or substrate utilization (Lupton *et al*., 1984).However, we cannot rule out the possibility that other electron transfer pathways substitute for hydrogen cycling when one of the hydrogenases is missing. It is plausible that the cells can re-route electron flow if one of several pathways is impaired. This would be the advantage of having dual or multiple pathways for electron flow, and sulfate reducers are recognized for their metabolic flexibility.

Chemiosmotic models for energy conservation have also been proposed in which electrons generated from substrate oxidation are transported through membrane-bound electron carriers to sulfate reduction (vectorial electron transport) and in the process translocate protons to the periplasm (vectorial proton transport) (Wood, 1978; Pereira *et al*., 2011) . Two membrane complexes, which were identified in the *D. gigas* genome, the Qmo and the Dsr complexes were

proposed to perform this function (Pires *et al*., 2003; Pires *et al*., 2006). An energy conservation process may result from electron transfer from the quinone pool to AprAB through the Qmo complex (Venceslau *et al*., 2010; Ramos *et al*., 2012), and also the Dsr complex may be involved in menaquinol oxidation with reduction of DsrC, associated with proton translocation (Pires *et al*., 2006; Oliveira *et al*., 2008). Furthermore, other electron transfer pathways to sulfate may involve Hdr-related proteins that could provide a soluble pathway from different donors (such as lactate, pyruvate, ferredoxin or H_2) to the reduction of DsrC in a flavin-based electron bifurcation mechanism for energy conservation (Pereira *et al*., 2011). Such a system may involve the HdrABC/FloxABCD proteins that are also encoded in the *D. gigas* genome.

Regarding the physiological role of hydrogenases, the periplasmic enzymes are generally presumed to be involved in H_2 oxidation. Previous deletions of periplasmic hydrogenases in *D. vulgaris* demonstrated that under lactate/sulfate or H_2/sulfate the absence of one periplasmic hydrogenase could be compensated by the others (Caffrey *et al*., 2007). In *D. gigas*, which has only the HynAB hydrogenase, the physiological and mRNA expression data indicates that this enzyme has a bidirectional role in terms of hydrogen metabolism. When hydrogen is the energy source for sulfate respiration, HynAB acts as the H_2 uptake hydrogenase, as expected, and the electrons from the oxidation of H_2 can then be shuttled to the cytoplasmic reduction of sulfate through cytochrome c_3, Qrc and Qmo (Venceslau *et al*., 2010). Thus, the absence of the *hynAB* genes impaired growth in hydrogen/sulfate. In the case where sulfate is absent, i.e. fermentative conditions, our results indicate that this enzyme acts in the opposite direction, as a hydrogen producing enzyme, as the HynAB deleted strain was not able to ferment pyruvate. Interestingly, Ech is not capable to substitute for the absence of HynAB, as could be expected, but this may also be due to the low level of expression of this enzyme in fermentative conditions.

In agreement with the above, higher levels of *hynAB* expression were observed during growth with H_2/sulfate and in pyruvate fermentation compared to

lactate/sulfate respiration. These levels were further increased in these conditions in the Δ*echBC* strain, which can account for the greater accumulation of H_2 when this strain is fermenting pyruvate. Our results are similar to what was observed in a *D. vulgaris* Hildenborough periplasmic [Fe] hydrogenase mutant strain (Δ*hyd*) (Voordouw, 2002), where this hydrogenase was required for pyruvate fermentation, in addition to its function in hydrogen uptake in hydrogen/sulfate medium. Also, in synthrophic growth a similar role of the periplasmic hydrogenase, acting as a H_2 producing enzyme, was observed in *D. vulgaris* Hildenborough cultures grown in lactate with a hydrogenotrophic methanogen (Walker *et al*., 2009). Furthermore, also in *Desulfovibrio alaskensis* G20, the HynBA hydrogenase seems to be the main enzyme responsible for H_2 production in synthrophic growth (Meyer *et al*., 2013).

However, in these previous studies, the presence of multiple hydrogenases prevented direct evidence of a periplasmic hydrogenase being responsible for H_2 production. In this paper, the inability of the Δ*hynAB* strain to grow with pyruvate demonstrated undoubtedly that this periplasmic hydrogenase is essential for fermentative growth and H_2 production. Furthermore, the absence of the *hynAB* gene caused a slower growth rate in pyruvate/sulfate, suggesting that this is the main hydrogenase in pyruvate metabolism.

Interestingly, accumulation of H_2 only started after pyruvate was consumed, as previously observed in *D. vulgaris* (Voordouw, 2002), suggesting that some intracellular cycling of H_2 may be occurring and/or that other fermentation products are accumulated inside the cell and later converted to H_2. The fact that the Δ*hynAB* strain cannot grow by pyruvate fermentation supports the idea that intracellular H_2 cycling is required, but this inability could also be due to the reduced expression of the Ech hydrogenase.

Regarding the cytoplasmic Ech hydrogenase, our results from physiological analysis and mRNA expression indicates that this hydrogenase is not essential for growth of the organism in any of the conditions tested. Actually, yield coefficients of the Δ*echBC* strain indicate that the deletion of this genes even slightly increase

the final cell yield, particularly whenever pyruvate was the energy source. Nevertheless, this enzyme shows a quite high expression during exponential growth in lactate/sulfate, suggesting that it is probably playing a role in this condition. Also, the growth rate of this mutant strain in lactate/sulfate is slower. In the stationary phase, the Ech is virtually not expressed in lactate/sulfate and pyruvate fermentation. Interestingly, transcriptomic analysis in *D.vulgaris* indicated an upregulation of this enzyme under H_2/sulfate when compared to lactate/sulfate (Pereira *et al*., 2008; Keller and Wall, 2011). However, in *D. gigas* the Δ*ech* mutant strain was able to reach a final cell density similar to the wild type with a smaller doubling time, when growing in H_2/sulfate.

Overall, it seems that the Ech hydrogenase does not play a central role in the energy metabolism in the conditions tested , which agrees with the fact that in many SRB, including *Desulfovibrio* spp. such as *D. alaskensis* G20 or *Desulfovibrio piger* no Ech hydrogenase has been identified in their genome (Pereira *et al*., 2011).

Our results also provide compelling evidence for the importance of obtaining expression data to complement studies of gene deletions. Indeed, the expression of each hydrogenase was significantly altered in the mutants. In particular, the expression of the Ech hydrogenase was almost completely abolished upon deletion of the HynAB enzyme, regardless of the energy source or type of growth. This suggests that HynAB may be somehow involved in the regulation of the *ech* genes. One interesting observation was the fact that the two hydrogenases have somewhat complementary expression, as the HynAB hydrogenase was more expressed during growth with H_2/sulfate and pyruvate fermentation, whereas the Ech hydrogenase was more expressed in lactate/sulfate and pyruvate/sulfate growth.

In conclusion, the HynAB hydrogenase appears to have a more predominant role in the metabolism of *D. gigas*, and is essential for growth with H_2/sulfate and pyruvate fermentation.

3.6 Acknowledgements

This work was supported by Fundação para Ciência e Tecnologia (FCT) grants (PTDC/BIA-MIC/104030/2008 to IACP/CRP and Pest-OE/EQB/LA0004/2011 to the Instituto de Tecnologia Química e Biológica – António Xavier (ITQB), 049/BI-BI/2011 to C.S and SFRH/BD/45211/2008 to FMS). We thank Eng. Maria Cristina Leitão for technical support with the HPLC quantifications, Ana Raquel Ramos for technical support in the Southern-blot analysis and Mónica Martins for methodological support and helpful discussions.

3.7 References

Broco, M., Rousset, M., Oliveira, S., and Rodrigues-Pousada, C. (2005) Deletion of flavoredoxin gene in Desulfovibrio gigas reveals its participation in thiosulfate reduction. *Febs Letters* **579**: 4803-4807.

Caffrey, S.M., Park, H.S., Voordouw, J.K., He, Z., Zhou, J., and Voordouw, G. (2007) Function of periplasmic hydrogenases in the sulfate-reducing bacterium Desulfovibrio vulgaris Hildenborough. *J Bacteriol* **189**: 6159-6167.

Casalot, L., De Luca, G., Dermoun, Z., Rousset, M., and de Philip, P. (2002a) Evidence for a fourth hydrogenase in Desulfovibrio fructosovorans. *J Bacteriol* **184**: 853-856.

Casalot, L., Valette, O., De Luca, G., Dermoun, Z., Rousset, M., and de Philip, P. (2002b) Construction and physiological studies of hydrogenase depleted mutants of Desulfovibrio fructosovorans. *Fems Microbiology Letters* **214**: 107-112.

Goenka, A., Voordouw, J.K., Lubitz, W., Gartner, W., and Voordouw, G. (2005) Construction of a [NiFe]-hydrogenase deletion mutant of Desulfovibrio vulgaris Hildenborough. *Biochem Soc Trans* **33**: 59-60.

Hedderich, R., and Forzi, L. (2005) Energy-converting [NiFe] hydrogenases: more than just H2 activation. *Journal of molecular microbiology and biotechnology* **10**: 92-104.

Keller, K.L., and Wall, J.D. (2011) Genetics and molecular biology of the electron flow for sulfate respiration in desulfovibrio. *Front Microbiol* **2**: 135.

Kunkel, A., Vorholt, J.A., Thauer, R.K., and Hedderich, R. (1998) An Escherichia coli hydrogenase-3-type hydrogenase in methanogenic archaea. *European Journal of Biochemistry* **252**: 467-476.

Li, X., McInerney, M.J., Stahl, D.A., and Krumholz, L.R. (2011) Metabolism of H2 by Desulfovibrio alaskensis G20 during syntrophic growth on lactate. *Microbiology* **157**: 2912-2921.

Li, X., Luo, Q., Wofford, N.Q., Keller, K.L., McInerney, M.J., Wall, J.D., and Krumholz, L.R. (2009) A molybdopterin oxidoreductase is involved in H2 oxidation in Desulfovibrio desulfuricans G20. *J Bacteriol* **191**: 2675-2682.

Lupton, F.S., Conrad, R., and Zeikus, J.G. (1984) Physiological-Function of Hydrogen Metabolism during Growth of Sulfidogenic Bacteria on Organic Substrates. *Journal of Bacteriology* **159**: 843-849.

Malki, S., De Luca, G., Fardeau, M.L., Rousset, M., Belaich, J.P., and Dermoun, Z. (1997) Physiological characteristics and growth behavior of single and double hydrogenase mutants of Desulfovibrio fructosovorans. *Archives of Microbiology* **167**: 38-45.

Matias, P.M., Pereira, I.A., Soares, C.M., and Carrondo, M.A. (2005) Sulphate respiration from hydrogen in Desulfovibrio bacteria: a structural biology overview. *Prog Biophys Mol Biol* **89**: 292-329.

Meuer, J., Kuettner, H.C., Zhang, J.K., Hedderich, R., and Metcalf, W.W. (2002) Genetic analysis of the archaeon Methanosarcina barkeri Fusaro reveals a central role for Ech hydrogenase and ferredoxin in methanogenesis and carbon fixation. *Proceedings of the National Academy of Sciences of the United States of America* **99**: 5632-5637.

Meyer, B., Kuehl, J., Deutschbauer, A.M., Price, M.N., Arkin, A.P., and Stahl, D.A. (2013) Variation among Desulfovibrio Species in Electron Transfer Systems Used for Syntrophic Growth. *J Bacteriol* **195**: 990-1004.

Noguera, Brusseau, Rittmann, and Stahl (1998) A unified model describing the role of hydrogen in the growth of desulfovibrio vulgaris under different environmental conditions. *Biotechnology and bioengineering* **59**: 732-746.

Odom, J.M., and Peck, H.D., Jr. (1981) Localization of dehydrogenases, reductases, and electron transfer components in the sulfate-reducing bacterium Desulfovibrio gigas. *J Bacteriol* **147**: 161-169.

Oliveira, T.F., Vonrhein, C., Matias, P.M., Venceslau, S.S., Pereira, I.A., and Archer, M. (2008) The crystal structure of Desulfovibrio vulgaris dissimilatory sulfite reductase bound to DsrC provides novel insights into the mechanism of sulfate respiration. *Journal of Biological Chemistry* **283**: 34141-34149.

Pereira, I.A., Ramos, A.R., Grein, F., Marques, M.C., da Silva, S.M., and Venceslau, S.S. (2011) A comparative genomic analysis of energy metabolism in sulfate reducing bacteria and archaea. *Front Microbiol* **2**: 69.

Pereira, P.M., He, Q., Valente, F.M., Xavier, A.V., Zhou, J., Pereira, I.A., and Louro, R.O. (2008) Energy metabolism in Desulfovibrio vulgaris Hildenborough: insights from transcriptome analysis. *Antonie Van Leeuwenhoek* **93**: 347-362.

Pires, R., Lourenço, A., Morais, F., Teixeira, M., Xavier, A., Saraiva, L., and Pereira, I. (2003) A novel membrane-bound respiratory complex from Desulfovibrio desulfuricans ATCC 27774. *Biochimica et biophysica acta* **1605**: 67-82.

Pires, R.H., Venceslau, S.S., Morais, F., Teixeira, M., Xavier, A.V., and Pereira, I.A. (2006) Characterization of the Desulfovibrio desulfuricans ATCC 27774 DsrMKJOP complex--a membrane-bound redox complex involved in the sulfate respiratory pathway. *Biochemistry* **45**: 249-262.

Plugge, C.M., Scholten, J.C., Culley, D.E., Nie, L., Brockman, F.J., and Zhang, W. (2010) Global transcriptomics analysis of the Desulfovibrio vulgaris change from

syntrophic growth with Methanosarcina barkeri to sulfidogenic metabolism. *Microbiology* **156**: 2746-2756.

Ramos, A.R., Keller, K.L., Wall, J.D., and Pereira, I.A. (2012) The Membrane QmoABC Complex Interacts Directly with the Dissimilatory Adenosine 5'-Phosphosulfate Reductase in Sulfate Reducing Bacteria. *Front Microbiol* **3**: 137.

Rethmeier, J., Rabenstein, A., Langer, M., and Fischer, U. (1997) Detection of traces of oxidized and reduced sulfur compounds in small samples by combination of different high-performance liquid chromatography methods. *Journal of Chromatography* **760**: 295-302.

Rodrigues, R., Valente, F.M., Pereira, I.A., Oliveira, S., and Rodrigues-Pousada, C. (2003) A novel membrane-bound Ech [NiFe] hydrogenase in Desulfovibrio gigas. *Biochem Biophys Res Commun* **306**: 366-375.

Rodrigues, R., Vicente, J.B., Felix, R., Oliveira, S., Teixeira, M., and Rodrigues-Pousada, C. (2006) Desulfovibrio gigas flavodiiron protein affords protection against nitrosative stress in vivo. *J Bacteriol* **188**: 2745-2751.

Silva, G., Oliveira, S., LeGall, J., Xavier, A.V., and Rodrigues-Pousada, C. (2001) Analysis of the Desulfovibrio gigas transcriptional unit containing rubredoxin (rd) and rubredoxin-oxygen oxidoreductase (roo) genes and upstream ORFs. *Biochem Biophys Res Commun* **280**: 491-502.

Soboh, B., Linder, D., and Hedderich, R. (2004) A multisubunit membrane-bound [NiFe] hydrogenase and an NADH-dependent Fe-only hydrogenase in the fermenting bacterium Thermoanaerobacter tengcongensis. *Microbiology-Sgm* **150**: 2451-2463.

Valente, F.M., Almeida, C.C., Pacheco, I., Carita, J., Saraiva, L.M., and Pereira, I.A. (2006) Selenium is involved in regulation of periplasmic hydrogenase gene expression in Desulfovibrio vulgaris Hildenborough. *J Bacteriol* **188**: 3228-3235.

Varela-Raposo, A., Pimentel, C., Morais-Silva, F., Rezende, A., Ruiz, J.C., and Rodrigues-Pousada, C. (2013) Role of NorR-like transcriptional regulators under nitrosative stress of the delta-proteobacterium, Desulfovibrio gigas. *Biochem Biophys Res Commun* **431**: 590-596.

Venceslau, S.S., Lino, R.R., and Pereira, I.A. (2010) The Qrc membrane complex, related to the alternative complex III, is a menaquinone reductase involved in sulfate respiration. *Journal of Biological Chemistry* **285**: 22774-22783.

Vignais, P.M., Billoud, B., and Meyer, J. (2001) Classification and phylogeny of hydrogenases. *Fems Microbiology Reviews* **25**: 455-501.

Volbeda, A., Charon, M.H., Piras, C., Hatchikian, E.C., Frey, M., and Fontecilla-Camps, J.C. (1995) Crystal structure of the nickel-iron hydrogenase from Desulfovibrio gigas. *Nature* **373**: 580-587.

Voordouw, G. (2002) Carbon monoxide cycling by Desulfovibrio vulgaris Hildenborough. *Journal of Bacteriology* **184**: 5903-5911.

Walker, C.B., He, Z.L., Yang, Z.K., Ringbauer, J.A., He, Q., Zhou, J.H. *et al*. (2009) The Electron Transfer System of Syntrophically Grown Desulfovibrio vulgaris. *Journal of Bacteriology* **191**: 5793-5801.

Welte, C., Kratzer, C., and Deppenmeier, U. (2010a) Involvement of Ech hydrogenase in energy conservation of Methanosarcina mazei. *FEBS J* **277**: 3396-3403.

Welte, C., Kallnik, V., Grapp, M., Bender, G., Ragsdale, S., and Deppenmeier, U. (2010b) Function of Ech hydrogenase in ferredoxin-dependent, membrane-bound electron transport in Methanosarcina mazei. *J Bacteriol* **192**: 674-678.

Wood, P. (1978) A chemiosmotic model for sulphate respiration. *FEBS letters* **95**: 12-18.

Chapter 4

Hydrogenase physiological role in non-sulfidogenic fermentative and respiratory conditions

The author of this thesis had a major contribution in the work presented in this chapter, namely in the planning of the experimental work, performing the experiments and analyzing the data.

4.1 Abstract

Although many biochemical and genetic studies have helped in understanding how energy is conserved during sulfate reduction, less information is available about how energy conservation is achieved under non sulfidogenic conditions in *Desulfovibrio* spp. It is known that in the absence of sulfate, these bacteria are able to grow by fermenting organic acids and alcohols. However, organic compounds, such as fumarate, can also be used as electron acceptors by SRB´s, during respiratory growth, in substitution of sulfate. In organisms that use H_2 or formate as electron donors to reduce fumarate, the respiratory chain comprises a hydrogenase or formate dehydrogenase, the menaquinone (MK) and fumarate reductase. We report, for the first time, the investigation of the physiological role of the two hydrogenases present in *Desulfovibrio gigas*, Ech and HynAB, during respiratory and fermentative growth with fumarate. Furthermore, hydrogenase function was also evaluated during lactate fermentation of *D. gigas* and *D. vulgaris* Hildenborough using hydrogenase mutant strains. The results obtained indicate that the absence of both *D. gigas* hydrogenases appears not to affect cell growth during fumarate fermentation. During lactate metabolism the Ech appears to be the main hydrogenase responsible for H_2 production in *D. gigas*. However, during lactate fermentation, both Ech and HynAB appear to produce H_2 from reducing equivalents generated during oxidation of substrate in a mechanism that appears to be common to *D. vulgaris* periplasmic hydrogenases.

4.2 Introduction

Sulfate-reducing bacteria are very versatile microorganisms that can use a variety of electron donors, such as organic acids, alcohol or H_2 as substrates for the reduction of sulfate, sulfite, or thiosulfate (Voordouw, 2002). The mechanisms of electron transfer from these substrates during sulfate respiration have been most intensively studied in the members of the δ-proteobacterial genus *Desulfovibrio* (Matias *et al*., 2005). Progress in the genetic manipulation of *Desulfovibrio* organisms has provided an opportunity to explore electron flow pathways during sulfate respiration (Keller and Wall, 2011).However, considerably less information is available regarding how these mechanisms contributing to energy conservation when sulfate is not the electron acceptor.

In absence of sulfate, *Desulfovibrio* spp. are able to grow by fermenting organic acids and alcohols or syntrophically with other organisms. Fermentation of lactate, one of the most common organic compounds used by the organisms, generates as main products, acetate, carbon dioxide and H_2 (Pankhania *et al*., 1988). Nevertheless, lactate oxidation in the absence of sulfate is a thermodynamically unfavorable reaction. As a consequence, sulfate reducers create syntrophic associations with hydrogen-consuming populations for its oxidation (McInerney and Bryant, 1981; Stolyar *et al*., 2007). Lactate oxidation during syntrophic associations between *Desulfovibrio* spp and methanogens has been recently described for *D. vulgaris* Hildenborough and *D. alaskensis* G20 (Walker *et al*., 2009; Plugge *et al*., 2010; Meyer *et al*., 2013). Nonetheless, the identity of the electron carriers involved in lactate metabolism remains elusive. For years, the exact mechanism by which lactate is oxidized in SRB has been under debate.

Other organic compounds which are found in their environment resulting from degradation of proteins and amino acids can also be used during fermentative growth. *Desulfovibrio* spp. are able to ferment C^4-dicarboxylic acids such as fumarate or malate with succinate, acetate and CO_2 as their main

products. In these fermentative conditions, referred as disproportionation, the substrate is used both as electron donor/carbon source and as electron acceptor. While malate disproportionation was already described in *D. gigas* (Chen *et al*., 1995), fumarate disproportionation was only investigated in *D. vulgaris* and *D. desulfuricans* strains (Zaunmuller *et al*., 2006). Furthermore, some *Desulfovibrio spp*. can also use organic compounds, such as the case of fumarate, as primary electron acceptor instead of sulfate (Rabus *et al*., 2006). Fumarate respiration is one of the most widespread types of anaerobic respiration (Kröger *et al*., 1992). The electron transport chain catalyzing this process is usually composed by either a hydrogenase or formate dehydrogenase, menaquinone (MK) and fumarate reductase (Kroger *et al*., 2002), where the hydrogenase usually contributes to the generation of a proton motive force. In *Desulfovibrio gigas* fumarate respiration and fumarate reductase have already been described (Barton *et al*., 1970; Odom and Peck, 1981a; Lemos *et al*., 2002a). As in the case of lactate, it is not yet known the mechanisms involved in the electron transfer and what is the role of the enzymes that participate in these processes.

Since hydrogenases play an important role in the energy metabolism of *Desulfovibrio* spp under respiratory conditions we decided to investigate their function in *D. gigas* fermentative metabolism as well. In addition, since hydrogenases could be involved in creation of a proton motive force during fumarate respiratory growth we evaluated the impact of their deletion in the ability of cells to grow using fumarate as the electron acceptor. Taking advantage of two mutant strains, *Δech* and *ΔhynAB*, already generated for this organism and the fact that the genome of *D. gigas* has only these two hydrogenases, we compared their growth profile *versus* the wild type strain (Morais-Silva *et al*., 2013). Quantification of substrates/products by HPLC as well as H_2 production by GC were assessed growing the strains in lactate and fumarate fermentative conditions as well as lactate plus fumarate conditions. In addition protein expression levels of the Ech hydrogenase, which appears to be involved in H_2 production from lactate was investigated by Western blot. The results obtained gave important information

about the participation of the hydrogenases in lactate fermentation and in fumarate metabolism.

4.3 Materials and Methods

Bacterial strains and growth conditions

D. gigas wild type (wt) ATCC 19364 and the Δ*echBC* and Δ*hynAB* mutant strains each lacking one the two hydrogenases found in this organism were used for the growth experiments (Morais-Silva *et al*., 2013). Bacteria were grown in 120mL flasks containing 50mL of lactate/sulfate medium. For the phenotypic analysis, 10% (v/v) of fresh pre-cultured cells were inoculated in basal media complemented with different electron donors and acceptors, as described in Morais-Silva 2013. For growth under respiratory conditions, lactate was used as electron donor, at a concentration of 40mM. As electron acceptor fumarate, at a concentration of 40mM, was used in substitution of sulfate. In fermentative conditions limiting amounts of sulfate, at a concentration of 5mM, were present in the media to allow favorable redox conditions for initial cell growth. Also fumarate was used alone at a concentration of 40mM for growth by disproportionation. Once again, a low concentration of sulfate, coming from the inocula, was necessary to initiate cell growth.

Growth was monitored by measuring optical densities at 600nm wavelength (OD_{600}). Biomass was estimated by correlating dry cell weight (dcw) and optical density values (OD_{600}), (one unit value of OD_{600} corresponding to $0.365 g_{dcw}/L$).

For the studies of H_2 production in *D. vulgaris* Hildenborough (DSM 644) wild-type and periplasmic hydrogenase mutants strains, Δ*hys* and Δ*hyd*Δ*hyn* (Caffrey 2007), cells were grown in modified Postgate medium C containing 0.5 g/L KH_2PO_4, 1 g/L NH_4Cl, 0.45 g/L Na_2SO_4, 0.06 g/L $CaCl_2.2H_2O$, 0.048 $MgCl_2.6H_2O$, 0.2 g/L yeast extract, 0.0071 g/L $FeSO_4.7H_2O$, 0.3 g/L sodium citrate tribasic dihydrate, 0.1 g/L ascorbic acid, 0.1g/L sodium thioglycolate, 4.5 g/L

sodium lactate and 0.3 mg/L resazurin. The effect of metal cofactors of hydrogenases (Fe, Ni and Se) on H_2 production by *D. vulgaris* and its mutants was evaluated by supplementing the medium with 1 µM nickel chloride or 1 µM of both nickel chloride and sodium selenite. 10% (v/v) inoculum was used in all experiments. Batch experiments were carried out at 37ºC using 120 ml serum bottles with a working volume of 20mL and N_2 in the gas headspace. The bottles were sealed with butyl rubber stoppers and aluminum crimp seals. Each experiment was carried out in triplicate.

Analytical procedures

H_2 quantification in the headspace volume of the 120ml culture flasks was performed by gas chromatography, with a THERMO Unicam Electron Cooperation Trace GC Ultra gas chromatograph fitted with a Alltech Molecular Sieve 5A 80/100 column in the same conditions as in Morais-Silva, 2013.

Quantification of substrate consumption during the growth experiments was achieved though HPLC analysis using a Waters chromatograph and an Aminex HPX-87H. Elution of the compounds identified in these experiments was carried out isocratically at a flow rate of 0.5mL. min^{-1}, with 0.005N of H_2SO_4 plus 6% of Acetonitrile. Injection volume was 20uL. Retention time of the expected compounds was compared with standards and quantification was obtained by peak area. Residual sulfate concentrations detected in all media was determined using SulfaVer4 method (Hach-Lange).

For malate quantification, a product of the oxidative degradation of sodium fumarate, peak identification was obtained through LC-MS system composed by an HPLC Surveyor Plus (Thermo Scientific) coupled to a mass spectrometer LCQ Duo Ion Trap Mass Spectrometer (Thermo Scientific) equipped with an electronspray ionization source and an ion trap mass analyzer. Separation of the compounds was obtained using an Aminex HPX-87H at room temperature. Elution was carried out isocratically, with a flow rate of 0.5mL·min^{-1}, with mobile phase

composed of 94% of 0.1% formic acid plus 6% Acetonitrile. The injection volume for each sample was 20uL. In the MS analysis, N_2 was used as nebulizing gas (30ua) as well as auxiliary gas (10ua). The potential applied to the capillar was 4.5 kV at a temperature of 220ºC. Pressure at the ionization source was 1.25 x 10^2 Pa, while at the analyzer He was used as thermalization gas at a pressure of 1.59 x 10^{-3} Pa. A mass range of *m/z* 60-300 was used and the analyses were performed in positive polarity. The Xcalibur v1.2 software from Thermo Scientific was used for acquisition and mass spectra processing. The peak corresponding to the malic acid was separated at 10.8min by HPLC and showed an ion of *m/z* of 133. Furthermore, random fragmentation of the compound by MS yielded ions of *m/z* 115, corresponding to ion products of malic acid, as described in (Bylund *et al*., 2007)

Protein extracts and Western-Blot analysis of hydrogenases

For *D. gigas* hydrogenase protein expression analysis, detected by Western-blot, total protein was extracted for wild type and hydrogenases mutant strains grown in the same conditions as in the phenotypical analysis. Cells were harvested at mid exponential (16h) and stationary phases (32h) though centrifugation at 10000rpm, during 15 min at 4°C and were ressuspended, at 1mL/g of cells, in buffer solution as described in (Silva *et al*., 2001). Cellular membranes were disrupted in a French® Pressure Cell Press (Thermo IEC), three to four times, with 900psi of pressure. Extracts were centrifuged at 14000 G´s during 20min, at 4°C, to remove cell debris and yielding total protein extracts. Quantification of the samples was performed by Bradford's method using a BioRAD Protein Assay as indicated by the manufacturer.

Samples were run in a 12% SDS-PAGE gel, with a total load of 25µg of total protein, for 1h at 100V for protein separation. Subsequently, they were transferred into a 0.45mm polyvinylidene difluoride (PVDF) membrane (Roche) using a trans-blot SD electrophoretic transfer cell (BioRAD) for 35 min at 20V.

Membranes were stained with Ponceau S to verify transfer efficiency and were bloqued in a 5% milk phosphate buffer solution composed of 40.03g of NaCl, 1.005g of KCl, 7.7g of Na_2HPO_4 and 1g of KH_2PO_4 per liter.

For the Ech hydrogenase detection, membranes containing total protein of wild type and Δ*hyn*AB strains were treated with a specific antibody raised against a synthesized antigenic polipetide of EchE from *D. gigas* diluted 1:1000 (Davis GmB Biotech). Immunodetection was done using an anti-rabbit immunoglobulin G-HRP conjugated diluted 1:5000 (Santa Cruz Biotechnology). Signal detection was achieved using Super Signal West Femto Maximum Sensitivity Substrate (Thermo Scientific) in a BioRAD Chemidoc XRS Plus device. Sample control was carried out using a commercial anti-σ70 antibody from *E. coli* (NeoClone), diluted 1:10000 and immunodetection was done using anti-mouse immunoglobulin G-HRP conjugated (Santa Cruz Biotechnology).

4.4 Results and Discussion

Two *D. gigas* mutant strains were previously generated, each containing a single active hydrogenase and the physiological function of each of these enzymes was analyzed during respiratory conditions in the presence of sulfate (Morais-Silva *et al*., 2013). We have further evaluated the function of Ech and HynAB hydrogenases in the absence of sulfate, during fermentation of lactate and fumarate, as well as in respiratory conditions where sulfate is replaced by fumarate as the main electron acceptor.

4.4.1 Lactate fermentation

Initially *D. gigas* wild type and both hydrogenase mutant strains were grown using limiting amounts of sulfate as the electron acceptor. After sulfate is reduced the cells start to ferment lactate (Fig 4.1).

As can be observed (Fig 4.1A), all strains are able to grow similarly while sulfate is still present, with production of acetate at the expected stoichiometry of 1:1 (Table 4.1). Once sulfate is completely reduced (~24h), cells cease to grow. The absence of either hydrogenase has no effect on the final cell density but differences can be noticed in the doubling time. The deletion of the cytoplasmic *ech* hydrogenase gene shows a strong effect in the doubling time, of around 10.5h, compared to the Δ*hynAB* mutant, of 8.5h, and against the wild type 7.5h.

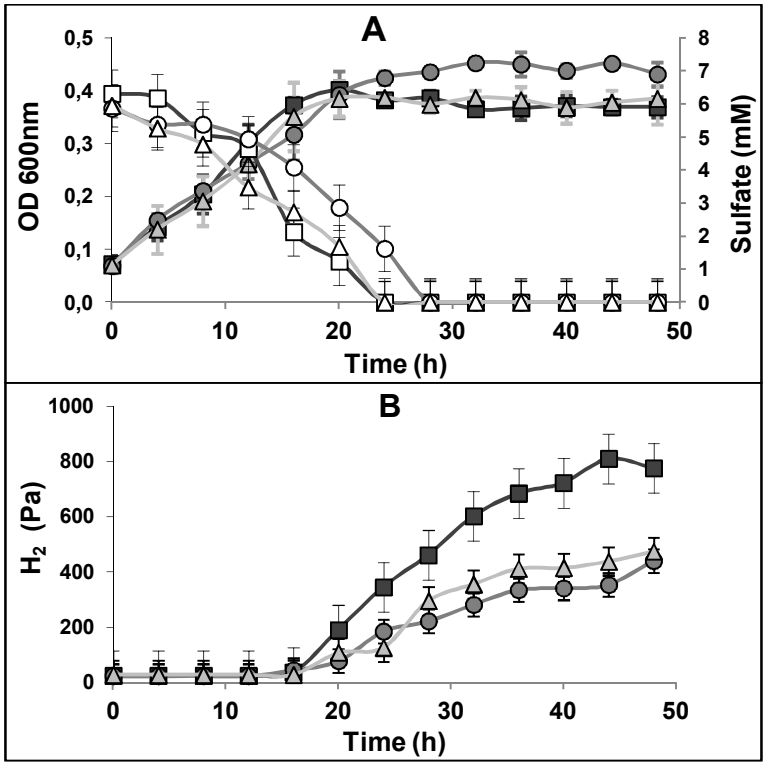

Fig 4.1. Growth curves (A) and H_2 accumulation (B) of WT *D. gigas* and hydrogenase mutant strains, Δ*echBC* and Δ*hynAB*, in medium containing 40mM of lactate and 5mM of sulfate. WT, squares; Δ*echBC* circles; Δ*hynAB* triangles. Open symbols represent sulfate while filled symbols represent OD_{600nm} in (A). Each point is the average of three independent growth experiments.

Growth Condition	Compound	Strains					
		WT		Δ*ech*		Δ*hynAB*	
		0h	48h	0h	48h	0h	48h
Lactate/Sulfate*	Lactate	46.9±2.9	29.4±4.7	43.6±2.7	27.8±1.9	46.9±4.5	31.4±3.3
	Acetate	0.0±0.1	14.8±1.0	0.0±0.1	15.9±0.8	0.0±0.1	13.2±0.7
	Sulfate	6.3±2.0	0.0±0.1	5.9±1.1	0.0±0.1	6.8±1.4	0.0±0.1
Fumarate	Fumarate	42.7±0.2	0.0±0.1	40.5±1.5	0.0±0.1	40.6±0.1	0.0±0.1
	Succinate	0.0±0.1	24.4±1.1	0.0±0.1	21.2±7.3	0.0±0.1	21.4±0.7
	Acetate	0.0±0.1	16.4±1.9	0.0±0.1	14.4±2.5	0.0±0.1	11.4±2.8
	Malate	0.0±0.1	2.2±1.6	0.0±0.1	0.0±0.1	0.0±0.1	2.3±2.0
	Sulfate	4.0±0.3	0.3±0.1	3.3±0.2	0.0±0.1	4.2±0.3	0.0±0.1
Lactate/Fumarate	Lactate	41.5±1.5	16.8±3.6	41.2±0.2	29.5±1.0	40.0±0.2	25.7±1.9
	Acetate	0.0±0.1	19.1±3.0	0.0±0.1	13.3±2.8	0.0±0.1	18.3±1.7
	Fumarate	43.0±1.5	2.5±0.6	42.2±3.3	21.1±9.7	41.4±1.7	8.4±1.3
	Succinate	0.0±0.1	23.7±1.2	0.0±0.1	9.3±1.7	0.0±0.1	20.0±0.2
	Malate	0.0±0.1	13.9±2.7	0.0±0.1	4.4±1.2	0.0±0.1	10.4±1.1
	Sulfate	4.1±0.2	0.0±0.1	3.2±0.1	0.0±0.1	4.3±0.3	0.0±0.1

Table 4.1. HPLC quantification of the substrates and products from of *D. gigas* wild-type (WT), Δ*ech* and Δ*hynAB* strains during growth with: Lactate 40mM / Sulfate 5mM*, Lactate 40mM / Fumarate 40mM and Fumarate 40mM. Each data point is the average of three independent growth experiments. Standard deviation for each value is shown.

Notably, a great decrease in H_2 accumulation can be observed for both mutant strains (Fig 4.1B). Molecular hydrogen starts to accumulate once sulfate is completely reduced and cell growth stops, reaching a concentration almost doubled in the wild type than in any of the mutant strains. In this situation, both enzymes appear to be producing H_2, irrespective of their cellular localization.

As such, contrary to what was observed previously in lactate plus sulfate respiratory conditions (Morais-Silva *et al.*, 2013) in the absence of sulfate both HynAB and Ech hydrogenases produces H_2 from the reducing equivalents generated during lactate oxidation. The periplasmic hydrogenase HynAB also acts as a hydrogen producing enzyme under these conditions, similarly to what was observed under pyruvate fermentation (Morais-Silva *et al.*, 2013).

Periplasmic hydrogen production during lactate fermentation was observed also in *D. vulgaris* Hildenborough (Voordouw, 2002). A mutant strain of *D. vulgaris* lacking the periplasmic [FeFe] Hyd hydrogenase showed decreased hydrogen production during lactate fermentation, suggesting that this enzyme could also be producing hydrogen under these conditions. Since a common mechanism of H_2 production by two periplasmic hydrogenases from different species and with different metal compositions in their active site was observed, we analyzed if other periplasmic hydrogenases of *D. vulgaris* Hildenborough could also be involved in H_2 production.

Taking advantage of the fact that hydrogenase mutant strains were available (Caffrey *et al.*, 2007), we have compared single (Δ*hys*) and double (Δ*hyd*_Δ*hyn*1) *D. vulgaris* Hildenborough periplasmic hydrogenase mutant strains growth profile againts the wild type growing during lactate fermentation

(unpublished results). Strikingly, as observed in *D. gigas*, all mutant strains lacking one or even two periplasmic hydrogenases accumulated much less molecular hydrogen than the wild type strain, regardless the metal content of the medium.

Put together, the results obtained with *D. gigas* and *D. vulgaris* strongly suggest that during lactate fermentation, periplasmic hydrogenases are reducing protons to H_2. Moreover, this seems to be a common mechanism in the *Desulfovibrio* spp, as different hydrogenases from different species behave in a similar manner.

This physiological role of H_2 production by periplasmic hydrogenases in *Desulfovibrio* spp growing in lactate media with sulfate limitation is similar to what is observed during syntrophic growth with methanogens (Walker *et al*., 2009; Meyer *et al*., 2013). During syntrophic growth, H_2 production by *Desulfovibrio* periplasmic hydrogenase, associated with continuous consumption of this compound by the methanogen, lowering H_2 concentration, enables energetically favorable conditions for continued lactate oxidation (Walker *et al*., 2009). As such, in the monocultures of *D. gigas* or *D. vulgaris*, these periplasmic enzymes apparently have a similar function of H_2 production.

4.4.2 Fumarate fermentative growth

Fumarate fermentative growth, known as disproportionation, was also evaluated in *D. gigas* wild type and hydrogenase mutant strains (Fig 4.2). Although all strains reached similar final optical densities, doubling time and substrate yields are different for each mutant strain compared to the wild type (Fig 4.2A). The ∆*echBC* mutant strain appears to grow slightly faster, with a doubling time of around 10.5h, compared to around 12h for the other strains. However, in terms of substrate yield, the ∆*hynAB* hydrogenase showed a maximum yield of 7g/mol, whereas in the wild type and ∆*ech* this value was around 9.5g/mol. It is also noticeable that regardless of the difference in these parameters, all strains reach much higher final optical densities, as well as higher substrate yield

coefficients, under fumarate fermentative conditions when compared to lactate fermentation.

The results observed in the quantification of substrate consumption and product formation (Table 4.1, Figs 4.2B and 4.2C), show that as expected fumarate disproportionation generates as main products succinate and acetate. The ratio of these two products observed in *D. gigas* wild type is very similar to what was described for fumarate disproportionation in *Desulfovibrio* spp. (Zaunmuller *et al*., 2006). For each mol of fumarate, in *D. gigas* 0.55 mol of succinate and 0.38 mol of acetate were produced. These values are closer to the ones observed for *D. vulgaris* Hildenborough compared to *D. desulfuricans* (Essex 6). In accordance, transient accumulation of malate is also observed in *D. gigas*, as in *D. vulgaris*, reaching its peak (22mM) after about 28h of growth. When we observed these values in the mutant strains, a major difference in the Δ*ech* strain is clear, while the Δ*hynAB* strain behaves similarly to the wild type.

Although all fumarate is oxidized in the Δ*ech*, considerable lower amounts of acetate and malate are produced (Fig 4.2C, Table 4.1). Despite that, this strain is able to reach same final optical densities having a faster cell doubling time than the wild type.

Furthermore, during fumarate disproportionation, sulfate is apparently not used as electron acceptor immediately (Fig 4.2A, open symbols). This observation was completely unexpected since sulfate is considered as primary electron acceptor for these organisms and it would be expected to be reduced as soon as possible. Fumarate plus sulfate growth was already reported for *D. gigas* (Lemos *et al*., 2002a). However, in these experiments the reduction of sulfate was not quantified during the course of growth. Our analyses suggest that sulfate reduction is linked to malate accumulation (Fig 4.2C). Once malate accumulation reaches its highest values it begins to be consumed, coupled to reduction of the small sulfate present in the media.

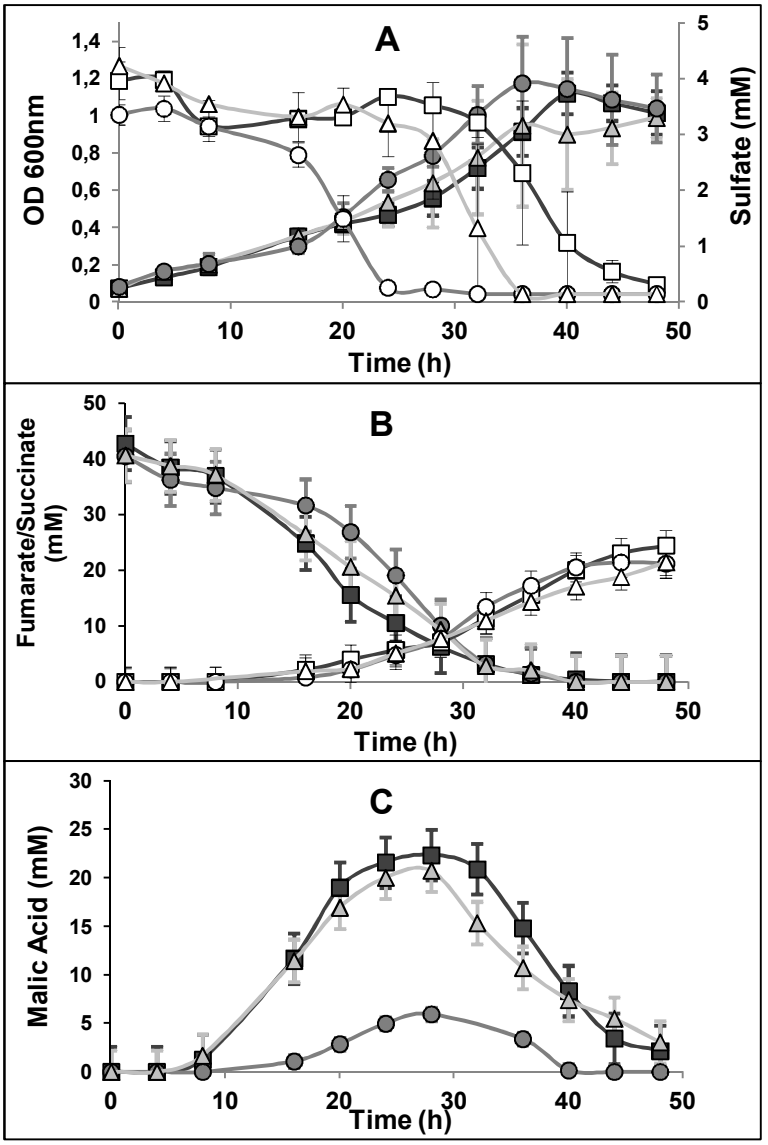

Fig 4.2. Fermentative growth on fumarate (40mM) in WT *D. gigas* and hydrogenase mutant strains, Δ*echBC* and Δ*hynAB*. WT, squares; Δ*echBC* circles; Δ*hynAB* triangles. Open symbols represent sulfate while filled symbols represent OD_{600nm} in (A). Each datum point is the average of three independent growth experiments.

As such, it is possible that under fumarate plus sulfate growth, fumarate is rather disproportionated in a fermentative process than used only as an electron donor for sulfate reduction. In addition, the *Δech* mutant strain behaves differently from the wild type and *ΔhynAB* strain, as it accumulates lower amounts of malate. The reason why the absence of a hydrogenase affects the production of malate is not known, but it does not affect cell growth. With respect to the participation of hydrogenases in fumarate fermentative growth, no molecular hydrogen is detected during the experiment and in any of the strains analyzed. This suggests that, despite the differences observed in the *Δech* mutant strain, hydrogenases are not essential enzymes and hydrogen is not being used as a mechanism for energy conservation during fumarate disproportionation.

Fumarate reduction to succinate is catalyzed by the membrane bound fumarate reductase (FRD), which is composed of three subunits, (FdrA, B and C). In some organisms, like *Bacillus subtilis*, a proton gradient is suggested to be generated upon fumarate reduction by the Frd enzyme, as the [H] used for this step is obtained from the cytoplasm, with electrons being transferred from NADH oxidation via the menaquinone (Schnorpfeil *et al*., 2001). However in some SRB, such as *Desulfovibrio alakensis* G20 and *Desulfobacterium autotrophicum* in the FrdC subunit there is the presence of a conserved Glu residue that is equivalent to Glu 180 of *Wollinela succinogenes*. The presence of this residue is involved in the dissipation of this proton potential generated by fumarate reductase activity, since it is part of a H^+ shortcut (`E-pathway`) (Lancaster, 2002; Haas *et al*., 2005; Lancaster *et al*., 2005; Zaunmuller *et al*., 2006). In *D. gigas*, in addition to the described Frd enzyme (Lemos *et al*., 2002a), the analysis of its recently available genome (Genbank CP006585, Chapter 2), revealed a second Frd, very similar to the already described one. Both of these enzymes present the conserved Glu residue in the FrdC subunit, similar to *D. alaskensis* G20 and *W. succinogenes*. This observation suggests that in *D. gigas* fumarate reduction does not generate a proton potential (Δp) that can be used for ATP production. Alternatively, in *W.*

succinogenes during respiratory conditions the creation of ∆p is accomplished with either H_2 or formate oxidation (Kröger *et al*., 1992). The electron transport chains catalyzing these reactions are composed of one or more dehydrogenases, menaquinone (MK) and fumarate reductase. The ∆p generation appears to be exclusively created by the electron transfer from H_2 (or formate) to MK (Kroger *et al*., 2002). Since no formate or H_2 are detected in *D. gigas* during fumarate disproportionation, this mechanism of energy conservation is also not operating. As such, in *D. gigas* wild type and mutant strains the energy generation during this metabolism (reaction a) is suggested to be obtained mainly by substrate-level phosphorylation of the fumarate pool oxidized to acetate (reaction b), while the electrons generated in the process are used reduction of the second pool of fumarate (reaction c).

3 Fumarate ---> 2 succinate + 1 acetate (a)

Fumarate ---> acetate + ATP + NAD(P)H + Fd_{red} (b)

Fumarate + [H] + e^- ---> succinate (c)

Since the electron transfer is not affected by the absence of any of the hydrogenases and formate is not present, other mechanisms for electron flow to fumarate reduction must be present (Fig 4.3). As depicted by Zaunmuller *et al*. 2006, the NAD(P)H formed upon the conversion of malate to pyruvate by the malic enzyme (L-malate:NADP+ oxidoreductase) could be involved in the electron pathway to the reduction of fumarate. As proposed for *D. gigas* this NAD(P)H could be converted to NADH, by the action of a transhydrogenase (Chen *et al*., 1995). This NADH could then be used to supply electrons for fumarate reduction to succinate, similarly to what is observed in *B. subtillis* (Schnorpfeil *et al*., 2001). An alternative mechanism could also involve the reduced ferredoxin (Fd_{red}) obtained from pyruvate oxidation to acetate since it appears to be the only redox product from this reaction. Electrons from Fd_{red} could be transferred to NADH by the action of the Rnf complex. This complex is proposed to carry out electron

transport from Fd_{red} to NAD+, coupled to electrogenic Na+ or H+ translocation (Muller *et al.*, 2008). However, further investigation must be performed to investigate if NADH could indeed be used to transfer electrons for the Frd via menaquinone in *D. gigas*.

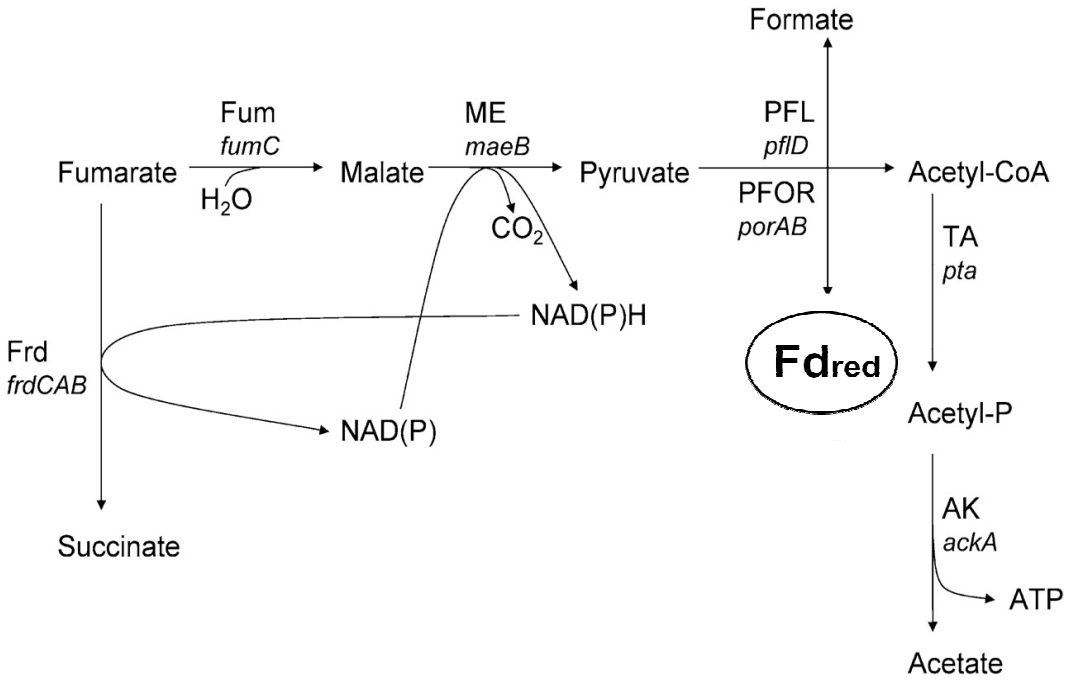

Fig 4.3. Fermentation pathway for fumarate disproportionation in *D. gigas*. Adapted from Zaunmuller *et al.* 2006.

4.4.3 Fumarate as the electron acceptor

It was demonstrated during lactate plus sulfate respiration, that the absence of either hydrogenase did not cause an effect on cell growth (Morais-Silva *et al*., 2013). In the mRNA expression analyzes it was found that *ech* gene expression is quite high during exponential growth in lactate plus sulfate. Also, the growth rate of this mutant strain in these same conditions was lower than the wild type strain.

Our results obtained during lactate fermentation reveal that the Δ*hynAB* mutant strain, containing only the Ech hydrogenase produced H_2. This suggests that this hydrogenase could indeed be participating as an H_2 producer during lactate metabolism. During sulfate reduction other soluble routes for electron could be operating. As such, we decided to replace sulfate by fumarate as the main electron acceptor. When acting as a terminal electron acceptor in respiratory growth, fumarate is reduced by a fumarate reductase in the membrane via a membrane electron transfer chain to which hydrogenases are possible electron donors (Lemos *et al*., 2002b). We evaluated cell growth and Ech hydrogenase expression using lactate as energy source and fumarate as the electron acceptors in *D. gigas* wild type and mutant strains (Fig 4.4).

In contrast to what was observe during fumarate fermentation, under these conditions the *D. gigas* mutant strains behave differently from wild type and between themselves in many aspects. *D. gigas* wild type is able to grow significantly more than both mutant strains (Fig 4.4A). Also, the Δ*hynAB* mutant can grow much better than the Δ*ech*, reaching final optical densities more similar to those of the wild type. Similarly to lactate fermentation, in lactate plus fumarate metabolism the Δ*ech* strain presents a slower doubling time (around 38h) compared to the Δ*hynAB* strain (36h). However in these conditions both mutants grow much slower than the wild type (around 26h) indicating that the presence of both genes contributes to cell growth and that hydrogenases participate actively in the energy metabolism.

Also in lactate/fumarate both hydrogenases appears to produce H_2 as both mutant strains accumulate molecular hydrogen after 20h of growth. The production of H_2 by both hydrogenases is similar to what was observed in the lactate fermentative conditions (Fig 4.4B). However, in these conditions the final concentration of H_2 is almost identical in all the strains and no deficit is observed in any of the mutants. Molecular hydrogen starts to accumulate after the consumption of the residual sulfate (~20h). In both mutant strains, this accumulation starts 4h of growth before the wild type.

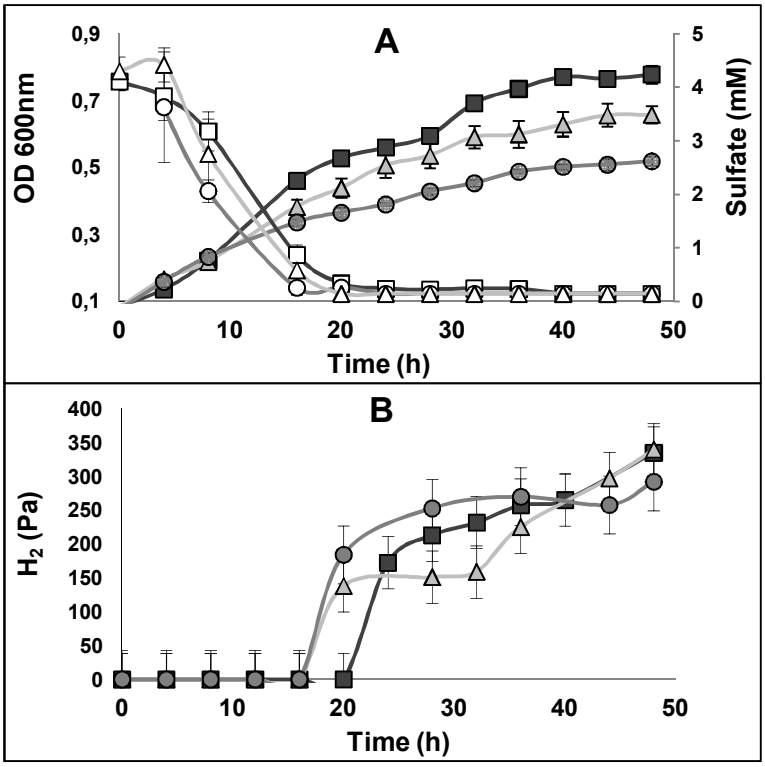

Fig 4.4. Growth curves (closed symbols) during lactate/fumarate growth condition and sulfate concentration (open symbols) (A) and H_2 accumulation (B) of WT *D. gigas* (squares) and hydrogenase mutant strains, Δ*echBC* (circles) and Δ*hynAB* (triangles), in medium containing 40mM of lactate and 40mM of fumarate. Each data point is the average of three independent growth experiments

When substrate consumption is observed it is clear that lactate is continuously oxidized after 20h of growth in the wild type strain, once residual sulfate coming from the inocula is completely reduced (Fig 4.5A and Table 4.1). In the case of the mutants, on the other hand, little or no lactate is further oxidized after 20h. Fumarate consumption is also higher in the wild type than in both mutant strains (Fig 4.5B). However in this case, the mutants behave differently as the Δ*hynAB* strain is able to consume much more fumarate than the Δ*ech* mutant. In fact, in the later, after 20h of growth, when lactate oxidation stops, little amounts

of fumarate are further consumed. As expected, the formation of succinate, the main reduction product of fumarate, is also markedly lower for the Δ*ech* strain than in the wild type, while in the Δ*hynAB*, succinate values are almost as high as in the wild-type. Most interestingly, malate production is observed (Fig 4.5C).

The production of malate suggests that fumarate disproportionation is occurring parallel to lactate oxidation. Once again, the Δ*ech* produces much less malate than the Δ*hynAB* and the wild type. Despite that, in this condition malate accumulates throughout growth and is not consumed.

When one observes the stoichiometry of the succinate in the wild type (0.77mol of succinate per mol of fumarate), it is markedly different from what is detected during fumarate fermentation, being close to the values observed for *D. vulgaris* and *D. desulfuricans* fumarate respiratory conditions using H_2 and formate as electron donors (Zaunmuller *et al*., 2006). As such, it is possible that a respiratory and a fermentative metabolism are operating at the same time. It is not clear though if in a respiratory metabolism where fumarate is the final electron acceptor the electrons are transferred directly from lactate oxidation via the menaquinone to the Frd or if H_2 is an intermediate in this process

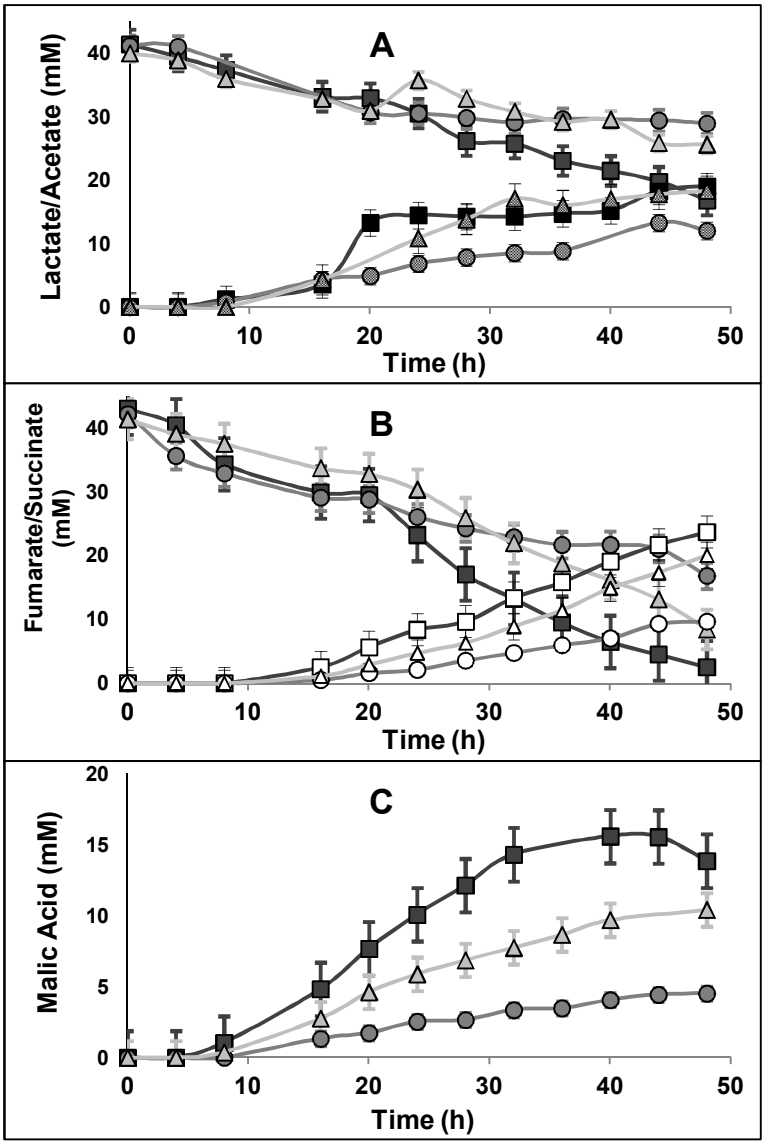

Fig 4.5. Consumption of substrates and product formation during growth of WT *D. gigas* (squares) and hydrogenase mutant strains, Δ*echBC* (circles) and Δ*hynAB* (triangles), in lactate plus fumarate media. (A) lactate (filled symbols) oxidation to acetate (open symbols); (B) fumarate (filled symbols) reduction to succinate (open symbols); and (C) accumulation of malate

The differences in lactate oxidation and succinate production in the hydrogenase mutant strains suggest that the electrons and protons of lactate oxidation are transferred via H_2. In this situation a respiratory growth where H_2 is the electron donor and sulfate or fumarate are the electron acceptors could be occurring in parallel to lactate and fumarate fermentation. During a lactate/fumarate respiratory process, a proton potential (Δp) for ATP production must be generated since the initial step of lactate oxidation to pyruvate is thermodynamically unfavorable and demands an energy input.

In *D. gigas*, as described, the generation of a Δp is not achieved by fumarate reduction and, due to the absence of *pfl* gene, formate is not formed. As such, H_2 could provide a route by which electrons from lactate oxidation generate a Δp during fumarate reduction, leading to ATP synthesis. In this scenario, the presence of both hydrogenases enables cells to oxidize H_2 that is generated from lactate oxidation, in a mechanism similar to the hydrogen cycling model (Odom and Peck, 1981b). Upon lactate oxidation to pyruvate the electrons generated would be used primarily by Ech to generate H_2 that would be oxidized by the HynAB in the periplasm. The electrons generated would be transferred to fumarate reduction creating a proton gradient and ATP. This ATP would then be used to oxidize lactate to pyruvate in a cyclic process.

The absence of either of the hydrogenases would affect negatively the growth of *D. gigas* as is observed. If ATP is not being generated through periplasmic hydrogen oxidation, the energy necessary to promote the endergonic oxidation of lactate to pyruvate would not be available and further lactate oxidation would not be possible. In the Δ*ech* strain the absence of the cytoplasmic hydrogenase would prevent that H_2 is produced from lactate oxidation. The H_2 accumulated by this strain is most likely produced by the HynAB hydrogenase to discard the excess of the reducing power from the lactate after the initial 20h of growth where residual sulfate was no longer present. In the case of Δ*hynAB* strain, the small oxidation of lactate and H_2 accumulation observed after 20h of growth is most likely due to some lactate fermentation, since Ech hydrogenase is still

present. However, once H_2 accumulates to a thermodynamically unfavorable level for further lactate oxidation, this process is impaired.

Moreover, the fact that the H_2 accumulation in the wild type is similar to both hydrogenase mutant strains also corroborates our hypothesis that hydrogen is an intermediate that is being produced and consumed. Fumarate is being used as the final electron acceptor during hydrogen oxidation.

However, regardless of this possible mechanism of energy conservation involving the participation of the hydrogenases during lactate oxidation, in their absence, cells would still be able to grow via fumarate fermentation as demonstrated in this report. This ability to growth by fumarate disproportionation could explain the continuous growth observed in both mutant strains at the expense of fumarate and without further lactate oxidation.

4.4.4 Hydrogenase expression profiles

The different levels of H_2 accumulation during lactate fermentation between wild type and the mutant strains could be due to a different expression of the remaining hydrogenase in the mutant strains. In addition, in the case of the lactate/fumarate conditions, it would be interesting to evaluate if the difference of growth between wild type and the mutant strains has any correlation with a high hydrogenase expression in the wild type.

During both growth conditions the Ech hydrogenases appears to be directly involved with lactate oxidation, as its mutant strain (*Δech*) reveals stronger effects in both doubling time and final optical cell densities. As such, we performed a Western-Blot analysis using an antibody designed specifically for the *D. gigas* Ech hydrogenase to evaluate its protein expression levels at 16h (mid-exponential) as well as at 32h (Fig 4.6). Relative quantification of the target protein in relation to the ribosomal protein, RpoD, was obtained for each sample (Fig 4.7).

As we can observe in Fig. 6, the Ech hydrogenase is expressed in both wild type and Δ*hynAB* mutant strain at mid-exponential and stationary phases

when lactate is the electron donor. We can notice under growth with lactate/limiting sulfate (LS*) that at mid-exponential phase the Ech protein levels are slightly higher in the Δ*hynAB* strain compared to the wild type (Fig. 4.7A).

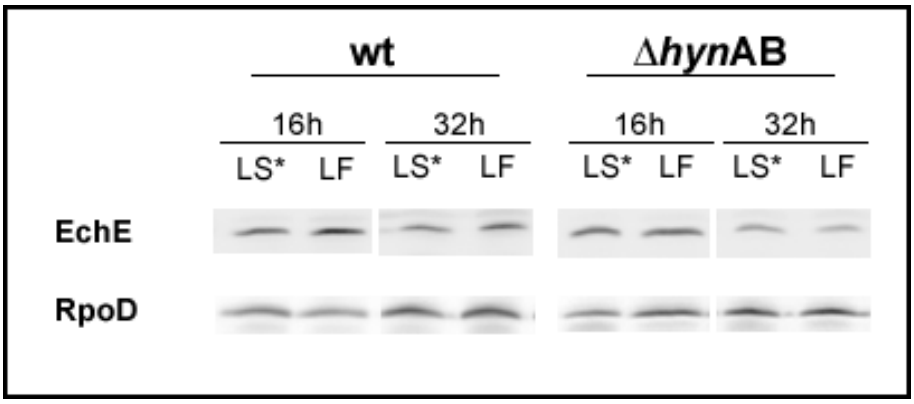

Fig 4.6. Western-blot of the EchE hydrogenase (37kDa) in *D. gigas* wild type and Δ*hynAB* mutant strains. An antibody against the ribosomal protein, RpoD (75kDa), was used as a loading control.

However at 32h, despite an overall decrease in its expression, the Ech protein levels are lower in the mutant strain compared to the wild type (Fig 4.7B). This could explain why, at the end of growth (48h), more H_2 is accumulated in the wild type when compared to the mutant strain.

In the lactate plus fumarate growth conditions, the Ech protein levels are higher in the wild type than in the mutant strain throughout growth. This indicates that this hydrogenase is indeed responsible for H_2 production under this condition. Also, the fact that there is a lower expression of Ech in the Δ*hynAB* mutant strain while the same amount of H_2 is observed in this strain and in the wild type reinforces our hypothesis that H_2 is being produced and consumed in the wild type, providing a mechanism of energy conservation that accounts for the difference in the cell growth.

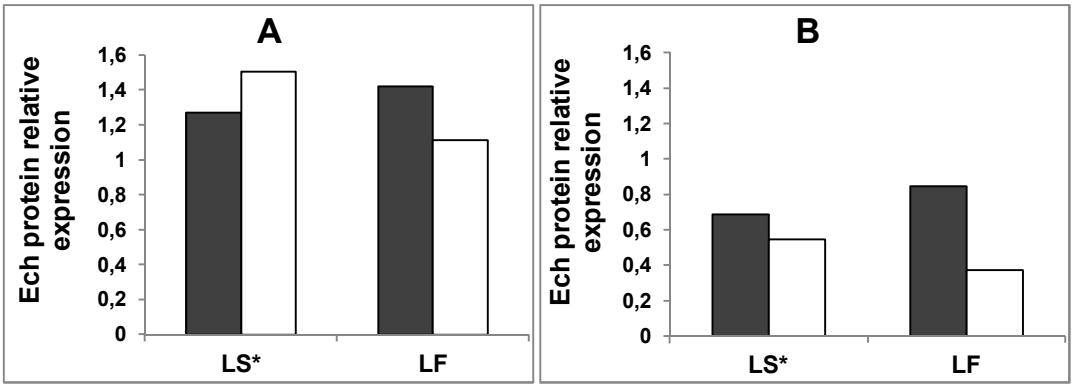

Fig 4.7. Relative quantification of Ech protein expression by Western-Blot analysis in *D. gigas* wild type (grey bars) and ∆*hynAB* (white bars) strains at 16h (panel A) and 32h (panel B).

4.5 Conclusion

The Ech hydrogenase has been shown to play a central and diverse role in the energy metabolism of methanogens, including hydrogen formation from reduced ferredoxin with energy conservation, as well as reduction of ferredoxin by hydrogen via reverse electron transport (Meuer *et al*., 1999; Meuer *et al*., 2002). The results obtained in this report using the *D. gigas* mutant strains clearly demonstrate that in this organism the Ech hydrogenase is a hydrogen producing enzyme when lactate is the organic substrate. Under lactate plus fumarate conditions it appears to be contributing to energy conservation, together with the periplasmic HynAB, enabling lactate oxidation and a higher cell growth. Furthermore, periplasmic hydrogenases of both *D. gigas* (HynAB) and *D. vulgaris* Hildenborough (Hys, Hyn1 and Hyd) function as H_2 producing enzymes during lactate fermentation, in what appears to be a common mechanism for different *Desulfovibrio* spp.

4.6 Acknowledgements

This work was supported by Fundação para Ciência e Tecnologia (FCT) grants (PTDC/BIA-MIC/104030/2008 to IACP/CRP and Pest-OE/EQB/LA0004/2011 to the Instituto de Tecnologia Química e Biológica – António Xavier (ITQB), 049/BI-BI/2011 to C.S and SFRH/BD/45211/2008 to FMS).

4.7 References

Barton, L.L., Le Gall, J., and Peck, H.D., Jr. (1970) Phosphorylation coupled to oxidation of hydrogen with fumarate in extracts of the sulfate reducing bacterium, Desulfovibrio gigas. *Biochem Biophys Res Commun* **41**: 1036-1042.

Bylund, D., Norstrom, S.H., Essen, S.A., and Lundstrom, U.S. (2007) Analysis of low molecular mass organic acids in natural waters by ion exclusion chromatography tandem mass spectrometry. *J Chromatogr A* **1176**: 89-93.

Caffrey, S.A., Park, H.S., Voordouw, J.K., He, Z., Zhou, J., and Voordouw, G. (2007) Function of periplasmic hydrogenases in the sulfate-reducing bacterium Desulfovibrio vulgaris Hildenborough. *Journal of Bacteriology* **189**: 6159-6167.

Chen, L., LeGall, J., Fareleira, P., Santos, H., and Xavier, A.V. (1995) Malate metabolism by Desulfovibrio gigas and its link to sulfate and fumarate reduction: purification of the malic enzyme and detection of NAD(P)+ transhydrogenase activity. *Anaerobe* **1**: 227-235.

Haas, A.H., Sauer, U.S., Gross, R., Simon, J., Mantele, W., and Lancaster, C.R. (2005) FTIR difference spectra of Wolinella succinogenes quinol:fumarate reductase support a key role of Glu C180 within the "E-pathway hypothesis" of coupled transmembrane electron and proton transfer. *Biochemistry* **44**: 13949-13961.

Keller, K.L., and Wall, J.D. (2011) Genetics and molecular biology of the electron flow for sulfate respiration in desulfovibrio. *Front Microbiol* **2**: 135.

Kroger, A., Biel, S., Simon, J., Gross, R., Unden, G., and Lancaster, C.R. (2002) Fumarate respiration of Wolinella succinogenes: enzymology, energetics and coupling mechanism. *Biochimica Et Biophysica Acta* **1553**: 23-38.

Kröger, A., Geisler, V., Lemma, E., Theis, F., and Lenger, R. (1992) Bacterial fumarate respiration. *Archives of Microbiology* **158**.

Lancaster, C.R. (2002) Wolinella succinogenes quinol:fumarate reductase-2.2-A resolution crystal structure and the E-pathway hypothesis of coupled transmembrane proton and electron transfer. *Biochimica Et Biophysica Acta* **1565**: 215-231.

Lancaster, C.R., Sauer, U.S., Gross, R., Haas, A.H., Graf, J., Schwalbe, H. *et al*. (2005) Experimental support for the "E pathway hypothesis" of coupled transmembrane e- and H+ transfer in dihemic quinol:fumarate reductase. *Proc Natl Acad Sci U S A* **102**: 18860-18865.

Lemos, R.S., Gomes, C.M., LeGall, J., Xavier, A.V., and Teixeira, M. (2002a) The quinol:fumarate oxidoreductase from the sulphate reducing bacterium Desulfovibrio gigas: spectroscopic and redox studies. *Journal of Bioenergetics and Biomembranes* **34**: 21-30.

Lemos, R.S., Fernandes, A.S., Pereira, M.M., Gomes, C.M., and Teixeira, M. (2002b) Quinol:fumarate oxidoreductases and succinate:quinone oxidoreductases: phylogenetic relationships, metal centres and membrane attachment. *Biochimica Et Biophysica Acta* **1553**: 158-170.

Matias, P.M., Pereira, I.A., Soares, C.M., and Carrondo, M.A. (2005) Sulphate respiration from hydrogen in Desulfovibrio bacteria: a structural biology overview. *Prog Biophys Mol Biol* **89**: 292-329.

McInerney, M.J., and Bryant, M.P. (1981) Anaerobic Degradation of Lactate by Syntrophic Associations of Methanosarcina barkeri and Desulfovibrio Species and Effect of H(2) on Acetate Degradation. *Appl Environ Microbiol* **41**: 346-354.

Meuer, J., Bartoschek, S., Koch, J., Kunkel, A., and Hedderich, R. (1999) Purification and catalytic properties of Ech hydrogenase from Methanosarcina barkeri. *Eur J Biochem* **265**: 325-335.

Meuer, J., Kuettner, H.C., Zhang, J.K., Hedderich, R., and Metcalf, W.W. (2002) Genetic analysis of the archaeon Methanosarcina barkeri Fusaro reveals a central role for Ech hydrogenase and ferredoxin in methanogenesis and carbon fixation. *Proceedings of the National Academy of Sciences of the United States of America* **99**: 5632-5637.

Meyer, B., Kuehl, J., Deutschbauer, A.M., Price, M.N., Arkin, A.P., and Stahl, D.A. (2013) Variation among Desulfovibrio Species in Electron Transfer Systems Used for Syntrophic Growth. *J Bacteriol* **195**: 990-1004.

Morais-Silva, F.O., Santos, C.I., Rodrigues, R., Pereira, I.A., and Rodrigues-Pousada, C. (2013) Roles of HynAB and Ech, the Only Two Hydrogenases Found in the Model Sulfate Reducer Desulfovibrio gigas. *J Bacteriol* **195**: 4753-4760.

Muller, V., Imkamp, F., Biegel, E., Schmidt, S., and Dilling, S. (2008) Discovery of a ferredoxin:NAD+-oxidoreductase (Rnf) in Acetobacterium woodii: a novel potential coupling site in acetogens. *Ann N Y Acad Sci* **1125**: 137-146.

Odom, J.M., and Peck, H.D., Jr. (1981a) Localization of dehydrogenases, reductases, and electron transfer components in the sulfate-reducing bacterium Desulfovibrio gigas. *J Bacteriol* **147**: 161-169.

Odom, J.M., and Peck, H.D.J. (1981b) Hydrogen cycling as a general mechanism for energy coupling in the sulfate-reducing bacteria Desulfovibrio sp. *Fems Microbiology Letters* **12**: 47-50.

Pankhania, I.P., Spormann, A.M., Hamilton, W.A., and Thauer, R.K. (1988) Lactate conversion to acetate, CO2 and H2 in cell suspensions of Desulfovibrio vulgaris (Marburg): indications for the involvement of an energy driven reaction. *Archives of Microbiology* **150**.

Plugge, C.M., Scholten, J.C., Culley, D.E., Nie, L., Brockman, F.J., and Zhang, W. (2010) Global transcriptomics analysis of the Desulfovibrio vulgaris change from

syntrophic growth with Methanosarcina barkeri to sulfidogenic metabolism. *Microbiology* **156**: 2746-2756.

Rabus, R., Hansen, T.A., and Widdel, F. (2006) Dissimilatory sulfate- and sulfur-reducing prokaryotes. In. Dworkin, M., Falkow, S., Rosenberg, E., Schleifer, K.H., and Stackebrandt, E. (ed).

Schnorpfeil, M., Janausch, I.G., Biel, S., Kroger, A., and Unden, G. (2001) Generation of a proton potential by succinate dehydrogenase of Bacillus subtilis functioning as a fumarate reductase. *Eur J Biochem* **268**: 3069-3074.

Silva, G., Oliveira, S., LeGall, J., Xavier, A.V., and Rodrigues-Pousada, C. (2001) Analysis of the Desulfovibrio gigas transcriptional unit containing rubredoxin (rd) and rubredoxin-oxygen oxidoreductase (roo) genes and upstream ORFs. *Biochem Biophys Res Commun* **280**: 491-502.

Stolyar, S., Van Dien, S., Hillesland, K.L., Pinel, N., Lie, T.J., Leigh, J.A., and Stahl, D.A. (2007) Metabolic modeling of a mutualistic microbial community. *Mol Syst Biol* **3**: 92.

Voordouw, G. (2002) Carbon monoxide cycling by Desulfovibrio vulgaris Hildenborough. *Journal of Bacteriology* **184**: 5903-5911.

Walker, C.B., He, Z., Yang, Z.K., Ringbauer, J.A., Jr., He, Q., Zhou, J. *et al*. (2009) The electron transfer system of syntrophically grown Desulfovibrio vulgaris. *J Bacteriol* **191**: 5793-5801.

Zaunmuller, T., Kelly, D.J., Glockner, F.O., and Unden, G. (2006) Succinate dehydrogenase functioning by a reverse redox loop mechanism and fumarate reductase in sulphate-reducing bacteria. *Microbiology* **152**: 2443-2453.

Chapter 5

General Discussion and Future perspectives

5.1 General Discussion

The work presented in this thesis allowed us to have a global view of the main genetic elements of the model sulfate reducing bacteria *Desulfovibrio gigas* ATCC19364. We were particularly interested to understand the direct impact of the enzymatic group of hydrogenases in the energy budget of this organism. Hydrogen is known to be not only an important energy substrate for *Desulfovibrio* spp., but it is also proposed to participate as a key intermediate during the mechanisms of energy conservation from degradation pathways of other substrates during respiratory and fermentative growth.

The decoding of *D. gigas* genome allowed us to have a complete overview of the proteins and regulatory mechanism of this organism. Unique elements that are present only in this species when compared to the other representatives of the *Desulfovibrio* genus were identified. Some of these elements, such as a second ATPase and a membranar complex (Mnh) may play a role in the energy metabolism and provide *D. gigas* with unique adaptation mechanisms. Also, gene duplications for enzymes related to substrate oxidation (fumarate and formate dehydrogenases) and that confer resistance to O_2 (superoxide dismutase) were identified. The presence of alternative enzymes for these functions may have a strong effect in the interpretation of how these metabolic pathways operate. The presence of a highly variable number and types of CRISPR elements and associated Cas genes indicates that these prokaryotic innate immune system in *Desulfovibrio* spp. resulted from a series of horizontal gene transfer events. In *D. gigas* the presence of a high number of CRISPR elements (six in total) may reflect a rather different evolutionary pathway when compared to the close related *D. vulgaris* and *D. desulfuricans* strains and could justify, in part, the difficulty to perform genetic manipulation of this strain.

Moreover, the possibility to identify and to look for specific features in *D. gigas* genome helped the identification of two transcriptional factors that are involved in the nitrosative stress response, named *norR1* and *norR2*. The function

of *norR1* in the regulatory mechanisms upon nitrosative stress was assayed and published (Varela-Raposo *et al*., 2013).

Regarding the presence of hydrogenases, the information obtained from the initial *D. gigas* genomic survey, later confirmed after its final analysis, revealed that this organism only possesses the two hydrogenases previously described: the cytoplasmic membrane-bound energy conserving [NiFe] Ech hydrogenase and the periplasmic uptake [NiFe] HynAB hydrogenase. Using Blast Tool, genomic sequences of different types of hydrogenases from related species, such as *D. vulgaris* Hildenborough, were used as models to identify the genes encoding the hydrogenase orthologous in *D. gigas*. Despite extensive comparison analysis, no other hydrogenase genes were identified. The presence of only two hydrogenases in a *Desulfovibrio* species is unusual. From the available drafts or full genomes analyzed in various *Desulfovibrio* strains, *D. gigas* contains the smallest number of representatives from this enzymatic group. Other described species from this genus contain a minimum of three hydrogenases. It is important also to mention that the species *Desulfovibrio sapovorans*, which was later reclassified as *Desulfobotulus sapovorans*, apparently does not have any hydrogenase described (Devereux *et al*., 1990). However, due to the fact that there is not yet any draft or genome sequence available it is possible that this organism contains unidentified genes coding for the hydrogenases. Another unique aspect of *D. gigas* is the absence of any hydrogenase of the [FeFe] type, either in the periplasm or in the cytoplasm, as both Ech and HynAB are from the [NiFe] family. With the exception of *D. piger*, which contains only one cytoplasmic monomeric [FeFe] enzyme, all *Desulfovibrio* spp. so far described present at least one copy of the soluble periplasmic [FeFe] HydAB and eventually other soluble cytoplasmic [FeFe] hydrogenases (Pereira *et al*., 2011). From the fact that only two [NiFe] hydrogenases are found in *D. gigas* genome it is reasonable to draw two important observations. The first one relates to the mechanism of regulation of the hydrogenases. The metal availability might affect differently *D. gigas* when compared to all other *Desulfovibrio* strains. For instance, while the absence of Ni

might enhance the expression of [FeFe] hydrogenases in *Desulfovibrio* spp., *D. gigas* cells would be unable to express any hydrogenase and, depending on the growth conditions, this could completely impair growth. The second and most relevant observation is the possibility to use *D. gigas* as unique and simple model, when compared to other *Desulfovibrio*, to test the importance of the hydrogenase enzymatic group in mechanisms of energy conservation such as the hydrogen cycling model. In other species such as *D. vulgaris* or *D. desulfuricans*, one has to deal with multiple hydrogenases in which the absence of one hydrogenase by genetic engineering could be compensated by another of these enzymes. Multiple mutations to knock out a specific group or number of these genes must be performed in order to observe the physiological impact in whole cell metabolism. As such, the evaluation of the role of individual hydrogenases is very difficult to assess. The choice of multiple markers for selection of correct transformants or protocols for simultaneous deletions, involves a laborious work. On the other hand, in *D. gigas*, which presents only one hydrogenase either in the periplasm or in the cytoplasm, a single gene deletion can not only demonstrate the physiological role of the remaining enzyme, but also reveal if H_2 is generated in one subcellular compartment or the other. This can give important clues regarding the flow of electrons between periplasm and cytoplasm and how proton motive force for ATP synthesis is achieved.

Taking advantage of these characteristics, the specific participation of each hydrogenase in the energy metabolism was analyzed by generating two hydrogenase mutant strains, Δ*ech* and Δ*hynAB*. To detect their function, both mutant strains were grown using different electron donors and acceptors and their growth profile was compared with the wild type strain under the same conditions. To assess the physiological role of the gene deletions, H_2 accumulation was measured by gas chromatography (GC), along with the quantification of substrates and products performed by high performance liquid chromatography (HPLC). As different electron donors we used H_2, lactate, pyruvate and fumarate, whereas as electron acceptors, in alternative for sulfate, fumarate was selected or no other

external electron acceptor was used. As such, we were able to create both respiratory and fermentative conditions. Growing the mutant strains in these different conditions we were able to evaluate which hydrogenase is involved in the H_2 production or H_2 consumption. Furthermore, this data provides insights into the energy conserving mechanisms operating as well as the pathways that might be used in these processes.

It was shown that the periplasmic HynAB hydrogenase is a truly reversible enzyme. On one hand it functions as an H_2 oxidizing enzyme during hydrogen respiratory growth (HS), since the Δ*hyn*AB is unable to grow in these conditions. Also, it is possible that during lactate and pyruvate respiratory growth (LS and PS, respectively) hydrogen produced by the Ech from oxidation of these electron donors is being oxidized by the HynAB in a hydrogen cycling mechanism of energy conservation as proposed by Odom and Peck (1984). This hypothesis is corroborated by the higher mRNAs expression level of *ech* at 16h of growth and subsequent increase in the mRNA expression of the *hynAB* at 32h in the LS conditions. On the other hand, during fermentation using lactate and pyruvate as substrates the HynAB functions as a H_2 producing hydrogenase. Although no growth was observed in the lactate plus limiting sulfate condition (LS*) after sulfate was completely reduced and cells started to ferment lactate, the accumulation of H_2 by the Δ*ech* strain shows that the HynAB produced some H_2 from lactate oxidation. When pyruvate is the substrate, with or without addition of sulfate (PS* and P, respectively), the Δ*ech* strain not only produces H_2, but does so at much higher rates than the wild type, a result that was unexpected. Furthermore, because pyruvate oxidation to acetate is a thermodynamically favorable reaction, cells are able to grow fermentatively after sulfate is completely reduced, as long as the HynAB hydrogenase is present. This can be observed by the absence of growth of the Δ*hynAB* strain during pyruvate fermentation (P) when sulfate is not added.

When the electron acceptor is fumarate and the electron donor is lactate (LF conditions), the same physiological function of the HynAB hydrogenase in H_2

production can be observed by the accumulation of H_2 in the Δ*ech* mutant. It is important to notice that, due to the intrinsic complexity of the LF conditions, as fumarate can be used as both electron acceptor and electron donor, the exact metabolism by which lactate is oxidized to acetate while fumarate is reduced to succinate remains elusive. From HPLC quantifications it is possible to deduce that more than one metabolic pathway is active during growth in those conditions and that both fermentation and respiration are occurring simultaneously. However, the HynAB enzyme does not appear to participate in the energy metabolism of the cell during fermentation of fumarate, because H_2 production is not observed in the Δ*ech* mutant strain and the Δ*hynAB* strain is able to grow as well as the wild type.

The same observation can be made with respect to the participation of the Ech hydrogenase in the fumarate fermentative metabolism as neither H_2 is produced in the Δ*hynAB* nor growth is affected in the Δ*ech* strain. Under pyruvate fermentative metabolism in contrast to what is observed for the HynAB hydrogenase, the Ech enzyme does not produce H_2. This observation is also unexpected, since transcriptomic analysis in *D. vulgaris* Hildenborough suggested Ech activity to be involved in the generation of H_2 from reduced ferredoxin formed from the oxidation of pyruvate (Pereira *et al*., 2008). Ech was also shown, in methanogens, to produce H_2 from electrons generated by the substrate oxidation in the cytoplasm (Meuer *et al*., 2002). As such, it would be expected that Ech and not HynAB would produce H_2 from pyruvate fermentation in *D. gigas*. Furthermore, the almost absence of *ech* hydrogenase gene expression observed (see Chapter 3) in both wild type and Δ*hynAB* strain confirm that Ech does not produce H_2 under pyruvate fermentation. In the HS conditions, as Ech cannot compensate the absence of *hynAB* gene when hydrogen is the electron donor, the Δ*hynAB* strain is unable to grow. In HS conditions *ech* gene expression is only observed in the wild type at 32h, time at which the cells have already stopped to grow. Under pyruvate respiratory conditions (PS and at 16h of growth during PS*), despite detectable expression of *ech* gene in the wild type, its absence does not affect growth.

The Ech hydrogenase activity and its expression appear to be involved only in H_2 production from oxidation of lactate. During lactate fermentative growth (LS*), Ech functions in H_2 production, as expected for an energy-conserving cytoplasmic hydrogenase. This can be observed by the H_2 accumulation in the Δ*hynAB* mutant strain. Although no hydrogen is formed by this strain in lactate respiratory growth (LS) and no difference in cell density is observed in the Δ*ech* compared to the wild type strain, *ech* gene expression is very high after 16h of growth. The absence of the *ech* affects also negatively the doubling time of its mutant strain when compared to the wild-type and Δ*hynAB* in these same conditions. It is possible then, that the Ech hydrogenase could produce H_2 that is later consumed by HynAB activity during LS growth. Finally, during the LF growth conditions, the production of H_2 by Ech can also be observed in the Δ*hynAB* strain. Moreover, H_2 generation from lactate appears to be primarily performed by Ech hydrogenase, as in its absence, the Δ*ech* mutant strain oxidizes smaller amounts of lactate when compared to the Δ*hynAB* and wild type. This is, most likely, the reason why this strain presents a lower final cell density than the Δ*hynAB* strain, which is able to oxidize higher amounts of lactate, and even lower growth when compared to the wild type, that can continuously oxidize lactate. In this later strain, however, the absence of the Ech is compensated at some degree by the HynAB hydrogenase as the Δ*hynAB* grows almost to the same levels as the wild type. Nevertheless, the presence of both hydrogenases contributes to a better growth of the wild type compared to any of the mutants. In these conditions it is possible that, in the presence of both hydrogenases, some H_2 produced by Ech as a result of lactate oxidation could be consumed by HynAB providing electrons for fumarate reduction. As such, oxidation of higher amounts of lactate to acetate with concomitant higher accumulation of succinate as the main product of fumarate reduction would be observed. Thus, the presence of both hydrogenases would provide another mechanism of energy generation that could account for the higher final cell densities reached by the wild type in comparison with the mutant strain

The analysis performed with the *D. gigas* hydrogenase mutant strains enable us to clearly identify the function of each hydrogenase, as H_2 producing or H_2 consuming enzymes, during different types of metabolism (respiratory vs fermentative) and with different electron acceptors and donors. In addition, the comparison of growth parameters, H_2 accumulation and expression of these hydrogenases, together with the identification of other elements, such as membrane complexes and electron carriers that participate in the electron transfer pathways allows us to elaborate on the mechanisms of energy conservation that might be contributing to cell growth.

During respiratory growth with hydrogen as the electron donor and sulfate as the electron acceptor, the periplasmic HynAB hydrogenase acts as the main hydrogenase enzyme and is essential for cell growth. Hydrogen is oxidized in the periplasm and its electrons are shuttled to cytoplasmic sulfate reduction via TpI-c_3 and a transmembrane electron complex. The Qrc complex could accept the electrons from the TpI-c_3 and transfer them to the menaquinone pool, where the Qmo complex in turn would transfer them directly to the APS reductase (Venceslau *et al*., 2010; Ramos *et al*., 2012). Both these enzyme complexes were identified in the *D. gigas* genome. This Qrc and Qmo redox loop would contribute to the energy conservation through the creation of a proton potential that is used by the ATP synthase to generate ATP. This is necessary to promote cell growth since the ATP energy directly obtained by H_2 oxidation is consumed during sulfate activation. Furthermore, another transmembrane complex that could participate in the energy conservation during hydrogen plus sulfate is the RnfABCDEF complex, since in the analysis of *D. vulgaris* Hildenborough transcriptome subjected to HS growth conditions, an up-regulation of *rnf* genes was observed in comparison to LS respiratory growth (Pereira *et al*., 2008). The presence of a cytochrome *c* gene in *D. gigas rnf* operon could provide a mechanism by which this complex could accept the electrons from periplasmic hydrogen oxidation via the TpI-c_3,coupling it with the oxidation of ferredoxin or NAD^+ and pumping protons in the process contributing to a proton gradient formation. In the case of Ech, although an up-

regulation of this hydrogenase gene in HS compared to LS was observed in *D. vulgaris* transcriptional analysis, in *D. gigas* its absence does not affect cell growth and the Δ*ech* mutant reaches similar final densities as the wild type. As such, it does not appear to have a key contribution for the creation of a proton potential in these conditions.

When lactate is the electron donor for sulfate respiration, the Ech hydrogenase could produce H_2 from reducing equivalents generated during lactate oxidation in the cytoplasm. This H_2 would is in turn be oxidized in the periplasm by the HynAB hydrogenase. Such mechanism is suggested by the presence of significant mRNA expression of both hydrogenases in the wild type. The electrons generated would be then shuttled to reduce the sulfate in the cytoplasm by the transmembrane complexes, such as DsrMKJOP or QrcABCD that could accept them from TpI-c_3. During LS growth, *D. vulgaris* transcriptomic analysis showed that the relative mRNA abundance of the genes encoding both these complexes were among the highest expressed during exponential growth phase (Keller and Wall, 2011). The protons generated from the oxidation of H_2 in the periplasm would in turn build a proton gradient used for ATP generation for cell growth, as the energy produced by pyruvate oxidation would be, as in the case of hydrogen, spent in sulfate activation. However, besides H_2 cycling, another mechanism of energy conservation involving directly the lactate dehydrogenase (Ldh) enzyme could be operating. The Ldh enzymes may be capable of transferring electrons directly to the menaquinone since these enzymes present iron-sulfur subunits belonging to the CCG family with high homology to HdrD-like proteins (Ldh1a and Ldh1b) (Pereira *et al*., 2011). Once transferred to the menaquinone, these electrons coming from lactate oxidation could be accepted by the Qmo complex and transferred to AprAB reduction in a process that may result in energy conservation. Relative mRNA abundance of *qmo* genes was also high during LS growth (Keller and Wall, 2011). Furthermore, the reduced ferredoxin generated by the pyruvate:ferredoxin oxidoreductase (PFOR) enzyme might be participating in the electron bifurcation processes involving the Rnf complex or NfnAB

transhydrogenases instead of being used by the Ech hydrogenase to reduce protons to hydrogen in its absence. In such mechanisms, electron transport from reduced Fd to NAD^+ is coupled to electrogenic proton pumping by the Rnf complex, while the reduction of $NADP^+$ by reduced ferredoxin is accomplished by the NfnAB enzyme. The NAD(P)H formed could then be used by the FloxABCD complex to supply electrons for HdrABC mediated sulfite reduction. Thus, such complexes could provide soluble alternative pathways for sulfate reduction, where H_2 is not an obligate intermediate. These pathways could work in parallel to the proposed hydrogen cycling, as suggested by Noguera´s dual pathway hypothesis (Noguera *et al*., 1998). With the deletion of each hydrogenase, hydrogen cycling would no longer be available and the mutant strains could compensate its absence by reversing all the electrons from lactate oxidation to these alternative pathways. This would also explain why no hydrogen accumulation is observed in any of the mutant strains and the cells are able to grow as well as the wild type.

Similarly to what is observed with lactate as the electron donor, in pyruvate respiratory growth dual pathways could be operating simultaneously. Reduced ferredoxin is the main electron carrier produced in these growth conditions. It could be used by the Ech hydrogenase to generate hydrogen to participate in a hydrogen cycling mechanism of energy conservation with the periplasmic HynAB enzyme. In effect, in early experiments performed by Peck *et. al*, hydrogen cycling was proposed during pyruvate plus sulfate growth using membrane-inlet mass spectrometry (Peck *et al*., 1987). However, as discussed above, the Rnf complex and the NfnAB transhydrogenase could provide alternative routes for electrons coming from reduced Fd. Interestingly, in the case of the Rnf complex, different transcriptional data analysis using *D. vulgaris* Hildenborough indicate an increased expression of this complex during PS growth when compared to the LS conditions (Pereira *et al*., 2008; Keller and Wall, 2011). Apparently this is an important pathway during this growth conditions and could compensate hydrogen cycling in the absence of any of the hydrogenases in *D. gigas*. As in LS, these soluble

alternative pathways could be the reason why no H_2 is detected in any of the mutant strains when sulfate is still present.

On the other hand in the absence of sulfate, the panorama appears to be different and a general mechanism for hydrogenase function appears to be present for both organic substrates *e.g.* production of H_2 (Fig 5.1). Both cytoplasmic and periplasmic hydrogenase uses H_2 as electron and proton sink due to the absence of sulfate, discarding an excess of reducing power resulting from substrate oxidation.

In the case of pyruvate, this mechanism appears to rely only in the activity of the periplasmic HynAB hydrogenase, since in its absence the cells are no longer able to grow and the pyruvate oxidation is prevented. A similar role for the periplasmic hydrogenases in H_2 production was proposed during syntrophic growth of *D. vulgaris* and *D. alaskensis* G20 with the metanogen (Walker *et al*., 2009; Plugge *et al*., 2010; Meyer *et al*., 2013). In *D. vulgaris* Hildenborough it was demonstrated that the deletion of the Hmc complex impairs syntrophic growth by pyruvate fermentation (Walker *et al*., 2009). It is possible that in *D. gigas*, similarly to what is observed in *D. vulgaris* syntrophic growth, the Hmc complex could be the transmembrane component that would transfer the electrons from cytoplasmic pyruvate oxidation, via TpI-c_3 to periplasmic H_2 production (Fig 5.1, [A]). Also, other transmembrane complexes could perform this function, *e.g.* the Tmc complex, which is highly similar to the Hmc, or the DsrMKJOP. In accordance, *D. vulgaris* transcriptional analysis has shown that during pyruvate fermentation, both Hmc and DsrMKJOP genes are up-regulated compared to LS conditions (Pereira *et al*., 2008).

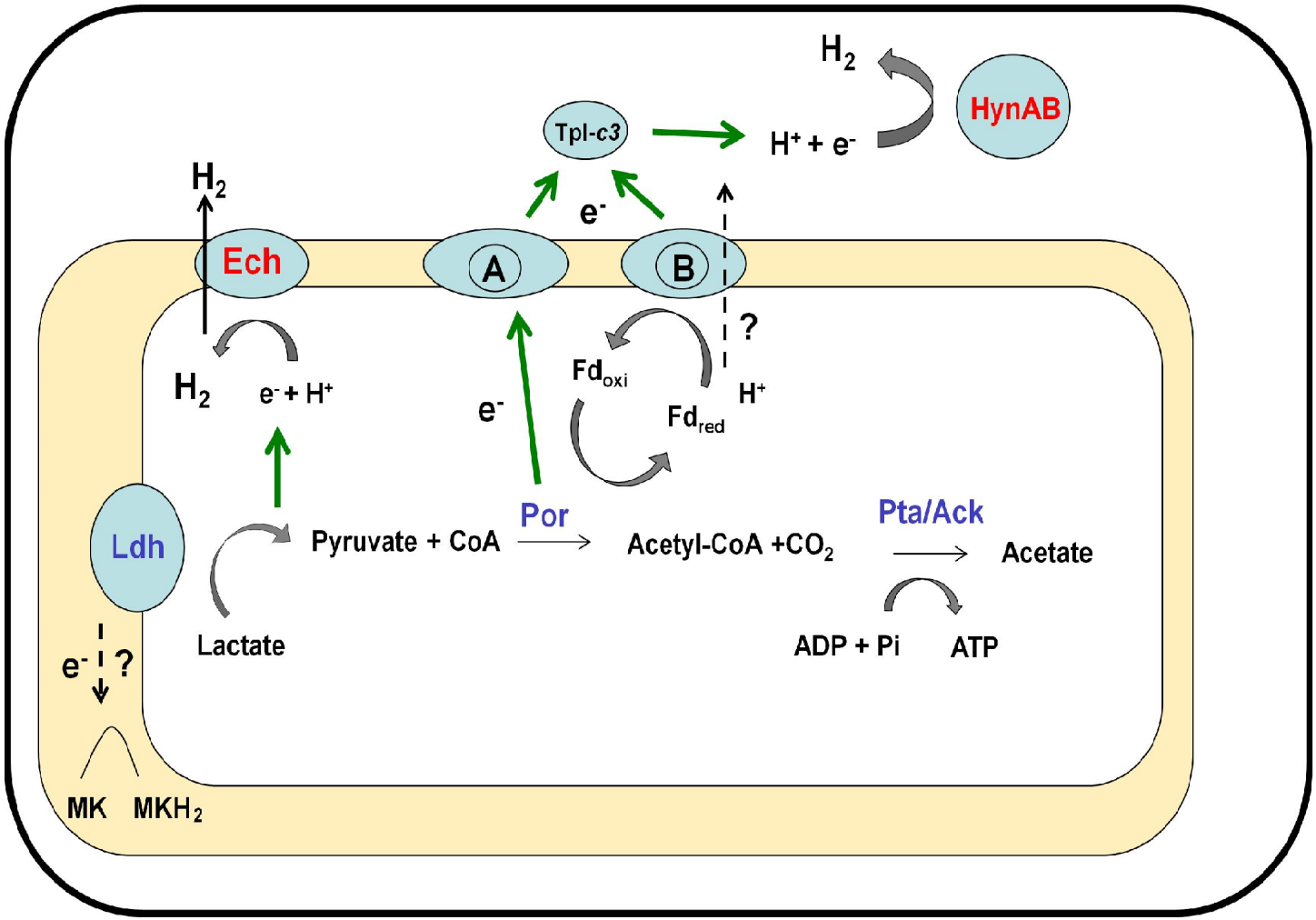
H2
HynAB
Tpl-c3
H+ + e-
H2
e-
Ech
A
B
?
Fdoxi
H+
Fdred
H2
e- + H+
e-
Por
Ldh
Pyruvate + CoA
Acetyl-CoA +CO2
Pta/Ack
Acetate
Lactate
ADP + Pi
ATP
e- ?
MK
MKH2

Fig 5.1. Proposed physiological function of *D. gigas* hydrogenases during lactate and pyruvate fermentative metabolism. Ldh: lactate dehydrogenase; Ech: cytoplasmic [NiFe] hydrogenase; Por: pyruvate:ferredoxin oxidoreductase; HynAB: periplasmic [NiFe] hydrogenase; Pta: phosphotransacetylase; Ack: acetate kinase; A: Hmc/Tmc transmembrane complex; B: Rnf transmembrane complex.

Unexpectedly, the Ech hydrogenase of *D. gigas* does not appear to be able to produce H_2 from reduced Fd, as the Δ*hyn*AB mutant does not accumulate significant amounts of H_2, being not able to compensate for the absence of the HynAB enzyme. Furthermore, in the Δ*ech* strain, the higher expression of the *hyn*AB genes when compared to the wild type strain might be translated into a greater production of H_2. Alternatively, this reduced ferredoxin generated by the pyruvate:ferredoxin oxidoreductase (PFOR) enzyme could be participating in the electron bifurcation processes involving the Rnf complex as proposed before (Fig 5.1, [B]).

However, during lactate fermentation we can clearly observe that the Ech hydrogenase has a similar function in the H_2 production, similarly to the HynAB, as the Δ*ech* mutant strain accumulate less H_2 (curiously, almost half the amount) than the wild type. The electrons produced from the oxidation of lactate, as mentioned before, could be transferred to the menaquinone by the Ldh enzyme. The electrons produced from the subsequent pyruvate oxidation could use the same routes as in pyruvate fermentative conditions to reach the periplasm where the HynAB would also contribute to H_2 production. Considering this situation our results apparently indicate that, as proposed by Keller and Wall there are two separate routes from the electrons coming from lactate oxidation to H_2 production by the Ech and HynAB respectively (Keller and Walker, 2001). In the absence of sulfate, H_2 is evolved by both enzymes as a mechanism of disposing of excessive reducing potential. However when its concentration accumulates and reaches a threshold, further oxidation of lactate coupled to H_2 production is unfavorable. Notably, the periplasmic hydrogen production during lactate fermentative

metabolism appears to be a common mechanism in some *Desulfovibrio* spp. as *D. vulgaris* Hildenborough mutant strains for periplasmic hydrogenases also accumulate less H_2 than the wild type (unpublished results). Although the periplasmic [FeFe] Hyd hydrogenase from *D. vulgaris* was proposed to be involved in hydrogen production during lactate fermentation, the results obtained here clearly demonstrate for the first time that other periplasmic hydrogenases such as the HynAB from *D. gigas* may also participate as H_2 evolving enzymes.

A completely different result was observed during fumarate fermentative growth. In such conditions, both Ech and HynAB do not seem to participate in any mechanisms of energy conservation or redox regulation in *D. gigas* cells growing by fumarate disproportionation. The corresponding mutant strains were able to grow as well as the wild type and no H_2 was accumulated in the process. Both fumarate reductases (FrdABC) enzymes present in *D. gigas* genome have the conserved Glu180 residue in the FdrC subunit indicating no proton potential is generated during fumarate reduction (Zaunmuller *et al*., 2006). This means that possible mechanisms of energy conservation must rely either on the NAD(P)H generate by malate reduction to pyruvate by the malic enzyme or in the reduced Fd that results from pyruvate oxidation. The electrons from NAD(P)H and reduced Fd could be transferred by HdrABC/FloxABCD and Rnf complexes, respectively, in electron bifurcation mechanisms of energy conservation creating the proton potential necessary for ATP synthesis.

Despite the fact that the absence of either hydrogenase does not affect growth of the mutant strains during fumarate fermentation, two observations can be made based on substrate and product quantifications. The first interesting observation is that although small amounts of sulfate (~3mM), coming from the inocula, are present during the fumarate fermentative conditions, it is not immediately reduced. Instead fumarate is being used as primary electron acceptor and it is reduced to succinate. This suggests than in both wild type and in the Δ*hynAB* mutant strain sulfate respiratory growth with fumarate as the electron donor is not preferable during the initial growth phase, being reduced only after

32h of growth. In contrast in the Δ*ech* strain, sulfate is rapidly consumed in the initial 20h. The second observation is that this same mutant strain, besides consuming the limiting amounts of sulfate after only 20h, also accumulates considerably less malate during exponential growth. Furthermore, the malate accumulated during fumarate fermentation appears to be directly involved in the reduction of the limiting sulfate present. After malate concentration reaches its peak, it starts to be consumed while sulfate is reduced, suggesting that sulfate can function as an alternative electron acceptor for malate oxidation.

A similar observation can be made during lactate plus fumarate growth conditions, as the Δ*ech* mutant strain once again accumulates less malate than the Δ*hynAB* and wild type strains. However these similarities between both growth conditions are the only ones seen. In these conditions, malate accumulates throughout growth and it is not re-oxidized. Also, all strains accumulate H_2 at similar levels confirming that both Ech and HynAB can produce H_2 from lactate oxidation. The absence of either hydrogenase affects cell growth, being the influence more visible in the Δ*ech* mutant strain. This strain oxidizes less lactate to acetate than the Δ*hynAB* mutant and considerably less than the wild type. At the same time, less fumarate is reduced to succinate resulting in much lower growth of the Δ*ech* strain when compared to the two other strains. These results obtained by the HPLC analyses indicate that during LF conditions, an overlap of metabolisms could be occurring and it is not clear if LF is a truly respiratory condition, where lactate serves as the electron donor for the reduction of fumarate. Due to the presence of simultaneous lactate oxidation and malate production, two parallel fermentative conditions could be operating. Lactate would be fermented to H_2 and fumarate disproportionated to acetate, succinate and malate. In addition, the limiting amounts of sulfate present in the beginning of growth could be reduced by the H_2 resulting from lactate oxidation. As such, the H_2 produced from lactate fermentation by one hydrogenase (ideally Ech) is re-oxidized by the second hydrogenase generating energy that allows the wild type to reach higher final cells yield. This would constitute a mechanism very similar to the hydrogen cycling and

reinforces our hypothesis that Ech is the primary enzyme to produce H_2 from lactate. In its absence no H_2 would be produced from lactate oxidation to be used as an alternative energy source leading to a stronger defect in cell growth. However in this strain, as observed under lactate fermentative conditions, the HynAB hydrogenase may also contribute to H_2 production to allow further lactate oxidation until H_2 concentrations reaches a limit where this reaction is no longer favorable.

Besides the analysis with the organic substrates mentioned in this thesis, the two *D. gigas* hydrogenase mutants, containing each a single hydrogenase enzyme, were also evaluated for their ability to grow and produce H_2 during fermentative conditions using formate as an electron donor, in a collaboration with the Bacterial Energy Metabolism laboratory. Due to the fact that both formate dehydrogenases identified in *D. gigas* genome present putative export signals, the oxidation of formate should be performed solely in the periplasm. In the case of H_2 production from formate, using both hydrogenase mutant strains it should be possible to determine which hydrogenase is involved in H_2 formation coupled to formate oxidation. The results obtained showed that both mutant strains are able to oxidize formate although the Δ*hynAB* mutant strain accumulated much less H_2 than the other two strains.

To conclude, in the work performed in this thesis we deciphered the genome of the sulfate-reducing bacterium *Desulfovibrio gigas* providing an extraordinary tool for the identification of all genetic elements present in this species. Also the work performed with two hydrogenase mutant strains gave key insights into the physiological function of the Ech and HynAB enzymes in *D. gigas* energy metabolism, suggesting that alternative mechanisms of energy conservation co-exist during respiratory and fermentative growth using different substrates.

5.2 Future Perspectives

With the results described in this thesis, several important questions regarding the features of *D. gigas* genome and the hydrogenase physiological function in this organism were answered.

While the publication of a genome sequence opens up a wide range of possibilities for future studies using *D. gigas* as a model organism, the results obtained with the hydrogenase mutant points out for two interesting analysis that can be performed to further elucidate the mechanisms of energy conservation in this bacterium, from which hydrogenases are one part of the whole process.

As can be observed during the discussion of the results obtained, transcriptomic analyses represent a powerful tool to try to elucidate the whole pathways involved in the energy conservation under given conditions. With the genome at hand, a microarray chip of *D. gigas* could be constructed similarly to what was performed for *D. vulgaris* Hildenborough. Transcriptional analysis comparing the wild type strain with the hydrogenase mutant strains could be analyzed under various growth conditions comparing the results with the phenotypes obtained in the physiological studies. This would greatly contribute to identify which transmembrane complexes might be participating in electron transfer reactions and providing alternative mechanisms of energy conservation. Furthermore, with the recent development of proteomic analyses, which are capable of measuring a great number of proteins in any biological system, a whole proteome analysis could complement microarray analyses (Bantscheff and Kuster, 2012).

Also, due to the fact that *D. gigas* presents only two hydrogenases and single mutant strains were already constructed, it would be very interesting to evaluate the effects of a double mutant in which the strain generated would be hydrogenase absent. This strain, if viable, could then be grown under different conditions to observe the real importance of hydrogen metabolism in the cell´s total energy metabolism. It is important to mention here that the creation of a

double mutant strain was already attempted during the course of this PhD thesis. However, we were unable to grow and isolate a double hydrogenase mutant in LS and PS medium. This could be due to the fact that the knockout of all hydrogenases in this strain is so deleterious that it becomes lethal to the cells. Alternatively, the selection for the transformants using simultaneously two antibiotics, kanamycin and cloramphenicol, could be too aggressive for an already weak mutated strain.

5.3 References

Bantscheff, M., and Kuster, B. (2012) Quantitative mass spectrometry in proteomics. *Anal Bioanal Chem* **404**: 937-938.

Devereux, R., He, S., Doyle, C.L.e.a., Orkland, S., Stahl, D., LeGall, J., and Whitman, W. (1990) Diversity and origin of Desulfovibrio species: phylogenetic definition of a family. *Journal of bacteriology* **172**: 3609-3619.

Keller, K.L., and Wall, J.D. (2011) Genetics and molecular biology of the electron flow for sulfate respiration in desulfovibrio. *Front Microbiol* **2**: 135.

Meuer, J., Kuettner, H.C., Zhang, J.K., Hedderich, R., and Metcalf, W.W. (2002) Genetic analysis of the archaeon Methanosarcina barkeri Fusaro reveals a central role for Ech hydrogenase and ferredoxin in methanogenesis and carbon fixation. *Proceedings of the National Academy of Sciences of the United States of America* **99**: 5632-5637.

Meyer, B., Kuehl, J., Deutschbauer, A.M., Price, M.N., Arkin, A.P., and Stahl, D.A. (2013) Variation among Desulfovibrio Species in Electron Transfer Systems Used for Syntrophic Growth. *J Bacteriol* **195**: 990-1004.

Noguera, Brusseau, Rittmann, and Stahl (1998) A unified model describing the role of hydrogen in the growth of desulfovibrio vulgaris under different environmental conditions. *Biotechnology and bioengineering* **59**: 732-746.

Peck, H.D., LeGall, J., Lespinat, P.A., Berlier, Y., and Fauque, G. (1987) A direct demonstration of hydrogen cycling by< i> Desulfovibrio vulgaris</i> employing membrane-inlet mass spectrometry. *Fems Microbiology Letters* **40**: 295-299.

Pereira, I.A., Ramos, A.R., Grein, F., Marques, M.C., da Silva, S.M., and Venceslau, S.S. (2011) A comparative genomic analysis of energy metabolism in sulfate reducing bacteria and archaea. *Front Microbiol* **2**: 69.

Pereira, P.M., He, Q., Valente, F.M., Xavier, A.V., Zhou, J., Pereira, I.A., and Louro, R.O. (2008) Energy metabolism in Desulfovibrio vulgaris Hildenborough: insights from transcriptome analysis. *Antonie Van Leeuwenhoek* **93**: 347-362.

Plugge, C.M., Scholten, J.C., Culley, D.E., Nie, L., Brockman, F.J., and Zhang, W. (2010) Global transcriptomics analysis of the Desulfovibrio vulgaris change from syntrophic growth with Methanosarcina barkeri to sulfidogenic metabolism. *Microbiology* **156**: 2746-2756.

Ramos, A.R., Keller, K.L., Wall, J.D., and Pereira, I.A. (2012) The Membrane QmoABC Complex Interacts Directly with the Dissimilatory Adenosine 5'-Phosphosulfate Reductase in Sulfate Reducing Bacteria. *Front Microbiol* **3**: 137.

Varela-Raposo, A., Pimentel, C., Morais-Silva, F., Rezende, A., Ruiz, J.C., and Rodrigues-Pousada, C. (2013) Role of NorR-like transcriptional regulators under nitrosative stress of the delta-proteobacterium, Desulfovibrio gigas. *Biochem Biophys Res Commun* **431**: 590-596.

Venceslau, S.S., Lino, R.R., and Pereira, I.A. (2010) The Qrc membrane complex, related to the alternative complex III, is a menaquinone reductase involved in sulfate respiration. *Journal of Biological Chemistry* **285**: 22774-22783.

Walker, C.B., He, Z.L., Yang, Z.K., Ringbauer, J.A., He, Q., Zhou, J.H. *et al*. (2009) The Electron Transfer System of Syntrophically Grown Desulfovibrio vulgaris. *Journal of Bacteriology* **191**: 5793-5801.

Zaunmuller, T., Kelly, D.J., Glockner, F.O., and Unden, G. (2006) Succinate dehydrogenase functioning by a reverse redox loop mechanism and fumarate reductase in sulphate-reducing bacteria. *Microbiology* **152**: 2443-2453.

Appendix

Supplemental material Chapter 1

General genome information and table of identified genes in the *D. gigas* genome.

GENERAL GENOME INFORMATION

CENTRAL METABOLISM

GENERAL METABOLISM

ENERGY CONSERVATION

MISCELLANEOUS

GENERAL GENOME INFORMATION

Table S0. Number of coding regions (CDS´s) associated with the general COG functions

Code	Value	Description
		Information Storage and Processing
K	86	Transcription
J	148	Translation, ribosomal structure and biogenesis
L	104	Replication, recombination and repair
B	1	Chromatin structure and dynamics
		Metabolism
C	184	Energy producing and conversion
F	55	Nucleotide transport and metabolism
H	97	Coenzyme transport and metabolism
Q	24	Secondary metabolites biosynthesis, transport and catabolism
I	36	Lipid transport and metabolism
P	112	Inorganic ion transport and metabolism
G	103	Carbohydrate transport and metabolism
E	208	Amino acid transport and metabolism
		Cellular processes and Signaling
U	23	Intracellular trafficking, secretion and vesicular transport
M	143	Cell wall/membrane/envelope biogenesis
V	37	Defense mechanisms
T	263	Signal transduction mechanisms
N	131	Cell motility
O	91	Posttranslational modification, protein turnover, chaperones
D	32	Cell cycle control, cell division, chromosome partitioning
		Poorly characterized
S	150	Function unknown
R	245	General function predicted only
-	999	No function

CENTRAL METABOLISM

Table S1. Alcohol metabolism

Encoded Protein	*D.gigas* ID	# AA	Gene symbol
Iron-containing Alcohol Dehydrogenase	0712	400	
Iron-containing Alcohol Dehydrogenase	1044	380	
Iron-containing Alcohol Dehydrogenase	1047	393	
Zinc-containing Alcohol Dehydrogenase	2585	323	
Zinc-containing Alcohol Dehydrogenase	3525	425	
Aldehyde Dehydrogenase	0746	477	ald

Table S2. ATP synthesis

Encoded Protein	*D.gigas* ID	# AA	Gene symbol
ATP synthase F0F1 subunit epsilon	0648	133	atpC
ATP synthase F1, beta subunit	0649	471	atpD
F0F1 ATP synthase subunit gamma	0650	293	atpG
F0F1 ATP synthase subunit alpha	0651	502	atpA
ATP synthase F0F1 subunit delta	0652	183	atpH
H+transporting two-sector ATPase subunit B/B'	0653	189	atpF
H+transporting two-sector ATPase subunit B/B'	0654	138	atpF1
ATP synthase protein I	1499	248	atpI
ATP synthase I	1500	156	uncI
ATP synthase F0 subunit alpha	1501	234	atpB
ATP synthase F0, C subunit	1502	110	atpE
V-type ATP synthase subunit K	3061	162	
V-type ATPase 116 kDa subunit	3062	622	
H(+)-transporting ATP synthase, vacuolar type, subunit D	3063	205	

V-type ATP synthase subunit B	3064	430	
V-type ATP synthase subunit A	3065	583	
Two-sector ATPase, V(1) subunit E	3067	214	

Table S3. Beta Oxidation

Encoded Protein	*D.gigas* ID	# AA	Gene symbol
N-acetyltransferase GCN5	2273	161	
Acyl-CoA Dehydrogenase domain-containing protein	1478	689	
Electron-transferring-flavoprotein Dehydrogenase	1479	618	
Electron Transfer Flavoprotein, Beta subunit	1480	268	etfB
Electron Transfer Flavoprotein, Alpha subunit	1481	339	etfA

Table S4. Embden-Meyerhof-Parnas Pathway

Encoded Protein	*D.gigas* ID	# AA	Gene symbol
Enolase (phosphopyruvate hydratase)	0704	441	eno
Fructose-bisphosphate Aldolase	0591	267	fbaB
Putative Phospho-2-dehydro-3-deoxyheptonate Aldolase	0592	267	fbaB2
Fructose-bisphosphate Aldolase	1026	257	fbaB1
Fructose-1,6-bisphosphatase	2524	349	fbp
Type I Glyceraldehyde-3-phosphate Dehydrogenase	2188	333	gap
Glyceraldehyde-3-phosphate Dehydrogenase, type I	2546	338	gap1
Glucokinase	1383	327	gck
Glycogen Phosphorylase	2153	855	glgP
Phosphoglycerate Mutase 1 family	1753	248	gpmA
2,3-Bisphosphoglycerate-independent Phosphoglycerate Mutase	3489	532	gpmB
PEP Synthase	2938	848	

Diphosphate--fructose-6-phosphate 1-Phosphotransferase	2195	456	pfkA
Phosphoglycerate Kinase	1347	391	pgk
Phosphoglucomutase, Alpha-D-glucose Phosphate-specific	0235	549	pgm
PTS System Mannose/fructose/sorbose IID component family protein	3110	462	
Phosphocarrier protein HPr	3111	162	ptsH
Phosphoenolpyruvate-protein Phosphotransferase	3112	594	ptsA
PTS System Sorbose subfamily transporter subunit IIB	2413	156	
PTS System Fructose IIA component family protein	2414	149	
PTS IIA-like Nitrogen-regulatory Protein PtsN	2416	149	ptsN
Pyruvate Kinase	0179	483	pyk
Triose-phosphate Isomerase	0332	249	tpi

Table S5. Entner-Doudoroff Pathway

Encoded Protein	***D.gigas* ID**	**# AA**	**Gene symbol**
Dihydroxy-Acid Dehydratase	0845	555	edd
Glucose-6-phosphate 1-Dehydrogenase	1385	523	zwf
Glucokinase	1383	327	gck

Table S6. Pentose Phosphate Pathway

Encoded Protein	***D.gigas* ID**	**# AA**	**Gene symbol**
Transketolase	1348	666	tkt
Glucose-6-Phosphate Isomerase	2341	552	gpi
Ribulose-Phosphate 3-Epimerase	1351	226	rpe
Translaldolase	2275	220	tal

6-Phosphogluconate Dehydrogenase, Decarboxylating	1384	301	gnd
Glucose-6-Phosphate 1-Dehydrogenase	1385	523	zwf
6-Phosphogluconolactonase	1386	242	pgl
Ribose-5-Phosphate Isomerase A	1387	236	rpi

Table S7. TCA Cycle

Encoded Protein	***D.gigas* ID**	**# AA**	**Gene symbol**
Aconitate Hydratase	0463	651	aco
Fumarate Hydratase	1571	278	fumA
Fe-S Type, Tartrate/fumarate subfamily Hydro-lyase subunit alpha	1573	181	fumC
Citrate Synthase I	1379	436	gltA
Isocitrate Dehydrogenase	1851	382	icd
Malic Protein NAD-binding protein	1574	437	mdh

Table S8. WoodLjungdahl Pathway

Encoded Protein	***D.gigas* ID**	**# AA**	**Gene symbol**
Acyl-CoA Synthetase (NDP forming)	0571	905	acsA
Homocysteine S-Methyltransferase	3461	816	acsE
Aerobic-type Carbon Monoxide Dehydrogenase, small subunit CoxS/CutS-like protein	3143	228	coxS
Aerobic-type Carbon Monoxide Dehydrogenase, large subunit CoxL/CutL-like protein	3144	782	coxL
Aerobic-type Carbon Monoxide Dehydrogenase, middle subunit CoxM/CutM-like protein	3145	325	coxM

Bifunctional 5,10-Methylene-tetrahydrofolate Dehydrogenase/ 5,10-Methylene-tetrahydrofolate Cyclohydrolase	0702	295	folD
5,10-Methylenetetrahydrofolate Reductase	0415	304	metF
Cobalamin B12-Binding domain Protein	2600	229	mtsB

Table S9. Glyoxylate cycle

Encoded Protein	***D.gigas* ID**	**# AA**	**Gene symbol**
Malate Synthase G	2708	725	glcB

Table S10. Oxidation of pyruvate to acetyl-CoA and acetate formation

Encoded Protein	***D.gigas* ID**	**# AA**	**Gene symbol**
Aldehyde Ferredoxin Oxidoreductase	1447	561	
Aldehyde Ferredoxin Oxidoreductase	3127	579	
Ferredoxin I	1020	62	
Ferredoxin II	0418	59	
Conserved hypothetical protein	2139	86	
Ferrodoxin-like protein	0869	81	vorC
2-Ketoisovalerate Ferredoxin Reductase	0870	353	vorA
Thiamine pyrophosphate binding domain-containing protein	0871	270	vorB
2-Oxoacid:ferredoxin Oxidoreductase, gamma subunit	0872	187	vorG
Indolepyruvate Ferredoxin Oxidoreductase	0081	201	
Indolepyruvate Ferredoxin Oxidoreductase subunit alpha	0082	632	iorA
Pyruvate-Ferredoxin Oxidoreductase	0996	1213	poR
Pyruvate Ferredoxin/Flavodoxin Oxidoreductase subunit beta	1712	283	porB

Pyruvate Flavodoxin/Ferredoxin Oxidoreductase domain protein	1713	563	porA
Biotin/Acetyl-CoA-Carboxylase Ligase	3401	326	pycA
Pyruvate Carboxylase	3402	1268	pycB
Pyruvate, water Dikinase., Phosphoenolpyruvate--protein Phosphotransferase	2250	1208	ppdk
Pyruvate, water Dikinase	3042	883	
Phosphoenolpyruvate Synthase/Pyruvate Phosphate Dikinase	3046	882	
Pyruvate, water Dikinase	2942	841	

Table S11. Lactate Metabolism

Encoded Protein	***D.gigas* ID**	**# AA**	**Gene symbol**
D-Lactate Dehydrogenase	1422	460	ldh
Glycolate Oxidase subunit GlcD	3110	462	
FMN-dependent Alpha-hydroxy Acid Dehydrogenase	1415	345	
Conserved hypothetical protein	1416	721	
Lactate Utilization Protein B/C	1417	208	
Putative L-Lactate Transport	1423	566	

Table S12. Beta-Lactamase proteins

Encoded Protein	***D.gigas* ID**	**# AA**	**Gene symbol**
Beta-Lactamase Domain-containing Protein	0607	242	
Beta-Lactamase Domain-containing Protein	0057	273	
Metallo-beta-lactamase	0043	546	ysh1
Beta-Lactamase	1117	405	ampC
Beta-Lactamase Domain-containing Protein	1546	252	

Beta-Lactamase	1809	241
Beta-Lactamase, class D	2558	266
Beta-Lactamase Domain-containing Protein	2610	281

Table S13. Formate Metabolism

Encoded Protein	*D.gigas* ID	# AA	Gene symbol
Chain B, Tungsten Containing Formate Dehydrogenase	1364	245	fdhB
Chain A, Tungsten Containing Formate Dehydrogenase	1366	1012	fdh A
Formate Dehydrogenase, alpha subunit	3334	1009	fdnG
Putative Fe-S-cluster-containing Hydrogenase component protein	3335	247	
Formate Dehydrogenase accessory protein	0759	315	fdhE
Formate Dehydrogenase subunit FdhD	0760	236	fdhD
Putative Formate Dehydrogenase, formation protein FdhE1	3336	303	fdhEI

Table S14. Fumarate Metabolism

Encoded Protein	*D.gigas* ID	# AA	Gene symbol
Fumarate Reductase Respiratory Complex	1568	218	fdrC
Fumarate Reductase, Flavoprotein subunit	1569	627	fdrA
Fumarate Reductase, Iron-sulfur subunit	1570	264	fdrB
Fumarate reductase Respiratory Complex, transmembrane subunit	0826	224	fdrCII
Fumarate Reductase, Flavoprotein subunit	0827	615	fdrAII
Fumarate Reductase, Iron-sulfur subunit	0828	255	fdrBII

Table S15. Methylglyoxal pathway

Encoded Protein	*D.gigas* ID	# AA	Gene symbol
putative Glyoxalase/bleomycin resistance protein/dioxygenase	0382	131	
lactoylglutathione lyase	2156	147	
carbamoyl-phosphate synthase large subunit	0189	1082	

GENERAL METABOLISM

Table S16. Sulfate metabolism

Encoded Protein	*D.gigas* ID	# AA	Gene symbol
Adenylylsulfate Reductase, subunit B	0458	167	aprB
Adenylylsulfate Reductase, subunit A	0457	666	aprA
Adenylylsulfate Kinase	1831	196	cycC
Desulforedoxin	3485	37	dsr
Cobyrinic Acid A,C-diamide Synthase	0687	487	
Dissimilatory Sulfite Reductase B	0688	75	dsrD
Dissimilatory Sulfite Reductase I (Dsri), subunit B	0689	386	dsrB
Dissimilatory Sulfite Reductase I (Dsri) subunit A	0691	437	dsrA
Dissimilatory Sulfite Reductase, gamma subunit	1681	105	dsrC
DsrE family protein	1238	118	
Nitrite and Sulfite Reductase, 4Fe-4S region	3367	217	
DsrE family protein	3368	106	
Phosphoadenosine Phosphosulfate Reductase	3007	273	paps
Sulfate Adenylyltransferase	0460	426	sat
DnaJ-like Protein	0854	132	
Protein of unknown function	0855	211	

Mammalian cell entry domain-containing protein	0856	310	
Sulfate-transporting ATPase	0857	259	
Protein of unknown function	0858	250	
Putative Sulfate Transport Protein CysZ	0923	214	
Putative Sulfate Transport Protein CysZ	2397	205	
Sulfate Permease family Protein	0373	561	sulP

Table S17. Nitrogen metabolism

Encoded Protein	***D.gigas* ID**	**# AA**	**Gene symbol**
Putative Nitrogenase Cofactor Biosynthesis Protein NifB	1271	423	
Putative Nitrogenase	1272	471	
Putative Nitrogenase MoFe Cofactor Biosynthesis Protein	1273	475	
Putative Nitrogenase Cofactor Biosynthesis Protein NifB	1275	403	
Putative Nitrogenase Molybdenum-iron Protein, beta chain	1276	461	
Putative Nitrogenase Molybdenum-iron Protein, subunit alpha	1277	555	
Putative Nitrogen Regulatory Protein P-II	1278	126	
Putative Nitrogen Regulatory Protein P-II	1279	118	
Nitrogenase Reductase	1280	274	nifH
Putative Nitrogen Regulatory Protein P-II	2553	112	glnB-1
Putative Ammonium Transporter	2554	402	amt
Putative Nitrate Reductase	0241	698	
Putative Nitrate Reductase	1101	640	
Putative Nitrate Reductase	1195	705	
Putative Transcriptional Regulator, NifA, Fis Family	1208	515	norR2L
Putative Fis family NifA subfamily Transcriptional Regulator	0080	525	norR1L
Putative Cytochrome c Nitrite Reductase, small subunit	1513	143	nrfH

Putative Nitrite Reductase	1514	488	nrfA
Putative Hydroxylamine Reductase	1496	545	
Putative cAMP-binding protein	1495	224	
Putative Nitroreductase	0813	174	
Putative Nitroreductase	1466	305	
Putative Nitroreductase	2864	169	
Putative Carbamoyl-phosphate Synthase, large subunit	0189	1082	
Putative Carbamoyl-phosphate Synthase, small subunit	0743	383	carA
Putative Ornithine Carbamoyltransferase	2162	301	argF
Putative Argininosuccinate Synthase	2161	403	argG
Putative Argininosuccinate Lyase	2160	462	
Putative Glutamate Synthase	2742	507	
Putative Glutamate Synthase (NADPH), homotetrameric	1689	481	nfnB
Putative Glutamine Synthetase, type I	1150	448	

Table S18. Transcriptional factors Sigma 54

Encoded Protein	***D.gigas* ID**	**# AA**	**Gene symbol**
Putative Sigma-54 dependent Transcriptional Regulator/Response Regulator	0875	458	
Putative two component, Sigma54 specific, Transcriptional Regulator, Fis family	0999	478	
Putative Fis family two component, Sigma-54 specific, Transcriptional Regulator	1046	453	
Putative two component, Sigma54 specific, Fis family Transcriptional Regulator	1069	486	
Putative Sigma-54 Factor Interaction domain-containing Protein	1255	468	
Putative two component, Sigma54 specific, Transcriptional Regulator	1424	507	

Putative Fis family Sigma-54 specific Transcriptional Activator	1482	338
Putative two component Sigma-54 specific Transcriptional Regulator	1580	470
Putative Fis family two component Sigma-54 specific Transcriptional Regulator	1653	473
Putative Fis family two component Sigma-54 specific Transcriptional Regulator	1941	479
Putative ECF subfamily RNA Polymerase Sigma-24 subunit	2673	202
Putative Sigma 54 interacting domain Protein	3035	844
Putative PAS modulated Sigma54 specific Transcriptional Regulator, Fis family	1702	441

Table S19. Response to oxygen

Encoded Protein	***D.gigas* ID**	**# AA**	**Gene symbol**
Superoxide reductase	1536	244	
Neelaredoxin, superoxide reductase	3082	130	nlr
Catalase	2858	502	cat
Bacterioferritin		177	bfr
Rubredoxin-like protein	1167	71	rub2
Chain A, Chain B, Rubredoxin-oxygen Oxidoreductase	1622	402	roo
Chain A rubredoxin	1624	52	rd
Cytochrome bd Quinol Oxidase, subunit I	1252	443	cydA
Cytochrome bd Quinol Oxidase, subunit II	1253	336	cydB
Desulforedoxin	3485	37	dsr
Peroxiredoxin	3518	222	prxU
Rubrerythrin	0750	165	rbr
Rubrerythrin	1055	156	rbr
Rubrerythrin	1714	162	

Coenzyme F390 synthetase	2876	421	
Coenzyme F390 synthetase	3140	441	
Coenzyme F390 synthetase-like	0910	433	

ENERGY CONSERVATION

Table S20. Membranar Energy Complexes

Encoded Protein	*D.gigas* ID	# AA	Gene symbol
Hdr-like Menaquinol Oxidoreductase Cytochrome b-like subunit	2334	338	dsrM
Cytoplasmic, binds 2 (4Fe-4S)	2335	542	dsrK
Periplasmic (Sec) Triheme Cytochrome c	2336	127	dsrJ
Periplasmic (Tat), binds 2(4Fe-4S)	2337	268	dsrO
Polysulphide Reductase NrfD	2338	386	dsrP
Sixteen Heme Cytochrome	0715	559	hmcA
4Fe-4S Ferredoxin	0716	364	hmcB
HMC redox complex, integral membrane protein HmcC	0717	416	hmcC
protein HmcD	0718	48	hmcD
HMC redox complex, integral membrane protein HmcE	0719	225	hmcE
protein HmcF	0720	470	hmcF
NAD(P)H-quinone Oxidoreductase subunit 3	0242	125	nuoA
NADH-quinone Oxidoreductase subunit B	0243	192	nuoB
NADH:ubiquinone Oxidoreductase 27 kD subunit	0244	568	nuoC/D
NADH Dehydrogenase (quinone)	0245	328	nuoH
NADH:ubiquinone Oxidoreductase chain I-like protein	0246	218	nuoI
NADH-ubiquinone/plastoquinone Oxidoreductase chain 6	0247	172	nuoJ
NADH-quinone Oxidoreductase subunit K 1	0248	113	nuoK
NADH/Ubiquinone/plastoquinone (Complex I)	0249	492	nuoL
hypothetical protein B193_0141	0250	90	
Monovalent cation/H+ Antiporter subunit D	0251	613	nuoN

Proton-translocating NADH-quinone Oxidoreductase subunit M	0253	521	nuoM
NADH Dehydrogenase (quinone)	0254	475	
4Fe-4S Ferredoxin	0255	169	
Permease	0256	378	nuoP
Conserved hypothetical protein	0257	219	
Multicomponent Na+/H+ Antiporter subunit E	2843	164	mnhE
Multiple Resistance and pH Regulation protein F	2844	100	mnhF
Multicomponent Na+/H+ Antiporter subunit G	2845	122	mnhG
Conserved hypothetical protein	2846	81	
Putative Monovalent cation/H+ Antiporter subunit B	0247	266	mnhB
Na(+)/H(+) Anitporter subunit MhnC	0248	129	mnhC
NADH/ubiquinone/plastoquinone	2849	465	
NADH Dehydrogenase (quinone)	2850	513	mnhA
Conserved hypothetical protein	2851	81	
Putative Monovalent cation/H+ Antiporter subunit D	2852	598	mnhD
Crp family Transcriptional Regulator	2853	164	
Hydrogenase, b-type Cytochrome subunit	0374	202	ohcC
Cytochrome c family protein	0375	545	ohcA
Iron-sulfur Cluster-binding Protein	0376	157	
4Fe-4S Ferredoxin	0377	323	ohcB
QmoD protein	0453	246	qmoD
Heterodisulfide Reductase	0454	393	qmoC
Quinone-interacting Membrane-bound Oxidoreductase	0455	768	qmoB
Heterodisulfide Reductase	0456	411	qmoA
Quinone-interacting Membrane-bound Oxidoreductase complex subunit C	2765	402	
Conserved hypothetical protein	2766	228	
Polysulfide Reductase NrfD	0130	411	qrcD
Molybdopterin Oxidoreductase, Iron-sulfur Cluster-binding subunit	0131	266	qrcC
Molybdopterin Oxidoreductase	0132	693	qrcB

Cytochrome C	0133	212	qrcA
CheY-like receiver, AAA-type ATPase, and DNA-binding domain containing response regulator	1424	507	
ApbE family Lipoprotein	1425	344	rnfF
4Fe-4S Ferredoxin	1426	293	rnfB
RnfABCDGE type electron transport complex subunit A	1427	191	rnfA
RnfABCDGE type electron transport complex subunit E	1428	239	rnfE
RnfABCDGE type electron transport complex subunit G	1429	193	rnfG
RnfABCDGE type electron transport complex subunit D	1430	318	rnfD
4Fe-4S Ferredoxin	1431	398	rnfC
Cytochrome c family protein	1432	245	
Transmembrane complex, Tetraheme Cytochrome c3	1698	137	tmcA
Iron-sulfur binding Protein	1699	444	tmcB
Conserved hypothetical protein	1700	219	tmcC
TmC complex protein, subunit D	1701	419	tmcD

Table S21. Hydrogenases

Encoded Protein	**D.gigas ID**	**# AA**	**Gene symbol**
hynD	2259	82	hynD
hynC	2260	165	hynC
hynB	2261	551	hynB
hynA	2262	288	hynA
echA	0034	647	echA
echB	0035	284	echB
echC	0036	147	echC
echD	0037	125	echD
echE	0038	358	echE
echF	0039	123	echF
(NiFe) Hydrogenase maturation protein HypF	0896	818	hypF
Hydrogenase expression/formation protein HypD	1098	372	hypD

Hydrogenase expression/formation protein HypE	1099	340	hypE
Hydrogenase accessory protein HypB	2238	219	hypB
HypA	2239	121	hypA

Table S22. Cytochromes

Encoded Protein	***D.gigas* ID**	**# AA**	**Gene symbol**
Cytochrome bd Quinol Oxidase subunit I	1252	443	cydA
Cytochrome bd Quinol Oxidase subunit II	1253	336	cydB
Cytochrome c class III	0326	133	
Cytochrome c3	0144	137	cyc
Di-Tetraheme Cytochrome C3	1464	112	
Cytochrome c554	0380	157	
Respiratory Nitrite Reductase specific menaquinol--cytochrome-c reductase (NrfH) precursor	1513	143	nrfH
Nitrite Reductase (cytochrome, ammonia-forming)	1514	488	nrfA
Conserved protein of unknown function	2209	47	
Cytochrome c assembly protein	2210	225	ccmC
ccmB family protein	2211	224	ccmB
Heme exporter protein CcmA	2212	226	ccmA
Cytochrome C assembly protein	2213	635	ccmF
Conserved hypothetical protein	2214	458	
Cytochrome c-type biogenesis protein CcmE	2216	140	ccmE
Protein of unknown function	2217	360	

Table S23. Hdr-like proteins

Encoded Protein	***D.gigas* ID**	**# AA**	**Gene symbol**
Heterodisulfide Reductase subunit C	1048	197	hdrC

CoB--CoM Heterodisulfide Reductase	1049	299	hdrB
Heterodisulfide Reductase, subunit A	1050	669	hdrA
Methyl-viologen-reducing Hydrogenase delta subunit	1051	149	floxD
Coenzyme F420 Hydrogenase/Dehydrogenase, beta subunit	1052	321	floxC
Hydrogenase, putative	1053	403	floxB
Dihydroorotate Dehydrogenase, electron transfer subunit protein	1054	277	floxA
FAD linked Oxidase domain-containing Protein	1343	1199	hdrD
Iron-sulfur cluster-binding protein	1416	721	
Iron-sulfur cluster-binding protein	1421	426	
Fe-S Oxidoreductase	3109	379	
Aldehyde Dehydrogenase, iron-sulfur subunit	0904	762	

Table S24. Nfn complex

Encoded Protein	***D.gigas* ID**	**# AA**	**Gene symbol**
FAD-dependent Pyridine Nucleotide-disulfide Oxidoreductase	1688	458	
Oxidoreductase	1689	481	nfnB
Ferredoxin-NADP(+) Reductase subunit alpha	1690	282	nfnA
Oxidoreductase	1577	475	
Ferredoxin-NADP Reductase	1578	261	

MISCELLANEOUS

Table S25. Selenocysteine-containing proteins

Encoded Protein	***D.gigas* ID**	**# AA**	**Gene symbol**
Selenocysteine-specific Translation Elongation Factor	1858	643	selB

L-seryl-tRNA Selenium Transferase	1861	470	selA
Conserved hypothetical protein	2096	106	
HesB-like domain-containing protein	2358	106	hesB
Selenide, water Dikinase	2804	325	selD
DsrE family protein	3368	106	
Cysteine Desulfurase / Selenocystein Lyase	2344	383	csdA
Selenium metabolism protein YedF	2272	215	yedF
Chain A, Tungsten Containing Formate Dehydrogenase	1366	1012	fdh IB

Table S26. CRISPR- associated proteins

Encoded Protein	***D.gigas* ID**	**# AA**	**Gene symbol**
CRISPR-associated Protein Cas1, YPEST subtype	1866	326	cas1
CRISPR-associated Helicase Cas3 family	1867	1109	cas3
CRISPR-associated Protein, Csy1 family	1868	443	csy1
CRISPR-associated Protein, Csy2 family	1869	309	csy2
CRISPR-associated Protein, Csy3 family	1870	345	csy3
CRISPR-associated Protein, Csy4 family	1871	186	csy4
Conserved hypothetical protein	2447	337	
CRISPR-associated Helicase	2448	982	cas3
CRISPR-associated Protein	2449	475	csb2
CRISPR-associated Protein	2450	404	csb1

Table S27. Chemotaxis proteins

Encoded Protein	***D.gigas* ID**	**# AA**	**Gene symbol**
CheB	0024	374	cheB
Hypothetical protein	0023	648	
CheR	0022	291	cheR

ParA family protein	0021	261	parA
CheW	0020	244	cheW
CheY	0019	372	cheY
CheA	0018	974	cheA
Putative methyl-accepting chemotaxis protein	3081	607	mcp
Chemotaxis protein CheW	3080	174	cheW
Superoxide dismutase	3082	130	nlr
Chemotaxis protein CheW	3083	168	cheW
Methyl-accepting chemotaxis protein	3084	649	mcp
Anti-sigma-factor antagonist	3079	102	
CheA signal transduction histidine kinase	3078	700	
Methyl-accepting chemotaxis protein	0120	599	
Methyl-accepting chemotaxis sensory transducer with Pas/Pac sensor	0338		
Methyl-accepting chemotaxis sensory transducer protein	0381	672	
Methyl-accepting chemotaxis protein	0398	676	
CheW protein	0399	162	
Hypothetical protein	0400	93	
Chemotaxis protein CheA	0401	691	
Methyl-accepting chemotaxis protein	0422	683	
CheW protein	0423	162	
Methyl-accepting chemotaxis sensory transducer	0498	710	
Methyl-accepting chemotaxis sensory transducer	0662	572	
Methyl-accepting chemotaxis protein	0682		
Response regulator receiver protein	0820	130	cheY
CheC, inhibitor of MCP methylation	0821	218	cheC
Chemotaxis protein CheA	0822	101	
Methyl-accepting chemotaxis sensory transducer with Pas/Pac sensor	0980	782	
Chemotaxis sensory transducer protein	0986	813	
Chemotaxis protein	1143	157	
Methyl-accepting chemotaxis sensory transducer	1240	604	

Chemotaxis sensory transducer protein	1382	779
Methyl-accepting chemotaxis protein	1490	600
Methyl-accepting chemotaxis protein	1602	544
Chemotaxis protein CheW	1665	158
Methyl-accepting chemotaxis sensory transducer with Cache sensor	1693	725
CheW protein	1942	166
CheR-type MCP methyltransferase	1943	477
Chemotaxis protein CheW	1944	212
Methyl-accepting chemotaxis sensory transducer	1945	583
CheA signal transduction histidine kinase	1946	776
Response regulator receiver modulated CheB methylesterase	1947	380
Multi-sensor hybrid histidine kinase	1948	1042
Anti-sigma-factor antagonist	1949	103
CheD family protein	1950	163
Methyl-accepting chemotaxis sensory transducer	2220	721
Methyl-accepting chemotaxis sensory transducer with Cache sensor	2263	572
Multi-sensor hybrid histidine kinase	2603	1195
CheW protein	2604	158
Methyl-accepting chemotaxis sensory transducer	2605	596
Hypotetical protein	2606	90
CheD-like chemotaxis protein	2639	160
Methyl-accepting chemotaxis sensory transducer	2675	679
Methyl-accepting chemotaxis sensory transducer	2707	583
Methyl-accepting chemotaxis protein	2714	576
Methyl-accepting chemotaxis sensory transducer	2743	676
Chemotaxis protei	2780	248
Methyl-accepting chemotaxis sensory transducer with Cache/Pas/Pac sensor	2999	
Chemotaxis protein	3056	167

Response regulator receiver protein	3057	156	
Methyl-accepting chemotaxis sensory transducer	3240	459	
Chemotaxis protein histidine kinase CheA	3241	701	cheA
Alkaline phosphatase synthesis transcriptional regulatory protei	3242	121	
Conserved hypothetical protein	3243	100	
Conserved hypothetical protein	3244	493	
Chemotaxis protein CheA	3245	696	
Response regulator receiver protein	3246	121	
Chemotaxis protein methyltransferase CheR	3247	283	
Conserved hypothetical protein	3248	220	
Chemotaxis-specific methylesterase CheB	3249	359	
Chemoreceptor glutamine deamidase CheD	3250	163	
CheW protein	3251	546	
Methyl-accepting chemotaxis protein	3252	650	
Response regulator receiver domain protein	3253	129	
Methyl-accepting chemotaxis protein	3422	879	
Response regulator with CheY-like receiver, AAA-type ATPase, and DNA-binding domains	3423	123	
Chemotaxis sensory transducer	3467	604	
Response regulator receiver protein	3468	120	
CheA signal transduction histidine kinase	3469	710	
Chemotaxis protein methyltransferase	3470	281	
Response regulator receiver modulated CheB methylesterase	3471	360	

Published papers related with this dissertation

Journal of Bacteriology

Roles of HynAB and Ech, the Only Two Hydrogenases Found in the Model Sulfate Reducer *Desulfovibrio gigas*

Fabio O. Morais-Silva, Catia I. Santos, Rute Rodrigues, Inês A. C. Pereira and Claudina Rodrigues-Pousada

J. Bacteriol. **2013, 195(20):4753. DOI: 10.1128/JB.00411-13.**
Published Ahead of Print 23 August 2013.

JB
Journals.ASM.org

Roles of HynAB and Ech, the Only Two Hydrogenases Found in the Model Sulfate Reducer *Desulfovibrio gigas*

Fabio O. Morais-Silva, Catia I. Santos, Rute Rodrigues, Inês A. C. Pereira, Claudina Rodrigues-Pousada

Instituto de Tecnologia Química e Biológica—António Xavier, Universidade Nova de Lisboa, Oeiras, Portugal

Sulfate-reducing bacteria are characterized by a high number of hydrogenases, which have been proposed to contribute to the overall energy metabolism of the cell, but exactly in what role is not clear. *Desulfovibrio* spp. can produce or consume H_2 when growing on organic or inorganic substrates in the presence or absence of sulfate. Because of the presence of only two hydrogenases encoded in its genome, the periplasmic HynAB and cytoplasmic Ech hydrogenases, *Desulfovibrio gigas* is an excellent model organism for investigation of the specific function of each of these enzymes during growth. In this study, we analyzed the physiological response to the deletion of the genes that encode the two hydrogenases in *D. gigas*, through the generation of Δ*echBC* and Δ*hynAB* single mutant strains. These strains were analyzed for the ability to grow on different substrates, such as lactate, pyruvate, and hydrogen, under respiratory and fermentative conditions. Furthermore, the expression of both hydrogenase genes in the three strains studied was assessed through quantitative reverse transcription-PCR. The results demonstrate that neither hydrogenase is essential for growth on lactate-sulfate, indicating that hydrogen cycling is not indispensable. In addition, the periplasmic HynAB enzyme has a bifunctional activity and is required for growth on H_2 or by fermentation of pyruvate. Therefore, this enzyme seems to play a dominant role in *D. gigas* hydrogen metabolism.

Hydrogenases are key enzymes in the hydrogen metabolism of *Desulfovibrio* spp. that catalyze the reversible oxidation of molecular hydrogen into protons and electrons (1). However, their role during sulfate respiration has not been clearly established. Odom and Peck proposed a hydrogen cycling model to explain energy conservation during growth on lactate and sulfate by *Desulfovibrio* spp., which belong to the deltaproteobacteria subgroup of the sulfate-reducing bacteria (SRB) (2). The model predicts that protons and electrons produced in the oxidation of lactate are used for the production of molecular hydrogen by a cytoplasmic hydrogenase. This hydrogen then diffuses across the membrane to the periplasm, where it is reoxidized by a periplasmic hydrogenase. Electrons are transferred back to the cytoplasm for sulfate reduction, thus creating a proton gradient across the membrane that leads to ATP formation. In this model, the presence of at least two hydrogenases on opposite sides of the membrane is a requirement for growth. In contrast, other studies suggested that the physiological role of these enzymes was to regulate the redox potential of the cell, controlling the flow of protons and electrons and generating a proton motive force (3). More recent models, proposed for *Desulfovibrio vulgaris*, suggested dual pathways for electron transfer from lactate to sulfate, one involving the cycling of H_2 and the other a route involving a membrane-associated electron transfer chain (4, 5). Several membrane complexes have been identified in SRB that could be involved in this process (reviewed in reference 6). It has been estimated that about 48% of the electrons transported from lactate to sulfate involve H_2 production (4).

Several studies have tried to elucidate the function of hydrogenases in *Desulfovibrio* spp., but because most of these organisms present a multiplicity of hydrogenases, in the periplasm and/or in the cytoplasm, identification of the role of each enzyme is complex. In addition, the expression patterns of different hydrogenases were shown to be different and to depend on the substrate, fermentative or respiratory growth, or metal availability (5, 7–13). Furthermore, the function of each hydrogenase in terms of hydrogen production or oxidation may vary depending on the conditions presented to the cell. Numerous studies have reported hydrogenase mutant strains of *Desulfovibrio fructosovorans* and in *D. vulgaris* Hildenborough (9, 14–17). However, in most cases, because of the multiplicity of enzymes present, these studies were not conclusive. This indicates that each hydrogenase may contribute to the overall energy metabolism of the cell and that the loss of one enzyme might be compensated for by the presence of the remaining ones. In spite of the extensive work performed with hydrogenase deletion strains and also transcriptomic analyses, the results obtained so far have not permitted a complete elucidation of the function and importance of each hydrogenase under different growth conditions.

Desulfovibrio gigas is an excellent biological model for investigation of the function and importance of hydrogenases in energy metabolism, since its genome, recently sequenced in our laboratory, encodes only two hydrogenases, the HynAB and Ech enzymes. Furthermore, because each hydrogenase is located in a different cell compartment, *D. gigas* is also an excellent model for the study of the importance of hydrogen cycling in energy conservation. The *D. gigas* periplasmic HynAB enzyme is one of the most extensively studied enzymes of the [NiFe] type and was the first [NiFe] hydrogenase to have its crystal structure solved (18). In *Desulfovibrio* spp., as in other bacteria, the periplasmic hydrogenases are believed to be involved in the consumption of hydrogen,

Received 9 April 2013 **Accepted** 5 August 2013
Published ahead of print 23 August 2013
Address correspondence to Claudina Rodrigues-Pousada, claudina@itqb.unl.pt, or Inês A. Cardoso Pereira, ipereira@itqb.unl.pt.
Supplemental material for this article may be found at http://dx.doi.org/10.1128/JB.00411-13.

doi:10.1128/JB.00411-13

coming either from the environment or from intracellular H_2 cycling, generating protons and electrons. The electrons are then shuttled to the cytoplasm through the type I cytochrome c_3 and the Qrc and Qmo complexes (19–21) to be used for sulfate reduction.

The *D. gigas* cytoplasmic Ech hydrogenase (22) belongs to the subgroup of multisubunit membrane-bound energy-conserving [NiFe] hydrogenases (23, 24), similar to the Ech hydrogenase from *Methanosarcina barkeri* (25, 26). These enzymes have subunits that show high similarity to energy-conserving complex I (NADH:quinone oxidoreductase). The Ech hydrogenase in methanogenic archaea can catalyze H_2 formation from reduced ferredoxin, generating a proton motive force, or the reduction of ferredoxin by H_2, driven by reverse electron transport (26–29). However, the function of the Ech hydrogenase in *Desulfovibrio* spp. is still not clear.

To elucidate the function of each of these two hydrogenases in *D. gigas* metabolism, we have generated single deletion (Δ*echBC* and Δ*hynAB*) mutants. These strains were tested under respiratory versus fermentative conditions with different energy sources (lactate, pyruvate, and H_2), and their hydrogenase expression profiles were studied at the mRNA level.

MATERIALS AND METHODS

Generation of mutants. To construct the mutant strains, recombinant cassettes containing the DNA fragments of the regions flanking the genes of interest were amplified from *D. gigas* wild-type (WT) ATCC 19364. A mutant *D. gigas* strain lacking a functional Ech hydrogenase (Δ*ech*) was produced by replacement of the *echB* (integral membrane subunit) and *echC* (electron transfer subunit) genes with a kanamycin resistance (*kan*) gene amplified from plasmid pJRD215 (27) by homologous recombination (30). Oligonucleotides (*ech*; see Table S1 in the supplemental material) were used to amplify ~1-kb adjacent DNA regions upstream of subunit *echB* (flank I) and downstream of subunit *echC* (flank II), respectively, from a DNA fragment containing the *ech* operon. *Pfx* DNA polymerase (Invitrogen) was used for amplification. The PCR products were ligated with T4 DNA ligase (Fermentas) into plasmid pZErO-1 (Invitrogen), and this construct was transformed in *Escherichia coli* XL-I Blue. Plasmid DNA was extracted with the plasmid purification kit from Eppendorf.

For the *hynAB* gene, a *D. gigas* mutant strain lacking the entire dicistronic operon was produced by replacement with *kan* as in the Δ*ech* mutant. Oligonucleotides (*hynAB*; see Table S1 in the supplemental material) were used to amplify ~1-kb adjacent DNA regions upstream and downstream of the operon directly from WT *D. gigas* genomic DNA (gDNA). *Phusion* high-fidelity DNA polymerase (Thermo Scientific) was used for amplifications. The PCR products were ligated and transformed into the vector YipLac211 according to the In-Fusion HD cloning kit (Clontech) protocol.

Kanamycin-resistant colonies of both constructs were selected, and their plasmids were analyzed by restriction enzyme pattern. These plasmids were used for *D. gigas* transformation.

D. gigas cells to be transformed were prepared as previously described (30) from 500 ml of an early stationary-phase culture. Immediately before transformation, 6 μg of the plasmid construct was mixed with the cells. Transformation was done aerobically in 0.1-cm cuvettes by electroporation in a Bio-Rad Gene Pulser Apparatus, setting the resistance to ∞ and using a 0.7-kV voltage and a 3-μF capacitance.

Immediately after electroporation, cells were inoculated into lactate-sulfate medium at 37°C. After a 5-h recovery period, kanamycin was added to the medium (50 μg/ml) and the cultures were allowed to grow overnight. Cells were then subcultured in lactate-sulfate medium with kanamycin (50 μg/ml) three consecutive times.

Colonies were grown for approximately 15 days to 1 month in medium supplemented with agar (15 g/liter) and kanamycin (50 μg/ml) in Hungate culture tubes by the roll tube technique and/or in plates inside an AnaeroPack Rectangular Jar 7L (Mitsubishi Gas Chemical Company, Inc.) with AnaeroPack System sachets (bioMérieux).

The deletions of the *echBC* and *hynAB* genes from the respective mutant strains were confirmed by PCR and Southern blot analyses (see the supplemental material).

Culture media and growth conditions. *D. gigas* cells were grown anaerobically at 37°C in 100-ml flasks with 50 ml of medium. All media were inoculated with 10% (vol/vol) fresh preculture cells grown in lactate-sulfate medium.

For most phenotypic analyses, WT and mutant strains were grown in basal medium modified from reference 14 and containing (per liter) 1 g NH_4Cl, 0.15 g $CaCl_2 \cdot 2H_2O$, 1 g NaCl, 0.5 g KCl, 0.4 g $MgCl_2 \cdot 7H_2O$, 4.9 g KH_2PO_4, 0.1 g yeast extract, and 1.5 ml of trace elements (31). This medium was then supplemented with either lactate or pyruvate as an electron donor at a concentration of 40 mM. Sulfate was added as an electron acceptor at either 40 or 5 mM or not added. The pH of all solutions was brought to 7.0 with NaOH. The growth conditions tested were lactate and sulfate at 40 and 40 mM, respectively; pyruvate and sulfate at 40 and 40 mM; pyruvate and limiting sulfate at 40 and 5 mM; and pyruvate at 40 mM.

For growth with H_2 as the sole energy source, cells were grown on modified Postgate medium C containing (per liter) 0.82 g sodium acetate, 0.5 g KH_2PO_4, 1 g NH_4Cl, 1.14 g Na_2SO_4, 0.05 g $CaCl_2 \cdot 2H_2O$, 0.5 g $MgSO_4 \cdot 7H_2O$, 0.2 g yeast extract, 0.0071 g $FeSO_4 \cdot 7H_2O$, 0.3 g sodium citrate, 0.1 g ascorbic acid, 0.1 g sodium thioglycolate, 1 μM Ni, 1 μM Se, and 0.1 μM Mo. The cultures were inoculated in 100-ml flasks containing 50 ml of medium and then gassed with H_2-CO_2 (80:20, vol/vol) at a pressure of 1 atm. The cultures were grown with the flasks at 37°C in a horizontal position to enhance the gas-liquid surface area.

Growth of the cultures was monitored by determining the optical density at 600 nm (OD_{600}). Biomass was determined by measuring the dry cell weight (dcw) and correlating it with the OD_{600}. One unit of OD_{600} corresponded to 0.365 g (dcw)/liter.

Analytical procedures. H_2 quantification in the headspace of culture-containing serum bottles was performed by gas chromatography with a Thermo Electron Corporation TRACE GC Ultra gas chromatograph fitted with a Alltech Molecular Sieve 5A 80/100 column. The carrier gas was N_2, and measurements were done at 130°C. Headspace volumes of 30 μl were withdrawn with a gas-tight syringe and injected into the gas chromatograph. The detection limit was 5 nmol of molecular hydrogen. Cultures of WT *D. gigas* and both mutant strains were compared.

Identification and quantification of the organic substrates and products generated during growth were performed by high-performance liquid chromatography (HPLC) analyses with a Waters chromatograph (Waters Chromatography, Milford, MA) consisting of a Waters 510 pump, a Waters 715 Autosampler, and a Waters temperature control module connected to an LKB 2142 Differential Refractometer detector (LKB, Bromma, Sweden). Chromatographic separation was undertaken with an Aminex HPX-87H column (300 by 7.8 mm) with a 9-μm particle size (Bio-Rad, Hercules, CA) at 45°C. Elution was carried out isocratically at a flow rate of 0.6 ml·min^{-1} with 0.005 N H_2SO_4, and the injection volume was 20 μl. The retention times of the compounds were compared with standards for identification, and the peak area was used for quantification.

Sulfate concentration was measured by HPLC analysis (32) and/or by the SulfaVer4 method (Hach-Lange). HPLC analyses were performed with a Hitachi LaChrom Elite HPLC apparatus with a photodiode array detector. Injections of 20 μl were made into a 10-μl loop operated in full-loop mode, and separation was achieved on a PRP-X100 (4.1 by 150 mm) with a 10-μm-particle-size column (Hamilton Company, Reno, NV) and a thermostat set at 25°C. Isocratic conditions of the mobile phase consisted of 3% (vol/vol) methanol and 97% (vol/vol) 4 mM 4-hydroxybenzoic acid (pH adjusted to 10). The flow rate of the eluent was 2 ml

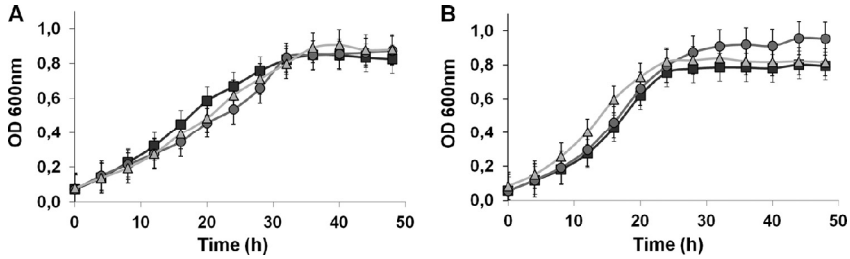

FIG 1 Growth curves of WT *D. gigas* and the Δ*echBC* and Δ*hynAB* mutant strains in medium containing 40 mM lactate and 40 mM sulfate (A) or 40 mM pyruvate and 40 mM sulfate (B). WT, squares; Δ*echBC* mutant, circles; Δ*hynAB* mutant, triangles. Each datum point is the average of three independent growth experiments.

min^{-1}. Indirect UV detection was done at 310 nm. The retention time of the compound was compared with a standard for identification, and the peak area was used for quantification.

RNA preparation and real-time quantitative reverse transcription-PCR (qRT-PCR) analyses. WT *D. gigas* and both mutant strains were grown at 37°C in the same medium composition as described for the growth experiments. Cells were harvested after 16 h (mid-exponential phase) or 32 h (stationary phase) of growth. Total RNA was extracted as described in references 33 and 34. However, DNase treatment with Turbo DNase (Ambion) had to be performed three times to avoid gDNA contamination in the RNA extracts. For each sample, 1 μg of total RNA was reverse transcribed with Transcriptor reverse transcriptase (Roche Diagnostics). Specific primers amplifying an ~100-bp region of *echE* and *hynB* were designed (see Table S2 in the supplemental material). The 16S rRNA gene was used as an internal reference gene for each sample analyzed. qRT-PCRs were performed in a LightCycler 480 real-time PCR system (Roche) with LightCycler Fast Start DNA Master SYBR green I (Roche). Relative standard curves and gene expression were calculated as described in reference 31. For the final results, three biological replicates and two technical replicates were used for each condition.

Nucleotide sequence accession numbers. The NCBI accession number of the *D. gigas* genome sequence described in this work is CP006585. In addition, the accession numbers of the hydrogenases and specific membrane complexes are as follows: *aprAB qmoABCD*, KF113859; *dsrMKJOP*, KF113860; *echABCDEF*, AY282786; *hdrABC floxABCD*, KF113861; *hynAB*, M18083; *qrcABCD*, KF113862.

RESULTS

A search of the *D. gigas* genome sequenced in our laboratory revealed the presence of genes encoding only the two known hydrogenases, the periplasmic HynAB and cytoplasmic Ech hydrogenases. Two mutant strains with these enzymes deleted, the Δ*echBC* and Δ*hynAB* mutant strains, were generated and then tested under different growth conditions. The deletions of *echBC* and *hynAB* were confirmed by both Southern blot and PCR analyses (see Fig. S1 and S2 in the supplemental material).

Mutant phenotype in sulfate respiration. The growth of WT *D. gigas* was compared to the growth of both the Δ*ech* and Δ*hynAB* single mutant strains. In the presence of an excess of sulfate (40 mM) with either lactate (Fig. 1A) or pyruvate (Fig. 1B), both mutant strains reached a final cell density similar to that of the WT. However, the doubling times of the Δ*echBC* mutant strain growing on lactate and the Δ*hynAB* mutant strain growing on pyruvate were higher than those of the WT (Table 1). Also, the cell yield coefficient observed for the Δ*echBC* mutant was higher than that of the WT, especially during growth on pyruvate.

Metabolite quantification (see Table S3 in the supplemental material) revealed that both mutations did not affect substrate consumption or product formation, compared to the WT. The electron acceptor, sulfate, was reduced in agreement with the expected stoichiometries of 2:1 and 4:1, relative to lactate and pyruvate, respectively, and at the same rate by the mutant strains and the WT. No significant amounts of H_2 accumulated during growth whenever sulfate was present. These results indicate that neither of the two hydrogenases is essential for growth under sulfate respiratory conditions with either lactate or pyruvate as the carbon source.

However, with H_2 as the energy source in the presence of sulfate, a different phenotype was observed (Fig. 2). The doubling time of the WT under this respiratory condition was much higher than that seen when an organic acid (lactate or pyruvate) was the energy source (Table 1). Also, the behavior of the mutant strains was quite different. The Δ*echBC* mutant strain reached a final cell density similar to that of the WT and had an even higher doubling time. In contrast, the Δ*hynAB* mutant strain did not grow at all, revealing that, as expected, the periplasmic hydrogenase is essential for growth under these conditions.

Mutant phenotype in sulfate limitation and fermentation. *Desulfovibrio* spp. are unable to grow fermentatively in the presence of lactate, unless H_2 partial pressures are kept low by hydrogenotrophic organisms such as methanogenic archaea. This is due to the fact that oxidation of lactate to pyruvate is an endergonic reaction. However, these bacteria can grow fermentatively with pyruvate. Thus, we evaluated the effect of deleting each hydrogenase under fermentative conditions in pyruvate. The WT and both mutant strains were grown in pyruvate with sulfate limitation (5 mM) or in its absence (Fig. 3A and B, respectively). In the

TABLE 1 Doubling times and cell yield coefficients of WT *D. gigas* and Δ*echBC* and Δ*hynAB* hydrogenase mutant strains during growth under different conditions

Growth condition	Doubling time (h)			Y_S (g [dry wt] cells/mol)		
	WT	Δ*echBC* mutant	Δ*hynAB* mutant	WT	Δ*echBC* mutant	Δ*hynAB* mutant
Lactate-sulfate	8.7	11.1	9.0	6.8	7.2	6.8
Pyruvate-sulfate[a]	6.7	6.7	7.9	6.0	7.3	6.1
Pyruvate-sulfate[b]	6.9	7.1	8.0	5.2	6.3	4.7
Pyruvate	14.2	16.7		4.8	6.7	
H_2-sulfate	33.3	24.1				

[a] Pyruvate-sulfate (40 mM–40 mM).
[b] Pyruvate-limiting sulfate (40 mM–5 mM).

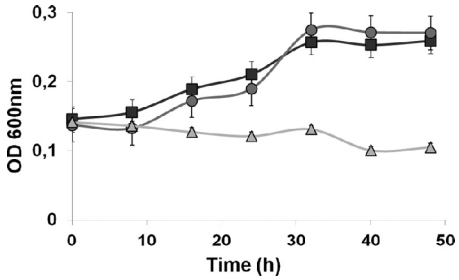

FIG 2 Growth curves of WT *D. gigas* and the Δ*echBC* and Δ*hynAB* mutant strains in H_2-sulfate. Cells were grown on modified medium C containing 10 mM acetate and 20 mM sulfate with a gas phase composed of H_2-CO_2 (80:20, vol/vol) at a pressure of 1 atm. WT, squares; Δ*echBC* mutant, circles; Δ*hynAB* mutant, triangles. Each datum point is the average of three independent growth experiments.

first case, although sulfate was limiting, the growth of the *D. gigas* WT and mutant strains reached cell densities similar to those seen when sulfate was present in excess (Fig. 1), revealing that enough sulfate was present to allow respiratory growth. In agreement with this, the doubling time was similar to pyruvate respiratory conditions and once again the deletion of the *hynAB* genes slowed growth (Table 1). When yield coefficients were compared, a decrease in cell yield was observed for all of the strains under this condition, especially in the case of the Δ*hynAB* mutant, which possibly correlates with the lower sulfate concentration available. Once again, it is noticeable that the absence of the *echBC* genes appears to increase the cell yield of the mutant strain over that of the WT.

Interestingly, after sulfate was completely reduced at 20 to 24 h (Fig. 3A), the cells stopped growing and started to accumulate H_2 (Fig. 3E), and the Δ*echBC* mutant strain, containing only the periplasmic hydrogenase, accumulated much more H_2 than did the WT strain. On the other hand, the Δ*hynAB* mutant strain,

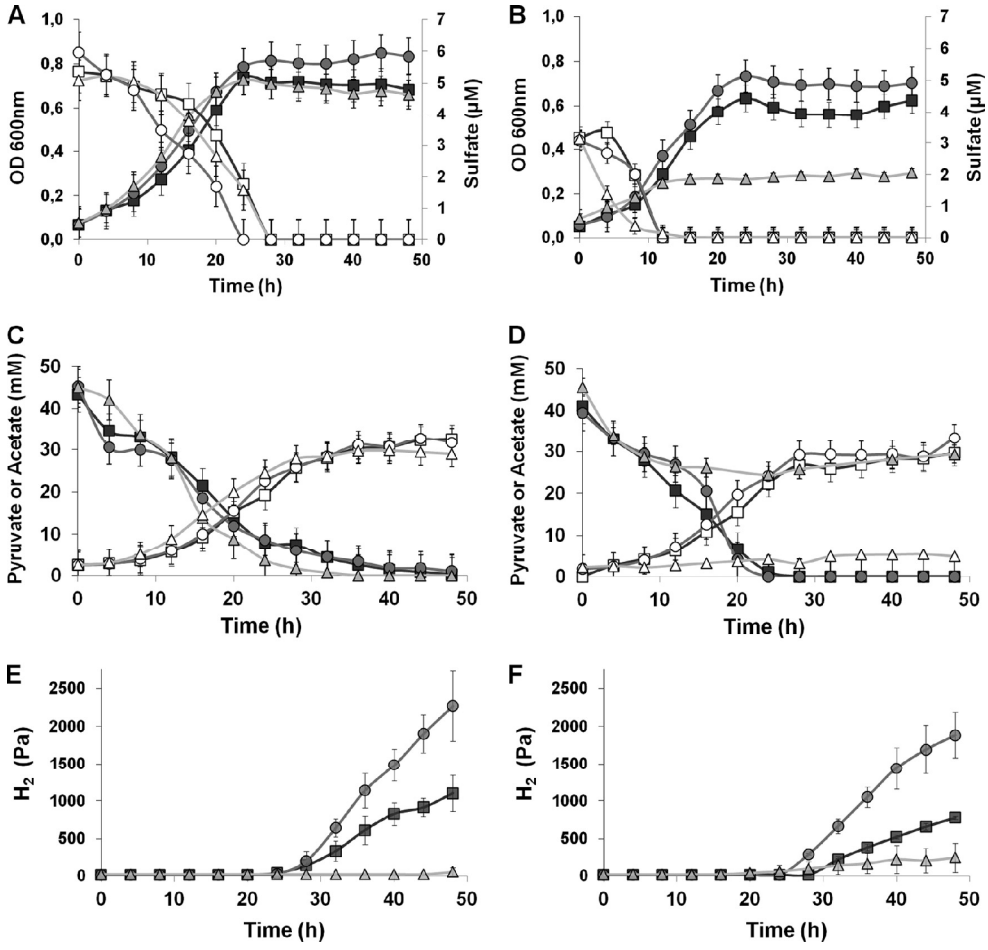

FIG 3 WT *D. gigas* and the Δ*echBC* and Δ*hynAB* mutant strains grown in pyruvate with sulfate limitation (A, C, and E) or with no sulfate added (B, D, and F). A and B, growth curves (filled symbols) and sulfate quantification (open symbols); C and D, quantification of pyruvate (filled symbols) and acetate (open symbols); E and F, hydrogen accumulation in the headspace. WT *D. gigas*, squares; Δ*echBC* mutant, circles; and Δ*hynAB* mutant, triangles.

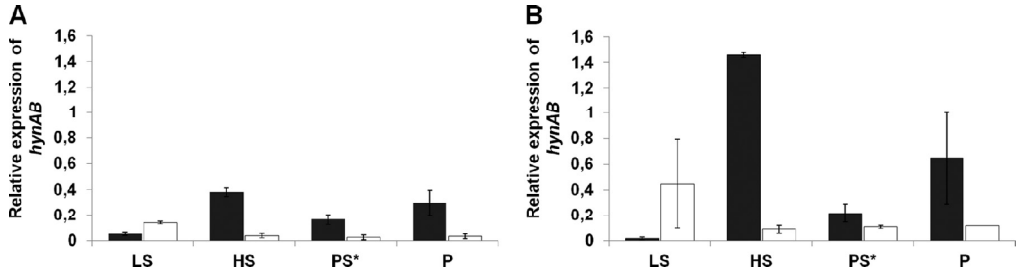

FIG 4 Quantification of the mRNA levels of the *hynB* hydrogenase gene by qRT-PCR in the mid-exponential (16 h) and stationary (32 h) phases of both the WT (A) and Δ*echBC* mutant (B) strains grown under the following conditions: LS, 40 mM lactate–40 mM sulfate; PS*, 40 mM pyruvate–5 mM sulfate; P, 40 mM pyruvate; HS, 1 atm H_2–20 mM sulfate. Black bars, 16 h; white bars, 32 h. The expression of the *hynAB* gene was normalized to that of the 16S rRNA gene. The standard errors of all values are shown.

having the cytoplasmic hydrogenase, did not accumulate any H_2. No difference in pyruvate consumption or acetate formation was observed, as shown in Fig. 3C, indicating that the difference in H_2 accumulation was due to HynAB activity.

Under fermentative conditions when no sulfate was added, a small amount of sulfate (~1 to 3 mM) was nevertheless present in the beginning of growth, coming from the inoculum. After this sulfate was reduced (~16 h), we observed a phenotype different from that seen during respiratory growth on pyruvate. The Δ*hynAB* mutant strain did not show fermentative growth once the small amount of residual sulfate was consumed, whereas the Δ*echBC* mutant and WT strains were able to grow, albeit to lower cell densities (Fig. 3B) and with reduced cell yields (Table 1) than in pyruvate-sulfate. Furthermore, the doubling times of these strains in pyruvate fermentation were at least double those seen when sulfate was present. From the metabolite analysis, it is clear that after the residual sulfate was reduced, the absence of the HynAB hydrogenase prevented the cells from fermenting pyruvate, resulting in the absence of fermentative growth of this strain (Fig. 3B and D). Furthermore, the expression of the *ech* genes is also lower under this condition in the Δ*hynAB* mutant strain than in the WT strain (see below), which may also have contributed to the lack of growth.

Similarly to what happened under sulfate-limiting conditions, H_2 accumulation in the Δ*echBC* strain was much higher than that in the WT (Fig. 3F). Interestingly, this accumulation started only after all of the pyruvate was consumed, as previously reported for *D. vulgaris* (39). A slight accumulation of H_2 could be observed in the Δ*hynAB* mutant strain as well, showing that the Ech hydrogenase can contribute to some H_2 production under these conditions.

These results indicate that under fermentative conditions, HynAB is an essential enzyme for cell growth and that cells are unable to ferment pyruvate in its absence. Furthermore, periplasmic HynAB is the main hydrogenase responsible for the H_2 accumulation observed under fermentative conditions.

Expression profiles of the *ech* and *hyn* genes. The higher H_2 accumulation by the Δ*echBC* mutant strain, relative to that by the WT, during pyruvate fermentation is very surprising, since it could be expected that the cytoplasmic Ech hydrogenase would be responsible for H_2 production from reduced ferredoxin produced by the pyruvate:ferredoxin oxidoreductase. To evaluate if this was due to an increase in HynAB transcripts in the deletion strain, we analyzed the expression levels of genes coding for both the HynAB and Ech hydrogenases in WT *D. gigas* and the deletion strains. Real-time qRT-PCR was performed to analyze the mRNA expression levels of the HynAB hydrogenase in both WT *D. gigas* (Fig. 4A) and the Δ*echBC* mutant strain (Fig. 4B) in the mid-exponential (16 h) and stationary (32 h) phases in pyruvate-limiting sulfate and pyruvate fermentation, as well as under lactate-sulfate and H_2-sulfate conditions, for which microarray expression data have been reported for other *Desulfovibrio* spp. (5, 7). Expression of the Ech hydrogenase was similarly evaluated in WT *D. gigas* (Fig. 5A)

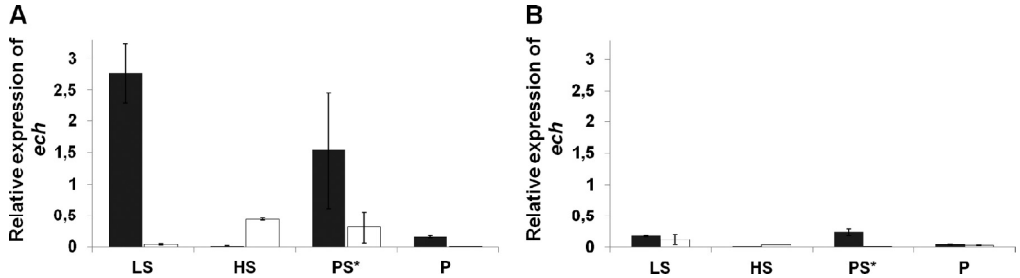

FIG 5 Quantification of the mRNA levels of the *echE* hydrogenase gene by qRT-PCR in the mid-exponential (16 h) and stationary (32 h) phases of both the WT (A) and Δ*hynAB* mutant (B) strains grown under the following conditions: LS, 40 mM lactate–40 mM sulfate; PS*, 40 mM pyruvate–5 mM sulfate; P, 40 mM pyruvate; HS, 1 atm H_2–20 mM sulfate. Black bars, 16 h; white bars, 32 h. The expression of the *echE* gene was normalized to that of the 16S rRNA gene. The standard errors of all values are shown.

and the Δ*hynAB* mutant strain (Fig. 5B). Quantification of all samples was performed relative to the 16S rRNA gene.

The expression of the *hynB* gene was highest in the WT strain during exponential growth in hydrogen respiration and in pyruvate fermentation (Fig. 4A), whereas it was lower in pyruvate-sulfate and even lower in lactate-sulfate. After cells entered stationary phase, *hynB* gene expression dropped to very low levels in hydrogen-sulfate, pyruvate-sulfate, and pyruvate fermentation, whereas it increased under lactate-sulfate conditions.

An increase in *hynB* gene expression, compared to that of the WT, was observed in the Δ*echBC* mutant strain under conditions in which the *hynAB* deletion prevented growth, i.e., hydrogen respiration and pyruvate fermentation (compare Fig. 4B and A). This increase was more prominent during the exponential phase but was also observed during the stationary phase, where we saw a more accentuated drop in the expression of *hynB* in the WT. Under respiratory conditions with organic substrates (lactate-sulfate and pyruvate-limiting sulfate), *hynB* expression in the exponential phase was similar to that of the WT, and once again an increase was observed in the stationary phase relative to the WT level. These increased levels of *hynB* in the stationary phase observed in the Δ*echBC* mutant may account for the greater accumulation of H_2 observed in pyruvate limitation fermentation during physiological analyses. Therefore, in the Δ*echBC* mutant strain, the absence of the Ech hydrogenase appears to be compensated for by an increased level of HynAB (except during exponential-phase growth in lactate-sulfate).

We also measured the levels of *echE* expression in the WT and Δ*hynAB* mutant strains. The *echE* mRNA levels were highest in the *D. gigas* WT strain during exponential growth on an organic substrate (lactate or pyruvate) in the presence of sulfate (Fig. 4A, 16 h). After cells entered the stationary phase (32 h), the levels of *echE* gene expression decreased significantly, especially during growth on lactate. During respiratory growth with H_2 as the energy source, the opposite behavior was observed, where the *echE* mRNA level was almost undetectable during the exponential phase (16 h) but increased after cells entered the stationary phase. During fermentative growth on pyruvate, the *echE* transcript levels were low in the exponential phase and decreased further to undetectable levels after cells entered the stationary phase. This suggests that Ech activity is related mainly to the initial phase of respiratory growth (i.e., when sulfate is still present) with organic substrates, whereas Ech appears to play a much less important role during fermentative growth.

When *echE* gene expression in the Δ*hynAB* mutant strain was analyzed (Fig. 5B), a major overall decrease in expression was observed under all conditions, compared to the WT level (Fig. 5A), suggesting that the HynAB hydrogenase is involved in the regulation of Ech expression. These results indicate that during hydrogen-sulfate respiration and pyruvate fermentation, the Ech hydrogenase is poorly expressed and thus cannot compensate for the absence of the HynAB hydrogenase, preventing growth under these conditions.

DISCUSSION

Previous studies have addressed the role of hydrogenases in *Desulfovibrio* spp. In a *D. vulgaris* strain with the periplasmic Hyn1 [NiFe] hydrogenase deleted, cells were able to grow to almost the same level as the WT in lactate-sulfate medium (17). Similar results were obtained with a *D. fructosovorans* periplasmic *hynABC* and cytoplasmic *hnd* hydrogenase double mutant that was able to grow under all of the conditions tested (14). A further triple mutant lacking all described periplasmic hydrogenases was also shown to grow in fructose-sulfate medium (16). However, in these studies, there were additional hydrogenases present that could compensate for the absence of the missing genes.

D. gigas is uniquely positioned among *Desulfovibrio* spp. for use in testing the function of hydrogenases and the importance of hydrogen cycling in energy conservation, since it contains only two enzymes, one periplasmic and one cytoplasmic. Furthermore, the genomic analyses revealed no sequences related to the pyruvate:formate lyase gene in *D. gigas*, and therefore, formate cycling should not be participating in the energy conservation processes as an alternative to hydrogen cycling.

The results obtained in this work demonstrate that neither of the two hydrogenases is essential for the growth of *D. gigas* under respiratory conditions on an organic substrate (lactate or pyruvate) in the presence of sulfate. In addition, the absence of the *hynAB* or *echBC* genes also did not lead to any significant accumulation of molecular hydrogen. Since no other hydrogenase, either periplasmic or cytoplasmic, is present in the genome of *D. gigas* and formate is not participating in the energy conservation process, this suggests that the hydrogen cycling pathway does not play a major part in the bioenergetics of *D. gigas*. The cell yield coefficients calculated for sulfate respiration with lactate and pyruvate are almost identical for the WT and hydrogenase mutant strains. Nevertheless, a slightly lower growth rate is observed for the Δ*echBC* mutant strain growing on lactate-sulfate and for the Δ*hynAB* mutant strain in both lactate-sulfate and pyruvate-sulfate, suggesting that a small fraction of the electron flow to sulfate may involve the production of H_2. In *D. vulgaris*, a mathematical model of metabolism, supported by experimental results, indicated that two simultaneous pathways for electron flow during growth in lactate-sulfate coexist, one requiring the obligate cycling of H_2 and the other not requiring it (4). The model estimated that 48% of the electron flow from lactate to sulfate involved H_2 production. Our results suggest that this value may be significantly lower for *D. gigas*. This would be in line with the reduced number of hydrogenases in this organism compared to *D. vulgaris*, which has seven hydrogenases. Nevertheless, we have been unable to date to generate a double hydrogenase mutant of *D. gigas*. However, given the difficulty in transforming this organism, we cannot clearly conclude that this is due to the required presence of at least one hydrogenase.

Thus, as suggested before, the mechanism of hydrogen cycling does not seem to be strictly essential for the *Desulfovibrio* genus (9) and may make different contributions to the overall electron flow in different organisms. This is not entirely surprising since it was previously shown that some SRB do not have any hydrogenases at all (e.g., *Desulfococcus oleovorans*) or have no cytoplasmic hydrogenases (like *Desulfomicrobium baculatum*, which is closely related to *Desulfovibrionaceae*) (6).

Thus, H_2 is not an obligatory intermediate in the oxidation of organic compounds by *D. gigas* since deletion of the hydrogenases does not affect the ability of cells to grow. This agrees with the observation by Lupton et al. that H_2 added to lactate-sulfate medium did not competitively inhibit the oxidation of lactate or increase growth or substrate utilization (3). However, we cannot rule out the possibility that other electron transfer pathways substitute for hydrogen cycling when one of the hydrogenases is miss-

ing. It is plausible that the cells can reroute electron flow if one of several pathways is impaired. This would be the advantage of having dual or multiple pathways for electron flow, and sulfate reducers are recognized for their metabolic flexibility.

Chemiosmotic models of energy conservation have also been proposed in which electrons generated from substrate oxidation are transported through membrane-bound electron carriers to sulfate reduction (vectorial electron transport) and in the process translocate protons to the periplasm (vectorial proton transport) (6, 35). Two membrane complexes that were identified in the *D. gigas* genome, the Qmo and Dsr complexes, were proposed to perform this function (21, 36). An energy conservation process may result from electron transfer from the quinone pool to AprAB through the Qmo complex (19, 37), and also the Dsr complex may be involved in menaquinol oxidation with reduction of DsrC, associated with proton translocation (36, 38). Furthermore, other electron transfer pathways to sulfate may involve Hdr-related proteins that could provide a soluble pathway from different donors (such as lactate, pyruvate, ferredoxin, or H_2) to the reduction of DsrC in a flavin-based electron bifurcation mechanism for energy conservation (6). Such a system may involve the HdrABC/FloxABCD proteins that are also encoded in the *D. gigas* genome.

Regarding the physiological role of hydrogenases, the periplasmic enzymes are generally presumed to be involved in H_2 oxidation. Previous deletions of periplasmic hydrogenases in *D. vulgaris* demonstrated that in lactate-sulfate or H_2-sulfate, the absence of one periplasmic hydrogenase could be compensated for by the others (9). In *D. gigas*, which has only the HynAB hydrogenase, the physiological and mRNA expression data indicate that this enzyme has a bidirectional role in terms of hydrogen metabolism. When hydrogen is the energy source for sulfate respiration, HynAB acts as the H_2 uptake hydrogenase, as expected, and the electrons from the oxidation of H_2 can then be shuttled to the cytoplasmic reduction of sulfate through cytochrome c_3, Qrc, and Qmo (19). Thus, the absence of the *hynAB* genes impaired growth in hydrogen-sulfate. When sulfate is absent, i.e., under fermentative conditions, our results indicate that this enzyme acts in the opposite direction, as a hydrogen-producing enzyme, as the HynAB-lacking strain was not able to ferment pyruvate. Interestingly, Ech is not able to compensate for the absence of HynAB, as could be expected, but this may also be due to the low level of expression of this enzyme under fermentative conditions.

In agreement with the above, higher levels of *hynAB* expression were observed during growth with H_2-sulfate and in pyruvate fermentation than during lactate-sulfate respiration. These levels were further increased under these conditions in the Δ*echBC* mutant strain, which can account for the greater accumulation of H_2 when this strain is fermenting pyruvate. Our results are similar to what was observed in a *D. vulgaris* Hildenborough periplasmic [Fe] hydrogenase (Δ*hyd*) mutant strain (39), where this hydrogenase was required for pyruvate fermentation, in addition to its function in hydrogen uptake in hydrogen-sulfate medium. Also, during syntrophic growth, a similar role of the periplasmic hydrogenase, acting as an H_2-producing enzyme, was observed in *D. vulgaris* Hildenborough cultures grown in lactate with a hydrogenotrophic methanogen (8). Furthermore, also in *Desulfovibrio alaskensis* G20, the HynAB hydrogenase seems to be the main enzyme responsible for H_2 production during syntrophic growth (12).

However, in these previous studies, the presence of multiple hydrogenases prevented the direct determination of whether a periplasmic hydrogenase is responsible for H_2 production. In this paper, the inability of the Δ*hynAB* mutant strain to grow with pyruvate demonstrated that this periplasmic hydrogenase is undoubtedly essential for fermentative growth and H_2 production. Furthermore, the absence of the *hynAB* gene caused a lower growth rate in pyruvate-sulfate, suggesting that this is the main hydrogenase in pyruvate metabolism.

Interestingly, accumulation of H_2 started only after pyruvate was consumed, as previously observed in *D. vulgaris* (39), suggesting that some intracellular cycling of H_2 may be occurring and/or that other fermentation products are accumulated inside the cell and later converted to H_2. The fact that the Δ*hynAB* mutant strain cannot grow by pyruvate fermentation supports the idea that intracellular H_2 cycling is required, but this inability could also be due to the reduced expression of the Ech hydrogenase.

Regarding the cytoplasmic Ech hydrogenase, our physiological analysis and mRNA expression results indicates that this hydrogenase is not essential for the growth of the organism under any of the conditions tested. Actually, the yield coefficients of the Δ*echBC* mutant strain indicate that the deletion of this gene even slightly increased the final cell yield, particularly whenever pyruvate was the energy source. Nevertheless, the expression of this enzyme is quite high during exponential growth in lactate-sulfate, suggesting that it is probably playing a role under this condition. Also, the growth rate of this mutant strain in lactate-sulfate is lower. In the stationary phase, Ech is virtually not expressed in lactate-sulfate and pyruvate fermentation. Interestingly, transcriptomic analysis in *D. vulgaris* indicated an upregulation of this enzyme under H_2-sulfate compared to lactate-sulfate (5, 7). However, the Δ*ech* mutant strain of *D. gigas* was able to reach a final cell density similar to that of the WT with a shorter doubling time when growing in H_2-sulfate.

Overall, it seems that the Ech hydrogenase does not play a central role in energy metabolism under the conditions tested, which agrees with the fact that no Ech hydrogenase has been identified in the genomes of many SRB, including *Desulfovibrio* spp. such as *D. alaskensis* G20 and *Desulfovibrio piger* (6).

Our results also provide compelling evidence of the importance of obtaining expression data to complement studies of gene deletions. Indeed, the expression of each hydrogenase was significantly altered in the mutants. In particular, the expression of the Ech hydrogenase was almost completely abolished upon deletion of the HynAB enzyme, regardless of the energy source or type of growth. This suggests that HynAB may be somehow involved in the regulation of the *ech* genes. One interesting observation was that the two hydrogenases have somewhat complementary expression, as the HynAB hydrogenase was expressed more during growth in H_2-sulfate and pyruvate fermentation, whereas the Ech hydrogenase was expressed more during growth in lactate-sulfate and pyruvate-sulfate.

In conclusion, the HynAB hydrogenase appears to have a more predominant role in the metabolism of *D. gigas* and is essential for growth with H_2-sulfate and pyruvate fermentation.

ACKNOWLEDGMENTS

This work was supported by Fundação para Ciência e Tecnologia (FCT) grants (PTDC/BIA-MIC/104030/2008 to IACP/CRP and Pest-OE/EQB/LA0004/2011 to the Instituto de Tecnologia Química e Biológica—

António Xavier [ITQB], 049/BI-BI/2011 to C.I.S and SFRH/BD/45211/2008 to F.O.M.-S.).

We thank Maria Cristina Leitão for technical support with the HPLC quantifications, Ana Raquel Ramos for technical support in the Southern blot analysis, and Mónica Martins for methodological support and helpful discussions.

REFERENCES

1. **Matias PM, Pereira IA, Soares CM, Carrondo MA.** 2005. Sulphate respiration from hydrogen in Desulfovibrio bacteria: a structural biology overview. Prog. Biophys. Mol. Biol. **89:**292–329.
2. **Odom JM, Peck HD, Jr.** 1981. Localization of dehydrogenases, reductases, and electron transfer components in the sulfate-reducing bacterium *Desulfovibrio gigas*. J. Bacteriol. **147:**161–169.
3. **Lupton FS, Conrad R, Zeikus JG.** 1984. Physiological function of hydrogen metabolism during growth of sulfidogenic bacteria on organic substrates. J. Bacteriol. **159:**843–849.
4. **Noguera DR, Brusseau GA, Rittmann BE, Stahl DA.** 1998. A unified model describing the role of hydrogen in the growth of Desulfovibrio vulgaris under different environmental conditions. Biotechnol. Bioeng. **59:**732–746.
5. **Keller KL, Wall JD.** 2011. Genetics and molecular biology of the electron flow for sulfate respiration in Desulfovibrio. Front. Microbiol. **2:**135. doi:10.3389/fmicb.2011.00135.
6. **Pereira IA, Ramos AR, Grein F, Marques MC, da Silva SM, Venceslau SS.** 2011. A comparative genomic analysis of energy metabolism in sulfate reducing bacteria and archaea. Front. Microbiol. **2:**69. doi:10.3389/fmicb.2011.00069.
7. **Pereira PM, He Q, Valente FM, Xavier AV, Zhou J, Pereira IA, Louro RO.** 2008. Energy metabolism in Desulfovibrio vulgaris Hildenborough: insights from transcriptome analysis. Antonie Van Leeuwenhoek **93:**347–362.
8. **Walker CB, He ZL, Yang ZK, Ringbauer JA, He Q, Zhou JH, Voordouw G, Wall JD, Arkin AP, Hazen TC, Stolyar S, Stahl DA.** 2009. The electron transfer system of syntrophically grown *Desulfovibrio vulgaris*. J. Bacteriol. **191:**5793–5801.
9. **Caffrey SM, Park HS, Voordouw JK, He Z, Zhou J, Voordouw G.** 2007. Function of periplasmic hydrogenases in the sulfate-reducing bacterium *Desulfovibrio vulgaris* Hildenborough. J. Bacteriol. **189:**6159–6167.
10. **Plugge CM, Scholten JC, Culley DE, Nie L, Brockman FJ, Zhang W.** 2010. Global transcriptomics analysis of the Desulfovibrio vulgaris change from syntrophic growth with Methanosarcina barkeri to sulfidogenic metabolism. Microbiology **156**(Pt 9)**:**2746–2756.
11. **Li X, McInerney MJ, Stahl DA, Krumholz LR.** 2011. Metabolism of H2 by Desulfovibrio alaskensis G20 during syntrophic growth on lactate. Microbiology **157**(Pt 10)**:**2912–2921.
12. **Meyer B, Kuehl J, Deutschbauer AM, Price MN, Arkin AP, Stahl DA.** 2013. Variation among *Desulfovibrio* species in electron transfer systems used for syntrophic growth. J. Bacteriol. **195:**990–1004.
13. **Valente FM, Almeida CC, Pacheco I, Carita J, Saraiva LM, Pereira IA.** 2006. Selenium is involved in regulation of periplasmic hydrogenase gene expression in *Desulfovibrio vulgaris* Hildenborough. J. Bacteriol. **188:**3228–3235.
14. **Malki S, De Luca G, Fardeau ML, Rousset M, Belaich JP, Dermoun Z.** 1997. Physiological characteristics and growth behavior of single and double hydrogenase mutants of Desulfovibrio fructosovorans. Arch. Microbiol. **167:**38–45.
15. **Casalot L, Valette O, De Luca G, Dermoun Z, Rousset M, de Philip P.** 2002. Construction and physiological studies of hydrogenase depleted mutants of Desulfovibrio fructosovorans. FEMS Microbiol. Lett. **214:**107–112.
16. **Casalot L, De Luca G, Dermoun Z, Rousset M, de Philip P.** 2002. Evidence for a fourth hydrogenase in *Desulfovibrio fructosovorans*. J. Bacteriol. **184:**853–856.
17. **Goenka A, Voordouw JK, Lubitz W, Gartner W, Voordouw G.** 2005. Construction of a [NiFe]-hydrogenase deletion mutant of Desulfovibrio vulgaris Hildenborough. Biochem. Soc. Trans. **33**(Pt 1)**:**59–60.
18. **Volbeda A, Charon MH, Piras C, Hatchikian EC, Frey M, Fontecilla-Camps JC.** 1995. Crystal structure of the nickel-iron hydrogenase from Desulfovibrio gigas. Nature **373:**580–587.
19. **Venceslau SS, Lino RR, Pereira IA.** 2010. The Qrc membrane complex, related to the alternative complex III, is a menaquinone reductase involved in sulfate respiration. J. Biol. Chem. **285:**22774–22783.
20. **Li X, Luo Q, Wofford NQ, Keller KL, McInerney MJ, Wall JD, Krumholz LR.** 2009. A molybdopterin oxidoreductase is involved in H_2 oxidation in *Desulfovibrio desulfuricans* G20. J. Bacteriol. **191:**2675–2682.
21. **Pires R, Lourenço A, Morais F, Teixeira M, Xavier A, Saraiva L, Pereira I.** 2003. A novel membrane-bound respiratory complex from Desulfovibrio desulfuricans ATCC 27774. Biochim. Biophys. Acta **1605:**67–82.
22. **Rodrigues R, Valente FM, Pereira IA, Oliveira S, Rodrigues-Pousada C.** 2003. A novel membrane-bound Ech [NiFe] hydrogenase in Desulfovibrio gigas. Biochem. Biophys. Res. Commun. **306:**366–375.
23. **Vignais PM, Billoud B, Meyer J.** 2001. Classification and phylogeny of hydrogenases. FEMS Microbiol. Rev. **25:**455–501.
24. **Hedderich R, Forzi L.** 2005. Energy-converting [NiFe] hydrogenases: more than just H_2 activation. J. Mol. Microbiol. Biotechnol. **10:**92–104.
25. **Künkel A, Vorholt JA, Thauer RK, Hedderich R.** 1998. An Escherichia coli hydrogenase-3-type hydrogenase in methanogenic archaea. Eur. J. Biochem. **252:**467–476.
26. **Meuer J, Kuettner HC, Zhang JK, Hedderich R, Metcalf WW.** 2002. Genetic analysis of the archaeon Methanosarcina barkeri Fusaro reveals a central role for Ech hydrogenase and ferredoxin in methanogenesis and carbon fixation. Proc. Natl. Acad. Sci. U. S. A. **99:**5632–5637.
27. **Soboh B, Linder D, Hedderich R.** 2004. A multisubunit membrane-bound [NiFe] hydrogenase and an NADH-dependent Fe-only hydrogenase in the fermenting bacterium Thermoanaerobacter tengcongensis. Microbiology **150**(Pt 7)**:**2451–2463.
28. **Welte C, Kratzer C, Deppenmeier U.** 2010. Involvement of Ech hydrogenase in energy conservation of Methanosarcina mazei. FEBS J. **277:**3396–3403.
29. **Welte C, Kallnik V, Grapp M, Bender G, Ragsdale S, Deppenmeier U.** 2010. Function of Ech hydrogenase in ferredoxin-dependent, membrane-bound electron transport in *Methanosarcina mazei*. J. Bacteriol. **192:**674–678.
30. **Broco M, Rousset M, Oliveira S, Rodrigues-Pousada C.** 2005. Deletion of flavoredoxin gene in Desulfovibrio gigas reveals its participation in thiosulfate reduction. FEBS Lett. **579:**4803–4807.
31. **Varela-Raposo A, Pimentel C, Morais-Silva F, Rezende A, Ruiz JC, Rodrigues-Pousada C.** 2013. Role of NorR-like transcriptional regulators under nitrosative stress of the delta-proteobacterium, Desulfovibrio gigas. Biochem. Biophys. Res. Commun. **431:**590–596.
32. **Rethmeier J, Rabenstein A, Langer M, Fischer U.** 1997. Detection of traces of oxidized and reduced sulfur compounds in small samples by combination of different high-performance liquid chromatography methods. J. Chromatogr. **760:**295–302.
33. **Rodrigues R, Vicente JB, Felix R, Oliveira S, Teixeira M, Rodrigues-Pousada C.** 2006. *Desulfovibrio gigas* flavodiiron protein affords protection against nitrosative stress in vivo. J. Bacteriol. **188:**2745–2751.
34. **Silva G, Oliveira S, LeGall J, Xavier AV, Rodrigues-Pousada C.** 2001. Analysis of the Desulfovibrio gigas transcriptional unit containing rubredoxin (rd) and rubredoxin-oxygen oxidoreductase (roo) genes and upstream ORFs. Biochem. Biophys. Res. Commun. **280:**491–502.
35. **Wood P.** 1978. A chemiosmotic model for sulphate respiration. FEBS Lett. **95:**12–18.
36. **Pires RH, Venceslau SS, Morais F, Teixeira M, Xavier AV, Pereira IA.** 2006. Characterization of the Desulfovibrio desulfuricans ATCC 27774 DsrMKJOP complex—a membrane-bound redox complex involved in the sulfate respiratory pathway. Biochemistry **45:**249–262.
37. **Ramos AR, Keller KL, Wall JD, Pereira IA.** 2012. The membrane Qmo-ABC complex interacts directly with the dissimilatory adenosine 5′-phosphosulfate reductase in sulfate reducing bacteria. Front. Microbiol. **3:**137. doi:10.3389/fmicb.2012.00137.
38. **Oliveira TF, Vonrhein C, Matias PM, Venceslau SS, Pereira IA, Archer M.** 2008. The crystal structure of Desulfovibrio vulgaris dissimilatory sulfite reductase bound to DsrC provides novel insights into the mechanism of sulfate respiration. J. Biol. Chem. **283:**34141–34149.
39. **Voordouw G.** 2002. Carbon monoxide cycling by *Desulfovibrio vulgaris* Hildenborough. J. Bacteriol. **184:**5903–5911.

Published papers not related with this dissertation

Biochemical and Biophysical Research Communications 431 (2013) 590–596

Contents lists available at SciVerse ScienceDirect

Biochemical and Biophysical Research Communications

journal homepage: www.elsevier.com/locate/ybbrc

Role of NorR-like transcriptional regulators under nitrosative stress of the δ-proteobacterium, *Desulfovibrio gigas*

Ana Varela-Raposo [a,1], Catarina Pimentel [a,1], Fabio Morais-Silva [a], Antonio Rezende [b], Jerônimo C. Ruiz [b], Claudina Rodrigues-Pousada [a,*]

[a] Instituto de Tecnologia Química e Biológica, Universidade Nova de Lisboa, Oeiras, Portugal
[b] Laboratório de Parasitologia Celular e Molecular, Centro de Pesquisa René Rachou – FIOCRUZ, Belo Horizonte, Minas Gerais, Brazil

ARTICLE INFO

Article history:
Received 21 December 2012
Available online 9 January 2013

Keywords:
D. gigas
Nitrosative stress
NorR-like
Transcription factors
Phylogenetic analysis

ABSTRACT

NorR protein was shown to be responsible for the transcriptional regulation of flavorubredoxin and its associated oxidoreductase in *Escherichia coli*. Since *Desulfovibrio gigas* has a rubredoxin:oxygen oxidoreductase (ROO) that is involved in both oxidative and nitrosative stress response, a NorR-like protein was searched in *D. gigas* genome. We have found two putative *norR* coding units in its genome. To study the role of the protein designated as NorR1-like (NorR1L) in the presence of nitrosative stress, a *norR1L* null mutant of *D. gigas* was created and a phenotypic analysis was performed under the nitrosating agent GSNO. We show that under these conditions, the growth of both *D. gigas* mutants Δ*roo* and Δ*norR1-like* is impaired. In order to confirm that *D. gigas* NorR1-like may play identical function as the NorR of *E. coli*, we have complemented the *E. coli* Δ*norR* mutant strain with the *norR1-like* gene and have evaluated growth when nitrosative stress was imposed. The growth phenotype of *E. coli* Δ*norR* mutant strain was recovered under these conditions. We also found that induction of *roo* gene expression is completely abolished in the *norR1L* mutant strain of *D. gigas* subjected to nitrosative stress. It is identified in δ-proteobacteria, for the first time a transcription factor that is involved in nitrosative stress response and regulates the *rd-roo* gene expression.

1. Introduction

Sulfate-reducing bacteria (SRB) are prokaryote microorganisms that use sulfate as the terminal electron acceptor in their metabolism and thus play a key role in sulfur cycling and are involved in several processes such as biomineralization, biocorrosion and metal metabolism. SRB are also capable of reductively precipitate redox metals, being often referred to as promising tools for bioremediation of environments contaminated with heavy metals [1,2]. They have been described as strict anaerobe organisms having an extreme respiratory flexibility [3]. These bacteria have to sense and respond to the chemical changes in their surroundings in order to survive in ever-changing environments. As such they use several mechanisms to avoid the unfavorable habitats and to approach the favorable ones.

Desulfovibro gigas, a member of the δ-proteobacteria, is a model SRB that has the ability of surviving in the presence of oxygen in its natural habitats. Indeed, these microorganisms exist in oxic environments as for instance in the interface of microbial mats as well as in oxygenated areas of aquatic spaces [4]. *D. gigas* contains oxygen detoxifying enzymes such as desulfoferredoxins and neelaredoxins which were shown to have superoxide-scavenging activity either as superoxide dismutase or superoxide reductases [5]. Furthermore, SRB and in particular *D. gigas* were shown to reduce oxygen to water having oxygen-reducing systems [6–8]. In this system rubredoxin (Rd), a small mononuclear iron protein transfers electrons between a NADH oxidase (NRO) and the terminal oxidase rubredoxin:oxygen oxidoreductase (ROO) [9].

ROO was also found to be involved in the protective mechanisms against NO (nitric oxide) in several *Desulfovibrio* species (*D. gigas*, *Desulfovibrio vulgaris* and *Desulfovibrio desulfuricans* among others) [10]. SRB has to cope with NO formed and released in the process of nitrite reduction by coexisting denitrifying microorganisms. Moreover, since *Desulfovibrio* organisms may inhabit the mammalian digestive tract, they are frequently challenged with NO, released by activated macrophages at the onset of infection and inflammatory processes [11,12]. Therefore bacterial response to NO is of considerable importance, occupying a central position in contemporary medicine, physiology, biochemistry and microbiology. A flavorubredoxin (Flrd) and its associated oxidoreductase (encoded by *norV* and

Abbreviations: GSNO, S-nitrosoglutathione; ROO, rubredoxin:oxygen oxidoreductase; NO, nitric oxide.

* Corresponding author.
E-mail address: claudina@itqb.unl.pt (C. Rodrigues-Pousada).

[1] Both authors contributed equally to this work.

0006-291X/$ - see front matter © 2013 Elsevier Inc. All rights reserved.
http://dx.doi.org/10.1016/j.bbrc.2012.12.130

norW, respectively) detoxify NO to form N_2O (nitrous oxide) under anaerobic conditions in *Escherichia coli* [13]. In this bacterium, the transcription of these genes is activated under nitrosative stress by the σ54-dependent regulator, NorR, a member of the bacterial enhancer-binding protein family [14,15]. This factor binds to three sites upstream of the *norV* promoter that contains inverted repeats with core consensus [GT-(N7)-AC], being conserved amongst the β- and γ-proteobacteria [16,17]. The fact that upstream of the *rd-roo* polycistronic unit of *D. gigas* were found two putative consensus sequences for a NorR-binding box led us to search in its genome the potential NorR binding factors [18]. We have found two coding units designated *norR1L* and *norR2L* genes by using bioinformatic tools. We have generated the *norR1L* mutant strain of *D. gigas* of which the growth was assayed in the presence of GSNO, a NO generator. Our results show that the growth of *D. gigas* mutant strain is impaired under these conditions and have also shown that *norR1L* encoding gene of *D. gigas* complements the sensitive phenotype of *E. coli norR* mutant strain. Accordingly *roo* gene expression was examined in the *norR1L* mutant strain revealing a complete abolishment of its induced mRNA levels.

2. Materials and methods

2.1. Bacterial strains and growth media

D. gigas wild-type (wt) ATCC 19364, Δ*roo* and Δ*norR1-like* mutants were grown at 37 °C, anaerobically in lactate–sulfate medium [19]. Kanamycin 50 μg/ml was added to the mutants. *E. coli* wt MC1000, Δ*norR* MC1003 and Δ*norR* MC1003 complemented with *D. gigas norR1-like* gene (amplified from *D. gigas* wt) were grown at 37 °C, aerobically in lysogeny broth medium as previously described [20] and anaerobically in the medium reported [21]. Kanamycin 50 μg/ml was added to Δ*norR* and ampicillin 100 μg/ml to the complemented mutant.

2.2. norR1-like deletion

A null mutant for *norR1-like* gene of *D. gigas* was generated by gene replacement with kanamycin resistance gene by homologous recombination as previously described [10,20].

2.3. Phenotypic analysis of D. gigas and mutant strains

D. gigas wt, Δ*roo* and Δ*norR1-like* mutant strains were grown overnight in lactate–sulfate medium. Cells were diluted in the same growth medium to OD ~0.05 and grown until early exponential phase (~0.3 to ~0.4 OD), when 10 μM of GSNO (NO donor) was added to the cultures. Growth of the cultures was monitored by OD_{600} measurement.

2.4. Functional complementation studies

D. gigas norR1-like gene was cloned into the expression vector pFLAG-CTC (Sigma) using restriction sites SmaI. The recombinant plasmid was confirmed by sequencing. Anaerobic cultures of *E. coli* Δ*norR* mutant cells transformed with either the pFLAG-CTC or pFLAG-CTC(*norR1-like* gene) were grown without shaking at 37 °C in medium as described previously [21] with ampicillin (100 μg/mL).

E. coli wild-type, *E. coli* Δ*norR* and *E. coli* Δ*norR* complemented with plasmid pFLAG-CTC (*norR1L* gene) were grown overnight aerobically at 37 °C in LB medium and transferred to their growth medium and grown anaerobicaly at 37 °C until OD_{600} of 0.6. Cells were diluted in the same growth medium to OD_{600} of 0.05 and grown until early exponential phase, when were either untreated or exposed to 500 mM of GSNO. Growth of the cultures was monitored by OD_{600} measurement.

2.5. RNA isolation and real-time reverse transcription quantitative-PCR (qRT-PCR) analysis

D. gigas wt and *D. gigas* Δ*norR1-like* were grown overnight in lactate–sulfate medium at 37 °C until they reached the early exponential phase. Cultures were then either untreated or treated with 10 μM of GSNO for several periods of time as indicated and harvested. Total RNA was extracted as previously described with minor modifications [10,18]. To eliminate the presence of DNA contamination in the RNA preparation, RNA samples were treated with turbo DNAse (Ambion) and total RNA (1 μg) was reverse transcribed with Transcriptor Reverse Transcriptase (Roche Diagnostics). Gene primer sequences used in the analysis of *roo* expression were 5′TCGATCCCAAAAAGATCGAC3′ and 5′GGCCAGTCCTTGTAATGGAA3′. qRT-PCR reactions were performed in a Light Cycler 1.5 Real-Time PCR System (Roche), using Light CyclerFast Start DNA Master SYBR Green I (Roche). Relative standard curves were constructed for each gene, using triplicate serial dilutions of cDNA. The relative expression of the genes was calculated by the relative quantification method with efficiency correction, using the LightCycler Software 4.1. The housekeeping gene 16S rRNA was used as the reference gene.

2.6. Sequence analysis

Conserved domain searches were performed by means of CDD: a Conserved Domain Database for the functional annotation of proteins [22].

The multiple sequence alignments were constructed using CLUSTALW (http://www.ebi.ac.uk/Tools/msa/clustalw2) and edited and shaded in the program GENEDOC (http://www.nrbsc.org/gfx/genedoc). Phylogenetic analysis was conducted with MEGA version 5 [23], using the neighbor-joining method with Poisson correction.

3. Results and discussion

3.1. Search of NorR-like sequences in D. gigas genome

NorR is a σ54-dependent transcription factor that belongs to the NtrC/NifA family, whose members are formed by a modular structure containing three highly conserved domains: a variable N-terminal regulatory domain (GAF), a central ATPase domain that binds the σ54 factor and a C-terminal DNA binding region of the helix-turn-helix type [24–27]. In the absence of NO the catalytic activity of the central domain of NorR is repressed by the N-terminal regulatory domain that contains a non-haem iron centre [24]. The binding of NO to this center results in the formation of a mononitrosyl iron species, promoting the activation of ATPase activity. It was suggested that the highly conserved GAFTGA loop in the ATPase domain is a target for intramolecular repression by the regulatory domain [28].

Taking advantage of the privileged access to the data generated by the ongoing *D. gigas* genome sequencing project (our unpublished results) we used the *E. coli* NorR [19] as a query sequence, to search genes encoding NorR-like proteins in *D. gigas* genome. Our search retrieved two sequences with the typical structural domain organization of the NtrC/NifA family members, sharing 39% of identity at the amino acid level, designated NorR1-like (NorR1L) and NorR2-like (NorR2L) (Fig. 1A). The alignment of the deduced amino acid sequences of both *D. gigas* NorRLs with those of NorR from *E. coli* [19] and NifA from *Klebsiella pneumonia* [29], indicated that their overall primary structure is close to NifA (40% of

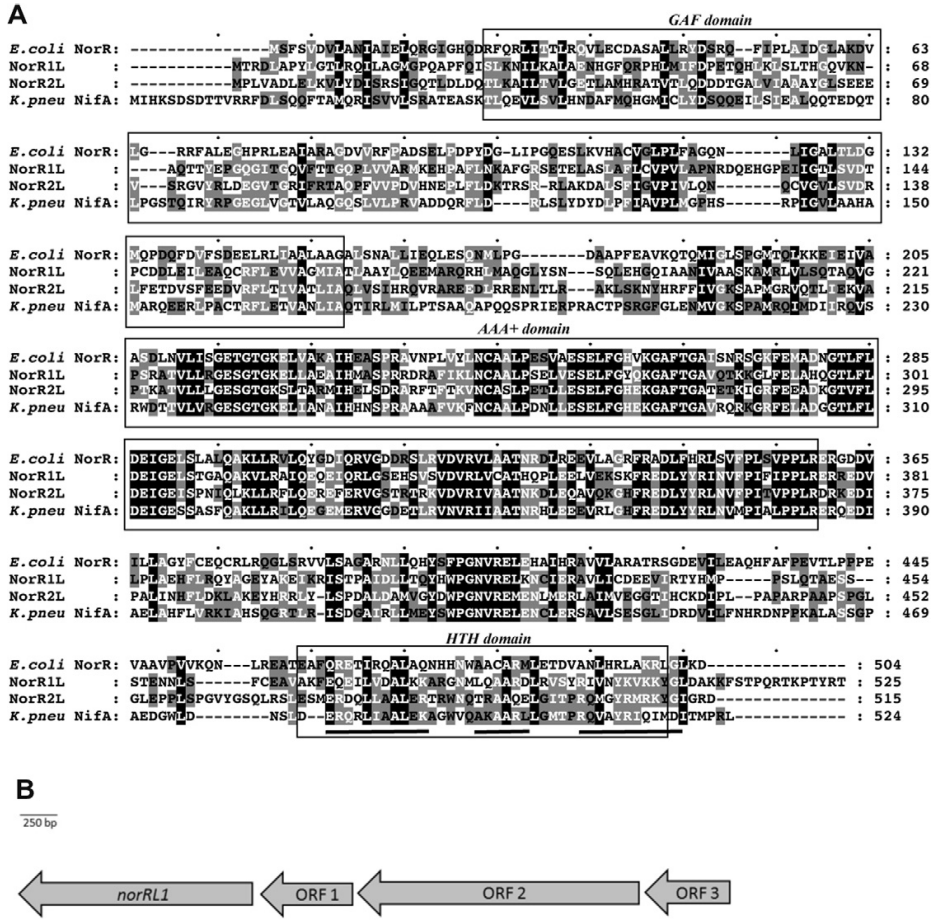

Fig. 1. Amino acid analysis and genetic organization of NorRLs. (A) Amino acid sequence alignment of NorR1L and NorR2L with NifA (*Klebsiella pneumonia*) and NorR (*Escherichia coli*). The three typical domains of the members of the Ntrc/NifA family are boxed. The amino acid residues of the HTH domain of NifA corresponding to the α-helical conformation are underlined. The four levels of shade correspond to 100% of similarity (black); 80–90% of similarity (grey with white symbols); 60–79% of similarity (grey with black symbols) and less than 60% of similarity (not shaded). (B) Gene organization in the surroundings of *norR1L*. ORF1 and ORF2 code for proteins that share a significant similarity with indolepyruvate ferredoxin oxidoreductase. In close vicinity of *norR2L* gene no further ORFS were found.

identity). At the level of the HTH domain, however, NorR1L shares the highest identity with the *E. coli* NorR (28%). Conversely, the DNA-binding domain of NorR2L is only 17% identical to the one of NorR, being close to the NifA corresponding domain (42% of identity). This observation prompted us to use NorR1L and not NorR2L in further studies.

Interestingly, some *Vibrio* species contain two *norR* paralogs that recognize slightly dissimilar *consensus* sequences and thus regulate different operons – *norVW* and *hcp-hcr* [30]. It was identified a member of the CRP/FNR family of transcription factors, HcpR, that regulates *hcp* and its associated ferrodoxin-like gene in *Desulfovibrio* species [31]. It seems therefore unlikely that either NorR1L or NorR2L factors regulate the *hcp-frdx* operon. Nevertheless, we cannot rule out the possibility that both NorR1L and NorR2L are functional and regulate different, yet unidentified, target genes.

The gene coding for NorR2L is monocistronic since no other coding units were found in its close vicinity. However, immediately upstream the *norR1L* gene we found three other putative ORFs (Fig. 1B). ORF1 and ORF2 encode proteins of 205 and 632 amino acid residues, respectively, with significant homology with an indolepyruvate ferredoxin oxidoreductase (IOR) from *Pyrococcus furiosus* [32]. IOR catalyzes the oxidative decarboxylation of aryl pyruvates generated by the transamination of aromatic amino acids, to the corresponding aryl acetyl-CoA [33]. The proximity of *norR1L*, ORF1 and ORF2, led us to admit that these genes are located in the same polycistronic unit, being thus subjected to the same transcriptional control. Northern blot analysis revealed however, that *norR1L* is transcribed as a monocistronic operon (data not shown).

3.2. Phylogenetic analysis of NorR(-like) sequences from different species

We searched the NorR-like orthologs encompassing the typical tri-modular structure in several *Desulfovibrio* genomes, by using the same strategy as described above. We found 2 paralog genes in the genomes of *D. vulgaris*, *D. desulfuricans*, *Desulfovibrio aespoeensis* and *Desulfovibrio magneticus*; 3 paralog genes in the genome of *Desulfovibrio salexigens* and 4 paralog genes in *Desulfovibrio*

alaskensis genome. Next, NorR-like amino acid sequences of *Desulfovibrio* genus were compared with those of gamma-bacteria and with two other *E. coli* nitrosative or nitrite/nitrate responsive factors – Nsr and FNR [34]. We found three distinct groups within the NorR-like sequences, on the basis of the resulting phylogenetic tree (Fig. 2). Group I comprises the best-studied NorRs from *E. coli* and *Ralstonia eutropha* [19,27]; group II includes NorR1L and two NorR-like sequences from *D. alaskensis* and *D. vulgaris* and group III encompasses NorR2L and NorR orthologs found in *D. aespoeensis*, *D. magneticus*, D. *salexigens* and *Desulfovibrio africanus* genome. The topology of the latter strongly suggests that the divergence of a common ancestor gene after speciation occurred rather than a convergent evolution, according to the 16S rRNA gene-based phylogeny of the genus *Desulfovibrio* as described by Gilmour et al. [35].

3.3. NorR1L functionally complements NorR from E. coli

In order to further confirm the functional relationship between *E. coli norR* and *D. gigas norR1L*, we carried out the complementation of *E. coli norR* mutant strain by expressing the plasmid-borne *norR1L* gene. The growth phenotypes of these strains were then assayed in presence of 500 mM GSNO. Our results revealed that wild-type and mutant strains of *E. coli* grow similarly under physiological conditions whereas in presence of 500 μM GSNO, the growth of *E. coli* Δ*norR* mutant strain is abrogated. However, after 6hr of GSNO treatment the growth of *E. coli* Δ*norR* mutant complemented with *norR1L* gene of *D. gigas* was resumed as illustrated in Fig. 3. Nevertheless it is worth noting that the complemented mutant takes longer time to reach the growth of the wildtype strain.

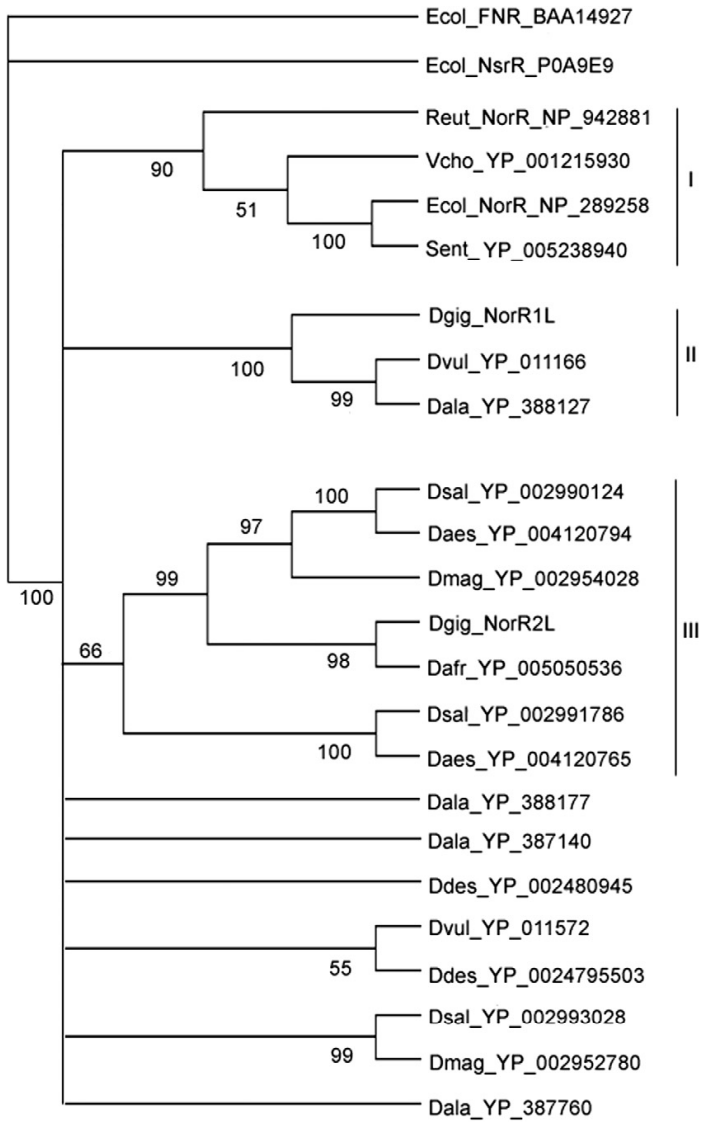

Fig. 2. Phylogenetic analysis of NorR-like amino acid sequences from different species. The phylogenetic analysis was carried out by the neighbor-joining method using MEGA. One thousand bootstrap replicates were calculated and bootstrap values are shown at each node. Nodes were collapsed to a single horizontal line whenever statistical support was less than 55%. The first letters in the sequence label indicate the species. The following characters indicate the sequence accession number.

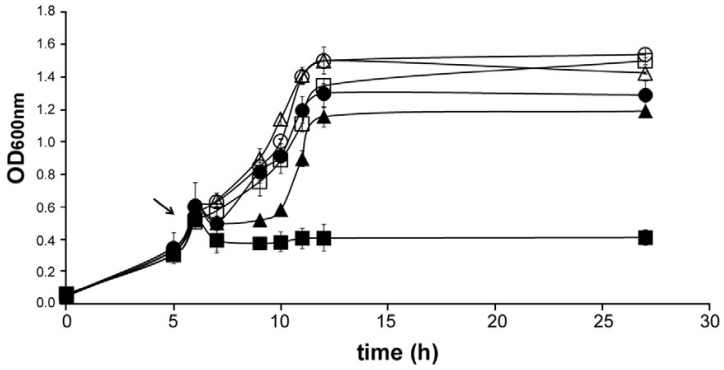

Fig. 3. Anaerobic growth of the *E. coli* strains MC1000 (wild-type), MC1003 (Δ*norR*) and MC1003 expressing a plasmid borne *D. gigas norR1L*, in the presence of GSNO. *E. coli* wild-type (circles), *E. coli* Δ*norR* (squares) and *E. coli* Δ*norR* complemented with pFLAG-CTC plasmid containing *D. gigas norR1L* (triangles) were induced (solid symbols) or not induced (open symbols) with 500 μM of GSNO (the arrow indicates the induction time). Each data point is the average of three independent growth experiments.

Our results obtained by complementation experiments strongly suggest that NorR1-like factor of *D. gigas* is playing the same role under NO stress as its counterpart of *E. coli*.

3.4. Genotypic and phenotypic analysis of *D. gigas* ΔnorR1-like mutant

To clearly evaluate the NorR1L function *in vivo*, we generated and characterized a *D. gigas ΔnorR1L* mutant. To this end, a plasmid containing the kanamycin resistance gene and the flanking regions of *norR1L* was constructed and used to transform the wt *D. gigas* as described in Material and Methods. After transformation and isolation of the colonies grown in presence of kanamycin, the *norR1L* deletion was confirmed by both PCR and Southern blot analysis. The results obtained by both techniques confirmed the deletion of *norR1L* gene via its replacement by the kanamycin resistance gene (Fig. S1).

We have next determined the growth phenotype of the *D. gigas ΔnorR1L* mutant strain, by assaying their growth in the presence of GSNO (as described in Materials and Methods). Our previous studies showed that 10 μM of GSNO inhibited the growth of the *D. gigas* Δ*roo* mutant [12], thus this was the concentration of nitrosating agent used in the present work.

We have verified that under standard growth conditions no differences were observed in *D. gigas* wild-type and the *D. gigas* mutant strain Δ*norR1L*. On the contrary, in the presence of 10 μM GSNO it is clear that growth of the mutant strains *D. gigas* Δ*norR1L* is severely impaired (Fig. 4). This is another indication that NorR1L factor is responsible for NO detoxification in *D. gigas*.

3.5. NorR1-like factor regulates the roo gene expression

E. coli NorR regulates *norVW* operon, which encodes for the nitric oxide reductase flavorubredoxin (NorV) and its associated reductase (NorW) [15,16]. NorR is activated in the presence of nitrosative stress under anaerobic conditions driving the induction of its target genes [17,18]. We therefore evaluated whether *D. gigas* NorR1L regulates the expression of *rd-roo*. Indeed, the *rd-roo* gene promoter contains two σ54 promoter motifs, CC**GG**CCAACCGGTG-**GA**G, at the positions 166 and 207 upstream of the *rd* ATG resembling the canonic sequence of σ54 found in several genes of pathogenic bacteria [36]. Remarkably, the σ54 sequence has a G + C content higher than the canonic one, which is in agreement with the high G + C content of *D. gigas* genome. Moreover, two putative consensus sequences for *norR1-like* gene [GT-(N7)-AC] box are found upstream the *rd-roo* promoter, respectively at 253 and 269 bp upstream of the *rd* ATG. The promoter of *norVW* operon of *E. coli* contains three functional boxes identical to the one we detected in *rd-roo* operon [37].

These features of *rd-roo* promoter together with the previous results led us to monitor the *roo* gene expression in *D. gigas ΔnorR1L* mutant by real time quantitative RT-PCR in the presence of GSNO. We found that *roo* expression is constitutively expressed

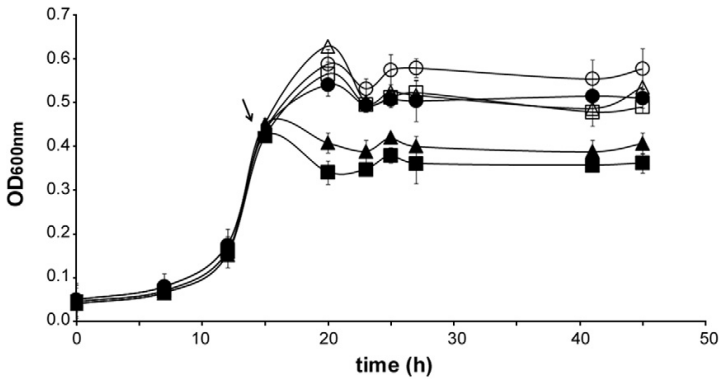

Fig. 4. Growth curves of *D. gigas* wild-type and *D. gigas* Δ*norR1L* in the presence of GSNO. Wild-type (circles) and mutant (squares) were treated (solid symbols) or not treated (open symbols) with 10 μM of GSNO (the arrow indicates the induction time). Each data point is the average of three independent growth experiments.

Table 1
Effect of 10 μM GSNO on *D. gigas roo* gene expression.

	Fold variation[a]		
	1 h	2 h	3 h
wt	1.17 ± 0.18	1.71 ± 0.36	1.32 ± 0.40
ΔnorR1L	1.00 ± 0.12	1.00 ± 0.02	1.00 ± 0.20

[a] Fold variation was calculated using the expression levels of *roo* immediately before and 1, 2 and 3 h after GSNO addition.

in wt strain and induced upon GSNO treatment. This induction is completely abolished in the Δ*norR1L* mutant strain (Table 1). It should be pointed out that as illustrated in Fig. 4 the Δ*roo* mutant strain exhibits a growth phenotype similar to the one of Δ*norR1L*.

Altogether our results show that *roo* gene induction is completely dependent on the regulation by NorR1L transcription factor under nitrosative stress playing an essential role in NO detoxification.

In the present work we have identified in the *D. gigas* genome, a transcription factor, NorR1L, which belongs to the Ntrc/Nif family and closely resembles the NorR factor from *E. coli*. The gene encoding NorR1L factor is able to functionally complement the growth phenotype sensitivity of *E. coli ΔnorR* mutant. In addition, NorR1L factor controls the expression of *roo* gene upon nitrosative stress. Another Ntrc/Nif factor was identified, NorR2L, of which the function is unknown. The *roo* gene besides being involved in nitrosative stress is also activated by oxidative stress [38]. Although Victor et al. by using molecular dynamics simulation reported that ROO does not exhibit any significant preference to accommodate both O_2 and NO [39] it might be possible that *roo* gene expression is regulated by different transcription factors depending on the stressors. In this context it is well possible that NorR2L factor would play a role in *roo* gene expression under oxidative stress conditions. Nevertheless we cannot exclude that NoR2L is regulating the expression of yet unidentified genes involved in nitrosative stress.

Acknowledgments

The authors are deeply indebted to Dr. Catarina Amaral for helpful suggestions and Cátia Santos for technical assistance. We thank Dr. Matthew Bush (John Innes Center, Norwich) for the generous gift of *E. coli* strains. This work was supported by Fundação para a Ciência e Tecnologia (FCT) through grants PTDC/BIA-MIC/70650/2006, given to CRP, and Pest-OE/EQB/LA0004/ 2011, given to Instituto de Tecnologia Química e Biológica. FCT fellowships supported CP (SFRH/BPD/35052/2007) and FS (SFRH/BD/45211/2008).

Appendix A. Supplementary data

Supplementary data associated with this article can be found, in the online version, at http://dx.doi.org/10.1016/j.bbrc.2012.12.130.

References

[1] D.R. Lovley, E.J. Philips, Reduction of uranium by *Desulfovibrio desulfuricans*, Appl. Environ. Microbiol. 58 (1992) 850–856.
[2] D.R. Lovley, P.K. Widman, J.C. Woodward, E.J. Phillips, Reduction of uranium by cytochrome c3 of *Desulfovibrio vulgaris*, Appl. Environ. Microbiol. 59 (1993) 3572–3576.
[3] D.J. Richardson, Bacterial respiration: a flexible process for a changing environment, Microbiology 146 (2000) 551–571.
[4] P. Fareleira, B.S. Santos, C. António, et al., Response of a strict anaerobe to oxygen: survival strategies in *Desulfovibrio gigas*, Microbiology 149 (2003) 1513–1522.
[5] G. Silva, S. Oliveira, C.M. Gomes, et al., *Desulfovibrio gigas* neelaredoxin: a novel superoxide dismutase integrated in a putative oxygen sensory operon of an anaerobe, Eur. J. Biochem. 259 (1999) 235–243.
[6] H. Abdollahy, J.W.T. Wimpenny, Effects of oxygen on the growth of *Desulfovibrio desulfuricans*, J. Gen. Microbiol. 136 (1990) 1025–1030.
[7] E.W.J. van Niel, J. Gottschal, Oxygen consumption by *Desulfovibrio* strains with and without polyglucose, Appl. Environ. Microbiol. 64 (1998) 1034–1039.
[8] L. Chen, M.Y. Liu, J. LeGall, et al., Rubredoxin oxidase, a new flavo-hemoprotein, is the site of oxygen reduction to water by the "strict anaerobe" *Desulfovibrio gigas*, Biochem. Biophys. Res. Commun. 193 (1993) 100–105.
[9] I. Moura, J.J.G. Moura, M.H. Santos, et al., Redox studies on rubredoxins from sulphate and sulphur reducing bacteria, FEBS Lett. 107 (1979) 419–421.
[10] R. Rodrigues, J.B. Vicente, R. Félix, et al., *Desulfovibrio gigas* flavodiiron protein affords protection against nitrosative stress in vivo, J. Bacteriol. 188 (2006) 2745–2751.
[11] J. Loubinoux, F.M. Valente, I.A. Pereira, et al., Reclassification of the only species of the genus *Desulfomonas*, *Desulfomonas pigra*, as *Desulfovibrio piger comb. nov.*, Int. J. Syst. Evol. Microbiol. 52 (2002) 1305–1308.
[12] G.R. Gibson, J.H. Cummings, G.T. McFarlane, Growth and activities of sulphate reducing bacteria in gut contents of healthy subjects and patients with ulcerate colitis, FEMS Microbiol. Ecol. 86 (1991) 103–112.
[13] A.M. Gardner, R.A. Helmick, P.R. Gardner, Flavorubredoxin, an inducible catalyst for nitric oxide reduction and detoxification in *Escherichia coli*, J. Biol. Chem. 277 (2002) 8172–8177.
[14] N.P. Tucker, B. D'Autreaux, S. Spiro, R. Dixon, Mechanism of transcriptional regulation by the *Escherichia coli* nitric oxide sensor NorR, Biochem. Soc. Trans. 34 (2006) 191–194.
[15] N. Tucker, B. D'Autreaux, S. Spiro, R. Dixon, DNA binding properties of the *Escherichia coli* nitric oxide sensor NorR: towards an understanding of the regulation of flavorubredoxin expression, Biochem. Soc. Trans. 33 (2005) 181–183.
[16] N.P. Tucker, B. D'Autreaux, D.J. Studholme, et al., DNA binding activity of the *Escherichia coli* nitric oxide sensor NorR suggests a conserved target sequence in diverse proteobacteria, J. Bacteriol. 186 (2004) 6656–6660.
[17] A. Busch, A. Pohlmann, B. Friedrich, R. Cramm, A DNA region recognized by the nitric oxide-responsive transcriptional activator NorR is conserved in β- and γ-proteobacteria, J. Bacteriol. 186 (2004) 7980–7987.
[18] G. Silva, S. Oliveira, J. LeGall, et al., Analysis of the *Desulfovibrio gigas* transcriptional unit containing rubredoxin (rd) and rubredoxin–oxygen oxidorreductase (roo) genes and upstream ORFs, Biochem. Biophys. Res. Commun. 280 (2001) 491–502.
[19] J. LeGall, G. Mazza, N. Dragoni, Cytochrome C3 of *Desulfovibrio gigas*, Biochim. Biophys. Acta. 99 (1965) 385–387.
[20] M. Broco, M. Rousset, S. Oliveira, C. Rodrigues-Pousada, Deletion of flavoredoxin gene in *Desulfovibrio gigas* reveals its participation in thiosulfate reduction, FEBS Lett. 579 (2005) 4803–4807.
[21] R.E.D. Silaghi-Dumitrescu, A. Coulter, L.G. Das, et al., A flavodiiron protein and high molecular weight rubredoxin from *Moorella thermoacetica* with nitric oxide reductase activity, Biochemistry 42 (2003) 2806–2815.
[22] A. Marchler-Bauer, S. Lu, J.B. Anderson, et al., CDD: a Conserved Domain Database for the functional annotation of proteins, Nucleic Acids Res. 39 (D) (2011) 225–229.
[23] K. Tamura, D. Peterson, N. Peterson, et al., MEGA5: molecular evolutionary genetics analysis using maximum likelihood, evolutionary distance, and maximum parsimony methods, Mol. Biol. Evol. 28 (2011) 2731–2739.
[24] M. Bush, T. Ghosh, N. Tucker, et al., Nitric oxide-responsive interdomain regulation targets the σ54-interaction surface in the enhancer binding protein NorR, Mol. Microbiol. 77 (2010) 1278–1288.
[25] N. Tucker, B. D'Autreaux, S. Spiro, R. Dixon, DNA binding properties of the *Escherichia coli* nitric oxide sensor NorR: towards an understanding of the regulation of flavorubredoxin expression, Biochem. Soc. Trans. 33 (2005) 181–183.
[26] A. Busch, A. Pohlmann, B. Friedrich, R. Cramm, A DNA region recognized by the nitric oxide-responsive transcriptional activator NorR is conserved in beta- and gamma-proteobacteria, J. Bacteriol. 186 (2004) 7980–7987.
[27] A. Klink, B. Elsner, K. Strube, R. Cramm, Characterization of the signaling domain of the NO-responsive regulator NorR from *Ralstonia eutropha* H16 by site-directed mutagenesis, J. Bacteriol. 189 (2007) 2743–2749.
[28] M. Bush, T. Ghosh, N. Tucker, X. Zhang, R. Dixon, Transcriptional regulation by the dedicated nitric oxide sensor, NorR: a route towards NO detoxification, Biochem. Soc. Trans. 39 (2011) 289–293.
[29] R. Pampa, K.J. Smith, R.A. Parslow, et al., Secondary structure and DNA binding by the C-terminal domain of the transcriptional activator NifA from *Klebsiella pneumoniae*, Nucleic Acids Res. 30 (2002) 3972–3980.
[30] D.A. Rodionov, I.L. Dubchack, A.P. Arkin, et al., Dissimilatory metabolism of nitrogen oxides in bacteria: comparative reconstruction of transcriptional networks, PLoS Comput. Biol. 1 (2005) 415–431.
[31] D.A. Rodionov, I. Dubchak, A. Arki, et al., Reconstruction of regulatory and metabolic pathways in metal-reducing deltaproteobacteria, Genome Biol. 5 (2004) R90.
[32] X. Mai, M.W.W. Adams, Indolepyruvate ferredoxion oxidorreductase from a hyperthermophilic archaeon *Pyrococcus furiosus*, J. Biol. Chem. 269 (1994) 16726–16732.
[33] Y. Ozawa, M.A. Siddiqui, Y. Takahashi, et al., Indolepyruvate ferredoxin oxidorreductase: an oxygen-sensitive iron–sulfur enzyme from the

hyperthermophilic archaeon *Thermococcus profundus*, J. Biosci. Bioeng. 114 (2012) 23–27.
[34] D.F. Browning, J.A. Cole, S.J. Busby, Transcription activation by remodelling of a nucleoprotein assembly: the role of NarL at the FNR-dependent *Escherichia coli* nir promoter, Mol. Microbiol. 53 (2004) 203–215.
[35] C.C. Gilmour, D.A. Elias, A.M. Kucken, et al., Sulfate-reducing bacterium *Desulfovibrio desulfuricans* ND132 as a model for understanding bacterial mercury methylation, Appl. Environ. Microbiol. 77 (2011) 3938–3951.
[36] C. Francke, T.G. Kormelink, Y. Hagemeijer, et al., Comparative analyses imply that the enigmatic sigma factor 54 is a central controller of the bacterial exterior, BMC Genomics 12 (2011) 385-1–385-21.
[37] M.C. Justino, V.M.M. Gonçalves, L.N. Saraiva, Binding of NorR to three DNA sites is essential for promoter activation of the flavorubredoxin gene, the nitric oxide reductase of *Escherichia coli*, Biochem. Biophys. Res. Commun. 328 (2005) 540–544.
[38] C.M. Gomes, G. Silva, S. Oliveira, J. LeGall, M.Y. Liu, A.V. Xavier, C. Rodrigues-Pousada, M. Teixeira, Studies on the redox centers of the terminal oxidase from *Desulfovibrio gigas* and evidence for its interaction with rubredoxin, J. Biol. Chem. 272 (1997) 22502–22508.
[39] B.L. Victor, A.M. Baptista, C.M. Soares, Dioxygen and nitric oxide pathways and affinity to the catalytic site of rubredoxin:oxygen oxidoreductase from *Desulfovibrio gigas*, J. Biol. Inorg. Chem. 14 (2009) 853–862.